Netrin signaling function in human and non-human primates' pluripotency regulation

Etienne Masfaraud

N°d'ordre NNT :
2021LYSE1229

THESE de DOCTORAT DE L'UNIVERSITE DE LYON
opérée au sein de
l'Université Claude Bernard Lyon 1

Ecole Doctorale N°340
Biologie Moléculaire, Intégrative et Cellulaire (BMIC)

Spécialité de doctorat : **Biologie Cellulaire**
Discipline : Biologie Cellulaire

Soutenue publiquement le 22/10/2021, par :
Etienne MASFARAUD

Netrin signaling function in human and non-human primates' pluripotency regulation

---

Devant le jury composé de :

KOCH, Manuel	Professeur, IEDMOMB, Cologne	Rapporteur
NAVARRO GIL, Pablo	Chercheur, Institut Pasteur, Paris	Rapporteur
AKSOY, Irène	CR, INSERM, SBRI, Lyon	Examinatrice
BERNET, Agnès	Professeure, CRCL, Lyon	Examinatrice
BŒUF, Hélène	DR, INSERM, BIOTIS, Bordeaux	Examinatrice
SAVATIER, Pierre	DR, INSERM, SBRI, Lyon	Directeur de Thèse

Rôle de la signalisation Nétrine dans la régulation de la pluripotence du primate humain et non-humain

Résumé

La pluripotence se définit comme la capacité d'une cellule à s'auto-renouveler et à se différencier dans les trois lignages primaires que sont le mésoderme, l'ectoderme et l'endoderme. Chez la souris, deux types de pluripotence ont été définis : la pluripotence naïve, trouvant son origine dans l'épiblaste pré-implantatoire, et la pluripotence amorcée, issue de l'épiblaste post-implantatoire. Ces deux types de pluripotence, bien que partageant les caractéristiques centrales précédemment citées, divergent sur les signaux moléculaires et les réseaux transcriptionnels qui les régissent. Chez les primates, la pluripotence naïve telle que définie chez la souris ne peut être capturée *in vitro*. En dépit de protocoles mis au point pour reprogrammer les cellules humaines amorcées vers un état « pseudo-naïf », cette problématique reste non résolue à ce jour, et suggère que la pluripotence chez le primate est régie par d'autres voies moléculaires encore non identifiées. Chez la souris, il a été récemment découvert qu'une molécule de la superfamille des laminines, Nétrine-1, est un régulateur de la pluripotence naïve, nous avons donc entreprit dans le présent projet de caractériser le rôle des Nétrines dans la pluripotence chez le primate. Nous avons démontré que l'expression de *NTN1*, contrairement au macaque et à la souris, n'est pas associée à la pluripotence chez l'homme, mais déclenche au contraire la différentiation des cellules souches pluripotentes humaines (CSPs) en lignages mésodermiques. L'antagoniste de NTN1, DRAXIN, est au contraire enrichi dans l'épiblaste pré-implantatoire humain et protège les CSPs de la différenciation induite par NTN1, constituant de ce fait un nouveau régulateur potentiel de la pluripotence chez l'homme.

Stem Cell and Brain Research Institute (SBRI), Inserm 1208; 18 Avenue du Doyen Jean Lépine, Bron.

Mots-clés : Pluripotence, Cellules souches, Primates, Humain, Embryologie, Embryogénèse

Netrin signaling function in human and non-human primates' pluripotency regulation

Abstract

Pluripotency is defined by the ability of a cell to self-renew and to differentiate in to the three primary germ layers, mesoderm, ectoderm and endoderm. In the mouse, two types of pluripotency have been defined: naïve and primed, the former originating from the naïve epiblast of the pre-implantation embryo, and the latter from the post-implantation epiblast. These two states, despite sharing the core characteristics of pluripotency, differ in the molecular pathways and transcriptional networks underpinning their regulation. In primates, naïve pluripotency as defined in mice cannot be captured *in vitro*. In spite of the many protocols established to reprogram primed human cells to a "naïve-like" state, the issue remains unsolved, suggesting that other regulators of primates' naïve pluripotency exist and remain to be identified. In the mouse, it has recently been shown that Netrin-1, a protein belonging to the Laminins superfamily, is a regulator of naïve pluripotency. In this work, we thus undertook to characterize Netrins family function in primates' pluripotency regulation. We demonstrated that, unlike for the mouse and macaque, *NTN1* expression is not associated with pluripotency in human, but rather triggers differentiation of naïve-like human pluripotent stem cells (PSCs) to mesodermal lineages. NTN1 antagonist DRAXIN, on the contrary, is enriched in the human pre-implantation epiblast and shields PSCs against NTN1-induced differentiating, therefore constituting a new potential regulator of pluripotency in human.

Stem Cell and Brain Research Institute (SBRI), Inserm 1208; 18 Avenue du Doyen Jean Lépine, Bron.

Keywords : Pluripotency, Stem cells, Primates, Human, Embryology, Embryogenesis

Acknowledgments/ Remerciements

Je souhaite dans un premier temps remercier Colette Dehay, directrice du Stem Cell and Brain Research Institute, de m'avoir accueilli au sein du laboratoire et d'avoir été attentive à mes commentaires et ceux de mes collègues doctorants concernant les Student Clubs. J'adresse également mes remerciements à Pascale Giroud, pour sa veille de tous les instants dans le laboratoire et les nombreux problèmes qu'elle a résolu et résout pour nous tous au quotidien.

J'adresse mes remerciements les plus chaleureux à Pierre Savatier, qui m'a accueilli au sein de son équipe, d'abord en stage de master puis en thèse, qui m'a longuement assisté dans la préparation du concours BMIC, les samedis, les dimanches, qu'il pleuve ou qu'il neige. Je le remercie de m'avoir accordé sa confiance et permis de travailler sur un sujet pour lequel il connait désormais ma passion, ainsi que pour toutes les discussions extrêmement intéressantes que nous avons eues ensemble. Je le remercie d'avoir été un chef d'équipe accessible et à l'écoute. Enfin, bien entendu, je le remercie pour les relectures attentives de ce manuscrit en plein mois d'août.

Je souhaite remercier les chercheurs de l'équipe, Marielle, garante du bon fonctionnement du P2, dans lequel j'ai passé de nombreuses heures, ainsi que Nathalie, et Pierre-Yves.

J'adresse également mes remerciements à Chandara et Véronique, qui m'ont à plusieurs reprises sauvé *in extremis* de déboires administratifs divers et variés, et dont le sourire et la bonne humeur ne faillissent jamais. Merci également à Thierry Blachère, la sentinelle des commandes, toujours prompt à répondre à nos réclamations paniquées d'anticorps, de milieu, de cônes, de pipettes ou d'à peu près n'importe quoi d'autre. Un grand merci également à Nathalie Doerflinger, qui a travaillé sur toutes les constructions génétiques de ce projet.

Je remercie infiniment mes collègues étudiants, les thésards, Wilhelm, Florence, Yannicke et Claire, mais aussi Charlotte, avec qui j'ai passé de si nombreux moments de (cri)golade, de procrastination, d'échange, de débats plus ou moins enflammés, mais aussi (parce qu'il en faut un peu) de travail. Je remercie également Tahereh, arrivée plus récemment, et lui souhaite toute la réussite possible pour sa thèse. Un grand merci également aux anciens : Antoine, Anaïs, Mouna, Synara, Lucas et Diana ; sans eux, ces années de thèse

n'auraient pas eu la même saveur, et merci à mes stagiaires, Alex, Julien et Nawel qui ont tous participé avec assiduité à l'acquisition des résultats de ce projet.

Merci à ma famille et à mes amis, Nico (les deux), Béa, Sémi, Mehdy, et tous ceux que j'oublie et qui m'en voudront (mais que j'aime bien quand même), d'avoir supporté des monologues sur des problèmes de labo auxquels, pour la plupart d'entre vous, vous ne compreniez rien. Merci aussi de tolérer mon esprit scientifique toujours prêt à saccager un débat sur les ovnis, les fantômes ou l'astrologie. Hélas pour vous, ce dernier point ne va pas prendre fin avec cette thèse…

Enfin, j'aimerais adresser des remerciements spéciaux aux personnes qui ont étroitement travaillé avec moi sur ce projet, et sans lesquelles il ne serait probablement pas arrivé à terme. Premièrement, à Guillaume Marcy, qui m'a enseigné à peu près tout ce que je sais en bioinformatique, avec lequel j'ai eu de longues et nombreuses discussions indispensables à ma réflexion, et sans qui ce manuscrit ne serait tout simplement que l'ombre de ce qu'il est.

Ensuite, à Cloé Rognard, que j'ai un jour qualifiée d'ange gardien de l'équipe, et qui l'a en tout cas certainement été pour moi. Les milliers d'heures passées au P2 auraient été ressenties au centuple sans elle, elle fut une aide indispensable de tous les instants en culture comme en biomol, une oreille patiente et attentive à toutes les difficultés ainsi qu'à toutes les plaisanteries (d'une qualité parfois franchement discutable) ; une merveilleuse collègue et une amie.

Enfin, j'adresse mes infinis remerciements à Irène Aksoy, qui m'a encadré de la plus excellente des manières durant mon stage de master (stage auquel, soit dit en passant, je n'aurais strictement rien changé…), et a continué de le faire en thèse. Tous les étudiants ne bénéficient pas d'un encadrement si étroit, tous ne sont pas défendus et soutenus comme je l'ai été par Irène. Je souhaitais initialement dédier ce manuscrit à ceux de mes professeurs d'école, de collège et même de lycée, qui disaient de moi que je n'étais bon qu'à récolter des heures de colle, mais c'est finalement à toi que je le dédie, Irène. Merci pour tout.

Table of Contents

Abbreviations

CNS	Central Nervous Sytem
DCC	Deleted in Colorectal Carcinoma
DE	Distal Enhancer
DNMT	DNA methyl transferase
DR	Dependence Receptor
DSCAM	Down Syndrome Cell Adhesion Molecule
ED	Embryonic Diapause
Epi	Epiblast
EpiLCs	Epiblast-Like Cells
EpiSCs	Epiblast-derived Stem Cells
ERVs	Endogenous retroviruses
ESCs	Embryonic Stem Cells
GPI	glycophosphatidilinositol
HDAC	Histone Deacetyl-transferase
hEPSCs	human Expanded Pluripotent Stem Cells
hESCs	human ESCs
ICM	Inner Cell Mass
INTPSCs	Intermediate Pluripotent Stem Cells
iPSCs	induced Pluripotent Stem Cells
KOSR	Knockout-Serum
MEFs	Mouse Embryonic Fibroblasts/Feeder Cells
mESCs	mouse ESCs
Neo1	Neogenin
OSKM	Oct4, Sox2, Klf4, c-Myc (iPS cocktail)
OSN	Oct4, Sox2, Nanog
OXPHOS	Oxidative Phosphorylation
PCA	Principal Component Analysis
PE	Primitive Endoderm **OR** Proximal Enhancer
PGCLCs	Primordial Germ Cells-Like Cells
PGN	Pluripotency Gene Network
PSCs	Pluripotent Stem Cells
RB	Retinoblastoma protein
TE	Trophectoderm
TEs	Transosable Elements
TET	Ten-Eleven Translocation enzyme
TFs	Transcription Factors
t-SNE	t-distributed Stochastic Neighbor Embedding
UMAP	Uniform Manifold Approximation and Projection
VPA	Valproic Acid
WiEpiSCs	Wnt-inhibited EpiSCs
XCI	X Chromosome Inactivation
Xi	inactivated X chromosome
YAP	Yes-associated proteins
VE	Visceral Endoderm
ExE	Extraembryonic Ectoderm

Figures and Tables Index

Introduction

Results

Discussion

Introduction

I/ The Pluripotency continuum – Lessons from the mouse model

Embryogenesis is characterized by the progressive specialization of stem cells, that commit as a matter of time into tissues of restricted function, giving the adult organism. This process of specialization is also called differentiation, and the potential of stem cells to a given extent of specialization is referred to as potency. Because mouse embryos are small sized, low cost and easy to obtain, mouse has become over the past decades the golden standard to study early stages of mammals' embryogenesis (Taft, 2008). It is in mouse that the fundamental concepts of pre-implantation development, and pluripotency, have been first and the most thoroughly described.

1. Pluripotency *in vivo*

Pre-implantation stages of eutherian mammals' embryogenesis are articulated around the segregation of embryonic and extra-embryonic tissues. In the mouse model, before E2.5, the embryo is constituted of blastomeres undergoing regular rounds of division. These blastomeres are totipotent, meaning they hold the capacity to give both embryonic and extra-embryonic lineages. At E3.0, the first differentiation event occurs, and these blastomeres segregate into two tissues: the trophectoderm (TE), contributing to the fetal portion of the placenta, and the Inner Cell Mass (ICM). The ICM undergoes the second round of differentiation of the embryo at E3.5, timepoint marking the beginning of the blastocyst stage. Two populations of cells arise then, the primitive endoderm (PE) and the epiblast (Epi). The former gives rise to the parietal and visceral endoderm of the yolk sac and to a subpopulation of cells in the early gut tube (Schrode et al., 2013). The latter is composed of Pluripotent Stem Cells (PSCs), entirely devoted to the formation of the embryo strictly speaking and holding the capacity to form any cell type in an adult organism (**Figure 1**).

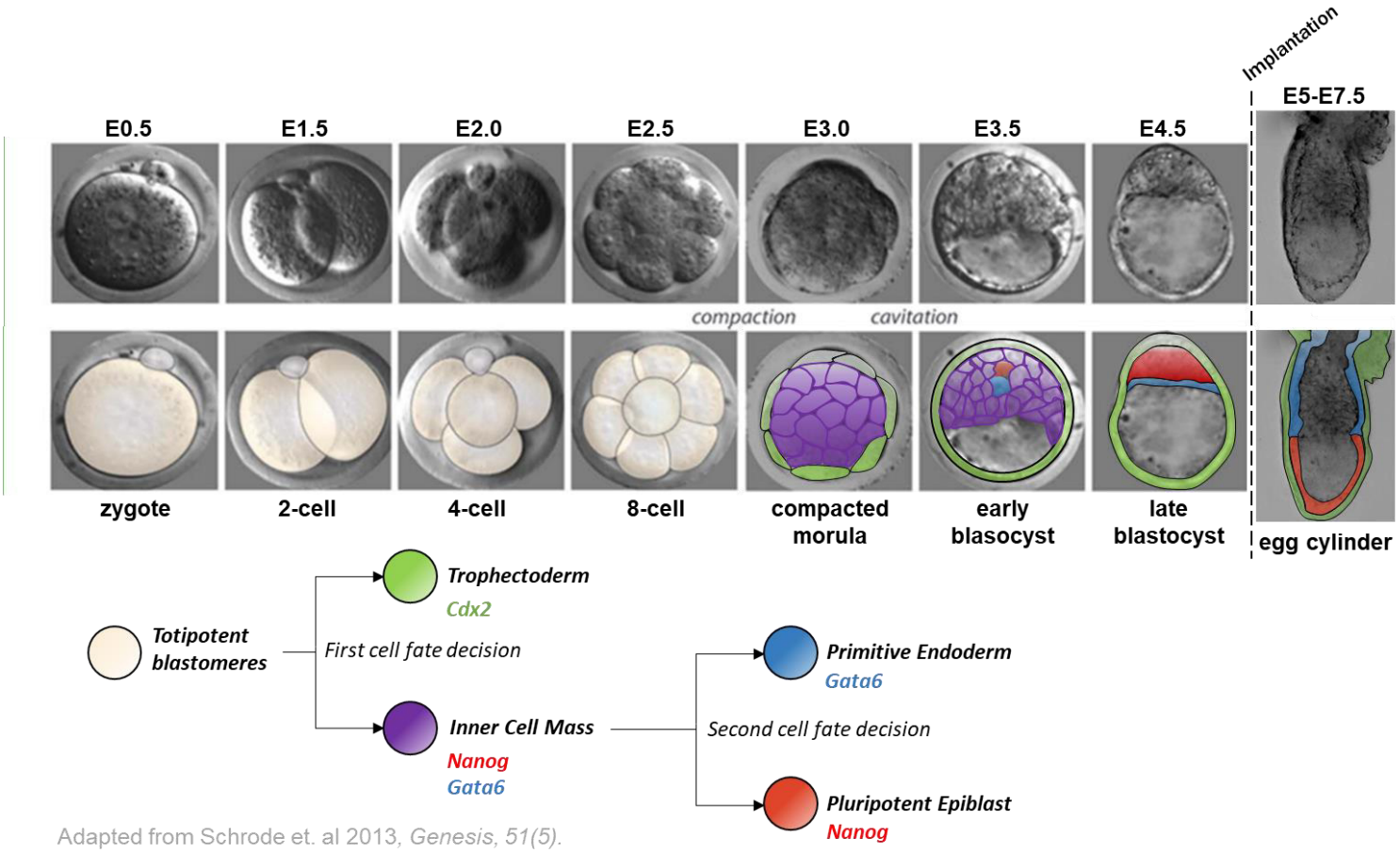

Figure 1. Pre- and peri-implantation stages of mouse embryonic development.
Pictures of mouse pre- and peri-implantation embryonic stages (first row) and their associated tissues (second row). Sequential cell fate decisions occuring between the 8-cell and late blastocyst stage are represented on the bottom diagram.

a) Molecular regulation of the ICM onset

Between the 8-cell and 32-cell stages of mouse development, the combination of symmetrical and asymmetrical divisions yields two populations of blastomeres: outer and inner (Humiêcka et al., 2017). Though identical in morphology and potency, these two populations start to diverge, i) in their polarity status, ii) in the differential expression of a subset of genes (Guo et al., 2010). Among those genes, three in particular have been shown to be critical in the ICM vs TE specification: Caudal-related homeobox 2 (*Cdx2*), *Nanog* and *Oct4*.

Cdx2 is detectable in a subset of blastomeres as soon as the 8-cell stage of development and is then significantly more expressed in outer blastomeres, until being fully restricted to the TE at the blastocyst stage (Ralston and Rossant, 2008). *Cdx2* -/- mutant embryos, although they form morphologically normal blastocysts, fail to implant. This is due to a complete lack of TE specification in said embryos (Strumpf et al., 2005). Cdx2 is therefore necessary to trigger TE allocation.

Oct4 (also known as Pou5f1), a POU family protein, is expressed in the oocyte and in all blastomeres of the cleavage stage embryo, and is then restricted to the ICM and Epiblast (Scholer et al., 1989). *Oct4* -/- mutant embryos, although they form blastocysts, do not develop an ICM and instead yield cells all committed to TE (Nichols et al., 1998). In complete opposition to Cdx2, Oct4 Is therefore necessary to ICM commitment, and its absence favors TE differentiation.

Nanog, a variant homeodomain protein, is expressed at the 8-cell stage and, as for Oct4, is subsequently maintained in the ICM and Epiblast. *Nanog* null mutants form an ICM, but when derived in vitro (surgical removal of TE), cells appear to not persist in undifferentiated masses, but instead entirely commit to a PE-like fate in 4 days (Mitsui et al., 2003; Silva et al., 2009). This demonstrates that Nanog, unlike Oct4, is not necessary to ICM formation, but is rather critical to its maintenance.

Altogether, Cdx2 and Oct4/Nanog therefore work in an ambivalent fashion, restricting each other's expression to promote respectively TE and ICM commitment (Niwa et al., 2005; Strumpf et al., 2005; Wang et al., 2010) (**Figure 2**). This process is also the founding step to the epiblast segregation, and therefore pluripotency establishment *in vivo*.

b) Emergence of the epiblast

After ICM establishment at E3.0, the cavitation process occurs, leading to the appearance of the blastocoelic cavity. This event marks the entrance in the blastocyst stage of development, at E3.5. In the meantime, ICM cells begin to differ in the expression of several factors, in a salt-and-pepper manner. Two subsets of cells can be distinguished then: those expressing *Nanog*, and those expressing *Gata6* (Chazaud et al., 2006; Gerbe et al., 2008; Kurimoto et al., 2006; Plusa et al., 2008; Rossant et al. 2003). The latter migrate toward the blastocoelic cavity and form an epithelialized layer, the PE, and the former stay in between the TE and newly formed PE epithelium, yielding the pluripotent epiblast. Before they are fully segregated into either Epi or PE, these cells are referred to as "biased", meaning their engagement in one or either way is not complete. Epi-biased cells, in addition to the expression of Nanog, upregulate the Fibroblast Growth Factor 4 (Fgf4), while PE-biased cells upregulate its receptor, Fgfr2 (Guo et al., 2010). Conversely, both proteins are respectively down-regulated in PE- and Epi-biased cells. Fgf4 binding to its receptor activates the MEK/ERK pathway, and leads to the upregulation of Gata6. Once expressed, *Gata6* in turns inhibits *Nanog* expression, promoting PE differentiation (**Figure 2**). Removal of Fgf4, Fgfr2 or any

downstream actor of the cascade leads to a failure of commitment into PE (Arman al., 1998; Chazaud et al., 2006; Feldman et al., 1995; Kang et al. 2013).

As stated earlier, *Oct4* is critical to the ICM establishment and maintenance, and its expression is maintained and just as mandatory in the epiblast. Nanog is paramount to the epiblast vs PE establishment. However, alongside Nanog and Oct4, a third factor is critical to the epiblast emergence: the SRY (Sex-determining Region Y) box 2 transcription factor, also known as Sox2. *Sox2* overlaps *Oct4* in terms of kinetics and patterning of expression in the early mouse embryo, but unlike Oct4, null mutants develop to the blastocyst stage and exhibit an ICM. This ICM though, fails to allocate an epiblast, while both PE and TE are present in the subsequent hours (Avilion et al., 2003). Oct4, Sox2 and Nanog are therefore altogether necessary to the epiblast emergence, and thus pluripotency *in vivo,* reason why they are often referred to as the triumvirate of pluripotency. Those three factors also appear to crosstalk and regulate one another (Liang et al., 2008). Oct4 and Sox2 form a transcriptional complex that regulates both Oct4 and Sox2 expression (Chew et al., 2005; Okumura-Nakanishi et al., 2005), and promotes Nanog upregulation (Kashyap et al., 2009; Rodda et al., 2005).

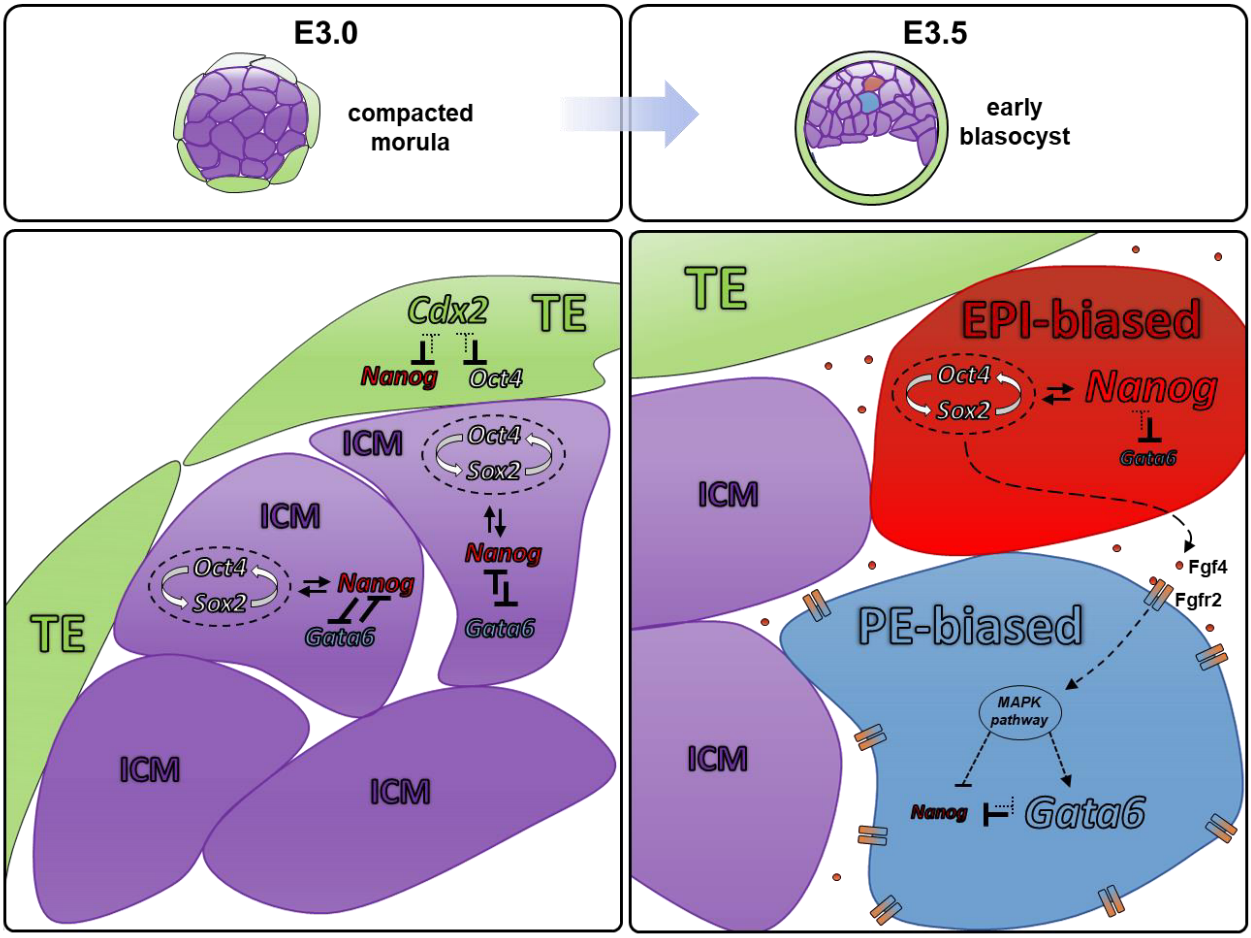

Figure 2. Molecular regulation of the mouse epiblast emergence.
Schematic of the molecular events occuring between E2.5 and E3.5 stages of mouse embryogenesis and leading to trophectoderm (TE), Inner Cell Mass (ICM), Epiblast (Epi) and Primitive Endoderm (PE) specifications. Dashed and solid lines respectively represent indirect and direct activation (arrows) or inhibition (bars).

2. Pluripotency *in vitro* - Pluripotent Stem Cells derivation

a) Conventional Embryonic Stem Cells (ESCs)

In 1981, a procedure to expand epiblast cells *in vitro* was developed (Evans and Kaufman, 1981; Martin, 1981). These cells, initially cultured on a layer of mitotically inactivated fibroblasts in a medium containing calf serum, were called Embryonic Stem (ES) cells. ES cells have a high nuclear/cytoplasmic ratio, form tightly packed, dome-shaped colonies and can be dissociated in single cells able to expand and form colonies *de novo*. This property is referred to as clonogenicity (Hackett and Azim Surani, 2014). As for the epiblast, ES cells can differentiate into any cell type from the three primary germ layers (ectoderm, mesoderm and endoderm) (Smith, 2013), and can be propagated *in vitro* indefinitely. This property of self-

replication without genetic impairment is called “self-renewal” and defines, along with differentiation into the three germ layers, pluripotency.

In addition to their *in vitro* potential, ES cells also hold the remarkable attribute to re-enter embryogenesis. Indeed, when injected in a host blastocyst, they are capable of participating in the development of the embryo, even if they have been precedingly manipulated and propagated *in vitro* (Bradley et al., 1984). Exogenous ESCs yield progeny in all tissues and organs of the host with no bias, proving that their potential remains intact. This unique capacity of embryo colonization is called chimeric competency, because the resulting embryo is a chimera between two distinct individuals.

In 1988, it was found that feeder cells used to co-culture ESCs could be replaced by a single cytokine, Leukemia Inhibitory Factor (LIF) (Smith et al. 1988; Williams et al. 1988). LIF is naturally secreted by the feeders in presence of ES cells, and its removal alone leads to their differentiation and the subsequent arrest of their propagation after a few days. It was shown that the molecular signal of LIF is transduced by the gp130 receptor (Yoshida et al., 1994) and inhibits differentiation through activation of the JAK-STAT3 pathway (Niwa et al., 1998). LIF triggers the cross phosphorylation of JAKs, that in turn recruits and phosphorylates STAT3, allowing it to enter the nucleus and activate the transcription of target genes (summarized on **Figure 3** and further discussed in part **I/2.d)).**

ES cells cultured in serum/LIF exhibit heterogeneity in terms of morphology and expression of several genes, among which notably, Nanog (Chambers et al., 2007; Hayashi et al., 2008). Serum batches need to be screened before use, and only a few mouse strains are permissive to ES cells derivation with such culture conditions. Therefore, replacing serum was critical to restrain variability and understand the extrinsic factors supporting pluripotency. It was observed that upon removal of serum and LIF, established ES cell lines preferentially differentiate into neurectodermal lineages (Ying et al., 2003b). In *Xenopus* embryo, the TGF-β superfamily growth factor BMP4 is known to suppress neuralization (Sasai et al., 1995). Based on this observation, BMP4 was used in replacement of serum in ES culture media, and was shown to be sufficient, through inhibition of Id target genes, to suppress differentiation in the presence of LIF (Ying et al., 2003a)

b) 2i/LIF ESCs

As stated in part **I/1.b)**, the ERK/MAPK pathway is activated in a non-cell autonomous manner through Fgf4-Fgfr2 binding in the mouse blastocyst, and promotes the second event of differentiation of ICM into PE. In line with this observation *in vivo*, chemically suppressing FGF/ERK *in vitro* with the MEK inhibitor PD098059 leads to an enhancement of self-renewal, and to an inhibition of differentiation in embryoid bodies formation assays (Burdon et al., 1999). In opposition to FGF/ERK, it was shown that Wnt pathway activation was associated to pluripotency maintenance in ES cells (Merrill, 2012). Wnt ligands trigger detachment of GSK3 from β-catenin, preventing its phosphorylation and degradation. Accordingly, inhibition of GSK3 with a pharmacological inhibitor, 6-bromoindirubin-3'oxime, in addition to LIF, maintains the undifferentiated phenotype of ES cells, although reducing their viability (Sato et al., 2004). On the basis of these findings, both inhibition of FGF/ERK and GSK3 was succeedingly attempted, with the combined use of PD098059 and CHIR99021 pharmacological inhibitors (Ying et al., 2008). This approach, called 2i, yields complete suppression of differentiation (**Figure 3**). When LIF is added, ES cells, contrary to their Serum/LIF counterparts, are largely homogeneous in morphology and gene expression (Wray et al., 2011). 2i/LIF (also referred to

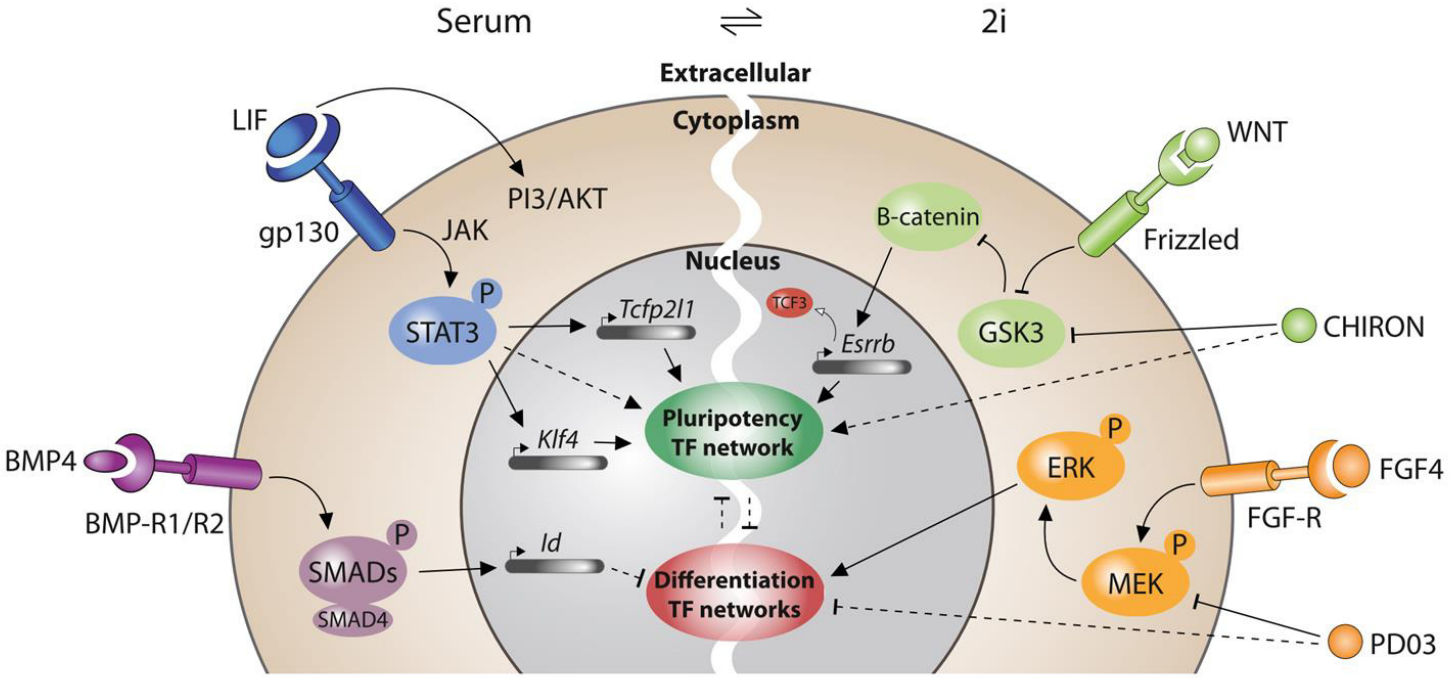

Hackett and Surani 2014, *Cell Stem Cell, 15(4).*

Figure 3. Extrinsic factors regulating mouse pluripotency.
Schematic of the extrinsic signals regulating pluripotency of mouse ES cells cultured in serum (Left) or 2i (right) + LIF conditions. Dashed and solid lines respectively represent indirect or direct effects and interactions.

as ground state condition, see part **I/3.e**)) is now widely adopted, and allows derivation of ES cell lines from otherwise restrictive mouse strains.

c) Epiblast-derived Stem Cells (EpiSCs)

After uterine implantation, the mouse embryo changes shape, and goes from blastocyst to a cup shaped structure called the egg cylinder (Kaufman, 1992). The epiblast does not cease to exist but is submitted to new molecular signals secreted by the trophoblast and the yolk sac. These include Bone Morphogenic Proteins (BMPs), Fibroblasts Growth Factors (FGFs) and Wnt family molecules (Beddington and Robertson, 1999). In XX embryos, post-implantation Epiblast cells also show random inactivation of one X, whereas both are maintained active during the pre-implantation period (Kalantry, 2011). These differences between pre- and post-implantation epiblast, however, do not appear to be associated with a loss of pluripotency after implantation, as both types of cells maintain the capacity to differentiate into any cell lineage from the primary germ layers.

In line with this observation, PSCs were derived from the post-implantation Epiblast (between E5.5 to 7.5) in 2007, and named post-implantation Epiblast-derived Stem Cells (EpiSCs). EpiSCs, just as ES cells, show the ability to self-renew and to differentiate into the three germ layers, and exhibit expression of the pluripotency triumvirate *Oct4*, *Nanog* and *Sox2* (Brons et al., 2007; Tesar et al., 2007).

d) Induced Pluripotent Stem Cells (iPSCs)

In 2006, Takahashi and Yamanaka identified 24 genes upregulated in either ESCs or tumors as potential candidates to induce pluripotency in somatic cells. By overexpressing each factor individually, no pluripotent characteristic could be observed, to the opposite of simultaneous expression of all 24 genes. Individual withdrawal of these factors allowed to break down the list to 4 critical factors whose absence did not allow to produce pluripotent colonies from somatic cells. These were Oct4, Sox2, Klf4 and c-Myc, known as the OSKM cocktail. Simultaneous overexpression of OSKM in mouse embryonic or somatic fibroblasts leads to effective conversion in pluripotent cells, named induced Pluripotent Stem cells (iPSCs). IPSCs can form teratomas, exhibit the growth properties and morphology of ESCs, and express gene markers specific of ESCs. Intriguingly, Nanog is dispensable to the reprogramming cocktail, as confirmed by double Knockout of *Nanog* in mouse embryonic

fibroblasts (MEFs) submitted to OSKM ectopic expression. After induction, *Nanog* -/- are efficiently reprogrammed to induced pluripotency, demonstrating that endogenous *Nanog* expression is not necessary to the process (Schwarz et al., 2014). Such cells, however, lack the capacity to produce adult chimeric mice, as wild-type first generation iPSCs, revealing a default in germline transmission. A proposed explanation is that *Nanog* is dispensable for the first steps of reprogramming, *i.e.* de-differentiation and acquisition of "pre-pluripotent characteristics", but paramount to germline-competency and acquisition of ground state pluripotency (further discussed in part **I/3.e)**) (Silva et al., 2009). Accordingly, the second generation of iPSCs achieved germline transmission with addition of *Nanog* overexpression, or specific selection of *Nanog*-positive colonies (Okita et al., 2007; Wernig et al., 2007).

3. From Naïve to Primed: The Continuum of Pluripotency

a) Discrepancies of ESCs and EpiSCs

When they were first derived, it was observed that EpiSCs exhibit a number of differences with ES cells (summarized on **Figure 4**). First, they are derived and maintained *in vitro* with a medium containing Activin A and FGF2, contrary to the conventional Serum-BMP4/LIF ES cells medium, and no EpiSC line can be derived and/or maintained with such conventional conditions. In addition, application of the activin receptor inhibitor SB431542 leads to rapid differentiation of EpiSCs, showing that their pluripotency, unlike that of ESCs, depends strictly on the activin/nodal pathway. Second, they are morphologically distinct from ES cells, growing as flat monolayered colonies rather than tight dome-shaped ones. Third, when passaged by molecular dissociation with trypsin, EpiSCs undergo widespread cell death contrary to ESCs, and need to be mechanically dissociated in smaller clumps for amplification. Fourth, EpiSCs show no expression of some pluripotency markers expressed in ESCs, such as *Rex1* (*Zfp42*), and strongly reduced expression of others such as *Gbx2*; they also express early lineage markers such as *Fgf5* (ectoderm), *Eomes*, *Brachyury* (mesoderm) and *Gata6* (endoderm) (Coronado et al., 2013). Fifth, Unlike ESCs, EpiSCs also appear to not express Germ line markers such as *Blimp1* and *Stella*. Sixth, their transcriptomic signature, as shown by microarray studies, is similar to the late epiblast but distinct from ESCs and ICM/early-epiblast cells, consistent with their origin. Lastly, when micro-injected in pre-implantation mouse embryos, EpiSCs are uncapable of colonizing the host and to yield chimeras, as opposed to ESCs (Brons et al., 2007; Tesar et al., 2007).

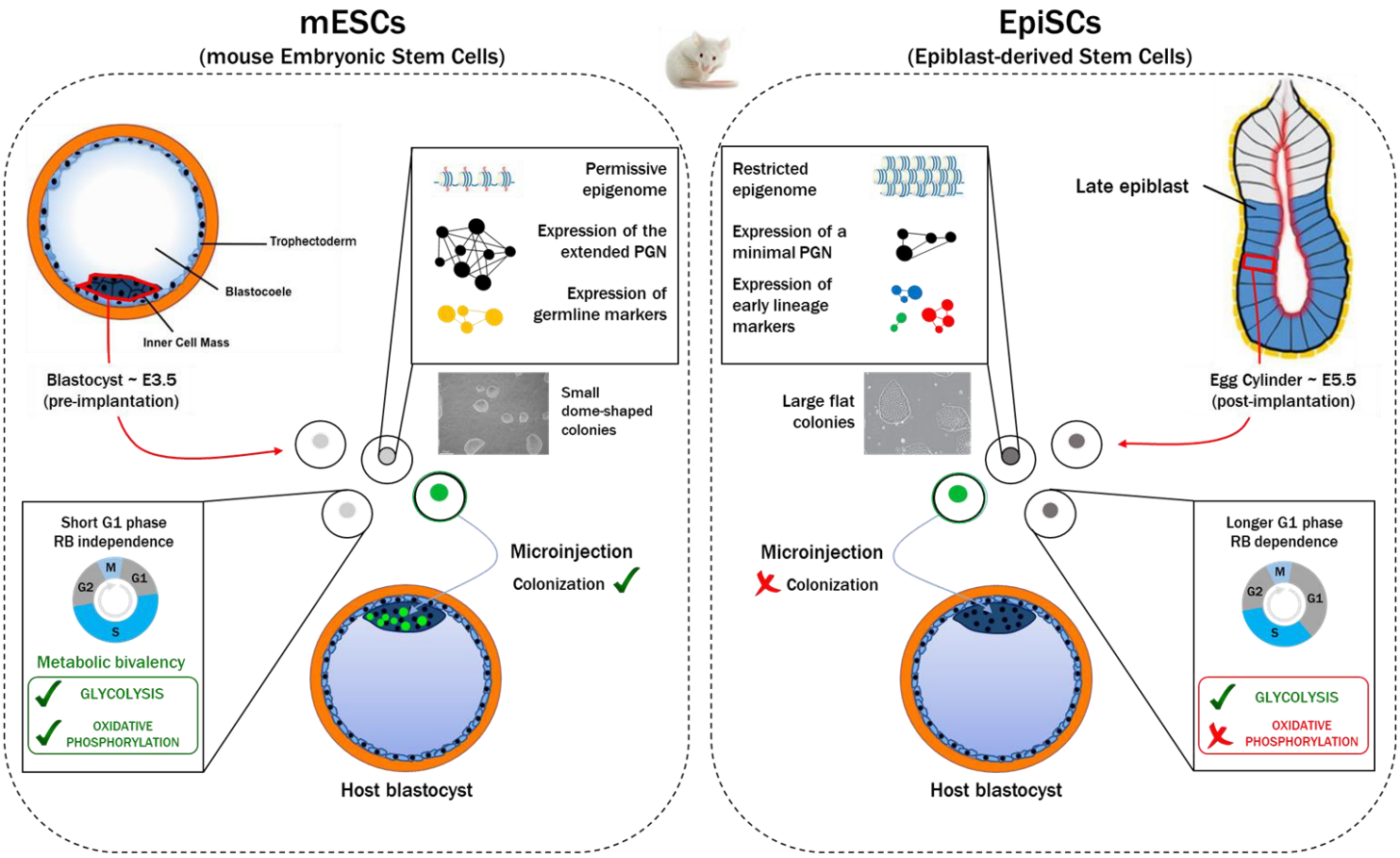

Figure 4. Discrepancies of mouse ESCs and EpiSCs.
Schematic of the main differences separating mouse Embryonic Stem Cells (mESCs, left panel) and Epiblast-Derived Stem Cells (EpiSCs, right panel). **PGN**: Pluripotency Gene Network ; **RB**: Retinoblastome.

b) Epigenetic landscape of ESCs and EpiSCs

Epigenome is defined by the accumulation of DNA and histones chemical modifications affecting the transcription of genes. These changes are of two main types: DNA methylation and histone modifications. DNA methylation plays a repressive role in gene transcription regulation, while histone modifications can be of two types, repressive or activating (Thiagarajan et al., 2014). During early development, global DNA demethylation occurs (Smith and Meissner, 2013), followed by selective *de novo* methylation. The early pluripotent epiblast is therefore characterized by a globally hypomethylated genome. Accordingly, ESCs exhibit low levels of DNA methylation, to the opposite of EpiSCs, derived from a later developmental stage (Takahashi et al., 2018). Histone modifications also differ sharply, particularly in enhancer sites, and also for genes that are expressed in both ESCs and EpiSCs. *Oct4*, for

example, is controlled by its distal enhancer (DE) in ESCs, and by its proximal enhancer (PE) in EpiSCs (Tesar et al., 2007). In the case of female cell lines, EpiSCs exhibit one inactive X chromosome, as shown by the presence of the H3K27me3 mark, unlike ESCs that display two active chromosomes. This is consistent with *in vivo* observations (mentioned in part **I/2.c)**) that female peri-implantation epiblast cells only show one active X chromosome versus two in pre-implantation epiblast.

Culturing ESCs in EpiSCs medium (*i.e.* with Activin and Fgf2) leads to their conversion in EpiSCs. The converse, however, is not possible without genetic modification or epigenetic reversion (Guo et al., 2009). Taken together, these observations suggest that a one-way epigenetic barrier exists between ESCs and EpiSCs, consistently with the latter being derived from a more developmentally advanced and more restricted tissue (Takahashi and Yamanaka, 2015).

c) Cell Cycle of ESCs and EpiSCs

ES cells have unusual proliferative capacities. They do not suffer contact inhibition, are anchorage-independent and never undergo cell-cycle arrest or quiescence in conventional culture conditions, suggesting they hold a unique regulation of cell-cycle (Burdon et al., 2002).

In somatic cells, proliferation is mainly controlled by the regulation of the G1 to S phase transition. This process is monitored by the phosphorylation status of the retinoblastoma protein (RB). During the G1 phase, RB is hypophosphorylated and sequesters the E2F family transcription factors, blocking entry into S phase. As G1 phase progresses, RB is sequentially phosphorylated by Cyclin/Cyclin-dependent-kinases (CDKs) tandems, Cyclin D/Cdk4 or Cyclin E/Cdk6, leading to the release of E2F that in turns allows expression of *Cyclin E*. The Cyclin E/Cdk2 complex subsequently finalizes RB phosphorylation, leading to complete release of E2F and entry into S phase (Harbour and Dean, 2000; Harbour et al., 1999). In addition to this RB/E2F pathway, the c-*Myc* gene has also been demonstrated to control the G1/S phase transition.

It has been shown that ES cells have an unusually short G1 phase of approximately 1h, and at the same time do not exhibit hypophosphorylated RB (Savatier et al., 2002). They are resistant to the Cyclin D/Cdk4-6 inhibitor p16ink4a, do not arrest in G1 phase at confluency (a process mediated by increasing hypophosphorylation of RB), and when triple knocked-out (TKO) for the RB family genes (*p107–/–, p130–/–, Rb–/–*), remain unaffected and carry on proliferating. These observations strongly suggest that ES cells escape from contact inhibition

and G1 checkpoint is at least in part due to shielding against RB regulating activity of the G1/S transition. Moreover, ES cells show low levels of Cyclin D1 and D3, and no Cyclin D2 at all. Cdk4 kinase activity is also undetectable. This reflects the state of pre-implantation epiblast cells, that also appear to have low amounts of D-type cyclins. Once gastrulation *in vivo* and differentiation *in vitro* start, however, D-type cyclins expression is strongly increased and Cdk4 kinase activity restored, showing that response to G1 regulatory control is recovered (Savatier et al., 1996).

When ESCs are converted in EpiSCs by treatment with FGF2 and Activin, the proportion of cells in G1 phase, monitored by FACS-sorting using a cell cycle phase-specific fluorescent system, drastically increases (from ~3% to ~25%) (Coronado et al., 2013). On the contrary, when conventional ESCs are transferred to 2i/LIF condition, only rare cells are found left to be in G1 phase. On the other hand, ESCs in G1 phase are more prone to differentiation, as evidenced by their response to Retinoic Acid (RA). When isolated from their population, ESCs in G1 submitted to a RA treatment form more mixed and differentiated colonies than their S and G2/M counterparts. This is also true, though to a lesser extent, for RA-untreated G1 cells, demonstrating that the G1 phase of the cell cycle is favorable to differentiation.

Thus, G1 phase lengthens as ES cells transit from 2i/LIF to Serum-BMP/LIF and Activin/Fgf2, demonstrating that ESCs and EpiSCs differ, in addition to their precedingly mentioned discrepancies, in their cell cycle and proliferation rate. This divergence, as the entirety of the properties of EpiSCs, suggest that they are more prone to differentiate than their ESCs counterparts, because G1 is the privileged phase for differentiation. This is consistent with their *in vivo* provenance of peri-implantation epiblast, poised to initiate gastrulation.

d) The Metabolic Switch of PSCs

Because ESCs are rapidly proliferating, energy must be balanced accordingly. Two modes of cellular energy production exist: glycolysis, yielding 2 molecules of ATP per molecule of glucose, and oxidative phosphorylation (OXPHOS), yielding ~38 molecules of ATP per molecule of glucose (Zhang et al., 2012). In conventional conditions, ESCs are able to use both OXPHOS and glycolysis metabolic pathways, though relying mostly on OXPHOS, more cost-effective, for faster proliferation. This ability is referred to as metabolic bivalency. As they shift toward differentiation or are converted into EpiSCs though, ESCs gradually lose their bivalency to rely exclusively on glycolysis. This phenomenon is termed metabolic switch, and is consistent with the lengthening of G1 phase observed between ESCs and EpiSCs and the associated difference in proliferation speed. Interestingly, forcing expression of the hypoxia-

inducible factor 1α (HIF1α) in conventional ESCs leads to their conversion in cells morphologically and metabolically similar to EpiSCs, with notably a drastic downregulation of ESCs marker *Esrrb* (Zhou et al., 2012). This suggest that the metabolic mode is not only a consequence to ESCs and EpiSCs respective states, but also an intrinsic driver of such states.

e) The Naïve, the Formative and the Primed

ESCs and EpiSCs are equivalent in their differentiation potential (*i.e.* pluripotent) but, as developed above, they also exhibit a considerable number of differences. This suggests that they are not strictly in the same state, but rather in two distinct states of pluripotency. ESCs epitomize the pre-implantation epiblast *in vivo*, a tissue of unbiased potential, of uncondensed, opened to transcription chromatin. EpiSCs on the other hand, epitomize the peri-implantation epiblast, poised to gastrulate and, as a matter of fact, already expressing differentiation factors (*I.g. Fgf5*, *Eomes, Brachyury, Gata6* and *FoxA2*). Consistently with their tissue of origin, EpiSCs are of reduced plasticity compared to ESCs, and biased in their differentiation potential. This led to name the pluripotent states associated to ESCs and EpiSCs respectively “Naïve” and “Primed” (Nichols and Smith, 2009).

Embryonic development is progressive, and tissues *in vivo* gradually change identity. For this reason, it is unlikely that pluripotency behaves as a binary switch from naïve to primed. Naïve cells (ESCs) are derived from the mouse embryo between E3.75 and 4.75, while primed cells (EpiSCs) are obtained between E6.0-6.5 and further. In between, pluripotency is neither naïve nor primed as precedingly defined. During 24 to 30h post-implantation, epiblast cells expand and stop expressing naïve markers, however, global gene expression analysis shows that they diverge from both the naïve pre-implantation epiblast and the gastrulating post-implantation epiblast (Smith, 2017).

Consistent with this observation, several pluripotency states have been captured *in vitro* that can be qualified of intermediates between naïve and primed. 2i/LIF ESCs passed in Activin/FGF with fibronectin and 1% of KnockOut Serum (KOSR) for instance, start to downregulate naïve markers after 2 days, such as *Stella*, *Klf4* and *Rex1*, but yet do not overexpress early lineage markers such as *Brachyury*, *FoxA2* or *Sox1*. These cells were named Epiblast-Like Cells (EpiLCs), and represent a pluripotent state just prior to gastrulation *in vivo*, slightly ahead of the primed state. Interestingly, EpiLCs hold the capacity, when exposed to BMP4**,** to differentiate into Primordial Germ Cells-Like Cells (PGCLCs) (Hayashi et al., 2011; Ohinata et al., 2009).

EpiLCs, though short-lived and heterogeneous, hold characteristics consistent with the existence of a conceptual phase of development and pluripotent state named “Formative” (Smith, 2017). This state corresponds to the period of time observed *in vitro*, where naïve cells subjected to differentiating cues are not immediately responsive and need to exit their naïve status first. During this time, a transient population appears able to differentiate into PGCLCs. The formative state is thus defined by both the ability to give rise to PGCLCs, and a transcriptional signature in between ESCs and EpiSCs, where naïve markers are shut down but early differentiation markers are not yet expressed (Kinoshita and Smith, 2018; Kinoshita et al., 2021). *In vivo*, such a population exists transiently between E5.5 and E6.75 (Ohinata et al., 2009).

Another intermediate state can be captured from the combination of both Activin and Fgf2 to one of the 2i inhibitors of the 2i/LIF condition, CHIR. These intermediate Pluripotent Stem Cells (INTPSCs) have, as their name judiciously suggests, mixed naïve and primed characteristics (Tsukiyama and Ohinata, 2014). INTPSCs conserve expression of some naïve markers (*e.g*. *Rex1*, *Esrrb* and *Klf4*), retain a naïve morphology of tight dome-shaped colonies, have two active X chromosomes in female lines and remain able to colonize a pre-implantation blastocyst. However, they also exhibit primed characteristics, though to a lesser extent than EpiSCs, such as increased expression of peri-implantation epiblast markers (*e.g Otx2* or *Fgf5*) (Morgani et al., 2017). Compared to EpiLCs, INTPSCs do not epitomize the formative state as precedingly defined, but are rather slightly upstream, between naïve and formative.

EpiLCs, INTPSCs and *in vivo* observations illustrate the gradually changing nature of development, and demonstrate that, accordingly, pluripotency is not a coin with two sides. The naïve and primed states are rather the endpoints of a continuum, starting with epiblast establishment and ending with gastrulation (**Figure 5**).

f) Refining Culture Conditions

f.1. The Ground State, Holy Grail of Pluripotency

In conventional culture conditions, ESCs exhibit important transcriptional heterogeneity, showing subpopulations with signature of pre-implantation epiblast, endoderm or peri-implantation epiblast. If such populations are isolated and cultured *de novo* in conventional Serum/LIF conditions, heterogeneity of the initial population is soon restored, demonstrating that these subpopulations are not representing stable fractions of cells, but rather a dynamic landscape of interconverting states. One explanation to this phenomenon is

the endogenous secretion of contradictory signals by conventional ESCs: LIF, that sustains self-renewal, and FGF, that promotes differentiation. In conventional conditions (*i.e.* Serum/LIF), the exogenous supplementation of LIF allows most cells to ultimately balance toward self-renewal, but does not prevent a part of the population to be on the edge of differentiation (Morgani et al., 2017). In the 2i/LIF condition, FGF pro-differentiating effect is countered by direct inhibition of the MAPK/MEK pathway through use of PD0032. This inhibition of differentiation is, in parallel, reinforced by GSK3 inhibition with CHIR99021 (Ying et al., 2008).

2i/LIF ESCs, unlike their conventional counterparts, are widely homogenous in their transcriptomic signature and functional capacity of chimeric formation. For this reason, they are considered as "true" naïve cells, representing more accurately pre-implantation epiblast cells than conventional ESCs. This *in vitro* captured state was named "ground state" of pluripotency, the pinnacle of the pluripotency spectrum. Rather than a different state *per se*, the ground state is a homogenous naïve state, devoid of any intermediate subpopulations and differentiation bias, corresponding to the *tabula rasa* of development *in vivo*.

f.2. WiEpiSCs

EpiSCs cultured in Activin/Fgf2 express high levels of germ layers markers, and have a high propensity to spontaneous differentiation. This differentiation, largely stochastic, is a source of heterogeneity in EpiSCs. While Activin and Fgf2 alone sustain self-renewal in the primed state, it was shown that combined with BMP and Wnt, they collaborate to promote epithelial-to-mesenchymal transition (EMT). Wnt, downstream of BMP, is also required for mesodermal differentiation (Huelsken et al., 2000; Liu et al., 1999). Blocking the Wnt pathway with inhibitors (such as XAV939, IWP2 and IWR1), or by genetically knocking down β-catenin, consistently leads to a more homogenous primed state. Such cells, named Wnt-inhibited EpiSCs (WiEpiSCs), are more permissive to clonal expansion in single cells and easier to derive (Kurek et al., 2015). They express reduced levels of mesodermal and endodermal markers, and increased levels of pluripotency markers compared to conventional EpiSCs. Because of their enhanced quality and homogeneity, WiEpiSCs are sometimes considered as representative of the "ground state" of primed pluripotency (Kim et al., 2013; Sumi et al., 2013; Tsakiridis et al., 2014; Wu et al., 2015).

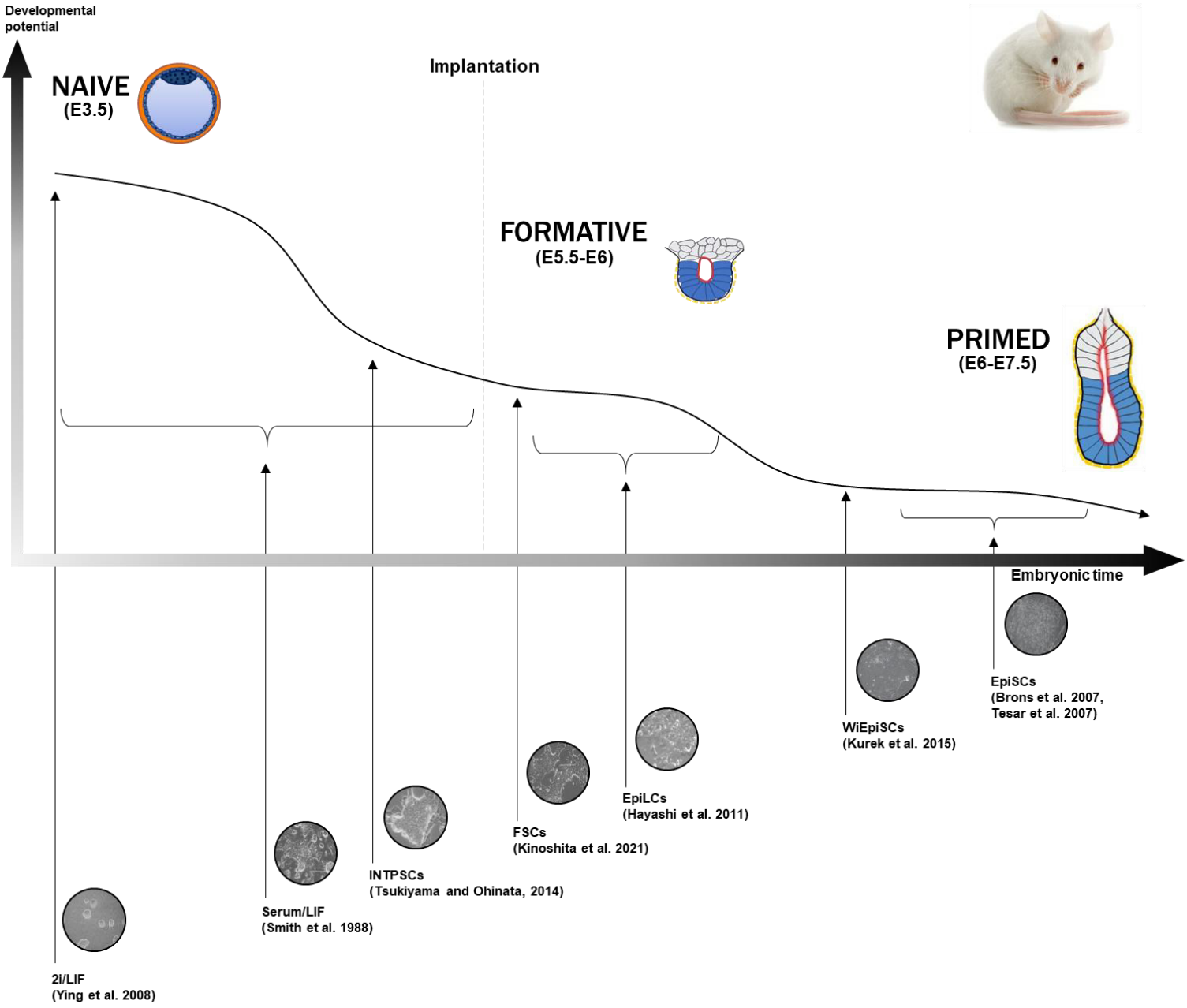

Figure 5. The different types of mouse PSCs and their *in vivo* equivalent – the pluripotency continuum.

Schematic showing the main types of mouse pluripotent stem cells and their relative position along the mouse early embryonic development timeline (x axis) and pluripotency continuum (y axis) passing from the naive through formative to primed states.

g) The Pluripotency Gene Network

Pluripotency is regulated at two levels: 1) Extrinsic signals, 2) intrinsic signals originating from a regulatory gene network. Those two layers of regulation are context-dependent, vary depending on the pluripotent state of the cell, and mainly rely on the action of transcription factors (TFs).

TFs are proteins that recognize and bind DNA sequences to either activate or repress their transcription. They can bind promoter-proximal DNA regions or more distal elements that can be from several tens of bases to hundreds of kilobases away. Enhancers, the elements involved in positive gene regulation, are bound by multiple TFs that can recruit both the transcription machinery, and chromatin regulators/ remodelers in order to allow access to promoter regions. In ESCs, as mentioned earlier, the OSN (Oct4, Sox2, Nanog) TFs are considered as the core triad of pluripotency, because their simultaneous expression is characteristic of pluripotency both *in vivo* and *in vitro* (Avilion et al., 2003; Masui et al., 2007; Mitsui et al., 2003; Nichols et al., 1998; Silva et al., 2009). OSN are the centerpieces of a regulatory circuitry governing pluripotency and behave so in two manners: One, by cooperating to positively regulate their own promoters; Two, by co-occupying genes, simultaneously repressing expression of those involved in lineage commitment and activating those involved in the maintenance of self-renewal (Young, 2011).

At the top of the pluripotency regulation system are extrinsic signals, *i.e.* LIF, Bmp4, Wnt, FGF and Activin, as detailed precedingly. Stat3, β-catenin and Smad1, the downstream effectors of LIF, Wnt and Bmp4, overlap with most part of OSN binding sites, thus coupling extrinsic signals with the intrinsic regulatory gene circuitry. This is the first level of pluripotency regulation.

Once OSN expression is established and maintained, forming the core of the Pluripotency Gene Network (hereafter PGN), naïve ESCs then express an “ancillary” set of genes, such as *Rex1, Esrrb, Klf4, Tbx3* and *Tfcp2l1,* that constitute the second layer of pluripotency regulation (**Figure 6**). Unlike OSN, these factors are individually dispensable for pluripotency establishment and maintenance, but they globally reinforce and stabilize the network to shield it against pro-differentiating cues. This extended PGN, much like OSN, is self-promoting through positive feedback loops, and its components stabilize each other’s expression (Festuccia et al., 2012; Hackett and Azim Surani, 2014; S.J. Dunn and G. Martello, B. Yordanov, S. Emott, 2014). In conventional ESCs populations, components of the extended PGN are heterogeneously expressed, stochastically on or off at the single-cell level. This is consistent with the heterogenous nature of such populations and the propensity of individual

cells to metastably shift close to the primed state (Chambers et al., 2007; Martello et al., 2012; Toyooka et al., 2008; Yamaji et al., 2013). This shift is at least in part due to the fact that, without GSK3 inhibition by CHIRON, conventional ESCs express the TCF3 factor that antagonizes OSN and destabilizes the network. With addition of 2i in the ground state condition, TCF3 expression is inhibited and the network is stabilized, heterogeneity is thus suppressed and ancillary factors expressed at high and stable levels in most cells (Wray et al., 2011). Though most members of the extended network are upregulated in 2i/LIF compared to Serum/LIF, some have a particularly higher expression in the former, such as *Tfcp2l1* and *Rex1*, and seem to play a critical role in the maintenance of the naïve state. *Tfcp2l1* alone, for instance, can drive EpiSCs to reprogram in the naïve state when overexpressed (Grabole et al., 2013; Martello et al., 2013).

Accordingly with the rest of their characteristics, the regulatory gene circuitry of ESCs and EpiSCs largely differs. Though EpiSCs express *Oct4* and *Sox2* to a comparable level to ESCs, *Oct4* expression in EpiSCs is controlled by its proximal enhancer, as mentioned in part **I/3.b)**. In the primed state, *Nanog* expression is also attenuated. In addition to these nuances in OSN expression, EpiSCs also and foremost do not express, or to very reduced levels, most of the extended pluripotency network. On the contrary, they do express lineage-associated factors and other TFs, such as *Otx2*, *Zic2, Zfp281, Zscan10*, and *Oct6*, not expressed in neither ground state nor conventional ESCs.

Interestingly, when ESCs are converted to EpiLCs (Fgf/Activin/Fibronectin/1% KOSR), Oct4 occupancy is drastically changed from genes associated with naïve pluripotency (*Klf4, Tbx3, Prdm14*) to post implantation epiblast/primed pluripotency-associated genes (*Fgf5, Oct6, Wnt8a*). This phenomenon goes along with a global transformation of the chromatin landscape. Oct4 also changes TFs interactors, switching from Esrrb and Klf4/5 (in addition to Sox2 and Nanog) to Otx2 and Zic2/3. The newly formed Oct4/Otx2 tandem has been shown to bind, in this context, previously inaccessible chromatin domains, triggering the expression of primed-associated genes (Buecker et al., 2014). This suggests that, as for naïve cells, primed cells express their own ancillary factors forming an extended primed pluripotency network.

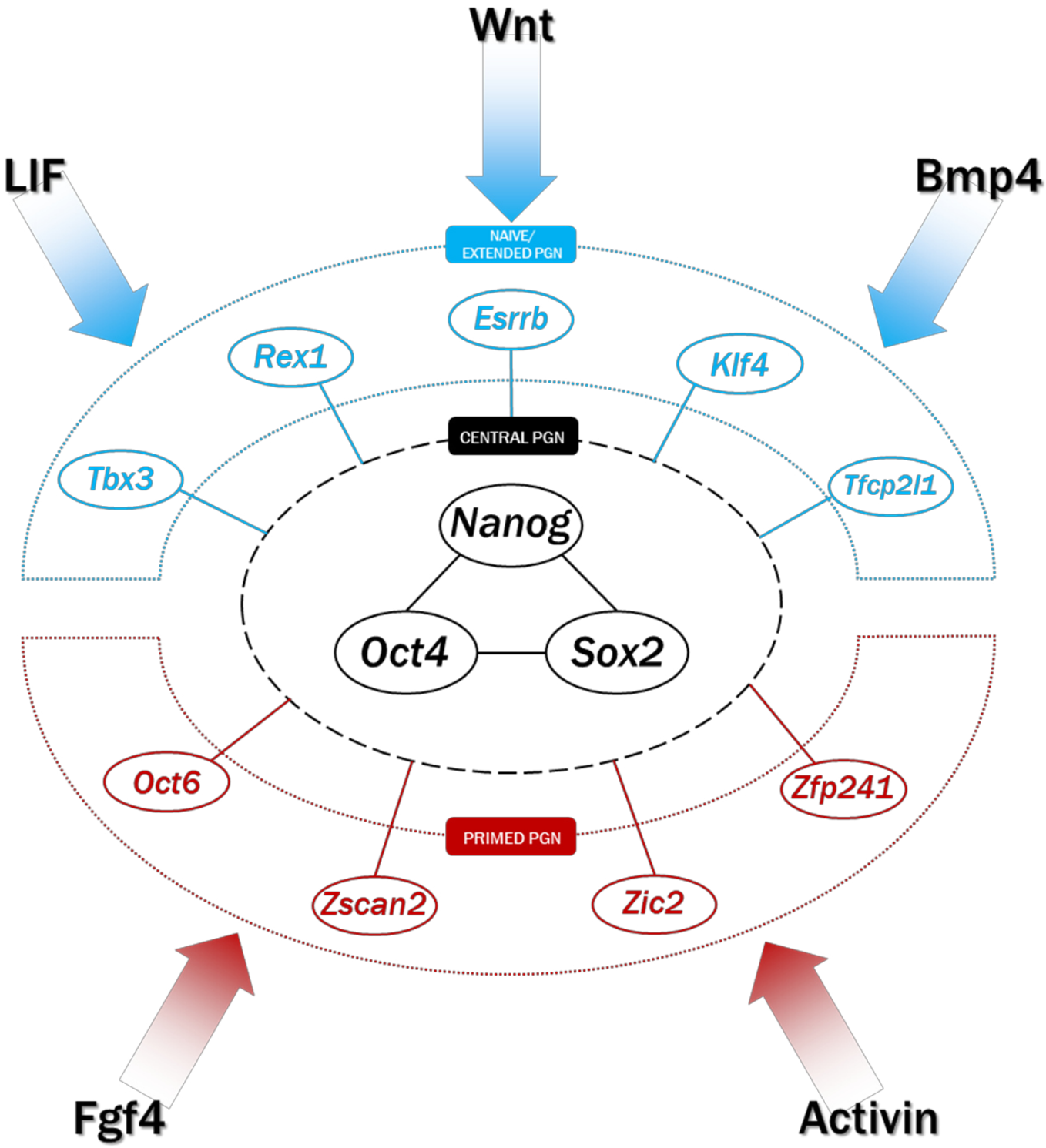

Figure 6. The mouse pluripotency gene network.
Schematic of the transcription factors genes network governing mouse primed, naive and central pluripotency. Arrows represent external cues postively regulating the networks.

II/ Pluripotency in Primates.

1. Human Embryonic Stem Cells (hESCs)

In 1998, ES cell lines were derived for the first time from human blastocysts (Thomson, 1998). These cells (hereafter named hESCs), although derived from the ICM like mouse ES cells (hereafter mESCs), do not share the same characteristics, however (Weinberger et al., 2016). First, they are not responsive to LIF, and need to be cultured in primed conditions instead (*I.e.* FGF/Activin A) to self-renew. In addition, hESCs lose pluripotency upon MEK-ERK inhibition in conventional conditions (Dahéron et al., 2004). Second, they have a primed morphology of flat, monolayered colonies and need to be passaged by mechanical dissociation. Third, most of the extended pluripotency network/naïve pluripotency network as defined in mouse is not expressed in hESCs (Chia et al., 2010). Fourth, hESCs epigenome differs largely with that of mESCs, with H3K27 histone repressive marks being appended to developmental genes and hESCs exhibiting one inactivated X chromosome (Xi) in female cell lines, like EpiSCs but unlike mESCs (Silva et al., 2008).

Thus, hESCs differ greatly from mESCs; however, they do not have all the primed characteristics from a mouse standard. They do not, for instance, express some of the classical EpiSCs markers such as *FGF5* or *CDH2*; but they do express some of the naïve markers such as *PRDM14* and *REX1* (Chia et al., 2010). hESCs genome methylation is also closer to that of conventional mESCs (although distinct from ground state mESCs) than to EpiSCs (Hackett et al., 2013; Shipony et al., 2014), and hESCs exhibit both a nuclear and cytoplasmic localization of the TFE3 factor, located either in one or the other in mouse ground state and primed conditions, respectively (Betschinger et al., 2013).

The question then arises of why hESCs diverge so much in their characteristics from mESCs. Although some similarities of hESCs with EpiSCs are striking, hESCs have a somewhat different phenotype, revealing a potential intermediate state between primed and naïve. However, it is worth reminding that both of these states have been discovered and characterized in mouse. A critical question thus arises: does the naïve state as defined in mouse exist in humans, and more generally, in primates? Answering this question requires a stricter definition of naïve pluripotency.

In mouse, the naïve state can be defined on the basis of either the functional (*i.e.* chimeric competency), molecular (reliance on cytokines and growth factors) or genetic (expression of the extended pluripotency network) characteristics of ground state ESCs. However, the primed and naïve pluripotent states are also and foremost defined by their tissue

of origin *in vivo*, *i.e.* the post- and pre-implantation epiblast, respectively. Defining naïve pluripotency in primates can thus not be extrapolated from either functional, molecular or genetic characteristics of mouse cells, but reclaims to define the identity of the primates' pre-implantation epiblast, and understand in what measure it diverges from that of the mouse.

2. The naïve state of primates' pluripotency *in vivo*

a) Early embryonic development of the mouse and primates

In 1994, Denis Duboule suggested the model of the "Developmental hourglass", based on the observation that all vertebrate species diverge in the earliest and latest stages of their embryonic development, but share more common characteristics during the mid-embryonic period, also called phylotypic (Duboule, 1994; Hanken and Carl, 1996). The phylotypic period starts when the common anatomical features of the basic body plan of a given phylum are established. In the particular case of mammals, this period starts after gastrulation, when neurulation, establishment of the antero-posterior axis and appearance of the mesodermal somites occur. In mouse, this period lies between E7.5 and E8.0, and is concomitant with the differentiation of the last pool of epiblast cells. In primates, and more specifically humans, it extends from E15 to E20, between the beginning of gastrulation and formation of the notochord (**Figure 7**) (Irie and Kuratani, 2014; Shahbazi and Zernicka-Goetz, 2018). According to the developmental hourglass model, important divergence in primates' and mouse embryogenesis before gastrulation should thus exist. This is proven correct in several aspects of development.

The first, maybe most obvious difference is that of timing. Mouse embryonic development lasts for 19 days, while human's extends to 9 months. This difference of duration is not only reflected by the final number of cells composing the individual, but also by a difference in their proliferation rate. Indeed, mouse late blastocysts (E4.5) consist of ~150 cells, which reflects a cell cycle comprised between 14 and 15h (Plusa et al., 2008) while at the same stage (E7), human blastocysts are formed of ~250 cells, reflecting a cell cycle of ~21h (Niakan and Eggan, 2013). In mouse, the rapid proliferation rate of ICM and early epiblast cells is due to a high expression of *Cdk2*, promoting a fast G1 to S-phase transition. High *CDK2* is not observed in human or marmoset ICM and early epiblast cells. Moreover, the key G2/M checkpoint kinase *WEE1* is highly expressed, exemplifying a different behavior in cell cycle regulation (Blakeley et al., 2015; Boroviak et al., 2015; Yan et al., 2013).

Another critical difference is that of structural organization upon implantation. At E5, the mouse embryo attaches to the endometrium and epiblast cells form a rosette-like structure,

embedded in between TE and PE. That rosette subsequently invaginates to form a cup-shaped structure called the egg-cylinder, conserved until the beginning of gastrulation at E7.5 (Shahbazi and Zernicka-Goetz, 2018). In primates the blastocyst, once implanted, forms a bilaminar embryonic disc composed of an apical layer of epiblast cells and a basal layer of visceral endoderm. At this stage compared to the mouse embryo, one more extra-embryonic tissue appears, the amniotic epithelium, only initiated upon gastrulation in rodents (**Figure 7**) (Boroviak and Nichols, 2017).

The third important difference between primates and rodents early embryogenesis is embryonic diapause. This process, also known as discontinuous development, is characterized in mammals by a delayed implantation when environmental conditions are unfavorable to postnatal development (Lopes et al., 2004). In eutherian mammals, it occurs at the blastocyst stage, where the embryo hatches from the zona pellucida and then remains in a so-called “dormant state”, *i.e.*, retains its full developmental potential but is under proliferation arrest. Embryonic diapause has been widely described in a number of placental species, including rodents, but has not yet been depicted in primates (Ptak et al., 2012).

In mouse, delayed blastocysts have been shown to be able to stay dormant for several weeks, and keep the ability to resume development afterwards in response to estrogens. Though mESCs can be derived from normal and diapaused embryos alike, the first mESCs lines derived were from diapaused embryos (Evans and Kaufman, 1981), and this appears to generally be a facilitating factor of derivation (Brook and Gardner, 1997). Embryonic diapause has been linked in mouse to LIF/gp130 signaling, c-Myc and mTOR activity (Bulut-Karslioglu et al., 2016; Nichols et al., 2001; Scognamiglio et al., 2016). Although the precise mechanisms underlying this phenomenon’s regulation are still poorly understood, the correlation with mESCs derivation efficiency and pluripotency-associated pathways raises the question of a link between this process and the naïve state *per se* in mouse. Whether the molecular tooling of embryonic diapause remains in primates, despite it not being used *in vivo*, and whether this absence can be correlated with difficulties to capture the naïve state remains to be elucidated.

In addition to these three major differences, Zygotic Genome Activation (ZGA) also occurs at different timings in mouse and primates, at the 2-cell stage in the former, and between the 4- and 8-cell stage in the latter (Blakeley et al., 2015) and mechanisms of X chromosome dosage compensation, process by which male and female cells conserve an equivalent number of X chromosome transcripts, also appear to differ (Petropoulos et al., 2016). Taken altogether, these differences could explain a divergence between mouse and primates pluripotency regulation, and thus, differences between hESCs and mESCs. However, the question of the proximity between hESCs and the pluripotent human pre-implantation

epiblast remains. More generally, the question is: how is the primates' naïve state defined *in vivo*?

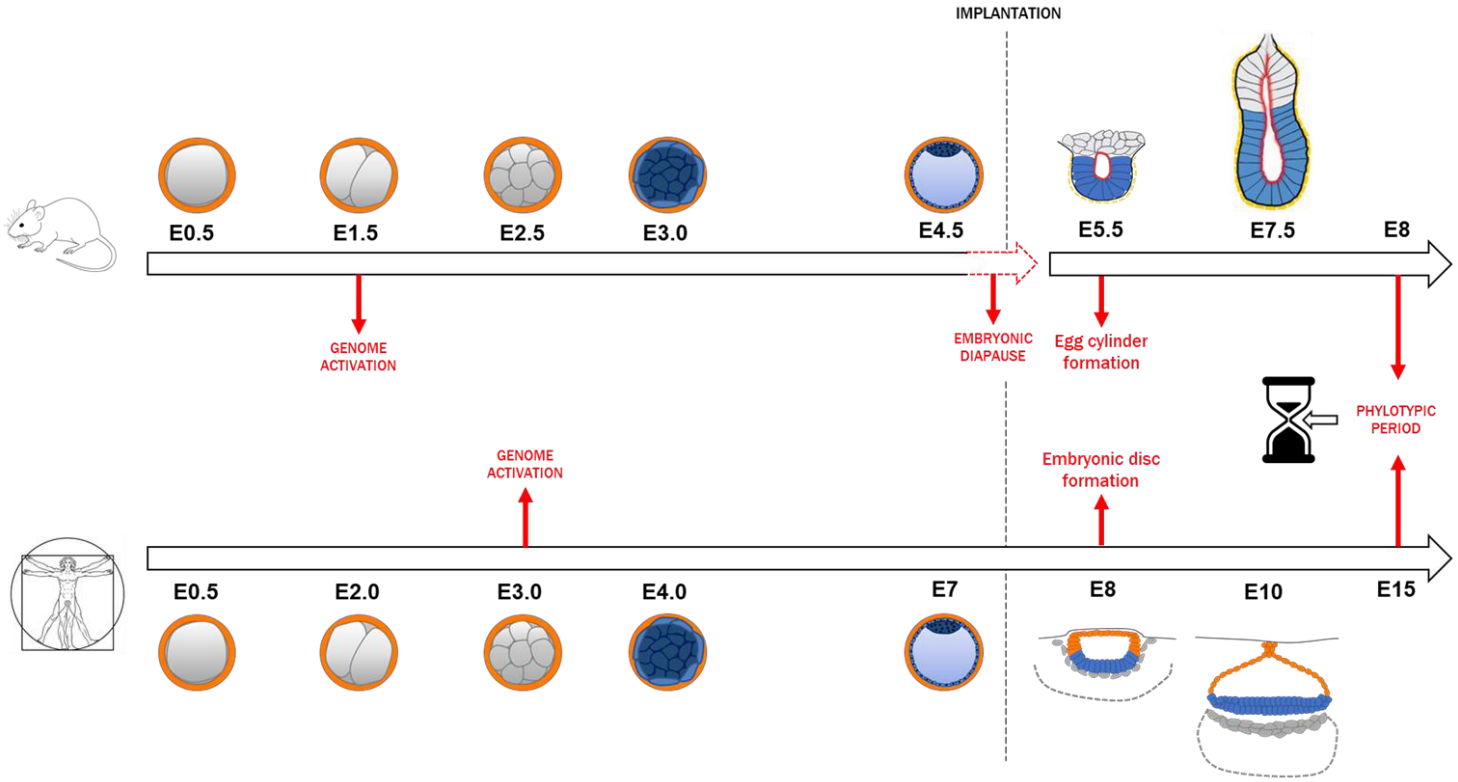

Figure 7. Early embryonic development of the mouse and human.
Schematic comparing pre- and peri-implantation timelines of mouse and human embryonic development until the beginning of the phylotypic period. Red arrows indicate key differences between the two models.

b) The hallmarks of the naïve primates' epiblast

In part I/3., we depicted the differences existing between mouse ESCs and EpiSCs, *i.e.* the naïve and primed pluripotent states *in vitro.* These differences reflect the identity of pre-implantation epiblast versus its post-implantation counterpart *in vivo*, and characteristics of the former define the hallmarks of naïve pluripotency in mouse. Such hallmarks are not yet entirely unraveled in primates, but are under active investigation and so far revealed at least eight

features, based on the identity of human and non-human primates' pre-implantation epiblast. These include ERK independence, apolarity, DNA hypomethylation and X chromosome activation, all of which are common with the mouse. Three features are specific to primates: the expression of a primates' specific naïve network, a primates' specific naïve transposable elements (TEs) signature, and the ability to differentiate into amniotic epithelial cells (**Figure 8**) (Boroviak and Nichols, 2017).

b.1 ERK independence

In mouse, the FGF/ERK pathway is a critical inducer of differentiation and in the blastocyst, PE specification is mainly controlled by FGF paracrine secretion (cf. part **I/1.b**))(Burdon et al., 1999) (Arman al., 1998; Chazaud et al., 2006; Feldman et al., 1995; Kang et al. 2013). When mouse cells shift from naïve to primed pluripotency, *i.e.* are converted into EpiSCs, they necessitate FGF for self-renewal. Similarly, hESCs, that closely resemble EpiSCs, rely on FGF signaling to self-renew. In primates' blastocyst, though additional signals are involved, FGF is as for mouse implied in PE specification. It was also shown for both human and marmoset that high *NANOG* expression could be maintained without FGF, showing independency to this pathway for self-renewal (Boroviak et al., 2015; Roode et al., 2012).

b.2 Apolarity

When grown in vitro, mESCs form small, tightly packed dome-shaped colonies. In conventional serum/LIF conditions, this morphology is heterogeneously distributed, but when cells are cultured in ground state 2i/LIF culture conditions, *i.e.* homogeneously naïve, this becomes the only morphology. Colonies of cells in primed conditions, on the other hand, adopt a flat, monolayered morphology. This difference between primed and naïve cells is attributed, at least in part, to polarity. *In vivo*, between the 16- and 32-cell stages of the morula, polarity is established in outer blastomeres and drives differentiation into TE. Inner cells on the contrary remain apolar, a characteristic critical to their adoption of a pluripotent identity (Anani et al. 2014, Boroviak and Nichols 2014). At the blastocyst stage, the pluripotent epiblast conserves an apolar status, while both PE and TE are polarized epithelia (Bedzhov and Zernicka-Goetz, 2014; Enders et al., 1986; Plusa et al., 2005). This changes only upon implantation, when Epi cells arrange in a rosette-like structure, form extensive adherens junctions and concentrate their organelles at apical ends (Bedzhov and Zernicka-Goetz, 2014; Enders et al., 1986). The apolar and polar status of pre- and post-implantation epiblast, respectively, is conserved in

primates. *In vitro*, EpiSCs and hESCs harbor ultrastructural characteristics of the post-implantation epiblast such as apical microvilli and tight junctions (Brons et al., 2007; Krtolica et al., 2007; Sathananthan et al., 2002; Tesar et al., 2007). Therefore, naïve primates' cells, in accordance with *in vivo* observations, should be apolar and recapitulate *in vitro* the dome-shaped morphology of 2i/LIF mESCs.

b.3 DNA Hypomethylation

During germline differentiation and pre-implantation development, the genome of both primates' and mouse undergo massive hypomethylation, allowing enhanced access to gene promoters for transcription (Seisenberger et al., 2013a,b). In the pre-implantation epiblast, genome-wide hypomethylation is observed, to the only exception of imprinted regions, and progressive methylation proceeds upon implantation until gastrulation (Guo et al., 2014; Smallwood et al., 2011; Smith et al., 2014, 2012). In mouse, this process is retrieved *in vitro* with mESCs in 2i/LIF, but not serum/LIF condition, while EpiSCs show higher levels of methylation, consistent with their tissue of origin. Accordingly, hESCs show high levels of methylation, in discordance with the hypomethylated human ICM and early epiblast. In both rodents and primates therefore, hypomethylation is a hallmark of naïve pluripotency *in vivo*.

b.4 X Chromosome Activation

In most mammalian species, including rodents and primates, random X chromosome inactivation (XCI) occurs in female cells to compensate for X-linked gene expression (Escamilla-Del-Arenal et al., 2011). In mouse, the paternal X chromosome is silenced at the 4-cell stage and transiently reactivated in the epiblast, concomitantly with naïve pluripotency establishment. Once the embryo implants, XCI occurs in the post-implantation epiblast as pluripotent cells transit from naïve to primed. Such a phenomenon is also observed in primates embryo (Dupont and Gribnau, 2013; Petropoulos et al., 2016), making dual activation of X chromosomes a mark of pre-implantation epiblast cells and thus, naïve pluripotency in both primates and rodents.

b.5 Primate-specific naïve network

Numerous single-cell RNA sequencing analyses (Blakeley et al., 2015; Boroviak et al., 2015; Liu et al., 2018; Nakamura et al., 2016; Petropoulos et al., 2016; Xue et al., 2013; Yan

et al., 2013) showed that primates (cynomolgus monkey, rhesus monkey, marmoset and human) and rodents epiblasts share common components of the pluripotency network. In addition to the core OSN triumvirate, some members of the extended network such as *KLF4*, *TFCP2L1*, *SALL4, TBX3* and *TDGF1* are expressed in primates. However, critical components of the mouse network are absent, namely *KLF2, ESRRB, BMP4, NR0B1* and *FBXO15*. It is becoming increasingly clear that primates indeed express their own extended, naïve-specific pluripotency network, though the exact nature and regulation of this network is still under investigation. Several members have been yet identified, notably *KLF17* (Guo et al., 2016), the activator protein-2 (AP2) transcription factor C (*TFAP2C*) (Pastor et al., 2018), *ARGFX*, and several members of the TGF-β signaling pathway, including *NODAL, GDF3, TGFBR1, LEFTY1, SMAD2, SMAD4* and *TDGF1* (see part **II/2.c**)) (Blakeley et al., 2015; Boroviak et al., 2015; Nakamura et al., 2016; Petropoulos et al., 2016).

b.6 *OCT4* expression control

In mouse, differential enhancer control of *Oct4* expression is a clear distinction between the primed and naïve states (cf part **I**/). Primed cells indeed rely on the proximal enhancer (PE) to express *Oct4* while naïve cells rely on the distal enhancer (DE) both of which are located upstream of the *Oct4* gene. In primates, pre-implantation blastocysts, both PE and DE are, surprisingly, inaccessible to the transcription machinery. However, two enhancers are located downstream of the *OCT4* transcription termination site. When these sequences are ablated in primed hESCs, normal *OCT4* expression is maintained, but if so is done in naïve-like reprogrammed hESCs (See part **II/3.b)**, *OCT4* expression is dramatically decreased (Pastor et al., 2018). The naïve primate marker *TFAP2C* appears to be the main activator of these downstream enhancers, confirming that they are naïve-specific regulators to the naïve state. Therefore, while upstream distal enhancer control of *OCT4* expression is not, contrary to what is observed in mouse, a discriminating hallmark of naïve pluripotency in primates, *OCT4* yet has a differential regulation in the primed and naïve states.

b.7 Primate-specific “transpocriptome”

Transposable elements (TEs) (or “jumping genes”) are DNA sequences able to change location within the genome through duplication or excision processes. In mammalian species, TEs count for approximately half of the genome and play a critical role in several biological processes such as transcriptional modulation, coding and long non-coding RNA metabolism

or germline and soma mutagenesis (Bourque et al., 2018). In 2015, Göke and colleagues investigated the function of endogenous retroviruses (ERVs), a subclass of TEs, based on the observation that hESCs express genes from active ERVs, and that ERVs are, in mouse, indicators of totipotency. It was found that ERVs are systematically transcribed in the human pre-implantation embryo, and that the long terminal repeats (LTRs) flanking ERVs can be used as stage-specific markers. More specifically, the LTR7- class of HERVHs are only expressed in *NANOG*-positive, *i.e.* naïve pre-implantation epiblast cells, along with members of the HERVK class (Göke et al., 2015). Therefore, *in vivo* naïve pluripotency of primates is characterized by a specific "transposcriptomic" (TEs transcriptome) signature, which is likely, however, to be species-specific.

b.8 Extra-embryonic potential

As mentioned precedingly, primates epiblast undergoes differentiation into amniotic epithelium before gastrulation, a major difference to mouse development (Boroviak and Nichols, 2017). This means that, theoretically, naïve primate cells should retain the capacity to differentiate into amniotic epithelial cells. However, the pathways governing this process are yet unknown, and the precise transcriptomic and epigenetic identity of the amniotic epithelium is still largely unraveled.

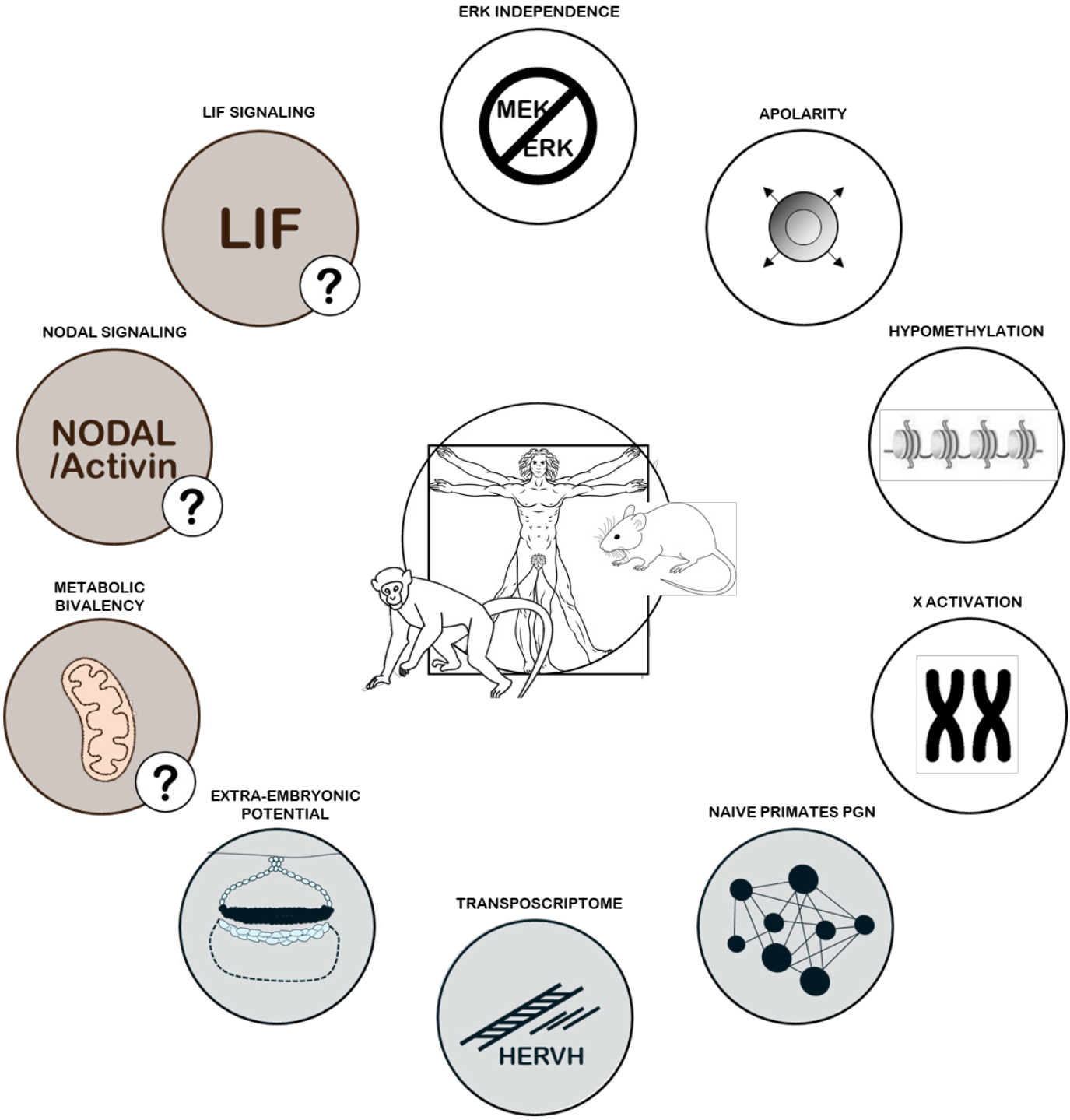

Figure 8. Hallmarks of naïve epiblast cells in mouse and primates.

Schematic of the main features of the mouse and primates naïve epiblast cells. White circles show common features of mouse and primates, light blue, primates specific features. Orange circles represent naïve characteristics demonstrated for the mouse, but not primates *in vivo.*

c) Questioning Hallmarks

c.1 Metabolism

As mentioned in part I, metabolism is a discriminating aspect of pluripotency in mouse. While mESCs are metabolically bivalent, *i.e.* able to switch from glycolysis to OXPHOS and *vice-versa*, EpiSCs exclusively rely on glycolysis. Although this distinction is very clear *in vitro*, the *in vivo*, complex embryonic microenvironment is not yet fully recapitulated by any culture conditions, and oxygen consumption rate as well as metabolites accumulation measurements are challenging to perform *in vivo*. The metabolic bivalency observed for mouse *in vitro* has been described in hESCs reprogrammed to naïve-like pluripotency (Wu and Belmonte, 2015a) (see part **II/3.b)**), however, this is not observed in all naïve-like reprogrammed hESCs, and does not result from a *in vivo* observation, therefore remaining as a questionable hallmark of the naïve primates epiblast.

c.2 NODAL/TGF-β signaling

Among the primate-specific pre-implantation epiblast genes, several are members of the NODAL/TGF-β signaling pathway (*NODAL, GDF3, TGFBR1, LEFTY1, SMAD2, SMAD4* and *TDGF1),* suggesting a critical role in naïve pluripotency identity. Interestingly, culture of human pre-implantation embryos with the NODAL/TGF-β inhibitor SB431542 leads to an increase in the number of *NANOG*-positive ICM cells (Van Der Jeught et al., 2014). However, performing the same experiment with higher concentrations leads to an opposed result of dramatic reduction of *NANOG* expression (Blakeley et al., 2015), and using another inhibitor, A83-01, on marmoset embryos (Boroviak et al., 2015) does not seem to provide modulation of *NANOG* expression. The function of NODAL/TGF-β signaling in primates pre-implantation epiblast thus remains elusive, and cannot be seen so far as a hallmark of naïve pluripotency *in vivo*.

c.3 LIF signaling/ JAK dependency

One paramount element of mESCs self-renewal is the phosphorylation and nuclear translocation of Stat3 in response to LIF. In human embryos, members of the JAK/STAT3 pathway (*IL6R, GP130/IL6ST, JAK1* and *STAT3*) are expressed at significantly higher levels in the pre-implantation epiblast than in the PE or TE (Bourillot et al., 2020) and treatment of

embryos cultured *in vitro* in serum-free conditions with LIF significantly improves blastocyst formation (Dunglison et al., 1996). Consistently, *LIFR* is expressed in all pre-implantation human lineages, demonstrating that human embryos are responsive to LIF. In the cynomolgus monkey, a subset of pre-implantation epiblast cells express *IL6R, GP130/IL6ST, STAT3*, but not *JAK1* at high levels. Interestingly, a drastic downregulation of those members occurs upon implantation, suggesting that LIF signaling is indeed a characteristic of the naïve primates pre-implantation epiblast (Bourillot et al., 2020; Nakamura et al., 2016). However, a compelling observation is the low level of expression of *LIF* itself in all human pre-implantation lineages or, in the case of the cynomolgus monkey, undetectable. On the strict basis of *in vivo* observations, LIF/STAT3 activation cannot be considered so far as a hallmark of the naïve primates' epiblast, however, it appears mandatory to any reprogramming method yielding naïve-like cells from hESCs (See part **II/3.b**)).

3. The naïve state of primates' pluripotency *in vitro*

a) Of the purpose of primates naïve cells

Capture of the naïve state in primates, and more specifically in humans, is desired for at least three reasons. The first is use of naïve hPSCs as a tool for regenerative medicine. Contrary to hESCs, naïve cells should be, as mESCs, more genetically stable (Fu et al., 2017; Nagaria et al., 2013), more amenable to genetic editing (Zwaka and Thomson, 2003) and free of any differentiation bias, allowing to efficiently derive any desired tissue with no epigenetic imprinting (Ying et al., 2008). Most hopes in using PSCs for regenerative medicine are based on iPSCs, however, current methods of hiPSCs generation yield cells with limited proficiency of lineage-specific differentiation, and epigenetic imprinting of donor cells (Kim et al., 2011). The *tabula rasa* of naïve-state conversion is hoped to solve such problems.

Another potential application, more controversial, is that of organ culture. In 2008, after establishment of the 2i/LIF protocol, Buehr and colleagues derived for the first time naïve cells from a rat blastocyst (Buehr et al., 2008). Two years later, naïve 2i/LIF rat cells were used by Kobayashi et al. in a major breakthrough experiment. Naïve rat cells were injected in a mouse *Pdx1-/-* blastocyst (pancreatogenesis disabled) and efficiently complemented pancreatogenesis, generating an interspecific chimera, a mouse with a functional rat pancreas (Kobayashi et al., 2010). More recently a similar experiment was performed in anephric *Sall1-/-* mutant rats, in which naïve mouse cells successfully complemented kidney formation (Goto et al., 2019). These experiments showed that naïve cells are not only able to form chimeras,

but to do so in other species in the proper conditions. Such approach, termed “blastocyst complementation”, raised hopes of similar success with human naïve cells injected in host species such as pigs or non-human primates, allowing human organ culture in non-human hosts to address donations shortage (Wu et al., 2016). Recently, a first step was performed toward this direction by Wu and colleagues who injected naïve-like human iPSCs in pig embryos and obtained chimerism, though to a limited extent (Wu et al., 2017).

Finally, the capture of the naïve state in primates is fundamental to the comprehension of primates early embryonic development, and would provide a valuable model to the investigation of the molecular and epigenetic mechanisms occurring before implantation. As a tool, human naïve cells would not only give insight in pre-implantation, but also in post-implantation development, as this period is, for obvious ethical reasons, challenging to investigate.

b) Reprogramming strategies to naïve-like pluripotency

In 2007, one year after the derivation of the first mouse iPS cells (hereafter miPSCs), Takahashi and Yamanaka successfully repeated the experiment on human cells. After induction with the OSKM cocktail, cells exhibited pluripotent properties, but did not display a similar morphology to miPSCs or mESCs (Takahashi et al., 2007). Additionally, they expressed some early lineage markers and conserved imprinting from their tissue of origin (Kim et al., 2011). Altogether, human iPSCs (hereafter hiPSCs) exhibited properties more similar to primed mouse cells or to hESCs than to naïve cells. This was not surprising, accounting to the fact that the first generation of miPSCs themselves displayed primed characteristics. The second generation, yielding cells resembling the naïve state, included addition of *NANOG* to the OSKM cocktail or subcloning of *NANOG*-positive clones among the reprogrammed population (Okita et al., 2007; Wernig et al., 2007).

In 2010, starting from this postulate, Buecker and colleagues attempted reprogramming of human fibroblasts with a doxycycline-inducible combination of OSKM and *NANOG*. This yielded human iPSCs with naïve properties, named “hLR5 iPSCs”. hLR5 displayed a dome-shaped morphology, expressed some mouse naïve pluripotency markers, could be passaged by trypsin dissociation and were dependent on LIF to self-renew. However, they remained dependent on the constant activation of their five transgenes (Buecker et al., 2010). The same year another approach was adopted by Hanna and colleagues, that combined overexpression of *OCT4*, *KLF4* and *KLF2*, with LIF stimulation and inhibition of both GSK3b and ERK1/2 (2i/LIF conditions) (Hanna et al., 2010). In both of these studies, despite the apparent naïve

characteristics of the cells, constitutive activation of the transgenes was mandatory (although forskolin, a protein kinase A agonist, could transiently compensate for absence of *OCT4*, *KLF4* and *KLF2* in the study of Hanna and colleagues) leaving many questions unanswered regarding the extrinsic regulation of the human PGN.

In 2013, Gafni and colleagues reported the first transgene-free reprogramming method of hESCs to a naïve-like state, using exclusively small molecules and growth factors. This protocol, termed NHSM, yielded cells with a number of naïve characteristics including, notably, the ability to colonize a mouse blastocyst (Gafni et al., 2013), although this last feature has been the subject of controversy, and was not retrieved in other hands afterwards.

These three experiments paved the way to the quest of human naïve pluripotency, and in the following years, a broad number of protocols blossomed, yielding variable proximity to the naïve human epiblast, and a diverse set of molecular and functional naïve characteristics. All of these methods are based on the simultaneous LIF stimulation and inhibition of GSK3 and ERK/MEK, though this can be combined with other approaches, thus leading to different outcomes and shedding light on different aspects of pluripotency regulation in humans (**Figure 9** and **Table 1**). In the subsequent paragraphs, we will detail these aspects, often overlapping between several protocols. It is worth noting that, although we mentioned the compelling role of LIF signaling *in vivo*, its necessity *in vitro* appears unquestionable and demonstrates that, as for the mouse, LIF/STAT3 signaling plays a critical role in primates naïve pluripotency regulation.

b.1 MEK/ERK reinforced inhibition

In addition to LIF stimulation and Wnt inhibition, reinforcement of FGF/ERK inhibition appears as a recurring way to induce naïve-like reprogramming. In their original protocol NHSM, Gafni and colleagues make use of a Protein Kinase C (PKC) inhibitor in addition to PD03 (classical MEKi), a strategy also used in the Reset (Takashima et al., 2014) and 5i/L/A protocols (Theunissen et al., 2014). PKC is part of a regulatory loop promoting MEK/ERK activation. PKC activates Ras, leading to the phosphorylation cascade activating ERK that in turn phosphorylates PKC (Krueger et al., 2009). Use of a PKCi (Gö6983) on mESCs has been shown to suppress differentiation (Dutta et al., 2011). In the 5i/L/A method of Theunissen and colleagues, the serine/threonine B-Raf and tyrosine kinase c-Src are also targeted in addition to MEK and PKC (Theunissen et al., 2014). B-Raf is a direct activator of MEK (Leonardi et al., 2012), while c-Src is an activator of Ras, upstream kinase of the MAPK pathways (Du et al., 2012). In the case of 5i/L/A, 4 simultaneous MEK/ERK actors are therefore inhibited. The last

inhibitor is IM-12, an alternative to CHIR99021 GSK3 inhibition. This suggests that in human cells, MEK inhibition with PD03 alone is not sufficient and/or specific enough to promote activation of the PGN. Reinforced MEK/ERK inhibition through other inhibitors is one strategy to overcome this problem.

b.2 Activin/Nodal activation

Nodal is a member of the Transforming Growth factor beta (TGF-β) superfamily, able to bind heterodimeric Activin receptors. When bound, Nodal or Activin activate the phosphorylation and nuclear translocation of SMAD2 and SMAD3 that in turn regulate transcription of their target genes. In *Xenopus*, Zebrafish and rodents, Nodal has been shown to regulate mesodermal and endodermal differentiation *in vivo.* In humans, it was shown *in vitro* that Nodal signaling inhibits neurectoderm differentiation, the default commitment path of hESCs in conventional culture media (Vallier et al., 2004), and that the Activin/Nodal and FGF pathways cooperate to maintain pluripotency (Vallier et al., 2005). SMAD2/3, as STAT3, are indeed able to co-occupy enhancers with OSN and thus, promote pluripotency (Hill, 2016). Consistently mouse EpiSCs, just as hESCs, reclaim both Activin and FGF to self-renew (Brons et al., 2007; Tesar et al., 2007; Thomson, 1998). On the contrary, mESCs differentiate in response to Nodal/Activin but rely on BMP4, another TGF-β superfamily member, in combination with LIF to self-renew (Fei et al., 2010). BMP4, in spite of being a TGF-β member, acts through SMAD1, 5 and 8 instead of SMAD2/3, thus having a different impact on transcription regulation (Miyazono et al., 2010).

If mESCs are taken as a reference, primates naïve ESCs should therefore require BMP4 for self-renewal, and differentiate in response to Nodal/Activin, intriguingly however, the converse is observed (Nemashkalo et al., 2017). Most reprogramming methods require addition of a layer of mouse embryonic fibroblasts (MEFs), also called feeder cells (see part I/). In addition to Wnt molecules and FGF, MEFs secrete TGF-β-I, Activin A and antagonists of BMPs (Villa-Diaz et al., 2009). When MEFs are not used, naïve-like human culture conditions (so called feeder-free) require Activin A (Theunissen et al., 2014) or TGF-β-I (Gafni et al., 2013). This suggests that Activin/Nodal activation is mandatory to primed and naïve-like cells self-renewal alike, consistently with the observation that Nodal signaling members are upregulated in the primates naïve epiblast (see paragraph **II/2.c.2**).

b.3 JNK and p38 inhibition

The MAPK superfamily, in addition to the MEK/ERK pathway, includes the JNKs (c-Jun N-terminal kinases) and p38 pathways (Neganova et al., 2017). In mouse, LIF withdrawal induces activation of JNK1 and 2 that in turn phosphorylate Klf4, inhibiting its transcription and transactivation activity (Yao et al., 2014). P38/MAPK, on the other hand, has been shown to promote mESCs differentiation into either neuronal or cardiomyocytes lineages (Aouadi et al., 2006; Wu et al., 2010).

JNKs, p38, or their upstream activator AMPK (Meisse et al., 2002), are targeted in several reprogramming protocols, namely NHSM (Gafni et al., 2013), 3iL (Chan et al., 2013), 4i (rhesus monkey-specific) (Fang et al., 2014), EPSCs (Gao et al., 2019) and, optionally, 5i/L/A (thus being 6i/L/A) (Theunissen et al., 2014). Although it was shown that JUNs, downstream effectors of JNKs, can co-occupy enhancers of OCT4, NANOG, SMAD2 and SMAD3 in hESCs (Li et al., 2019), the process by which JNK/JUN pathway inhibition and, even more so, that of p38 and AMPK promotes the human and rhesus monkey naïve state remains to be elucidated.

b.4 Transitory PGN reinforcement

In their Reset protocol, Takashima and colleagues use a doxycycline-inducible system to overexpress *NANOG* and *KLF2* in primed hESCs, an approach shown to convert mouse EpiSCs to the ground state of pluripotency (Hall et al., 2009). After overexpression, cells are cultured in 2i/LIF with a reduced concentration of CHIR (GSK3i) compared to classical 2i/LIF conditions, and with a PKC inhibitor (Gö6983). Interestingly, reprogrammed hESCs would conserve naïve characteristics after dox withdrawal, suggesting that *NANOG* and *KLF2* overexpression is sufficient to ignite the extended PGN, that subsequently self-maintains without ectopic expression of any factor.

A similar approach was adopted by Chen and colleagues in 2015, who demonstrated that a transient reinforcement of STAT3 signaling through a tamoxifen-inducible system successfully reprograms hESCs to a naïve-like state (Chen et al., 2015). Upon withdrawal of tamoxifen, reprogrammed hESCs can subsequently be cultured with 2i/LIF, in FGF2- and feeder-free conditions, suggesting, as for Reset cells, that transitory PGN reinforcement is sufficient to elicit naïve pluripotency.

b.5 Epigenome resetting

The epigenome of a cell is characterized by both its global DNA methylation level and the apposition pattern of repressive and activating histone marks (Smith and Meissner, 2013; Thiagarajan et al., 2014). DNA methylation is carried out by DNA methyltransferases (DNMTs) while demethylation is operated by ten-eleven translocation (TET) enzymes. In part **I**/, we mentioned that early development is characterized by global demethylation followed by progressive *de novo* methylation. As a consequence, pre-implantation (naïve) epiblast cells exhibit a hypomethylated genome compared to post-implantation (primed) epiblast cells, more developmentally advanced. The epigenome of primed and naïve cells is not only a consequence, but also an intrinsic determinant of their state. A dynamic interplay exists between chromatin state and transcription factors activity determining which genes are expressed, and thus what regulatory loops are triggered (Thiagarajan et al., 2014). Accordingly, reprogramming somatic cells to induced pluripotency triggers widespread epigenetic changes resembling that of epiblast cells (Takahashi and Yamanaka, 2006; Takahashi et al., 2007), but the converse is also true: By using chromatin remodelers, transcriptomic status of a cell can be changed, as exemplified by Esteban and colleagues who used L-Ascorbic acid (Vitamin C), a known TET activator, to enhance iPSC generation in both mouse and human (Esteban et al., 2010).

Several naïve-reprogramming protocols consistently exploit chromatin remodelers to enhance reprogramming (Duggal et al., 2015; Gao et al., 2019), or as a direct catalyst of the process (Guo et al., 2018; Ware et al., 2009). In their 2iL/Toggle protocol, Ware and colleagues first use a mixture of Histone deacetylase inhibitors (HDACi) to erase histone repressive marks of hESCs, and then culture them, successfully, in 2i/LIF conditions (Ware et al., 2009). A similar approach was chosen by Guo and colleagues, who culture cells in three successive media, the first containing Valproic Acid (or VPA), a HDAC inhibitor (Guo et al., 2018).

Whether epigenome resetting/remodeling is used as a reprogramming driver or not, all naïve-reprogramming protocols to this day yield cells with altered epigenomes, resembling that of primates/human pre-implantation epiblast to different degrees. This demonstrates how critical the epigenetic status of a cell is in its identity, and in this case, in its route toward naïve pluripotency.

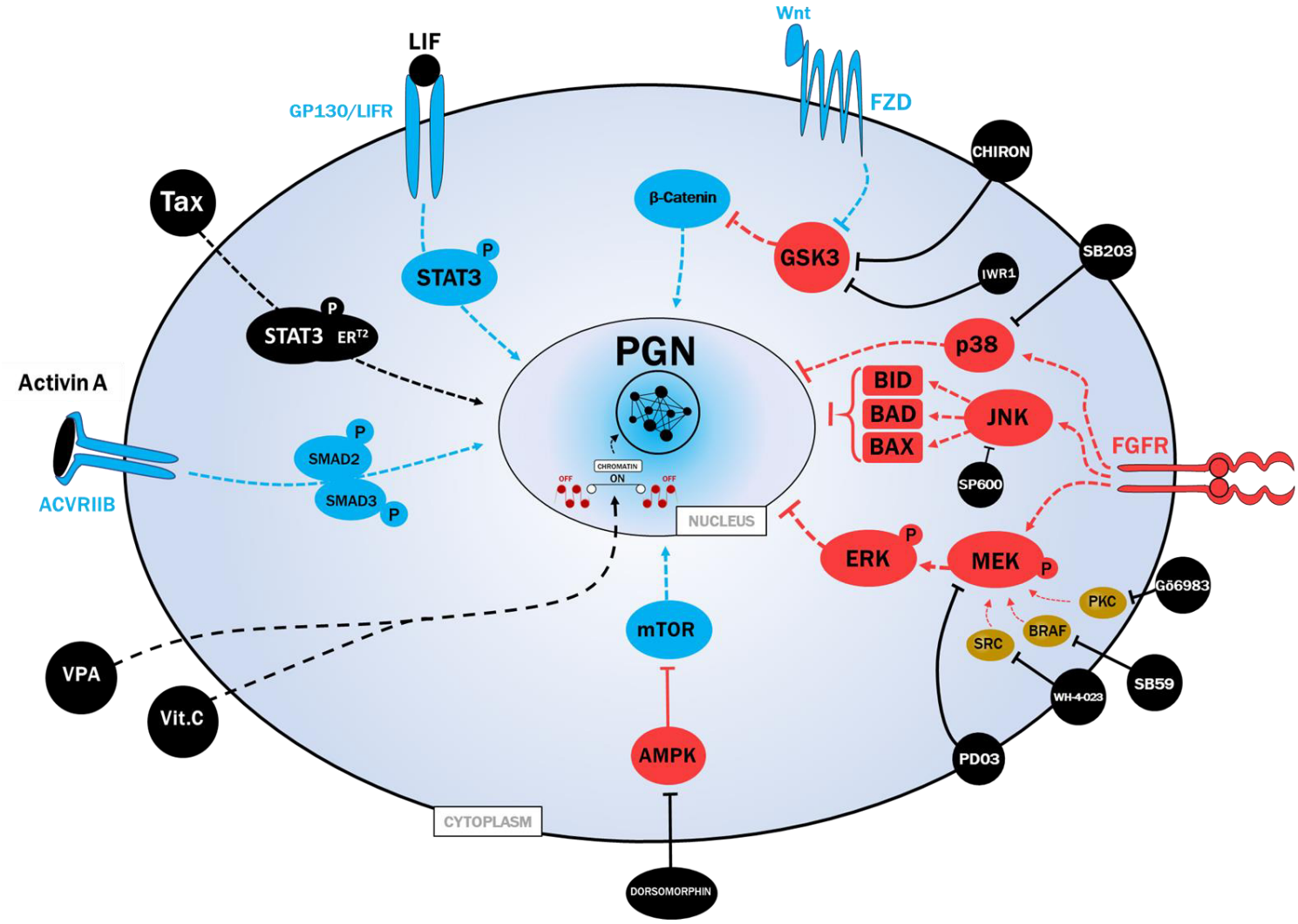

Figure 9: Molecular targets of human naïve-reprogramming protocols.

Schematic of the molecular pathways targeted in human/primates naïve-reprogramming protocols. Elements shown in light blue positively regulate the PGN and self-renewal in the naïve state, while elements in red negatively do so. Elements in black represent the small molecules, inhibitors and exogenous proteins used in one or several protocols to activate and reinforce the PGN. Arrows and bars respectively represent activations or inhibtions, indirect (dashed line) or direct (full line).

b.6 CDK8/19 inhibition

Mediator is a transcription complex located nearby potent enhancers called super-enhancers (SEs), able to recruit RNA pol II in the vicinity of their associated genes. One specific module of Mediator is composed of the cyclin-dependent kinases CDK8 and its paralog CDK19. When active, CDK8/19 prevent RNA pol II recruitment by Mediator and thus, are transcription repressors (Allen and Taatjes, 2015). Moreover, CDK8/19 are able to

phosphorylate TFs, leading to their degradation (Jeronimo and Robert, 2017). In the context of cancer cells, it was shown that CDK8/19 inhibition leads to global hyperactivation of enhancers and thus, hypertranscription (Pelish et al., 2015).

In a recent study, Lynch and colleagues targeted CDK8/19 in hESCs in the aim of promoting extended human PGN expression and reprogram hESCs to naïve pluripotency. Combination of CDK8/19i with 2i yielded cells with features of naïve pluripotency including morphology, naïve-ERVs and naïve-specific transcription factors expression (Lynch et al., 2020). Interestingly, factors of the MEK signaling pathway (RAF, SRC, PKC, p38, JNK, MEK, and ERK) targeted in different naïve-reprogramming protocols as detailed in part b.1 and b.2, have all been shown to regulate CDK8 activity (McDermott et al., 2017; Staab et al., 2013) suggesting that CDK8/19 might be the common effectors of these pathways in naïve pluripotency destabilization.

b.7 Hippo pathway inhibition/ YAP activation

Yes-associated proteins (YAP) are signaling effectors inhibited by the Hippo pathway. They have been shown to be upregulated in several types of cancer (Mo et al., 2014), in mouse progenitor and stem cells, including mESCs (Ramalho-Santos et al., 2002) and *in vitro*, the Hippo pathway is a barrier to iPSCs reprogramming (Qin et al., 2012, 2014). Consistently, Qin and colleagues demonstrated that YAP overexpression or Hippo inhibition with Lysophosphatidic acid (LPA) elicits naïve-like characteristics in hESCs, termed Yin-PSCs (YAP-induced naïve PSCs) (Qin et al., 2016). However, transcriptomic analysis of Yin-PSCs suggests they might be more closely related to cleavage stages embryos than to the ICM/naïve epiblast.

b.8 Tankyrase inhibition

In 2016, Zimmerlin and colleagues generated naïve-like hESCs from conventional primed hESCs by culture in 2i/LIF supplemented with the Wnt pathway modulator XAV939 (Zimmerlin et al., 2016). These culture conditions, termed LIF-3i, allowed direct reprogramming from Activin/FGF primed culture medium, while transfer to 2i/LIF conditions usually triggers immediate cell differentiation of hESCs (Hanna et al., 2010; Theunissen et al., 2014). Though XAV939 is an inhibitor of Tankyrase, known when used alone to favor B-catenin destabilization and destruction (Huang et al., 2009), it paradoxically acts in synergy with CHIR99021 (GSK3i) to increase Axin expression and thus, Wnt signaling and B-catenin targets transcription in

mouse EpiSCs (Kim et al., 2013). In both LIF-3i culture and EPSCs culture conditions from Gao and colleagues (Gao et al., 2019), joint use of XAV939 and CHIR99021 is adopted. Though the effect of this combination may be to strictly increase Wnt activation, it remains to be investigated if it acts through other molecular pathways.

b.9 MUC1* activation

In several types of cancer, the Mucin 1 receptor *MUC1* is found to be strongly upregulated. It has been shown that the truncated form of MUC1, MUC1-C/MUC1* is capable of functioning as an independent growth factor receptor, binding the Nucleoside diphosphate kinase A (NME1/NM23) ligand (Mahanta et al., 2008). In primed hESCs, it was shown that undifferentiated colonies are NM23-negative and MUC1*-positive, while differentiated cells lose expression of NM23 and express only the full-length form of MUC1 (Hikita et al., 2008). Culturing hESCs with either a dimeric form of NM23 (NM23-H1) (Smagghe et al., 2013) or a recombinant form of its paralog NME7 (Carter et al., 2016) reportedly triggers a conversion to a pluripotent state exhibiting naïve properties without use of LIF, FGF or any inhibitor. The naïve-like cells thus produced need to be further characterized and, so far, the mechanisms that underpin the function of MUC1* remain poorly understood. However, it is worth noting that the full-length MUC1 is able to block the phosphorylation-mediated degradation of B-catenin by GSK3B (Huang et al., 2005) although this capacity has not been yet verified for cleaved MUC1*.

c) Assessing naïve-reprogramming protocols

c.1 Transcriptomic analyses

In 2014, Takashima and colleagues incorporated in their Reset-reprogramming protocol study a Principal Component Analysis of single-cell RNA sequencing (scRNA-seq) and microarray data available on all reprogrammed human cell lines of that time. This analysis revealed that the transcriptome of naïve-like hPSCs was a) Significantly different from primed hPSCs, and b) significantly different between cell lines reprogrammed with different protocols (Takashima et al., 2014). Later the same year, Huang and colleagues compared transcriptomes of different reprogrammed hPSCs lines with that of human pre-implantation embryos and demonstrated that they displayed improved but variable similarity with the human epiblast compared to primed cells (Huang et al., 2014).

As new reprogramming methods and scRNA-seq analyses were published along the recent years, these observations only tended to be confirmed (Aksoy et al., 2021; Gao et al., 2019; Guo et al., 2018; Messmer et al., 2019; Yang et al., 2017) and remain true to this day : human naïve-like PSCs display variable transcriptomes, reflecting the diversity of methods used for their reprogramming, and some of them only (Chen et al., 2015; Guo et al., 2018; Theunissen et al., 2014) closely resemble the human epiblast. In all the considered studies, however, transcriptomic comparison is obtained by either calculating the expression foldchange for a selected set of genes between two populations, or by graphical representations such as Principal Component Analysis (PCA), t-distributed stochastic neighbor embedding (t-SNE) or Uniform manifold approximation and projection (UMAP). In PCA representations two or three dimensions are selected to be displayed, representing each a fraction of the differentially expressed genes of the dataset. T-SNE and UMAP, on the other hand, perform a 2- or 3D projection of all dimensions (genes) of the dataset. In both cases, the resulting visualizations are approximations of the transcriptomic distance between cells (single-cell RNA-seq) or populations of cells (Bulk RNA-seq). This gives a robust overview of coarse differences, but hardly suffice to highlight finer changes between close populations. Thus, although such analyses have sometimes been relied on to claim the full efficiency of primates' PSCs naïve-reprogramming, they by no means constitute such evidence, and could even be considered to demonstrate the opposite.

c.2 Cell-surface markers

RNA-sequencing analyses, despite the diversity of information they provide, remain limited to the transcriptome and cannot thus reflect the entire biological reality. Another layer of analysis, taking into account the translated proteins is therefore necessary.

In 2005 Andrews and colleagues demonstrated that hESCs displayed heterogeneity in their self-renewal capacity, and that this was reflected at the population level by expression of surface antigens. The Specific Embryonic Antigen 3 (SSEA3) was found to be expressed only in the undifferentiated fraction of cells that accounted for most of the colony forming ability (Enver et al., 2005). In another study two markers (tetraspannin CD9 and the pericellular matrix proteoglycan GCTM-2) were demonstrated to be co-expressed with *OCT4* by hESCs at levels inversely correlated with the differentiation state of the cells (Hough et al., 2009).

Since then, a broad number of surface markers have been identified, not only reflecting pluripotency in human, but also discriminating the primed and naïve-like states (Bredenkamp

et al., 2019; Collier and Rugg-Gunn, 2018; Collier et al., 2017; Pastor et al., 2016; Shakiba et al., 2015). The analysis of expression of these markers by sc-RNA seq and flow cytometry offers a new layer of characterization for reprogrammed hPSCs, and demonstrates further that they largely differ depending on the method used for their conversion. Interestingly, only a fraction of these cells express the Sushi Containing Domain 2 (SUSD2) marker, recently identified as a surface marker of the human pre-implantation epiblast (Bredenkamp et al., 2019).

c.3 Chimeric competency

As reviewed above, reprogramming methods to naïve primates' pluripotency are diverse and numerous. Cells obtained with these methods, despite displaying common features of putative naïve pluripotency, also exhibit many discrepancies with one another. This is in apparent contradiction with the definition of the naïve state, expected to be at the high end of the pluripotency spectrum, and thus mostly homogenous. Two reasons could explain these differences: 1) Naïve-like cells are incompletely reprogrammed, and on different positions in the pluripotency spectrum. 2) Reprogramming methods "force" the cells out of the primed state toward an artificial state adapted from the culture conditions. Although these cells would share some characteristics with the naïve primates' epiblast, they would be in a state of their own, only partially overlapping with the pluripotency spectrum (**Figure 9B**).

In part **II/1**., we mentioned that all the criteria defining the naïve state could fall into three categories: I) molecular*, i.e.,* the activated and repressed pathways underpinning self-renewal in the naïve-state, II) Genetic, the gene network expressed in response of such cues, and contributing to maintain them. III) Functional, the ability of naïve cells to re-enter embryonic development at the time-point they originate from. In the preceding sections **II/3.c.1** and **c.2**, we showed that aspects I) and II) have been largely characterized in human naïve-like cells, and so far demonstrate their heterogeneity. While transcriptomic proximity of some hPSCs with the human epiblast exist (Chen et al., 2015; Guo et al., 2018; Theunissen et al., 2016), it was until recently unknown if they retained the functional capacity to re-enter development. The ability to form chimeras, and even more so, interspecies chimeras, is the litmus test for ground state pluripotency in mouse and, in the current state of knowledge, should be so in primates.

Although colonization of naïve-like human and rhesus monkey cells in mouse blastocysts has been described in early studies (Fang et al., 2014; Gafni et al., 2013), we mentioned that these results failed to be reproduced in subsequent attempts by other groups (Masaki et al., 2015; Theunissen et al., 2016). Furthermore in a more recent work, naïve-like

human iPSCs were injected in pig embryos, and although survival could sometimes be observed at pre-implantation stages, most cells were not able to survive past implantation, resulting in very low fetus colonization rates (Wu et al., 2017).

These rather inconclusive data were put in perspective again this year by two studies. The first, published by Tan and colleagues, described the fate of human extended PSCs (hEPSCs) injected in cynomolgus macaque early blastocysts (Tan et al., 2021). In this work, all blastocysts injected were reported to retain hEPSCs, although proliferation could not be demonstrated, as the number of human cells found in the host never exceeded the number of initially injected cells (25). Additionally, although the authors reported colonization of human cells at post-implantation stage d.p.f. (day post fertilization) 19, this observation was not supported by visual evidence.

In the second study, Aksoy and colleagues systematically assessed the capacity of naïve-like macaque monkey PSCs reprogrammed with a broad variety of methods (TL2i, NHSM-v, E-NHSM , 4i/L/b, t2iLGöY, 5iL/A and LCDM) and human iPSCs (TL2i and t2iLGöY) to colonize rabbit blastocysts, phylogenetically as distant to primates as rodents, but exhibiting structural and timing features closer to primates (Aksoy et al., 2021). These experiments revealed poor surviving and colonization capacity of both macaque monkey and human reprogrammed cells, with the best results being however obtained with t2iLGöY (Guo et al., 2018) and TL2i (Chen et al., 2015) cells. This was in sharp contrast with what was obtained with mouse 2i/LIF, *bona fide* naïve cells, that did not only yield excellent survival rates but also actively proliferated. In the same work, colonization was assessed in macaque embryos, and did not provide better results than with more distantly related species. Further characterization demonstrated that injected cells, both human and macaque, either underwent apoptosis or prematurely differentiated and were unable to remain as mitotically active as their mouse counterparts.

These results reveal that reprogrammed primates' cells lack the naïve-defining capacity of colonizing a pre-implantation blastocyst. Unlike their mouse counterparts, they are unable to remain seamlessly proliferating after dissociation or when re-introduced in an unfavorable environment, and thus cannot participate in the development of the host. Taken collectively with all the characterization of primates naïve-like PSCs performed so far, this questions their very nature and suggests that no current reprogramming method allows self-renewal in a true naïve-state, *i.e.*, a state faithfully mirroring the primates' naïve epiblast. This implies that gaps remain in our understanding of human and non-human primates' pluripotency regulation, and that potential new molecular and genetic regulators are to be yet identified.

III/ Netrin signaling

1. Netrin-1 discovery

Netrins, from the Sanskrit “Netr”, one who guides, are a family of molecules belonging to the superfamily of laminins and sharing with them homology in the N-terminal domains. The first Netrin, unc-6, was discovered in the worm *C. elegans*, in a screen aiming at identifying key genes in neural development (Hedgecock et al., 1990). In pioneer studies, the *unc-6* gene was found to code for a 591 amino-acids secreted protein able to bind two transmembrane receptors, unc-5 and unc-40 (Ishii et al., 1992; Leung-Hagesteijn et al., 1992). A gradient of unc-6 was shown, in the worm, to guide the newly formed axons along the epidermis toward their tissue of destination, depending on the type of receptor they express. A few years later, two *unc-6* homologs were discovered in the chicken and were named Netrin-1 and -2 (Serafini et al., 1994). These proteins were shown to share important homology (~50%) with their worm counterpart, but also to be involved in a very similar process of axon guidance during embryogenesis. At the end of neurulation, Netrin-1 is secreted by the floor plate cells and diffuses in a gradient toward the roof plate, reaching the newly differentiated commissural neurons. These detect the signal through structures called growth cones, and subsequently outgrow axons toward the floor plate and the ventral midline (Kennedy et al., 1994; Serafini et al., 1996). Depending on a) the type of receptor expressed by the axon growth cone and b) the type of ligand expressed by the neighboring cells and target tissues, the axon is either attracted or repelled by Netrin-1 and other chemoattractant signals until it reaches its destination and connects to the target area (Barallobre et al., 2005) (**Figure 10**).

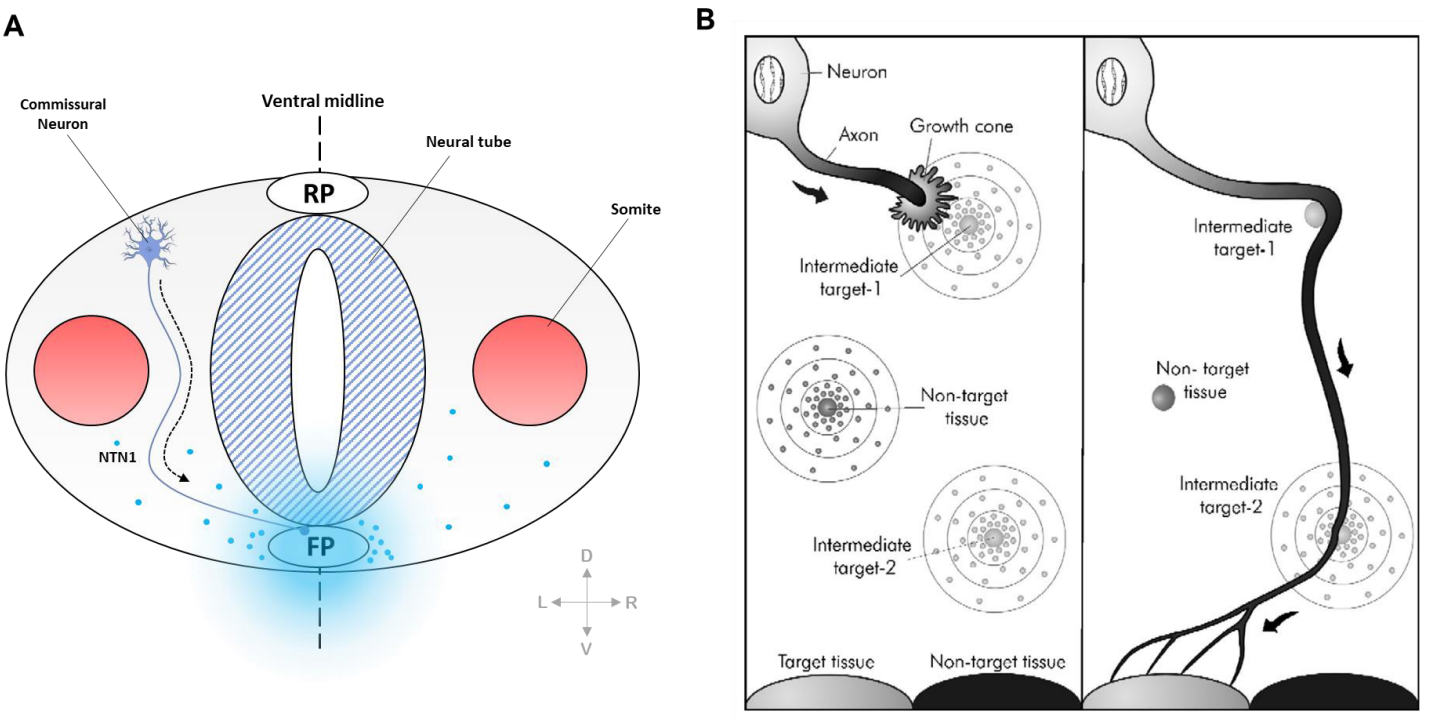

Barallobre et al. 2005, *Brain Research Reviews, 49(1).*

Figure 10. Netrin-1 drives commissural axonogenesis during vertebrates neural development.

(**A**) Diagram representing a transversal section of the neuralting mammalian embryo (human E18-21, mouse E8.5). RP, Roof Plate; FP, Floor Plate. Dashed arrow represents the migration direction of the commissural axons toward the NTN1 gradient produced by the FP. Key: D, Dorsal; V, Ventral, L, Left; R, Right. (**B**) Diagram depicting an axon growth scenario depending on two distinct guiding molecules gradients (Barallobre et al. 2005).

Since the establishment of this model, *Netrin-1* homologs have been identified in many other invertebrate and vertebrate species, including mammals (Gan et al., 1999; Harris et al., 1996; Matus et al., 2006). As it turns out, both the amino-acid sequence and the function of the protein in neurogenesis are well conserved across bilateral species, though it has been found to be also involved in many other developmental and somatic processes such as pancreatic branching morphogenesis, angiogenesis and spatial control of lung-bud development (Cirulli and Yebra, 2007).

2. The Netrin family

a) Netrin ligands

Since Netrin-1 discovery, other Netrins were identified. They all share homology in their N-terminal regions with the amino-terminal domains of laminins, classifying them as members of the laminin superfamily (Rajasekharan and Kennedy, 2009). In mammals, and more specifically primates, six Netrins have been identified so far: Netrin-1, -3, -4, -5, -G1 and -G2. The Netrin-2 homolog identified in the chick, duplication of the Netrin-1 gene, does not appear to exist in mammalian species. Netrins can be divided in two categories, depending of the homology they share with laminins. Netrin-1, -3 and -5 share homology with the γ-chain of laminins and are thus also referred to as γ-Netrins. Netrin-4, -G1 and -G2 are closer related to the β-chain, and thus named β-Netrins (**Figure 11A**).

In addition to their structural relation to laminins, Netrins also diverge in their own specific structures. Netrin-1, -3, -4 and -5 are secreted proteins, producing gradients involved in neurogenesis and other developmental processes. Netrin-G1 and -G2 (also named G-Netrins), however, are evolutionary and structurally more distant and are attached to the cell membrane by glycophosphatidylinositol (GPI) anchors instead of being secreted (Cirulli and Yebra, 2007; Rajasekharan and Kennedy, 2009). In the current state of knowledge, G-Netrins are thus reported to act as receptors binding their own ligands, NGLs (Netrin-G Ligands), are not able to interact with the other Netrins receptors, and likely support different molecular pathways than the rest of the family (Sun et al., 2011).

b) Netrin receptors

Aside from G-Netrins, secreted Netrins are able to bind two types of receptors: the DCC/Neo1 (DCC and Neogenin) family, and the UNC5 (primates' UNC5A-D and mouse UNC5H1-4) family. Both groups are closely related members of the immunoglobulin superfamily and composed of an extracellular domain, a single-pass transmembrane region, and a cytoplasmic domain (Bradford et al., 2009; Sun et al., 2011) (**Figure 11B**). Although it does not appear to be their preferential receptor, Netrins have also been reported to bind the DS Cell Adhesion Molecule (DSCAM), which is expressed by commissural axons during neurogenesis, participating in their pathfinding to the floor plate (Andrews et al., 2008; Liu et al., 2009).

c) Draxin

In addition to all Netrin members and receptors, another protein associated to the family was identified in 2009. This molecule, named Draxin has been first described *in vivo* in the mouse embryo (Islam et al., 2009) and then reported in the chick, where it is secreted by the roof plate during later stages of neurulation. It was shown that Draxin is able to directly bind Netrin-1, forming an opposing gradient and preventing it to act on its receptors, regulating its guiding action (**Figure 11A**). Another ability of the protein is reportedly to bind at least two of said receptors, DCC and Neo1, thus also acting as a competitive inhibitor of Netrin-1 (Gao et al., 2015).

Interestingly, the *DRAXIN* gene was reported in humans, and DRAXIN protein was shown to retain the same capacity of interaction and antagonism with human NTN1, suggesting a conserved function in molecular regulation (Gao et al., 2015).

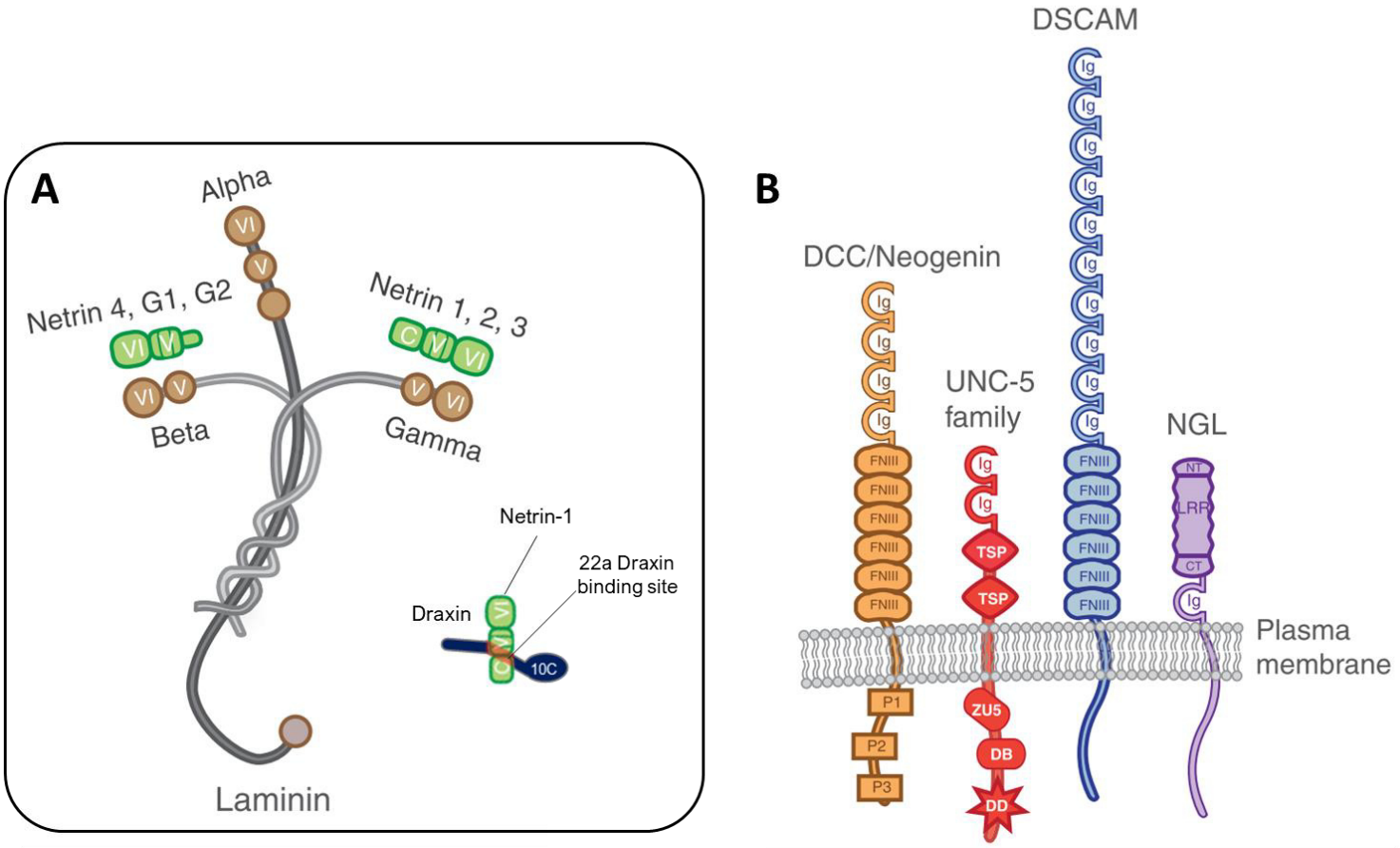

Adapted from Sun et al. 2011, *Development, 138(11).*

Figure 11. The Netrin protein family.
Diagram representing the Netrin ligands and Netrin-1 antagonist Draxin (**A**) and the Netrin receptors (**B**).

3. Netrins in cancer

Colorectal Carcinoma is often associated with a deletion in the chromosomal region 18q21. In 1990, it was found that when the deletion was present, suppression of a specific gene located in the area was responsible for the phenotype. This gene was named Deleted in Colorectal Carcinoma (*DCC*), and later found to be the receptor of Netrin-1, homolog of *unc-40* in *C. elegans* (Fearon et al., 1990; Keino-Masu et al., 1996).

Further studies demonstrated that DCC was not only active in response to Netrin-1 binding, but could also induce cell death in absence of it (Mehlen et al., 1998). This type of behavior was previously described for other receptors that were termed “dependence receptors” (DRs) (Bredesen et al., 1998; Rabizadeh et al., 1993). DRs, as their name suggests, rely on the presence of their ligand to trigger a broad variety of responses (survival, proliferation, differentiation) but instead of being inactive in absence of it, trigger pro-apoptotic signals. Thus, when correctly expressed, DRs regulate the balance between proliferation and cell death, participating in the maintenance of one tissue’s homeostasis and leading to overgrowth when suppressed or downregulated. The finding that DCC belonged to the DRs category opened a new avenue in cancer research (Bredesen et al., 2004; Mehlen and Bredesen, 2004), and numerous other receptors were subsequently found to behave in a similar manner. Among these, having the same dependence to Netrin-1 as DCC, are the Neogenin and UNC5 human family receptors (Guenebeaud et al., 2010; Llambi et al., 2001; Tanikawa et al., 2003).

Mechanistically, it was shown that, in the absence or their ligand, both DCC/Neo and UNC5 receptors are accessible and cleaved in their intracellular domain by caspase 3 (**Figure 12B**). On the contrary, binding of Netrin-1 blocks access to the cleavage site of caspases, at least in part through a dimerization process changing the configuration of the intracellular domains. Caspase 3 is then still recruited, but has no proteolytic effect on DCC/Neo or UNC5H receptors. Instead, it is the first link of several possible molecular chains leading to various effects (Arakawa, 2004). Though those are still probably not all identified, activated pathways reported so far include PI3k/Akt (Lv et al., 2015b; Yin et al., 2017), p53 (Tanikawa et al., 2003), ERK1/ERK2, (Forcet et al., 2002), FAK (Huyghe et al., 2020; Liu et al., 2004; Ren et al., 2004) and YAP/TAZ (Yin et al., 2018) (**Figure 12**).

Involvement of Netrin-1 and its receptors in tumorigenesis is now broadly demonstrated (Bernet and Fitamant, 2008; Boussouar et al., 2020; Goldschneider and Mehlen, 2010; Grandin et al., 2016; Sung et al., 2019), but other members of the Netrin family such as Netrin-

4 (Lee et al., 2020; Lv et al., 2015a; Xu et al., 2017), Netrin-3 (Jiang et al., 2021) and Netrin-G1 (Francescone et al., 2021) have been since found to be implied in oncogenic mechanisms, suggesting that the diversity of action of the family is still to be unraveled.

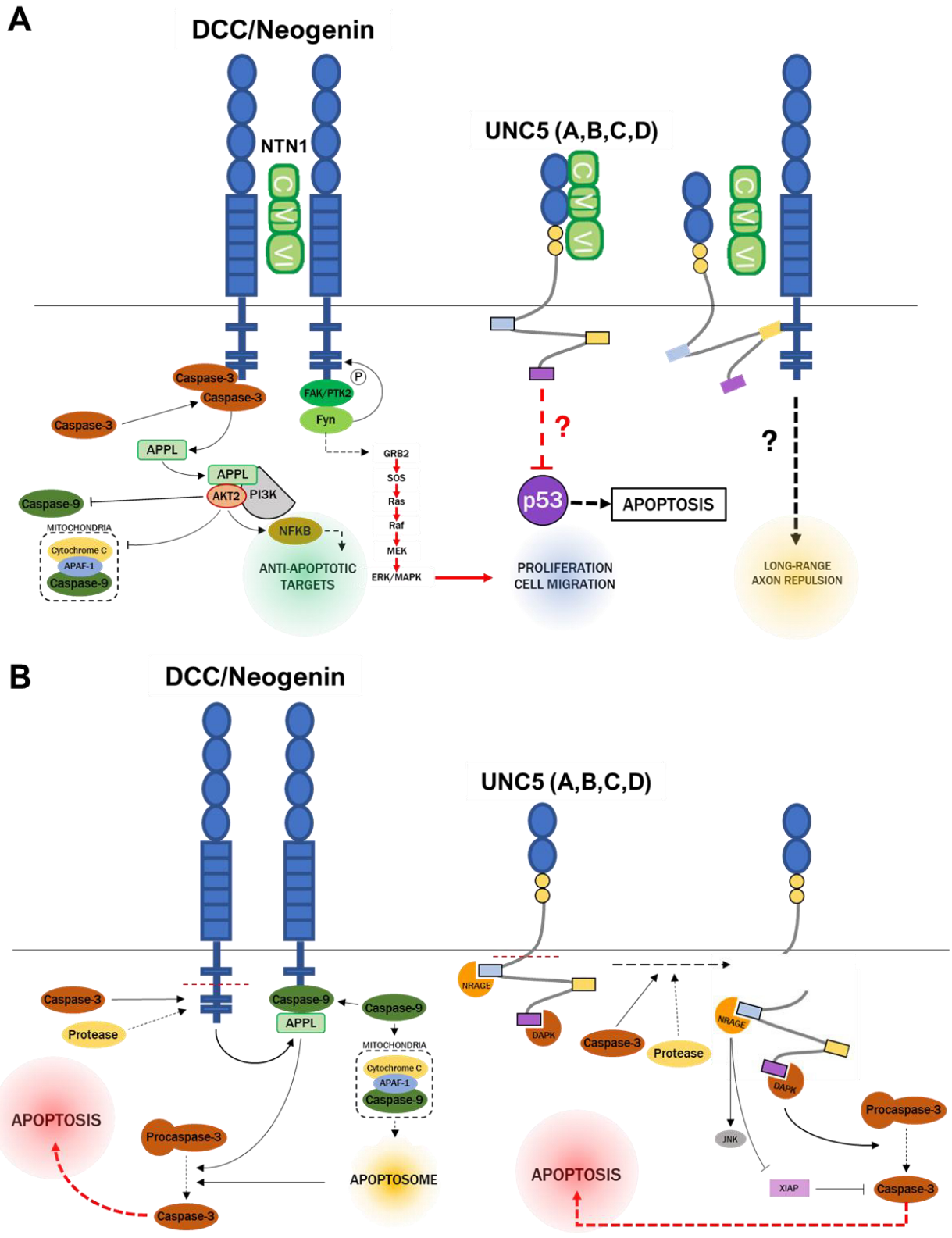

Figure 12. The Netrin receptors DCC, Neo1 and UNC5A-D are dependence receptors.

Schematic showing some of the known molecular pathways activated by the DCC/Neo1 and UNC5A-D families of receptors in presence (**A**) or absence (**B**) of their ligands (here NETRIN1). Arrows and bars respectively represent activations or inhibtions, indirect (dashed line) or direct (full line). A simple dashed red line indicates a Caspase-3 mediated cleavage.

4. Netrin-1 in mouse pluripotency

In 2015, starting from the postulate that Netrin-1, through the binding of its receptors, can control proliferation and cell death, Lavial and colleagues investigated the action of the protein on mouse iPSCs reprogramming (Ozmadenci et al., 2015). By adding recombinant Netrin-1 to the OSKM cocktail, the authors observed a significant enhancement of the reprogramming yield, normally associated with widespread cell death. This improvement was found to be mainly allowed by the anti-apoptotic effect of Netrin-1, binding an increasingly expressed DCC along the conversion process.

In the same study, *Ntn1* was overexpressed in mouse ESCs cultured in serum/LIF. By doing so, a significant improvement of self-renewal was observed in the dishes, with a higher fraction of cells being fully undifferentiated, compared to the classically heterogenous serum/LIF populations (**Figure 13A**). Although binding of UNC5B was shown to be partially responsible, this finding was compelling because it did not imply a simple inhibition of apoptosis. Indeed, commitment to differentiation and self-renewal were here affected and thus, pluripotency *per se*.

This intriguing observation led to a recently published study by the same group (Huyghe et al., 2020). In this work, Serum/LIF (heterogenous naïve state) and 2i/LIF ("ground state" / homogenous naïve state) mESCs transcriptomes were compared, and the Ntn1-Unc5b-Neo1 axis was found to be a specific component of the latter, suggesting an involvement in naïve pluripotency regulation. In serum/LIF cells, Ntn1-Unc5b-Neo1 activation was shown to increase Nanog levels, as well as that of the naïve mouse pluripotency marker Esrrb. *Ntn1* over-expression in mouse ES cell lines combined with LIF treatment was also found to supplement for 2i (MEK and GSK3 inhibitors) and to sustain self-renewal in a ground-like state for several passages, indicating that the Ntn1-Unc5b-Neo1 axis replaces, at least on the short run, MEK and GSK3 inhibition. In concluding mechanistic analyses, the authors demonstrated that the Ntn1-Unc5b-Neo1 promotes naïve pluripotency through FAK activation, leading to 1) Indirect ERK1/2 inhibition, a pathway promoting differentiation and 2) GSK3 destabilization, allowing stronger Wnt pathway activation (**Figure 13B**).

In regard of these recent findings, we thus decided to investigate the function of Netrin-1 and the Netrins family as a whole in primates pluripotency regulation. We investigated the expression of the family in both human and non-human primates single-cell RNA-seq data sets, and generated a human cell line, hSTAN1, conditionally overexpressing the *NTN1* gene to address the effect of NTN1-signaling exogenous activation in human pluripotent stem cells.

A

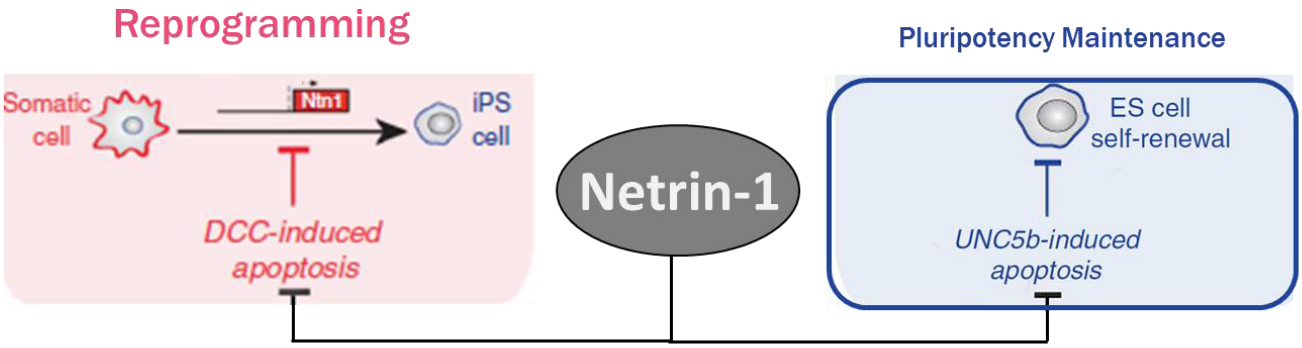

Adapted from Ozmadenci et al. 2015, *Nature Communications.*

B

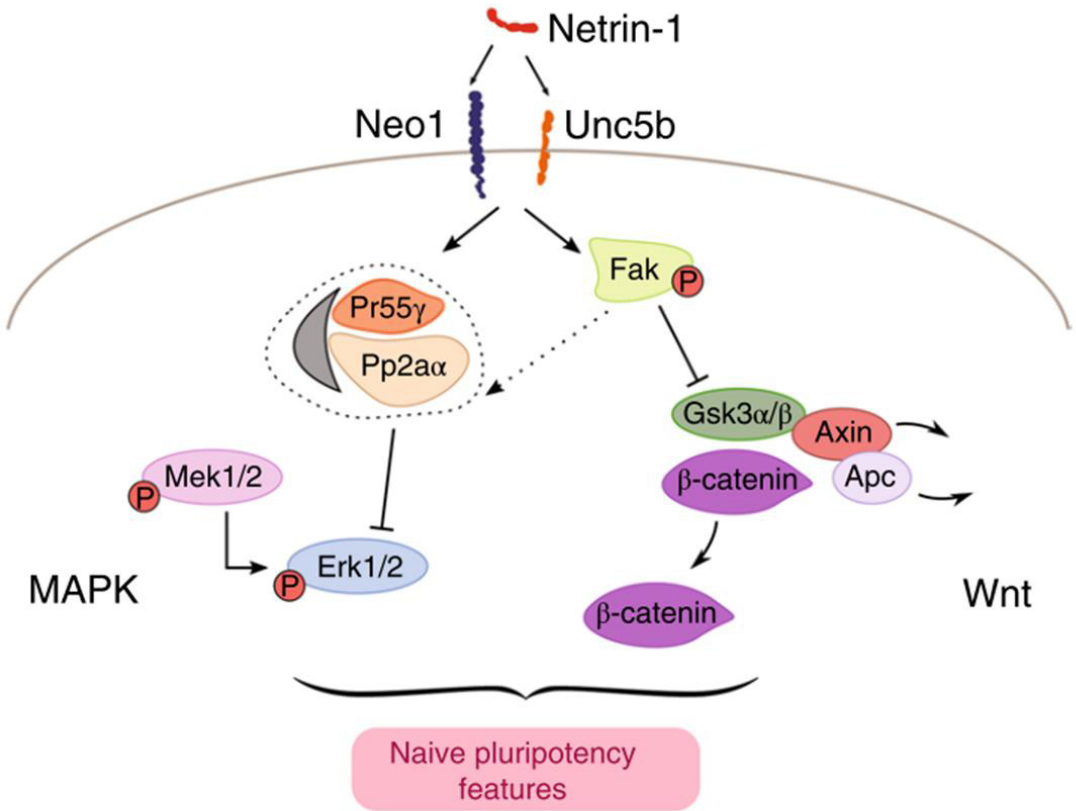

Huygue et al. 2020, *Nature Cell Biology, 22(4).*

Figure 13. Netrin-1 positively regulates survival and self-renewal of mouse PSCs.

(**A**) Schematic illustrating the effect of recombinant Netrin1 on mouse iPSCs generation, and Netrin1 overexpression effect in mESCs (Ozmadenci et al. 2015). (**B**) Schematic of the molecular mechanisms underlying Netrin-1 effect on mESCs (Huygues et al. 2020)

Results

I. Netrins in the human and non-human primates' embryo

I.1. Netrin family genes in the mouse naïve compartment

To investigate the function of Netrins in primates' pluripotency regulation, we first analyzed publicly available single-cell RNA-sequencing datasets published in the recent years, to establish an overview of the netrins' family genes expression in the primates' pre-implantation embryo. As a reference, we started by analyzing several datasets published in the mice early embryo and PSCs (Cheng et al., 2019; Kolodziejczyk et al., 2015; Nowotschin et al., 2019; Wu and Belmonte, 2015b). We observed in the embryo that *Ntn1*, *Unc5b* and *Neo1* are the only members of the family to be expressed in the epiblast, regardless of the stage (**Figure 14A**). While *Unc5b* and *Neo1* are expressed from E4.5 (pre-implantation) to E7.5 (post-implantation / pre-gastrulation), *Ntn1* expression is confined to the early (E4.5) epiblast, accordingly with what was described in previous work. Upon implantation, however, *Ntn1* switches from the EPI to visceral endoderm (VE), while *Unc5b* and *Neo1* remain expressed in EPI, VE and ExE (Extraembryonic ectoderm) (**Figure 14B** and **C**). In line with these observations, we found that mouse PSCs cultured in conditions supporting naïve pluripotency express the same three members of the netrin family as the EPI cells: *Ntn1*, *Unc5b* and *Neo1* (**Figure 14D**). Interestingly, ESCs cultured in 2i/LIF or alternative 2i/LIF (SRC inhibition instead of ERK inhibition), both epitomizing the ground state (homogenous naïve state) of pluripotency, display higher levels of *Ntn1* and *Neo1* compared to their serum/LIF (heterogenous naïve state) counterparts (**Figure 14E**). From a dataset generated from primed EpiSCs (Wu et al., 2015) we finally found that, although *Neo1* and *Unc5b* are present at high levels, *Ntn1* expression is replaced by *Ntn3* and *Ntn4* (**Figure 14F**). These results recapitulate what was previously demonstrated *in vitro*, and confirm that *Ntn1-Unc5b-Neo1* form the axis of netrins family genes in the mouse naïve pluripotency context.

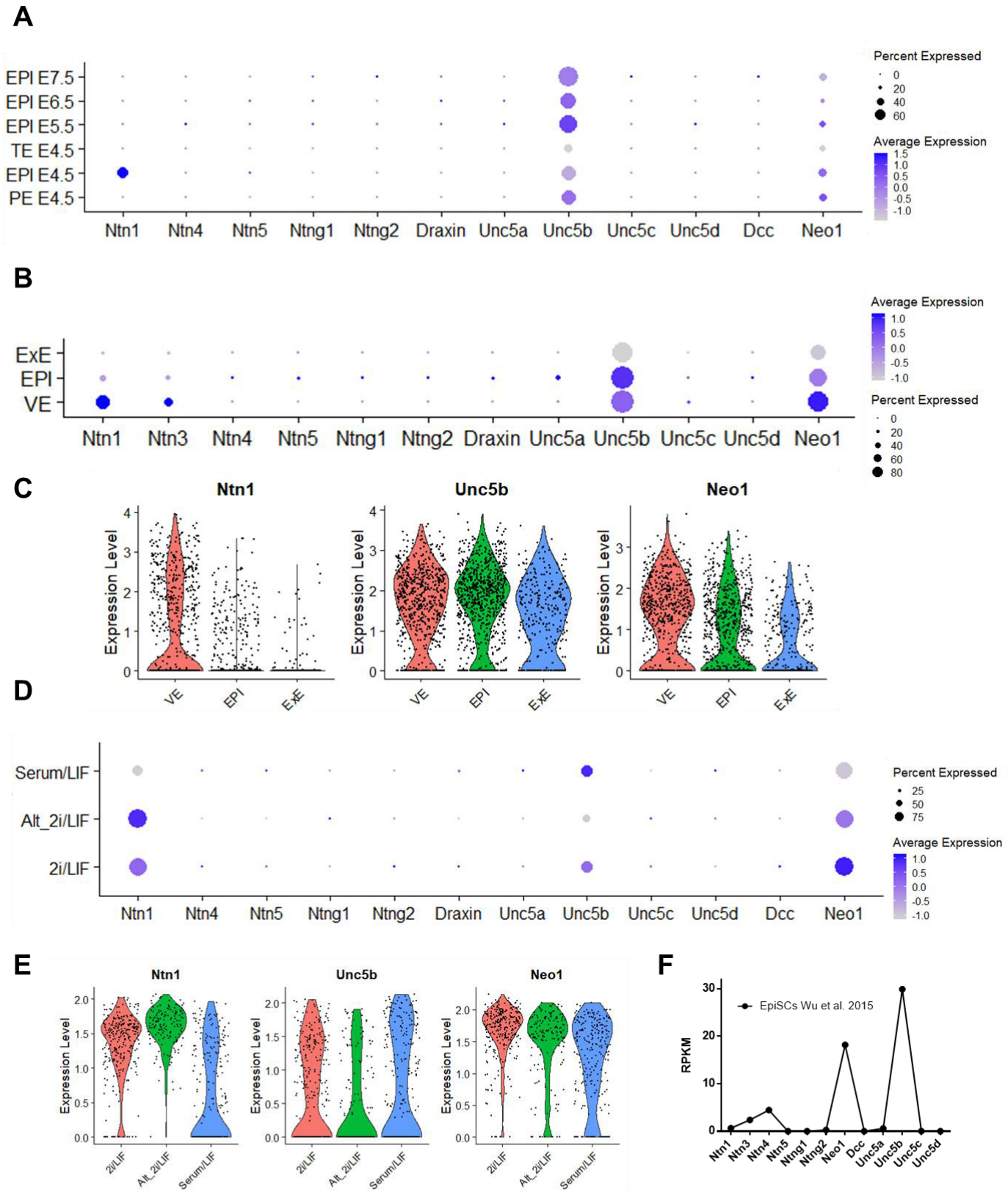

Figure 14. Naive mouse cells express *Ntn1*, *Unc5b* and *Neo1 in vivo* and *in vitro*.
(**A**) Dotplot of Netrin family genes expression in mouse pre- and post-implantation embryonic tissues (Nowotschin et al. 2019). EPI, Epiblast; TE, Trophectoderm; PE, Primitive Endoderm. (**B**) Dotplot of Netrin family genes expression in mouse peri-implantation embryonic tissues (Cheng et al. 2019). VE, Visceral Endoderm; ExE, Extraembryonic Ectoderm. (**C**) Violin plots of *Ntn1*, *Unc5b* and *Neo1* expression in mouse peri-implantation embryonic tissues (Cheng et al. 2019). (**D**) Dotplot of Netrin family genes expression in mouse Serum/LIF, 2i/LIF or alternative 2i/LIF (Alt_2i) embryonic stem cells (original data set from Kolodziejczyk et al 2015, *Cell Stem Cell*). (**E**) Violin plots of Netrin family genes expression. (**F**) Expression of Netrin family genes in mouse EpiSCs (Dataset from Wu et al. 2015).

I.2. Netrin family genes in the non-human primate embryo

With this reference in mind, we then examined netrins family genes in the cynomolgus macaque embryo, by exploring a single-cell RNA-seq dataset published by Nakamura and colleagues in 2016 (Nakamura et al., 2016). We found that, in addition to *NTN1*, *UNC5B* and *NEO1*, genes coding for two other Netrin family members are expressed in the primate's pre-implantation embryo: the membrane-anchored NTNG1, and the NTN1 antagonist DRAXIN. Both are enriched in PE, although *DRAXIN* was detected at lower levels in all other pre-implantation tissues (**Figure 15A**). As for the mouse, we observed that *NTN1* is strongly enriched in the early EPI and impoverished in other tissues, albeit expressed at low levels in mid- and late-EPI. While the *UNC5B* and *NEO1* receptors were found to be expressed in all pre-implantation tissues, *UNC5B* is enriched in the early-, and subsequently late-EPI, while *NEO1* shows only one peak in the late-EPI (**Figure 15B**). This suggests a pattern similar to the mouse, where *NTN1* and *UNC5B* are the privileged actors of naïve pluripotency/early epiblast regulation (Huyghe et al., 2020). To verify this hypothesis, we asked whether *NTN1*+ cells of the pre-implantation macaque embryo exhibit higher levels of expression of pluripotency markers, and observed that *NANOG*, *OCT4* and *SOX2* are all expressed at higher levels in *NTN1*+ cells compared to *NTN1*- (**Figure 15C**). Interestingly, NTN1-antagonist *DRAXIN* expression does not seem to affect pluripotency, as *DRAXIN*+ cells show similar expression of OSN compared to *DRAXIN*-. Upon implantation, we noticed that in addition to *NTN1*, *NTNG1*, *DRAXIN*, *UNC5B* and *NEO1, NTN4* and *UNC5D* are expressed (**Figure 15D** and **E**). We observed that after its peak of expression at E6, *NTN1* is swiftly downregulated and is not expressed again until E16-17, stages preceding the onset of gastrulation (**Figure 15F**). In sharp contrast, *DRAXIN* expression is strongly rising, along with *UNC5B* and *NEO1*, upon implantation until E20. *NTN4* and *UNC5D* have a distinct pattern, both being expressed solely at the peri-gastrulation stages. Collectively, these data show that mouse and macaque monkey share expression of the *NTN1-UNC5B-NEO1* axis at pre-implantation stages, with an enrichment of *NTN1* in the naïve epiblast.

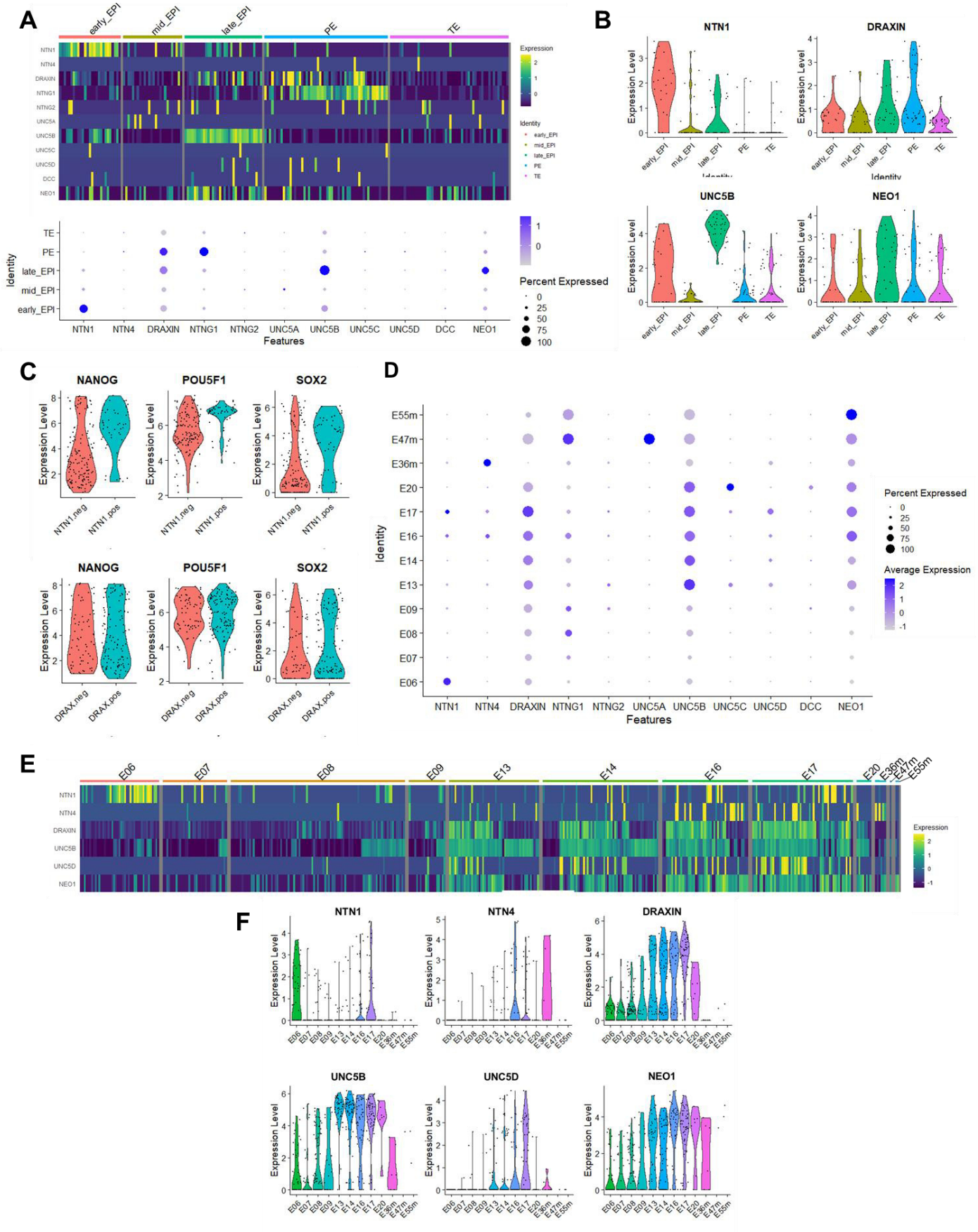

Figure 15. Netrin signaling in the macaque monkey early embryo.
Netrin family genes expression in the pre- (**A-C**) and post-implantation (**D-F**) tissues of the macaque monkey embryo. (**A**) Heatmap (top) and dotplot (bottom) of the netrin family genes expression. (**B**) Violin plots of *NTN1*, *DRAXIN*, *UNC5B* and *NEO1* expression. (**C**) Violin plots of *NANOG*, *OCT4* and *SOX2* in the *DRAXIN*+/- and *NTN1*+/- pre-implantation cell populations. (**D**) Dotplot of the netrin family genes expression. (**E**) Heatmap of *NTN-1,-4, DRAXIN, UNC5-B, -D* and *NEO1* expression. (**F**) Violin plots of *NTN-1,-4, DRAXIN, UNC5-B, -D* and *NEO1* expression.

I.3. Netrins and DRAXIN in the human pre-implantation embryo

We then asked if Netrin family genes are expressed in a similar fashion in the human pre-implantation embryo, and inspected to this end other publicly available single-cell RNA sequencing data (Blakeley et al., 2015; Stirparo et al., 2018). We first investigated expression of Netrin ligands (*i.e.*, secreted *NTN1, -3, -4* and *-5*), G-Netrins and *DRAXIN*. While *NTN*5 was very weakly detected, and *NTN3* absent in all tissues, *NTN1*, *-4* and *-G2* were found to be strongly expressed in the zygote and rapidly downregulated at the 8-cell stage (**Figure 16A-B**). Surprisingly, unlike the mouse and macaque, *NTN1* expression is completely extinguished from the compacted morula stage onwards. Only three genes were detected from this point: *NTN4*, *NTNG1* and *DRAXIN* (**Figure 16C***)*. Accordingly with its temporal pattern of expression, we found that *NTN1* is associated with lower expression levels of core pluripotency markers *NANOG*, *OCT4* and *SOX2* (**Figure 16D**). On the contrary, the *DRAXIN*+ population was enriched for *NANOG* and *OCT4* compared to *DRAXIN*- cells, although *SOX2* exhibited a similar level between the two groups. Neither *NTN4* or *NTNG1*, on the other hand, seem to have an influence on core pluripotency, as illustrated by strictly similar *OSN* patterns of expression between *NTN4+ and -* or *NTNG1+ and -* populations. Altogether, these observations indicate that despite their relative genetic proximity, macaque and human display critical differences of Netrins, and more specifically *NTN1* expression during early embryogenesis.

I.4. DRAXIN-positive cells of the human pre-implantation embryo

Because *DRAXIN*+ cells of the human pre-implantation embryo are specifically enriched in the EPI and PE and display higher levels of *OCT4*, *SOX2* and *NANOG*, we decided to further characterize this population. We generated volcano plots of the differentially expressed genes (DEGs) of the *DRAXIN*+ vs – groups and observed that aside from *OSN*, several other pluripotency genes are upregulated in the former, including the naïve markers *SUSD2* and *DPPA4* (**Figure 17A** and **B**). Interestingly, we also noticed that elements of NODAL signaling, including *NODAL* itself, *GDF3* and *LEFTY2* represent some of the most upregulated genes of the *DRAXIN*+ population. On the contrary, the PE marker *GATA6* is the most downregulated gene of the group (p-value and Foldchange considered). Accordingly, *DRAXIN* and *GATA6* show robust anti-correlation among the dataset (**Figure 17C**). To define more clearly the phenotype of *DRAXIN*+ cells, we interrogated the KEGG (Kyoto Encyclopedia of Genes and Genomes) database with the most up- and down-regulated genes of the population (Log_2(FC)>0,25 or <-0,25) and found that *DRAXIN*+ cells are enriched for several

terms associated with active amino acids biogenesis and metabolism (**Figure 17D**). Among the most enriched terms are “Signaling pathways regulating pluripotency of stem cells” and “Oxidative phosphorylation”, regrouping 30 genes each. On the contrary, downregulated genes return only one term, “Cell cycle”, suggesting that *DRAXIN*- cells proliferate faster than their *DRAXIN*+ counterparts. We performed a similar analysis with the Gene Ontology (GO) database using most upregulated genes of the *DRAXIN+* population, and observed that numerous terms are consistent with rich amino-acid metabolism and active oxidative phosphorylation (**Figure 17E**). GO analysis also returned terms associated with planar cell polarity and epithelium establishment, including activation of the Wnt signaling pathway. Collectively, these findings strongly suggest that *DRAXIN*+ cells epitomize the naïve pluripotent compartment of the human pre-implantation embryo, *i.e.,* the early epiblast, exhibiting expression of naïve markers and genes associated with oxidative phosphorylation, the preferential metabolic mode of naïve cells *in vitro*.

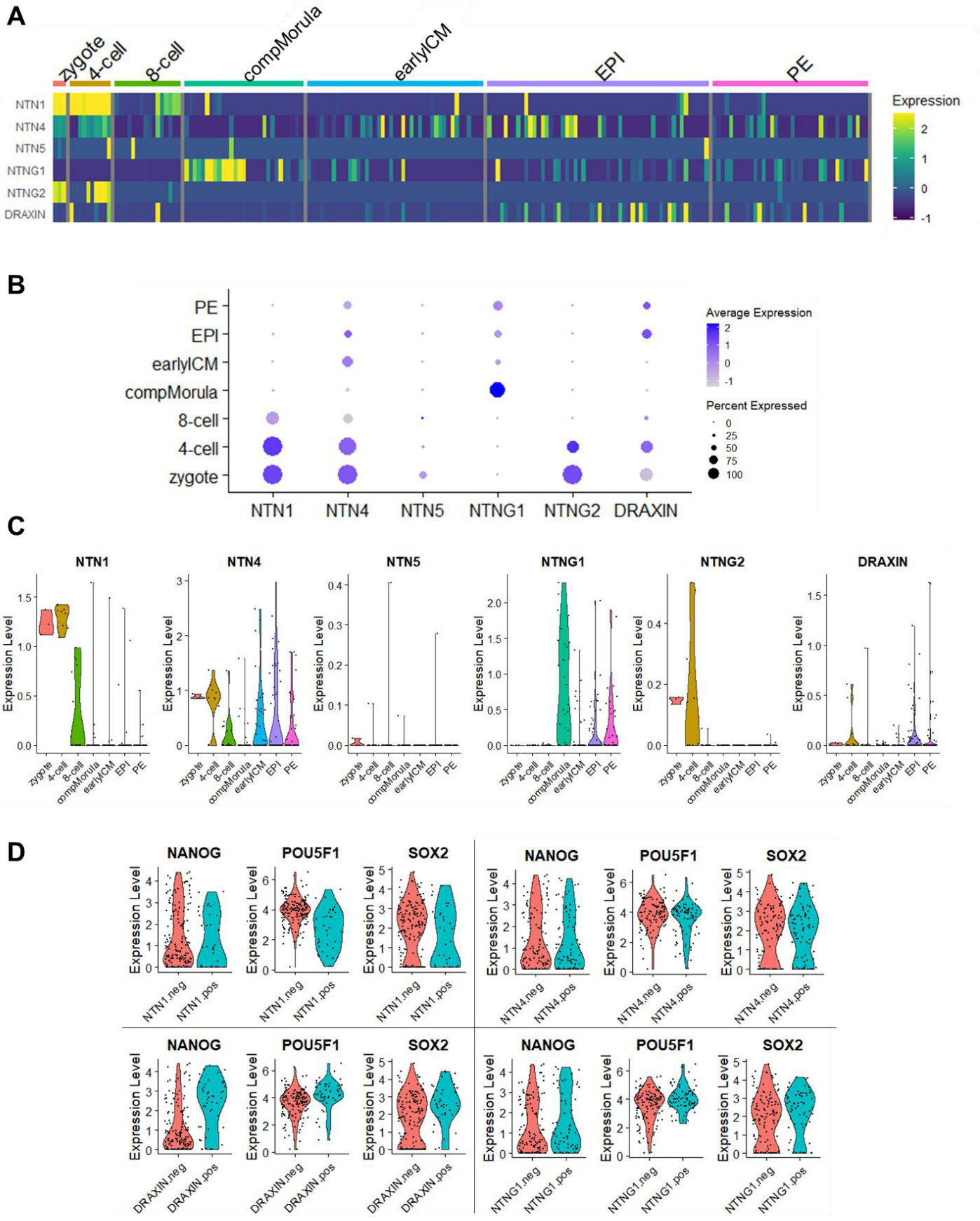

Figure 16. The human pre-implantation epiblast is devoid of *NTN1* transcript.

Overview of the Netrin family genes expression in the human pre-implantation embryo (original dataset from Stirparo et al. 2016). (**A-B**) Heatmap and dotplot of the netrin family genes expression in the human pre-implantation tissues. compMorula, compacted morula.(**C**) Violin plots of *NTN1-4*, *NTNG1-G2* and *DRAXIN* expression. (**D**) Violin plots of *NANOG*, *OCT4* and *SOX2* expression in *NTN1,4, DRAXIN* and *NTNG1*-positive or –negative cells.

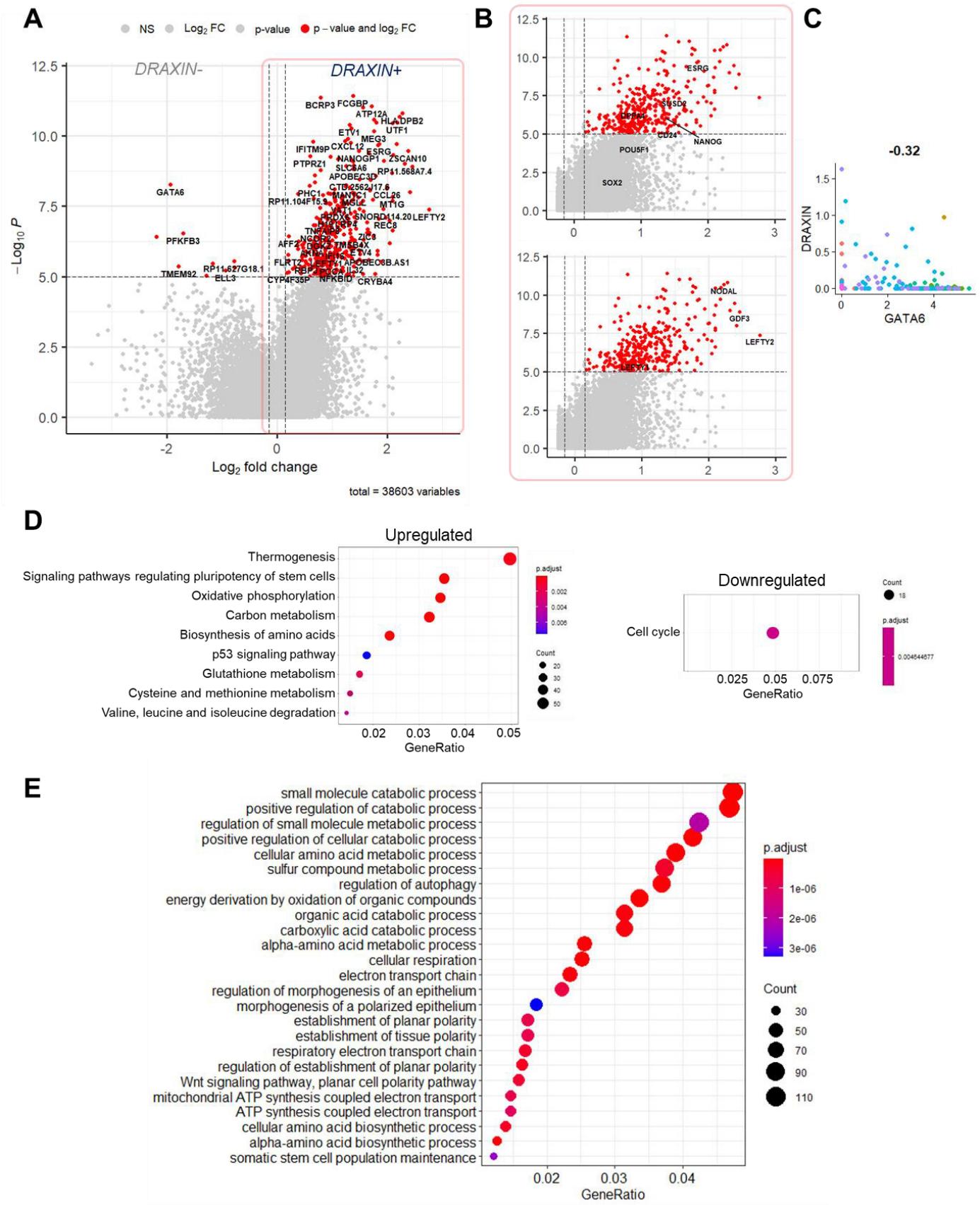

Figure 17. *DRAXIN*-positive cells of the human pre-implantation embryo are pluripotent and display active Wnt and NODAL signaling.

(**A**) Volcano plot of DRAXIN+ vs DRAXIN- DEGs of the human pre-implantation embryo. (**B**) Enlargement of the red-framed part of (**A**) highlighting pluripotency (top panel) and Nodal (bottom panel) signaling associated genes. (**C**) Correlation plot and coefficient of *GATA6* vs *DRAXIN* expression in the human pre-implantation embryo. (**D**) KEGG pathway analysis performed on DEGs (average Log2(FC)>0,25 and <-0,25) of DRAXIN+ (left panel: upregulated) vs DRAXIN- (right panel: downregulated) cells. (**E**) Gene Ontology analysis performed on upregulated genes (average Log2(FC)>0,25) of DRAXIN+ vs DRAXIN- cells.

I.5. Netrin receptors in the human pre-implantation embryo

We next explored expression of netrin receptors (*UNC5A-D*, *DCC* and *NEO1*) in the same dataset. We observed that all receptors, except *UNC5B,* exhibit zygotic expression followed by a rapid downregulation at the 8-cell stage (**Figure 18A** and **B**). Among these, only *NEO1* sustains a high and steady level at the compacted morula, early ICM and blastocyst (both EPI and PE) stages, while others (*UNC5A*, *-C*, *-D* and *DCC*) are expressed at very low levels and/or by a negligible fraction of cells. *UNC5B* shows a sharply different pattern, mostly undetected until the blastocyst stage where it is strongly upregulated in both *EPI* and *PE* (**Figure 18C**). Because only *NEO1* and *UNC5B* are expressed at this developmental point, we decided to further characterize the *NEO1*+ and *UNC5B*+ populations. We found that, while *UNC5B*+ cells show higher levels of *NANOG* and *OCT4*, the converse is true for *NEO1*+ cells, exhibiting lower *NANOG* and *OCT4* than their negative counterparts. In both *UNC5B*+ and *NEO1*+ populations, *SOX2* expression is unaffected (**Figure 18D**). In addition to these findings, we observed that *NEO1* and *UNC5B* expression anti-correlate in the dataset, despite their overlap at the blastocyst stage. Furthermore, *UNC5B* was found to strongly correlate with *NANOG* and anti-correlate with the PE marker *GATA6* (**Figure 18E**). Taken together, these observations indicate that, while *NEO1* is ubiquitously expressed in the human pre-implantation embryo, *UNC5B* expression is likely a marker of the early epiblast.

To further demonstrate this hypothesis, we studied *UNC5B*+ cells transcriptome by generating volcano plots of *UNC5B*+ vs *UNC5B*- DEGs. Similarly to the *DRAXIN*+ population, we found multiple pluripotency-associated genes to be upregulated in *UNC5B*+ cells, including the naïve marker *DPPA4.* Consistently with our preceding observations, *SOX2* is the only pluripotency marker considered that exhibits a similar level of expression between *UNC5B*+ and – cells. We observed that enrichment in pluripotency genes expression in *UNC5B*+ is accompanied by a strong enrichment for NODAL signaling members such as *GDF3*, *LEFTY1*, *-2*, *TDGF1* and *NODAL* (**Figure 19A** and **B**). KEGG pathway and GO analyses with the most differentially expressed genes from the *UNC5B*+/- populations showed that *UNC5B*+, as *DRAXIN*+ cells, are enriched for terms associated with pluripotency, oxidative phosphorylation and active amino acids biogenesis and metabolism (**Figure19C** and **D**). Altogether, these results confirm that *UNC5B* expression in the human pre-implantation embryo is correlated to naïve pluripotency and likely epitomizes the early epiblast, thus phenotypically overlapping with *DRAXIN*+ cells.

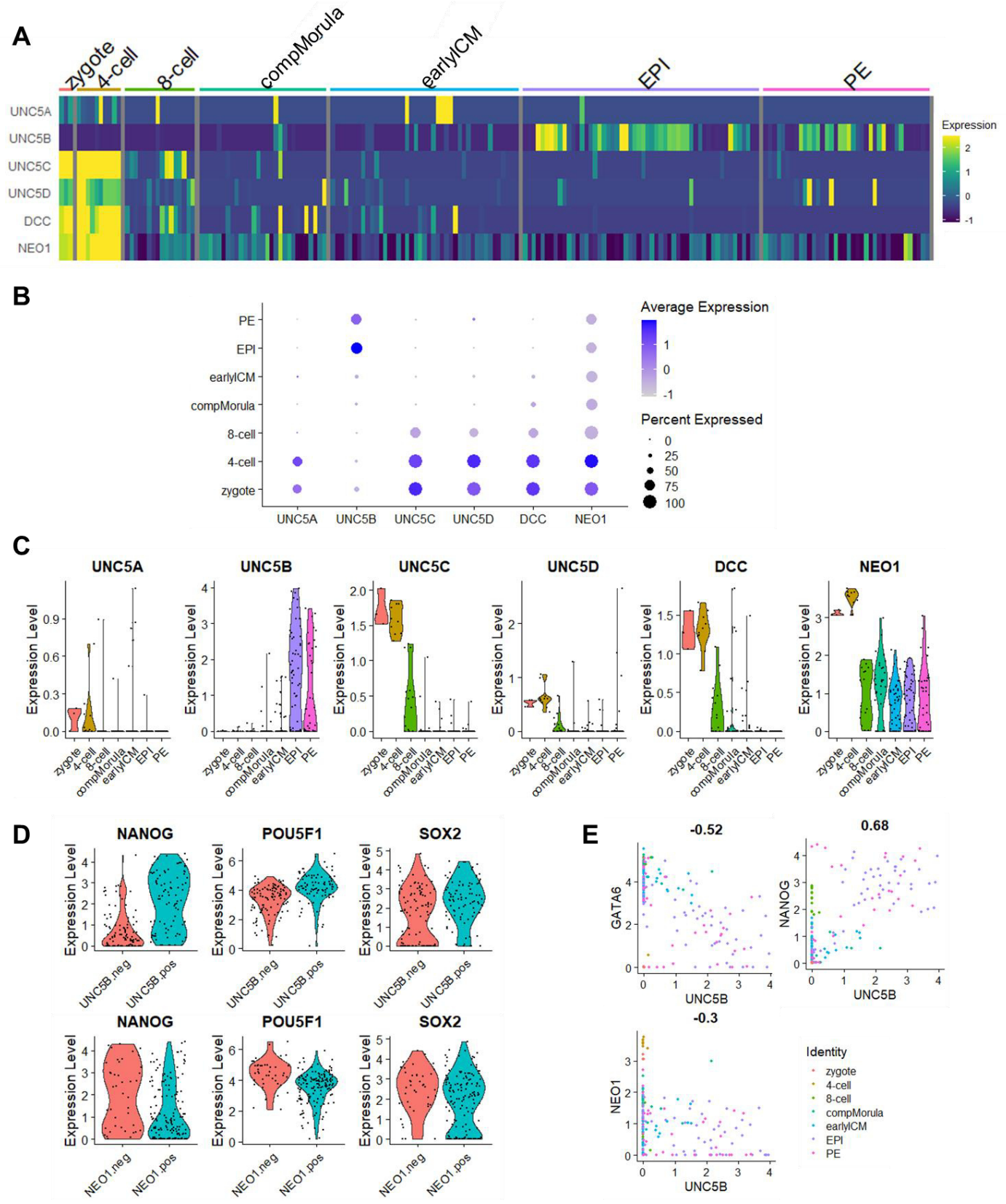

Figure 18. *NEO1* is ubiquitously expressed in the human pre-implantation embryo while UNC5B is specific to the Epiblast and Primitive Endoderm.

(**A**) Overview of the Netrins receptors expression in the human pre-implantation embryo (original dataset from Stirparo et al. 2016). (**A-B**) Heatmap and dotplot of the netrins receptors expression. compMorula= compacted morula.(**C**) Violin plots of *UNC5A-D, DCC* and *NEO1* expression at different embryonic stages. (**D**) Violin plots of *NANOG*, *OCT4* and *SOX2* expression in *UNC5B* and *NEO1*-positive or –negative cells. (**E**) Correlation plots and coefficients (displayed as title of each plot, -1<p<1 ; p=-1, complete anti-correlation, p=1, complete correlation, p=0, no correlation) of *UNC5B* vs *GATA6, NANOG or NEO1* expression at all pre-implantation stages.

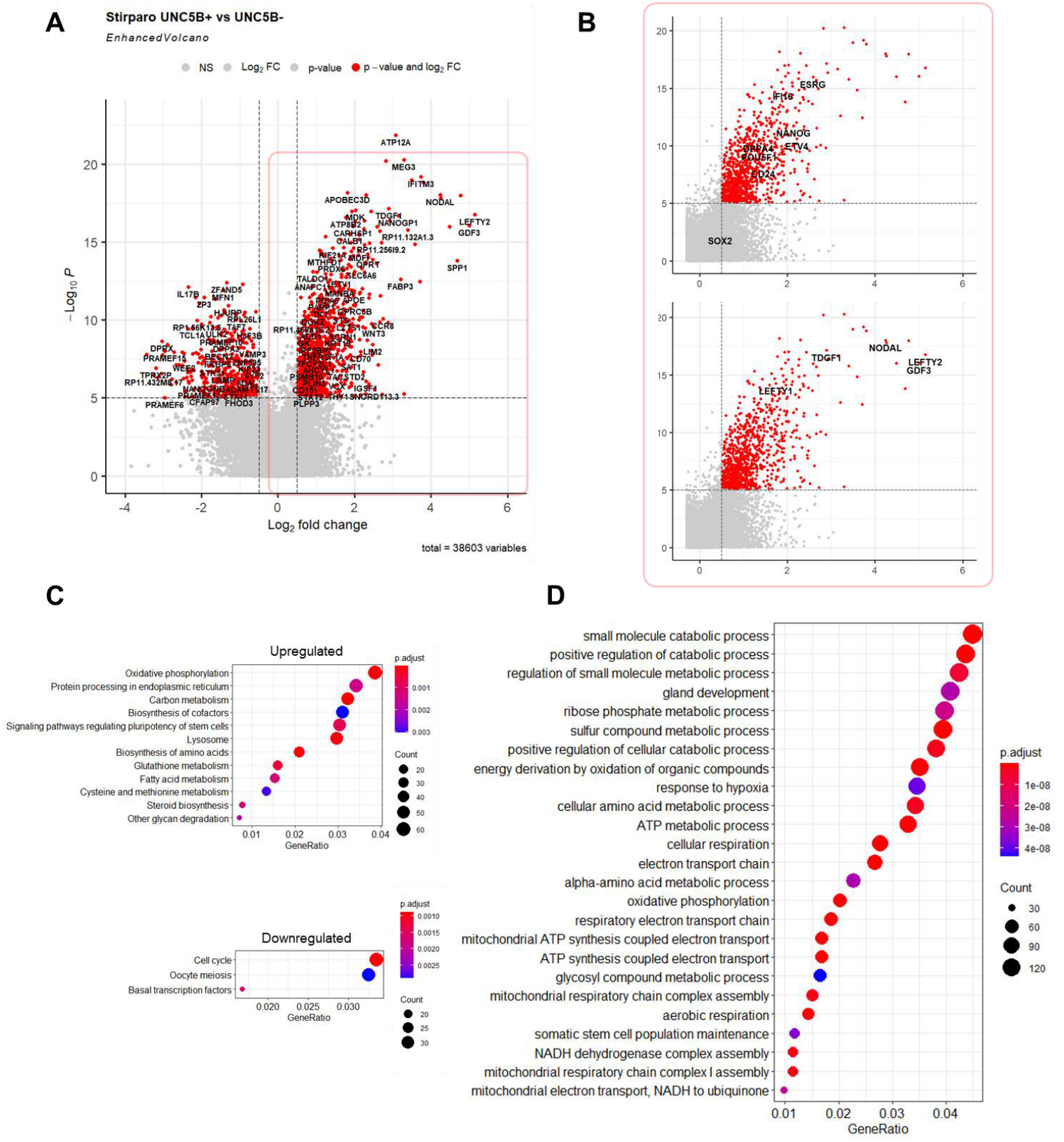

Figure 19. *UNC5B*-positive cells of the human pre-implantation embryo epitomize the naive epiblast compartment.

(**A**) Volcano plot of UNC5B+ vs UNC5B- DEGs of the human pre-implantation embryo. (**B**) Enlargement of the red-framed part of (**A**) highlighting pluripotency (top panel) and Nodal (bottom panel) signaling associated genes. (**C**) KEGG pathway analysis performed on DEGs (average Log2(FC)>0,25 and <-0,25) of UNC5B+ (top panel: upregulated) vs UNC5B- (bottom panel: downregulated) cells. (**D**) Gene Ontology analysis performed on upregulated genes (average Log2(FC)>0,25) of UNC5B+ vs UNC5B- cells.

To obtain a complete overview of Netrin family genes patterns in the human pre-implantation embryo, we finally analyzed *NEO1*+ cells transcriptome. As previously mentioned, this population spans from the zygote to blastocyst stages with high enrichment in all tissues, including the EPI and PE. We found that, despite their representation in the pluripotent compartment, *NEO1*+ cells are strongly downregulated for *NANOG*, *OCT4*, and *SUSD2*. The NODAL signaling members found upregulated in the *UNC5B*+ population are also all downregulated in *NEO1*+ cells (**Figure 20A** and **B**). In line with these observations, we found through KEGG pathway analysis that *NEO1*+ cells are impoverished for genes associated with oxidative phosphorylation (**Figure 20C**), while GO databases returned numerous terms associated with meiosis and ciliogenesis. This suggests that *NEO1*, despite being expressed in the human epiblast, is not a marker of naïve pluripotency and is likely involved in different early embryogenesis mechanisms.

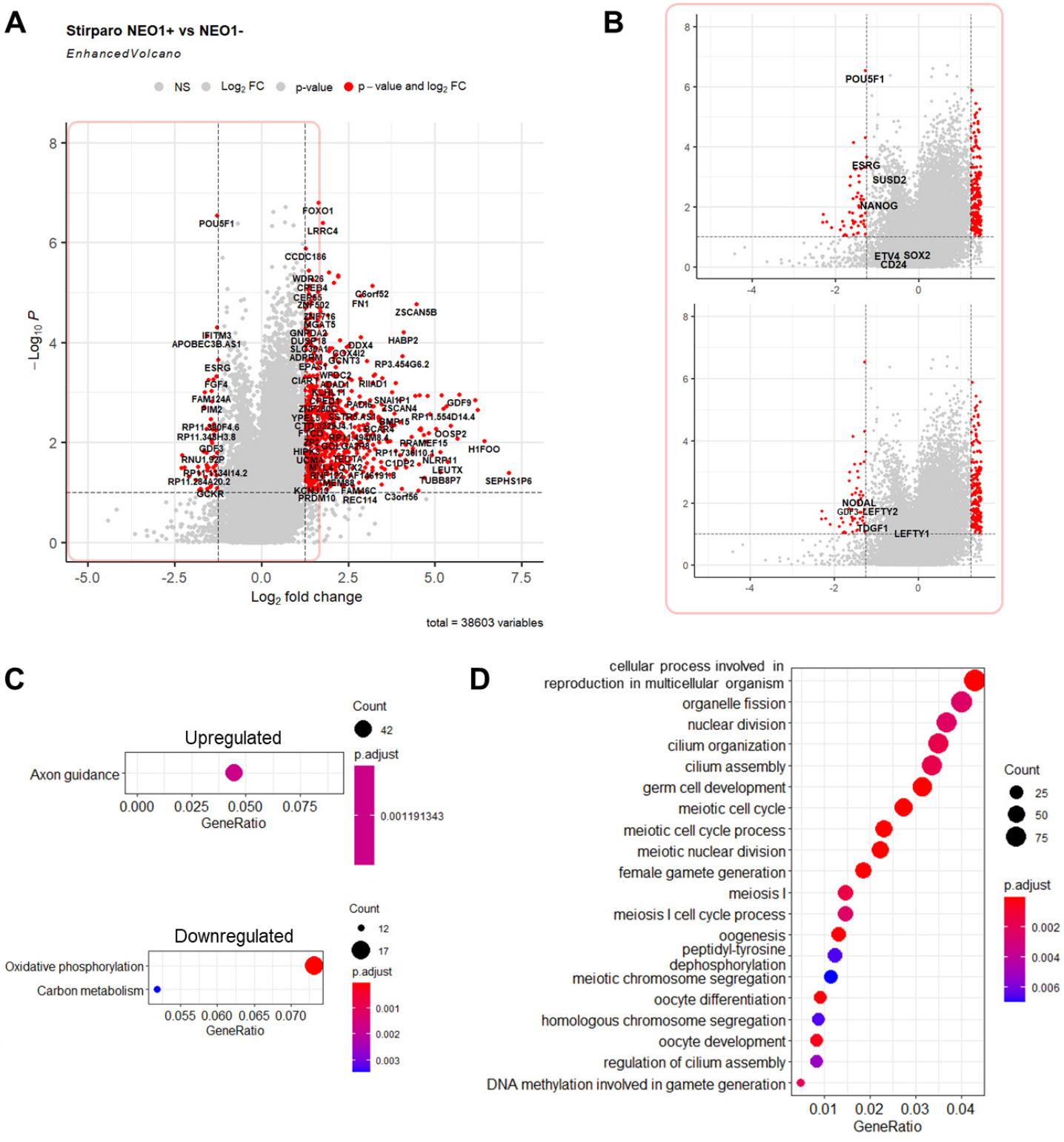

Figure 20. *NEO1*-positive cells of the human pre-implantation embryo are impoverished for pluripotency markers and undergo processes associated with differentiation.

(**A**) Volcano plot of NEO1+ vs NEO1 DEGs of the human pre-implantation embryo. (**B**) Enlargement of the red-framed part of (**A**) highlighting pluripotency (top panel) and Nodal (bottom panel) signaling associated genes. (**C**) KEGG pathway analysis performed on DEGs (average Log2(FC)>0,25 and <-0,25) of NEO1+ (top panel: upregulated) vs NEO1- (bottom panel: downregulated) cells. (**D**) Gene Ontology analysis performed on upregulated genes (average Log2(FC)>0,25) of NEO1+ vs NEO1- cells.

II. Netrin family genes in primates Pluripotent Stem Cells

II.1. Netrin family genes in non-human primate PSCs

In order to know if our observations *in vivo* could be verified *in vitro*, we then decided to explore netrin family genes expression in primates PSCs. We first performed bulk RNA-sequencing on rhesus monkey PSCs (LyonES cell line, characterized by Wianny et al., 2008.) in the primed state or reprogrammed to naïve-like pluripotency with three methods : ENHSM (modification of the original NHSM protocol from Gafni et al., 2013), 4i (Fang et al., 2014) and TL2i (Chen et al., 2015). In primed cells, we noticed very low levels of *NTN1*, but high *DRAXIN*, *NTN4, NEO1*, *UNC5B* and UNC5D, consistently with our observations in the post-implantation macaque embryo (**Figure 21A**). Unlike the embryo however, *NTN5* expression was here detected. After reprogramming with the 4i and TL2i method, we observed a slight increase of *NTN1*, a decrease of *DRAXIN* and *UNC5D*, and almost complete disruption of *NTN4* and *-5* expression. In these cells, the *NTN1-UNC5B-NEO1* triad is thus expressed along with *DRAXIN*, similarly to what was found in the macaque early epiblast. Cells reprogrammed with the third method, ENHSM, however showed a pattern of netrin family genes expression almost exactly similar to the primed condition. This is consistent with previous reports showing weak or partial acquisition of naïve characteristics from NHSM cells (Aksoy et al., 2021; Theunissen et al., 2014). We confirmed these results with quantitative PCR (qPCR) analysis on rhesus PSCs reprogrammed with the three protocols already mentioned and two more, LCDM (Yang et al., 2017) and TLCDK8i (Original protocol from Lynch et al., 2020 combined with STAT3ER activation). When comparing these cells with their primed counterparts, we observed an upregulation of *NTN1*, *NEO1*, a downregulation of *NTN4* with all reprogramming methods, and an upregulation of *UNC5B* with TL2i, 4i and TLCDK8i (**Figure 21B**). This is in accordance with our findings in bulk RNA-seq, and consistent with observations made in the embryo. A compelling observation, however, is the co-increase of *NTN3* and *NTN1,* observed neither *in vivo* nor *in vitro* through bulk RNA-seq.

II.2. Netrin family genes in human PSCs

We next explored netrin family genes expression in human PSCs, and for this first looked over raw microarray data from naïve-like 5i/L/A cells (Original data from Theunissen et al., 2014). We observed that Netrin ligands and *DRAXIN* are weakly expressed compared to *NANOG*, and that among the receptors, *UNC5B*, *NEO1* and *DCC* exhibit the highest expression levels, two or three-fold higher than their ligands (**Figure 21C**). We additionally

compared human cell lines reprogrammed with the 5i/L/A or t2iLGöY / Reset (Takashima et al., 2014) methods to their primed counterparts, and noticed important discrepancies in netrin family genes between the two protocols. While 5i/L/A cells upregulate all genes of the family upon reprogramming except the *UNC5B* and *-D* receptors, t2iLGöY only show weak upregulation of *NTN3* and *-4*, and downregulation of *DRAXIN*, *NEO1*, *DCC* and *UNC5D* (**Figure 21D**). These results suggest that, contrary to the macaque and mouse, culture of human PSCs in media sustaining self-renewal in a naïve-like state does not trigger a systematic upregulation of *NTN1*, and yield overall various outcomes in Netrin family genes expression.

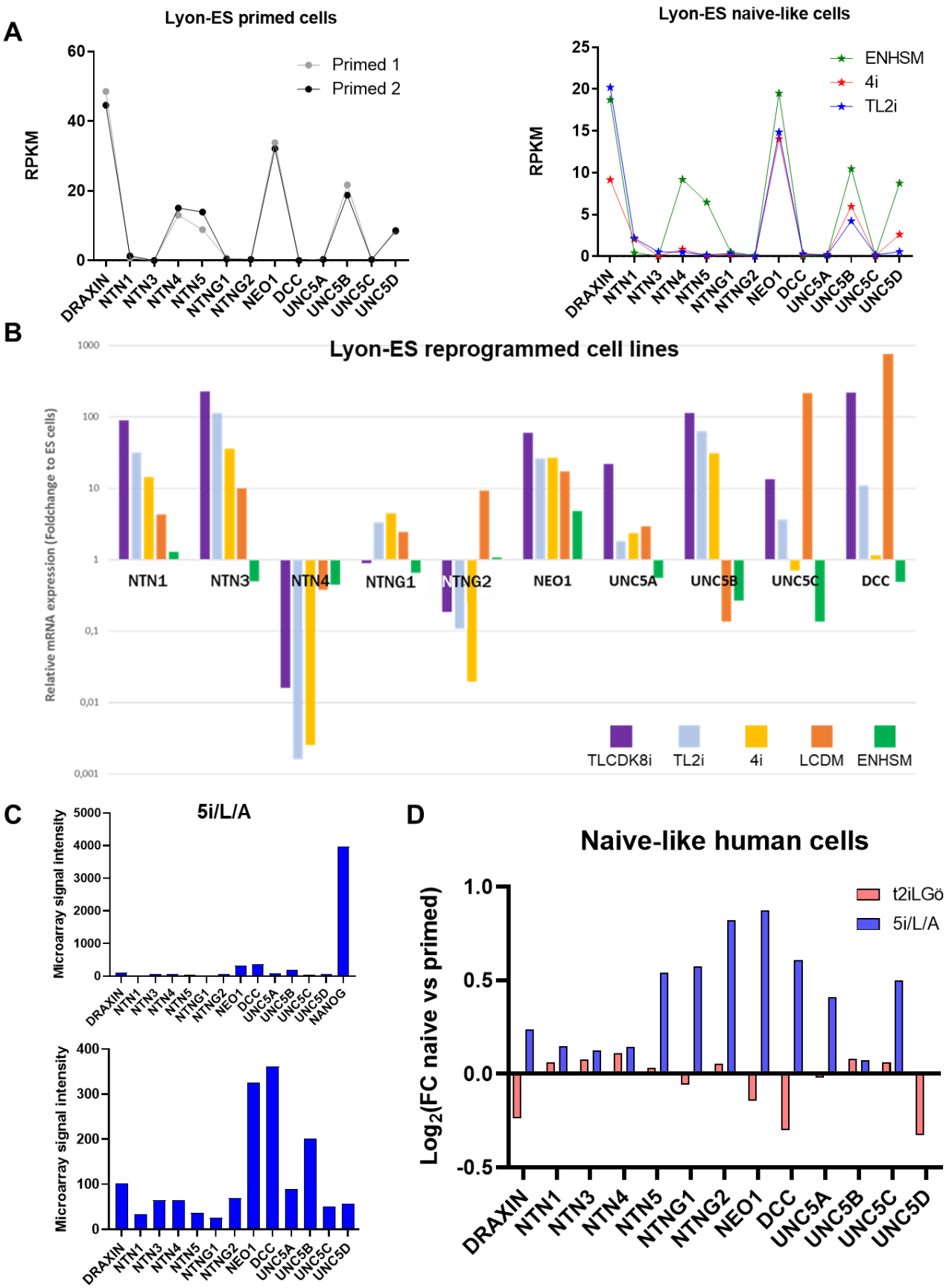

Figure 21. Netrin Signaling in primates pluripotent stem cells.

(**A**) Expression of Netrin family members in Primed (left plot) and Naive-reprogrammed (right plot) LyonES rhesus macaque PSCs (Bulk RNA-seq data from Aksoy et al. 2021). (**B**) qPCR analysis of Netrin family genes expression in naive-like rhesus macaque PSCs compared to primed rhesus macaque ESCs.(**C**) Raw microarray data from human 5i/L/A cells (Theunissen et al. 2014) (**D**) Ratio of Netrin family genes expression from microarray data of t2iLGö (Takashima et al. 2014) and 5i/L/A (Theunissen et al. 2014) cells compared to their primed counterparts.

III. *NTN1* overexpression in primates Pluripotent Stem Cells.

III.1. *NTN1* overexpression in rhesus PSCs – STAN1 cells

To investigate the effect of Netrin signaling in primates' pluripotency, we decided to overexpress *NTN1* in primed LyonES rhesus cells. For this, we used a Tet-On 3G, doxycycline-inducible PiggyBac system called "XLone", for which robust transgene induction in 24h has been demonstrated in human PSCs (Randolph et al., 2017). We replaced Xlone's GFP cassette by a *NTN1-HA*-tag fusion gene and electroporated LyonES rhesus cells with the XLone-NTN1-HA construction, resulting in the creation of the STAT3ER-NTN1 (STAN1) cell line (**Figure 22A**). After selection of the clones, we confirmed induction efficiency through western blot analysis, and selected two clones for further characterization (**Figure 22B**). To explore a potential dose-effect of *NTN1* induction, we submitted STAN1 cells to a doxycycline (hereafter dox) scale comprising five different concentrations (0, 100, 500, 1000 and 2000 ng/mL) for 72h. For both clones, we observed discrete morphological changes at the highest (1000 and 2000 ng/mL) dox concentrations, with a light flattening and thinning of colonies (**Figure 22C**). After 72h, no cell death or marked change of proliferation could be observed in any +dox condition compared to the -dox control. We analyzed the transcription profile of induced STAN1 clones by qPCR, using as a reference non-induced STAN1 cells. We first confirmed gradual and efficient induction of *NTN1-HA* in response to the dox scale, and observed that other Netrin genes are either not detected (*NTN3* and-*5*) or not affected (*NTN4* and *DRAXIN*) by *NTN1* induction (**Figure 22D**). Among the receptors, only *NEO1* shows a light and gradual increase in response to *NTN1* induction in both clones, while *UNC5B* and *-D* exhibit different behaviors from one clone to another with no clear increase. We then tested expression of several core, primed and naïve pluripotency, as well as early lineage differentiation markers, and did not observe significant downregulations in any case. Several genes from the pluripotency categories (*KLF5*, *FGF5*, *PITX2*, *DPPA5* and *ICAM1*) are upregulated upon induction in both clones, albeit with foldchanges not exceeding 3 with the highest dox concentrations. Most of the differentiation genes tested however, are unaffected by *NTN1* induction, with the exception of *GATA6* that exhibits a slender increase in the 1000 and 2000 ng/mL dox conditions. Collectively, these data suggest that *NTN1* overexpression only triggers discrete morphological and transcriptomic changes in macaque primed PSCs.

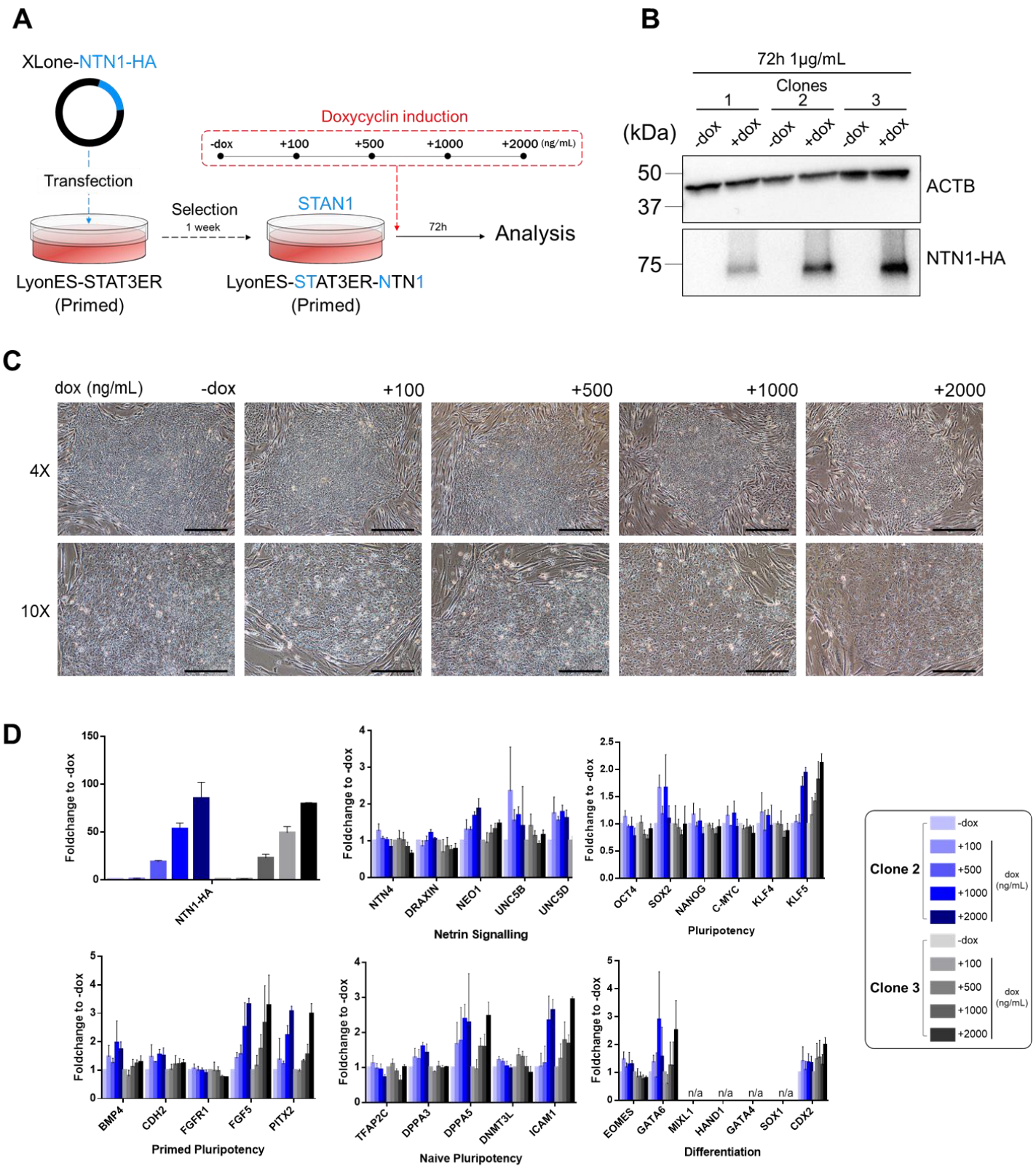

Figure 22. Rhesus monkey STAN1 ESCs are weakly affected by *NTN1* overexpression.

(**A**) Scheme describing the rhesus STAN1 cell line creation and protocol followed for (**B**) and (**C**) analyses. Primed STAN1 cells were submitted to gradual dox concentrations (0,100, 500, 1000, 2000 ng/mL) for 72h. (**B**) Western blot of *NTN1-HA* protein expression in three rhesus STAN1 clones with or without doxycyclin induction (72h, 1µg/mL). (**C**) Brightfield photos of primed rhesus STAN1 colonies submitted to increasing dox concentrations. Scale bars, 4X: 500µM; 10X: 200µM (**D**) Quantitative-PCR analysis of STAN1 rhesus ESCs submitted to the dox scale applied in (**C**).

III.2. *NTN1* overexpression in primed human PSCs – hSTAN1 cells

Because of the minor changes observed in rhesus PSCs, and because such cells show increased instability compared to human PSCs when cultured in media initially designed for the latter, we decided to carry on experiments with human PSCs. We used for this the male ES cell line F-OS3-10, expressing a *STAT3-ER* transgene (derived and characterized by Chen et al., 2015). Using a similar protocol to STAN1 cells creation, we thus generated human STAN1 (hSTAN1) cells (**Figure 23A**). We verified hSTAN1 clones' induction by western blotting and immunostaining, and selected two clones (c10 and c15) for subsequent work (**Figure 23B**). After a 72h dox induction at 1µg/mL, we noticed that hSTAN1 colonies homogeneously express the NTN1-HA protein, although net-like aggregates form at the periphery (**Figure 23C**). We submitted hSTAN1 cells to a dox scale modified from our previous experiments, adding very low concentrations (10, 30, 100, 300 and 1000ng/mL) to explore a possible low-dose effect of induction. Upon treatment, we observed sharp morphological changes in both clones from the +100 to +1000 points (**Figure 23D**). Phenotype is stronger but comparable to STAN1 cells, with a flattening and thinning of colonies without size change. After 72h of induction, we noticed no increase of cell death or proliferation in +dox dishes in comparison to the control. By qPCR, we analyzed the transcriptome of induced hSTAN1 cells compared to their non-induced counterparts. Increase of *NTN1* transcripts in response to dox was confirmed but, contrary to what was observed in rhesus cells, we found an overall decrease of several pluripotency markers upon induction, including *NANOG*, *OCT4*, and the gene coding for a primed surface marker *CD24* (**Figure 24A**). Three pluripotency genes: *SOX2*, *BMP4* and *CDH2* are unaffected by dox treatment. Despite the overall downregulation of pluripotency, we however did not notice an equivalent upregulation of early lineage markers *EOMES*, *GATA6* and *NESTIN*. Among the netrin genes family, only *UNC5B* and *DRAXIN* returned detectable levels of expression, both decreasing upon *NTN1* induction. Interestingly, we observed that 11 (*NANOG, OCT4, PITX2, C-MYC, KLF4, FGF5, DPPA5, DRAXIN, UNC5B*, *EOMES* and *GATA6*) out of the 18 genes tested show a peak of expression at the 30 ng/mL dox point. By immunostaining, we confirmed that the NANOG, OCT4 and CD24 proteins are visibly downregulated at the +300 and +1000ng/mL dox points, but could not observe any peak of signal at +30ng/mL (**Figure 24B**). At the highest dox concentration, we noticed that NANOG and OCT4 expression is extinguished in most of the cells, but that both proteins remain co-expressed in patches in the central part of colonies. We observed a similar pattern for the primed cell-surface marker CD24. The SOX2 protein, on the other hand, is homogeneously expressed in all hSTAN1 colonies regardless of the dox treatment applied, consistently with our previous results. Altogether, these data show that primed hSTAN1 cells

undergo marked morphological changes upon *NTN1* induction and, unlike rhesus STAN1 cells, undergo pluripotency exit in a cluster fashion.

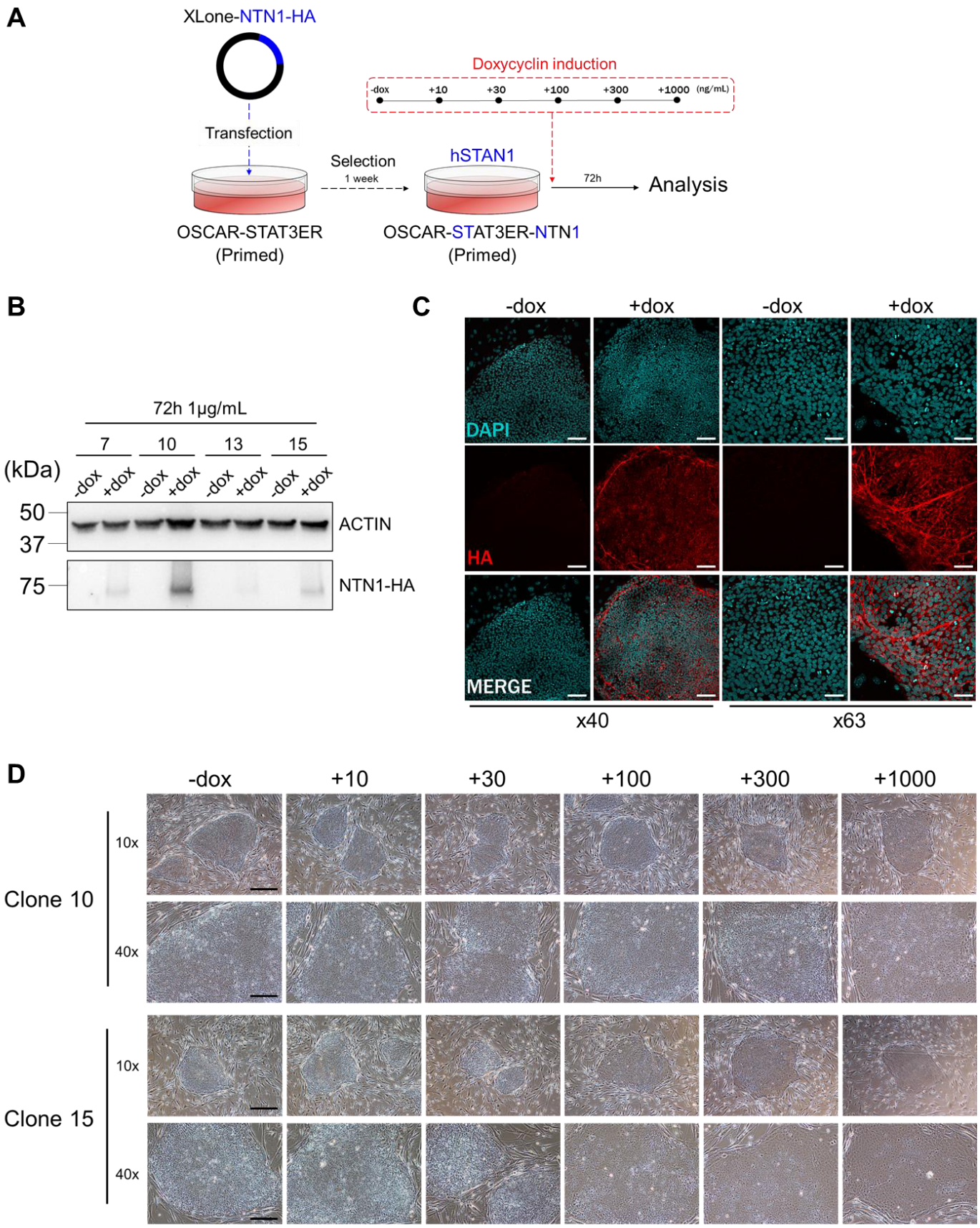

Figure 23. Creation of the human STAN1 (hSTAN1) cell line.

(**A**) Scheme describing the protocol followed for hSTAN1 cell line creation and (**B-D**) analyses. Primed hSTAN1 cells were submitted to gradual dox concentrations (0, 10, 30, 100, 300 and 1000 ng/mL) for 72h. (**B**) Western blot of NTN1-HA protein expression in four hSTAN1 ESCs clones with or without doxycyclin induction (72h, 1µg/mL). (**C**) Immunostaining of HA (NETRIN1) in primed hSTAN1 cells treated with 1µg/mL dox for 72h. Scale bars: 40x, 50µm; 63x, 35µm (**D**) Brightfield photos of primed hSTAN1 cells submitted to the dox scaled described in (**A**); Scale bars: 10x, 200µm; 4x, 500µm.

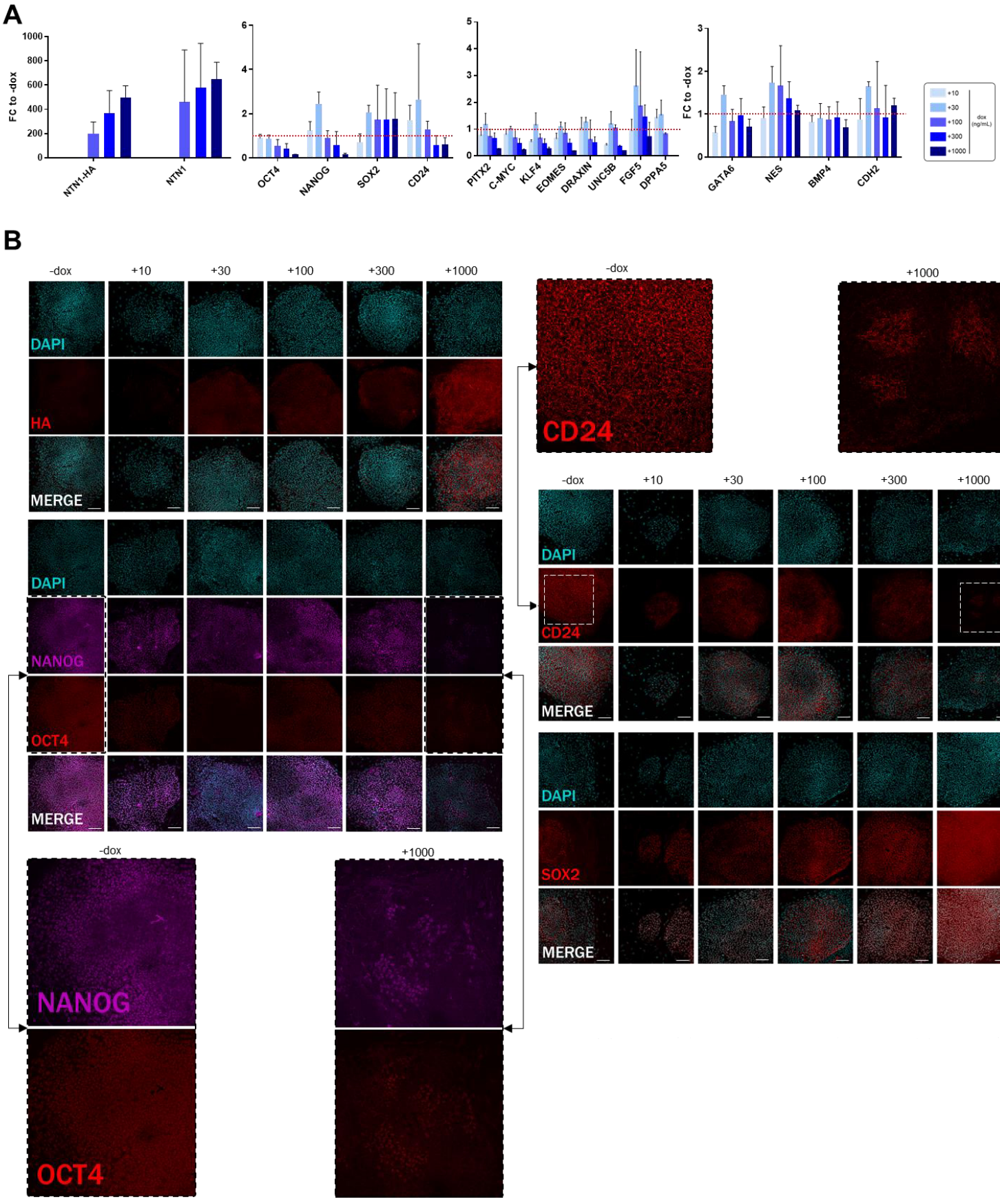

Figure 24. Primed hSTAN1 cells undergo pluripotency collapse upon induction.

(**A**) qPCR analysis of primed hSTAN1 cells submitted to different dox concentrations for 72h. (**B**) Immunostaining of HA(NETRIN1), NANOG, OCT4, CD24 and SOX2 in primed hSTAN1 cells submitted to different dox concentrations (ng/mL) for 72h. Scale bars, 50µm.

III.3. *NTN1* overexpression in reprogrammed human PSCs – TL2i-hSTAN1 cells

To address if *NTN1* overexpression has a similar effect on pluripotency in a naïve versus to primed context, we next reprogrammed our hSTAN1 cells with the TL2i method. After reprogramming, TL2i-hSTAN1 displayed the typical naïve-like morphology and characteristics reported in previous publications (Aksoy et al., 2021; Chen et al., 2015). Upon treatment with the dox scale applied on primed hSTAN1, we observed a change of morphology gradually accentuating with concentration (**Figure 25A**). Induced TL2i-hSTAN1 colonies are flattened with an overall increase of size, reaching a point close to confluency after 72h in the +1000 condition. By applying the same doxycycline treatment to a control TL2i-OS3 cell line, no morphological transformation could be seen at any concentration, confirming that changes observed with TL2i-hSTAN1 are caused by the XLone-NTN1 transgene activation. We next analyzed TL2i-hSTAN1 transcriptome through qPCR and found, similarly to primed hSTAN1, that *NTN1* expression is efficiently induced in response to dox (**Figure 25B**). While we observed a slight increase of *NTN3*, all other netrin ligands, receptors and *DRAXIN* share a similar pattern, with a peak of expression at +10 and +30 ng/mL dox (*NTNG1, UNC5A-C*) or +30 ng/mL (*DRAXIN*, *NTN4*, *NEO1* and *UNC5D*) followed by a gradual downregulation. We found a similar behavior for core, primed and naïve pluripotency markers with the exception of *KLF5*, the only pluripotency gene upregulated upon induction (**Figure 25C**). As reported for primed hSTAN1, commitment to early lineage differentiation could not be demonstrated, as no endodermal (*GATA6*, *SOX17*), ectodermal (*FST*, *PAX6*) or mesodermal (*EOMES*) marker is upregulated as a matter of induction. Instead, all rather exhibit a pattern similar to pluripotency markers, with a single peak of expression at +30 followed by a downregulation. To gain better insight on the contrasting low- vs high-dose effects, we performed immunostaining on cells treated with the lowest (+10, +30) and highest (+1000) dox concentrations. We found faint expression of NTN1-HA at the lowest doses, while strong signal is visible at the +1000 concentration (**Figure 25D**). As observed for primed hSTAN1, we noticed that NTN1 is thoroughly expressed in TL2i-hSTAN1 colonies, but enriched in a net-like structure at the periphery. OCT4 staining revealed that, as for primed hSTAN1, reprogrammed cells heterogeneously lose expression of the core pluripotency marker, and remaining signal is located in the central area of colonies. Unlike what was suggested by our qPCR analysis, we did not find an increase of OCT4 staining in the +30ng/mL condition compared to untreated cells. Collectively, these data show that naïve-like hSTAN1 cells, as their primed counterparts, change morphology and lose pluripotency in a dose-dependent fashion upon *NTN1* induction.

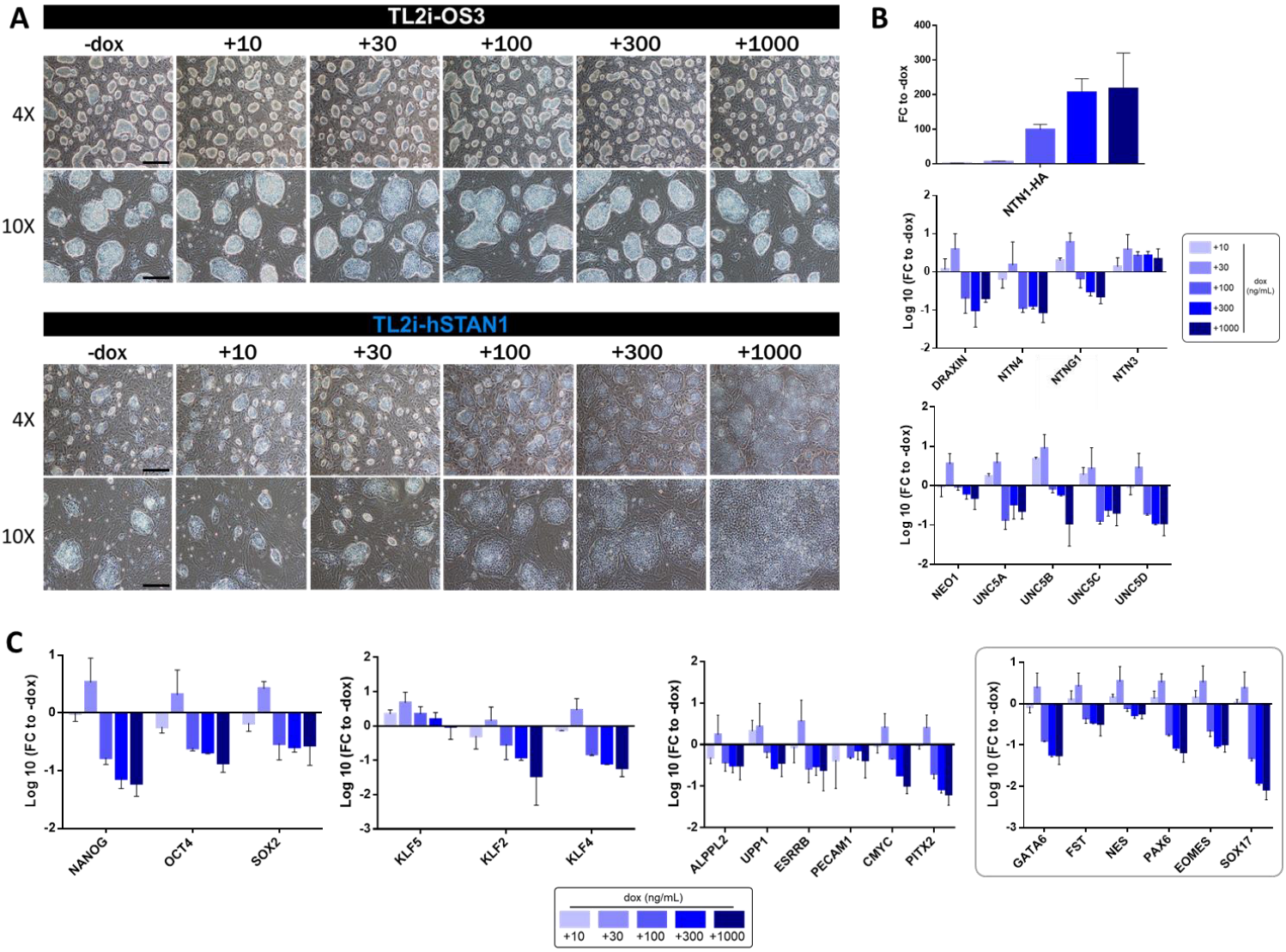

(legend on next page)

In both cases, however, no commitment to early-lineage differentiation could be demonstrated, and transcriptomic analyses returned a peak of expression in discordance with protein observations at the lowest doxycycline doses.

Figure 25. NTN1 overexpression in naive-like hSTAN1 cells triggers pluripotency collapse and morphological transformation.

(**A**) Brightfield photos of TL2i-reprogrammed OS3 (control, top panel) and hSTAN1 (bottom panel) cells submitted to gradual dox concentrations for 72h. Scale bars: 4X, 500µm; 10X, 200µm. (**B**) qPCR analysis of Netrin family genes in TL2i-hSTAN1 cells upon dox induction. (**C**) qPCR analysis of pluripotency-associated and differentiation (gray frame) genes in TL2i-hSTAN1 cells upon dox induction. (**D**) Immunostaining of HA (NETRIN1) and OCT4 in TL2i-hSTAN1 cells with or without dox induction. Scale bars: 40X, 50µm; 63X: 35µm.

IV. Single-cell RNA sequencing of TL2i-hSTAN1 cells.

To further investigate *NTN1* overexpression effect on human naïve-like cells, we decided to perform single-cell RNA sequencing on TL2i-hSTAN1 cells. We selected a clone (c15) that displayed the strongest morphological changes in response to induction, and treated it with, low (+10, +30ng/mL), high (+1000), or no dox for 72h. After trypsinization, cells were sorted out and collected by fluorescence-activated cell sorting (FACS), and a cDNA library preparation followed by sequencing were performed using the 10X genomics Chromium Single-cell 3' end protocol (**Figure 26A**). Because TL2i-hSTAN1 are cultured on mouse embryonic fibroblasts, we then mapped out and removed cells aligning with mouse genome (**Figure 26B**), and filtered out apoptotic debris and mitochondrial residues in the remaining population (**Figure 26C**). We thus obtained a final dataset comprised of an average 2100 cells per condition, with a mean read counts of 52000 (**Figure 26D**).

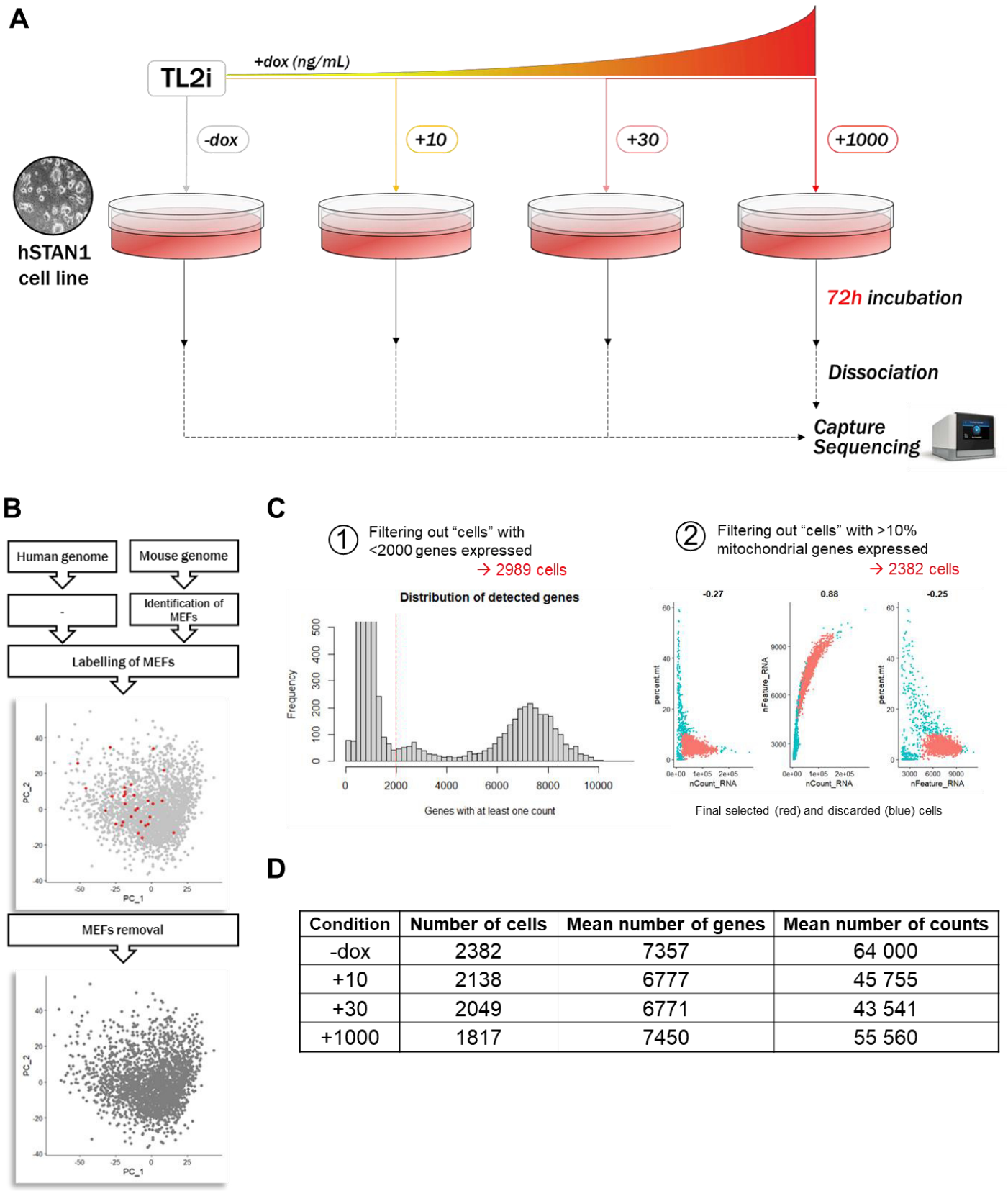

Condition	Number of cells	Mean number of genes	Mean number of counts
-dox	2382	7357	64 000
+10	2138	6777	45 755
+30	2049	6771	43 541
+1000	1817	7450	55 560

Figure 26. hSTAN1 10X Single-cell RNA-sequencing experiment overview.
(**A**) Schematic of the experimental design. (**B**) Mapping approach and removal of Mouse Embryonic Fibroblasts. (**C**) Library profiling : removal of dying cells and mitochondria (example displayed : dox0 condition). (**D**) Summary of the final number of cells, average number of genes and counts per cell sequenced.

IV.1. TL2i-hSTAN1 cells commit to mesodermal lineage after dox induction.

IV.1.a. TL2i-hSTAN1 cells undergo pluripotency exit upon induction

To characterize *NTN1* overexpression effect, we first evaluated the induction efficiency of our system. In absence of treatment (-dox condition), we found that most cells (91.9%) express no detectable *NTN1* (hereafter NTN1-zero population*)*; however, 7.6% display low levels of the transcript (**Figure 27A** and **B**). We termed that *NTN1* expression interval "endogenous" (NTN1-endo population). Upon dox treatment, we observed emergence of cells expressing *NTN1* up to 10-fold higher than the NTN1-endo levels. Cells expressing *NTN1* levels in that interval represent 46.6% of the population at the +10 ng/mL dox concentration, and increase to 79.2 and 84.5% at the +30 and +1000 doses, respectively (**Figure 27B**). As such levels of expression were not observed in the -dox condition, we considered this as product of the XLone-NTN1 system's induction, and refer to it as exogenous *NTN1* (NTN1-exo population). Interestingly, these observations are in sharp contrast with the kinetics of induction initially reported by Randolph and colleagues, where plateau phase is reached at the +1000 dox dose, and transgene-positive cells do not exceed 40% of the population with doses under 200ng/mL (Randolph et al., 2017), versus 10ng/mL in our hands. Incidentally, we noticed that few cells (0.4%, or 9 cells) from the -dox condition express exogenous levels of *NTN1*. This could be indicative of a system's leak; however, we did not observe any differentially expressed genes in these cells compared to their *NTN1-zero* counterparts (data not shown).

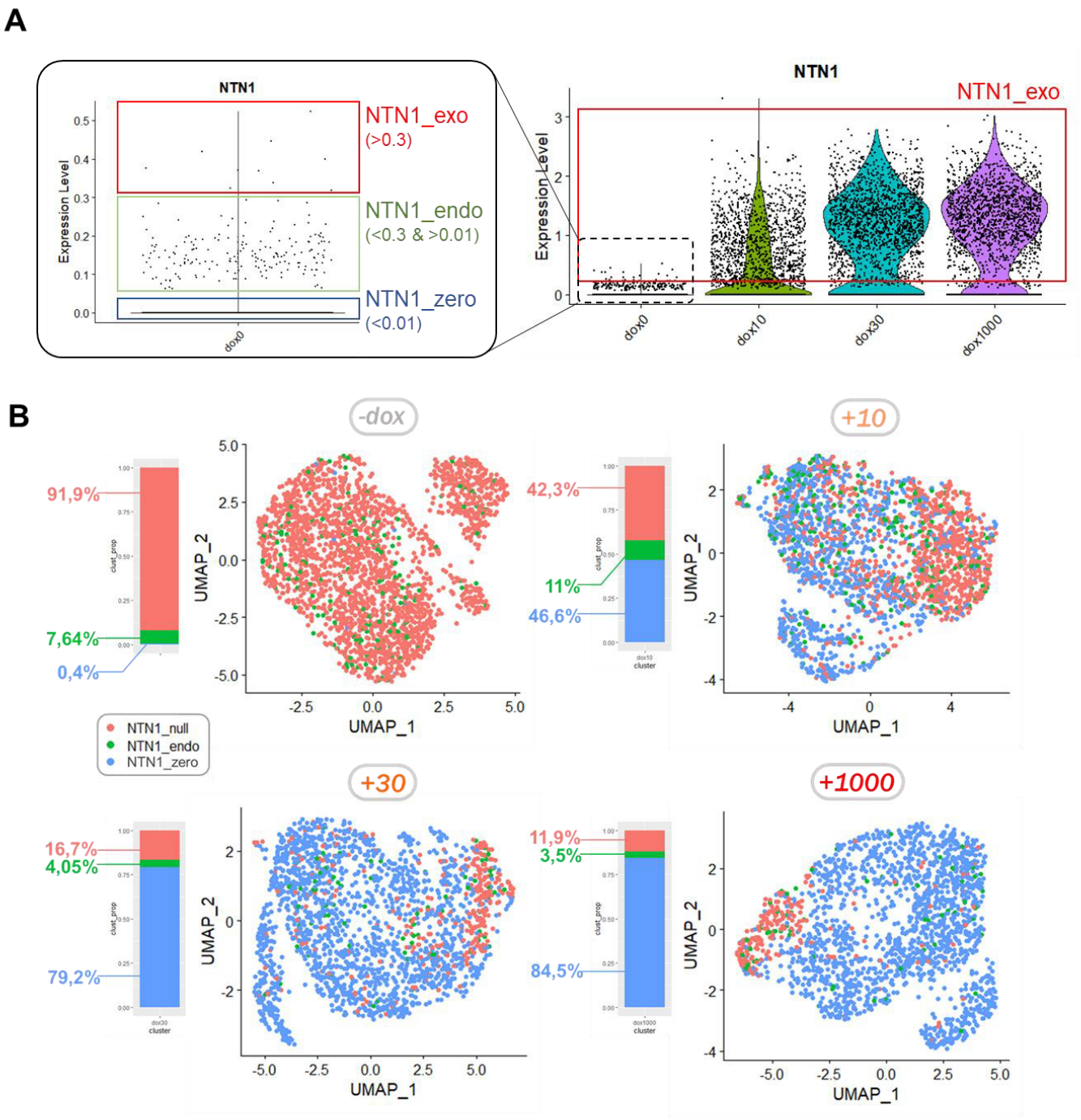

Figure 27. Induction efficiency and *NTN1* subpopulations of hSTAN1 cells.
(**A**) Violin plots of NETRIN1 expression used to establish the 3 subpopulations NTN1_exo (exogenous), NTN1_endo (endogenous) and NTN1_zero. Left: dox0 condition only, right: all conditions. (**B**) Feature plots of UMAPs and bar plots displaying the fraction of each *NTN1* subpopulation in each condition.

Next, we sought to evaluate if TL2i-hSTAN1 cells, as suggested by our previous findings, lose pluripotency upon induction. For this, we performed Uniform manifold approximation and projection (UMAP) for each of the four conditions, and generated feature plots of *NANOG* expression. As expected, we found that the -dox population exhibits widespread *NANOG* expression, while *NTN1* is limited to low levels in rare cells (**Figure 28A**). Upon induction, a drastic change occurs, with a strong decrease of *NANOG*+ cells and converse increase of *NTN1*+. This phenotype gradually accentuates with dox concentration. By generating violin plots of *NANOG* expression in NTN1-zero, NTN1-endo and NTN1-exo sub-populations for each condition, we noticed that NTN1-zero cells retain high *NANOG,* in contrast to NTN1-exo that show almost complete extinction of the gene in the +dox conditions (**Figure 28B**). NTN1-endo cells exhibit an intermediate behavior, with reduced but not entirely downregulated *NANOG* compared to NTN1-zero. This anti-correlation of *NANOG* and *NTN1-HA* is in accordance with our previous findings, and strongly suggests pluripotency exit of hSTAN1 cells in response to induction. To confirm this hypothesis, we investigated expression of additional markers of core, primed, formative and naïve pluripotency in the whole dataset. With heatmap and dotplot representations, we observed that non-induced TL2i-hSTAN1 cells express strong core pluripotency markers *OCT4*, *NANOG*, *SOX2* and the naïve marker *TFAP2C* (**Figure 29A**). Surprisingly, however, we found other naïve markers (*TFCP2L1, KLF4, HHLA1*) to be expressed by a relatively small fraction of cells. Conversely, primed and formative markers were both expressed at significant levels. This suggests, as outlined in introduction and in previous work (Aksoy et al., 2021), that naïve-like human cells are more heterogenous than their mouse counterparts and not fully recapitulate naïve characteristics.

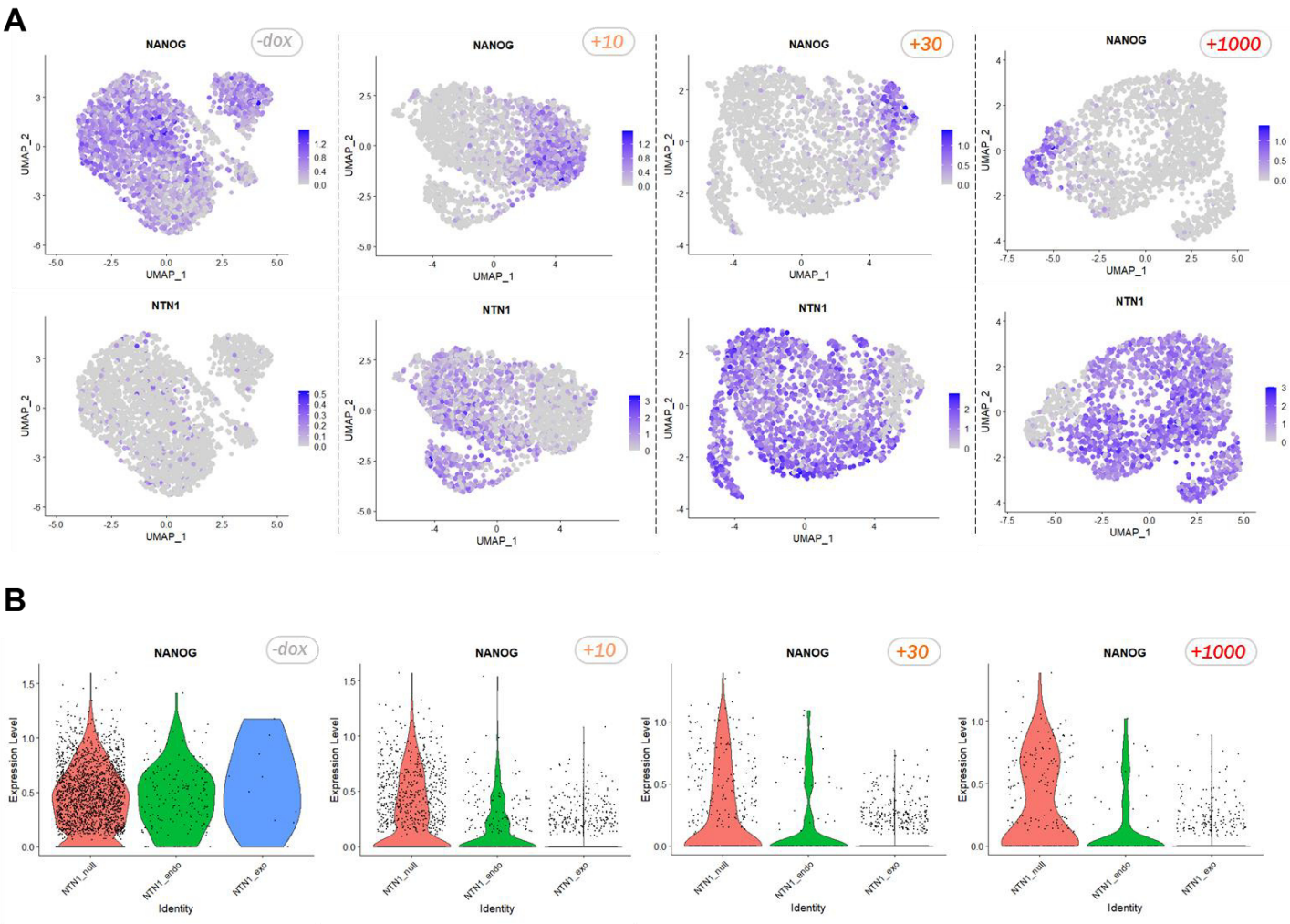

Figure 28. *NTN1* and *NANOG* anti-correlate upon induction.
(**A**) Feature plots of *NTN1* and *NANOG* expression in all dox conditions. (**B**) Violin plots of *NANOG* expression in NTN1-exo, -endo and –null subopopulations of all conditions.

Upon dox induction, we observed a gradual downregulation of all the pluripotency genes analyzed, to the one exception of *SOX2*, consistently with our previous data on TL2i-hSTAN1. With violin plot representations, we confirmed for *NANOG* a reduction both in the fraction of positive cells and average level of expression compared to -dox, but noticed a different pattern for *OCT4*, expressed by an equivalent number of cells in the +dox conditions versus -dox, but spanning out lower, more heterogenous levels in +dox (**Figure 29B**). *SOX2*, on the other hand, exhibits a slight increase upon induction, but remains stable and otherwise unaffected by dox concentration changes. Altogether, these results confirm our previous findings that hSTAN1 cells undergo pluripotency exit upon treatment, we thus next tried to determine if early lineage specification is occurring. We explored expression of mesoderm, endoderm and ectoderm markers and found that uninduced TL2i-hSTAN1 express both early

mesodermal (*MIXL1, TBXT, EOMES, LEFTY1, CER1*) and ectodermal (*VIM, NES, FST*) genes in an heterogenous fashion (**Figure 29C**). Endodermal markers (*GATA4, -6* and *SOX17*) are also expressed, though to a lesser extent. Upon treatment, we observed a sharp dose-dependent downregulation of all early lineage genes, with the exception of *NESTIN* that shows a slight increase following induction. As previously described by qPCR analysis, these results suggest that, although they exit pluripotency, induced TL2i-hSTAN1 cells do not commit to early-lineage differentiation.

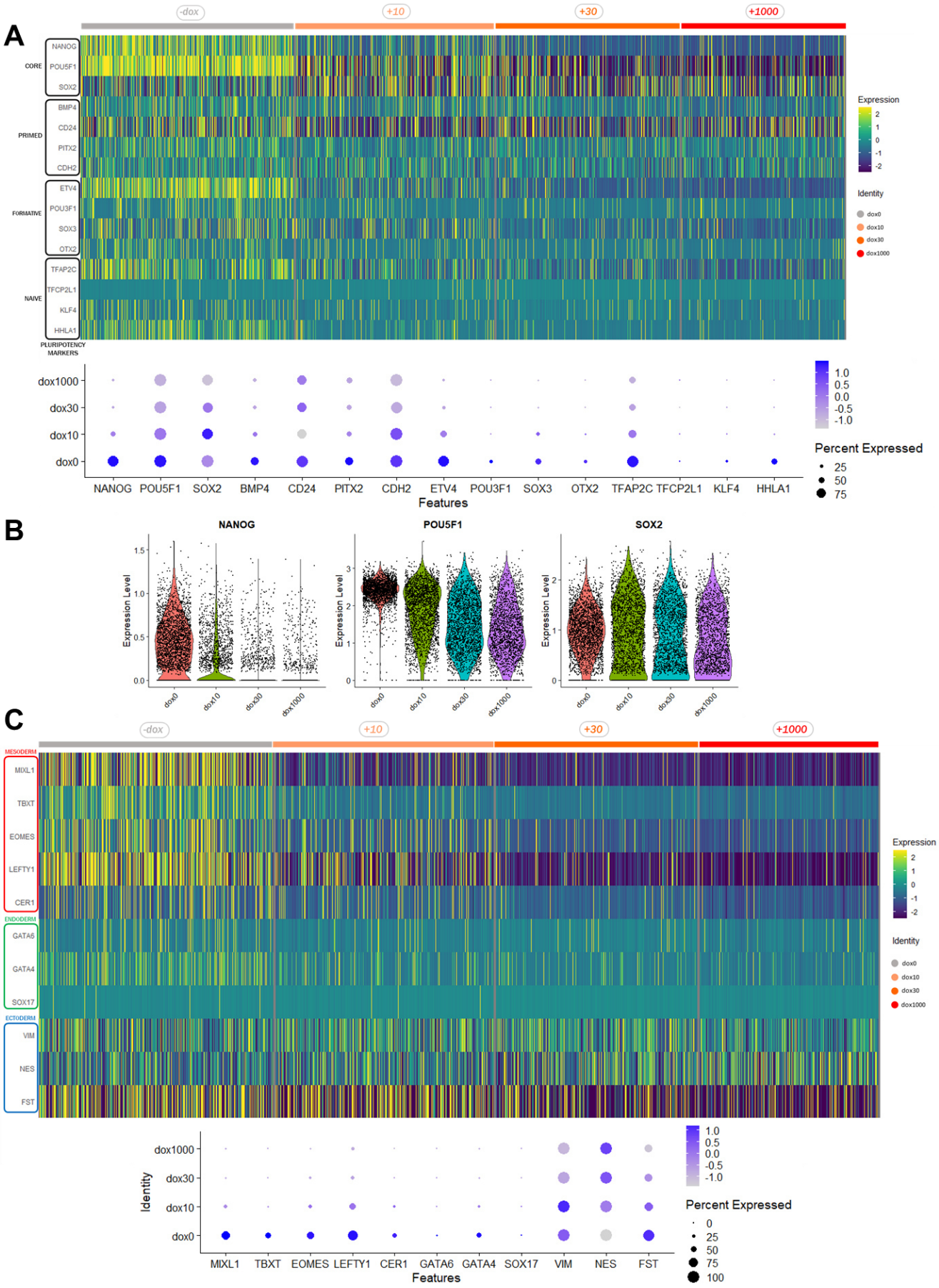

Figure 29. *NTN1* induction leads to pluripotency collapse of hSTAN1 cells, but is not associated with commitment to early lineages.

(**A**) Heatmap and dotplot of pluripotency-associated markers in all four dox conditions of hSTAN1 cells. (**B**) Violin plots of *NANOG*, *OCT4* (*POU5F1*) and *SOX2* expression in all four dox conditions of hSTAN1 cells. (**C**) Heatmap and dotplot of early lineages-associated markers in all four dox conditions of hSTAN1 cells.

IV.1.b. NTN1-exo cells commit to striated muscle differentiation

To gain better insight on NTN1 effect on TL2i-hSTAN1 cells, we undertook to characterize the NTN1-exo populations of the +dox conditions. For this we isolated NTN1-exo cells in all treated conditions and compared them to their null counterparts (**Figure 30A**). With the most differentially expressed genes (average $Log_2FC>0,25$ or $<-0,25$) thus obtained, we interrogated GO databases, and found that NTN1-exo cells are enriched for terms associated with muscle system processes, including myofibril assembly, sarcomere and actomyosin structures organization and striated muscle differentiation (**Figure 30B**). We also found several terms associated with Golgi-vesicle organization, transport and budding, consistent with active NTN1-HA translation and secretion. We performed GSEA analysis with all DEGs from NTN1-exo cells and confirmed enrichment for Golgi-transport, protein secretion, actin-based structure organization, but also cilium organization (~200 genes) (**Figure 30C**). We noticed that NTN1-exo cells are downregulated for terms associated with ribosome biogenesis and ribosomal RNA processes, consensus transcriptomic terms for naïve-like human cells (Huang et al., 2014), which confirms their disengagement from naïve pluripotency.

We then asked if the NTN1-exo phenotype observed is varying depending on dox concentration. When generating GO and GSEA analyses on NTN1-exo DEGs from +10, +30 and +1000 conditions individually, we found similar terms enriched compared to the pooled +dox populations, with only slight differences of order (data not shown); we thus decided to evaluate the transcriptomic distance between our four experimental conditions by comparing the most differentially expressed genes (average $Log_2FC>0,25$) of the +10, +30 and +1000 conditions compared to -dox. We found a significant overlap of 170 genes between the three treated conditions, and noticed that the +30 and +1000 points share the highest proximity index (**Figure 30D**). This was confirmed by hierarchical clustering representation, on which all +dox conditions cluster together, but +30 and +1000 segregate a separate branch. Altogether, this indicates that NTN1 triggers striated muscle differentiation of TL2i-hSTAN1 cells, but does not yield a different phenotype at low compared to high dox concentrations. More likely, commitment is gradual and dose-dependent.

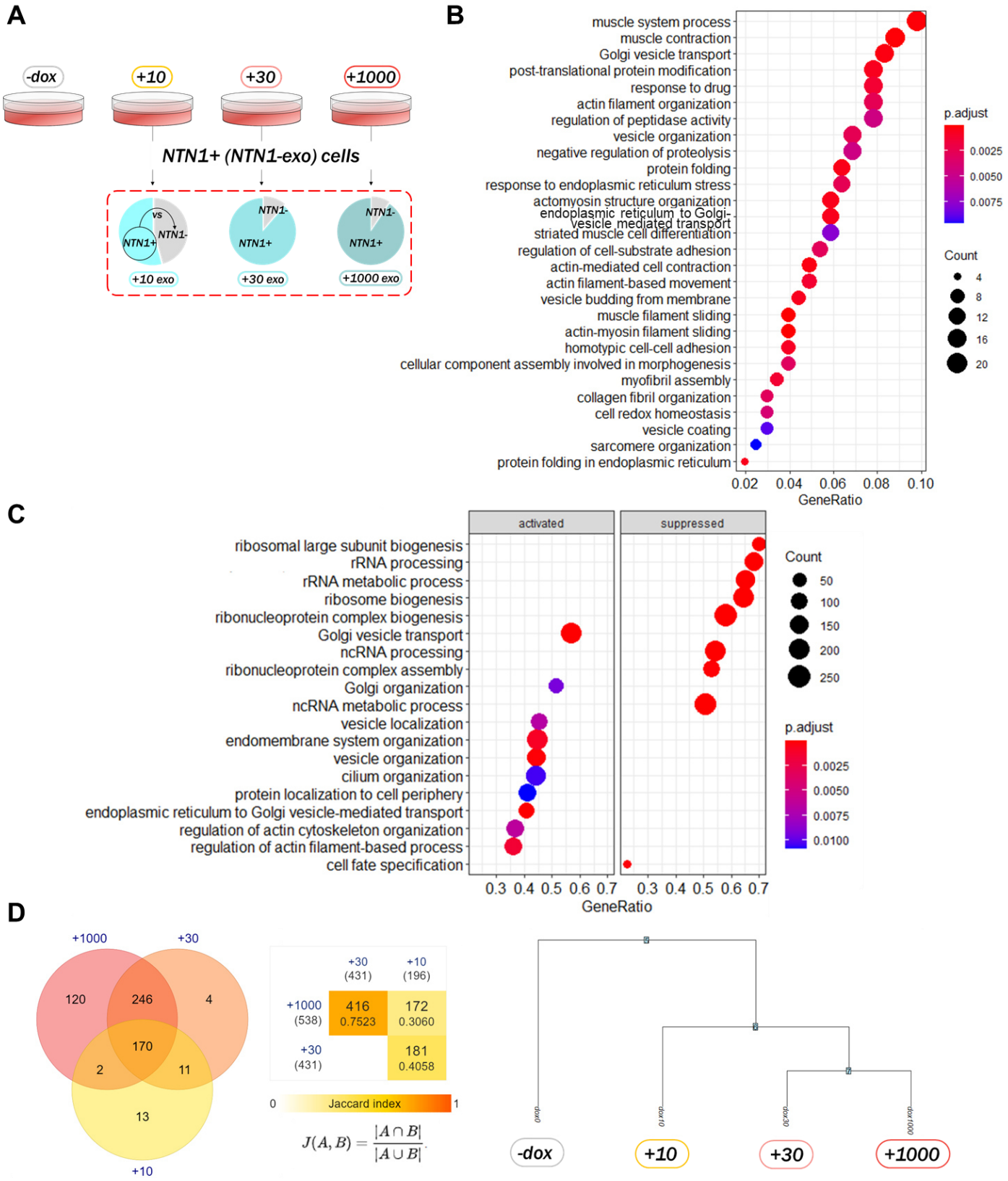

Figure 30. *NTN1* induction leads to a gradual commitment to skeletal muscle differentiation.
(**A**) Scheme representing the genes expression comparison performed for the subsequent analyses. (**B**) Gene Ontology analysis performed on upregulated genes (average Log2(FC)>0,25) of the pooled +10-exo, +30-exo and +1000-exo populations. (**C**) Gene Set Enrichment Analysis performed on all DEGs of the pooled +10-exo, +30-exo and +1000-exo populations. (**D**) Left: Venn diagram of the DEGs (average Log2(FC)>0,25) in the +10, +30, or +1000 dox condition compared to the –dox condition and Jaccard Index displaying the relative proximity (1, strongest ; 0, weakest) between the +10, +30 and +1000 conditions. Right: Hierarchical clustering of all conditions based on DEGs of +10, +30 and +1000 versus -dox.

IV.1.c. NTN1 overexpression has a paracrine differentiating effect

Because NTN1 is a secreted protein and has been extensively demonstrated to act, in different contexts, as a short- and long-range signal, we then asked if in addition to its autocrine effect on the NTN1-exo population, NTN1 has a paracrine effect on the NTN1-zero neighboring cells. To address this question, we compared the transcriptomes of NTN1-zero cells in induced context to the NTN1-zero population of the control (-dox) condition (**Figure 31A**). As precedingly, we performed successive GO analysis and GSEA, and found that, as NTN1-exo cells, NTN1-zero are enriched for muscle system processes, though to a lesser extent than NTN1-exo (**Figure 31B**). We also found enrichment for “ossification” and “osteoblast differentiation”, a cell type belonging, as straited muscle cells, to late mesodermal lineages. Through GSEA, we found for +dox NTN1-zero cells terms associated with a single family of enrichment, ciliogenesis, and a converse downregulation of ribosomal biogenesis and rRNA processes (**Figure 31C**). Collectively, these data suggest that NTN1 paracrine and autocrine signals trigger effects partially similar, but the latter has power to induce commitment in a different late mesodermal lineage.

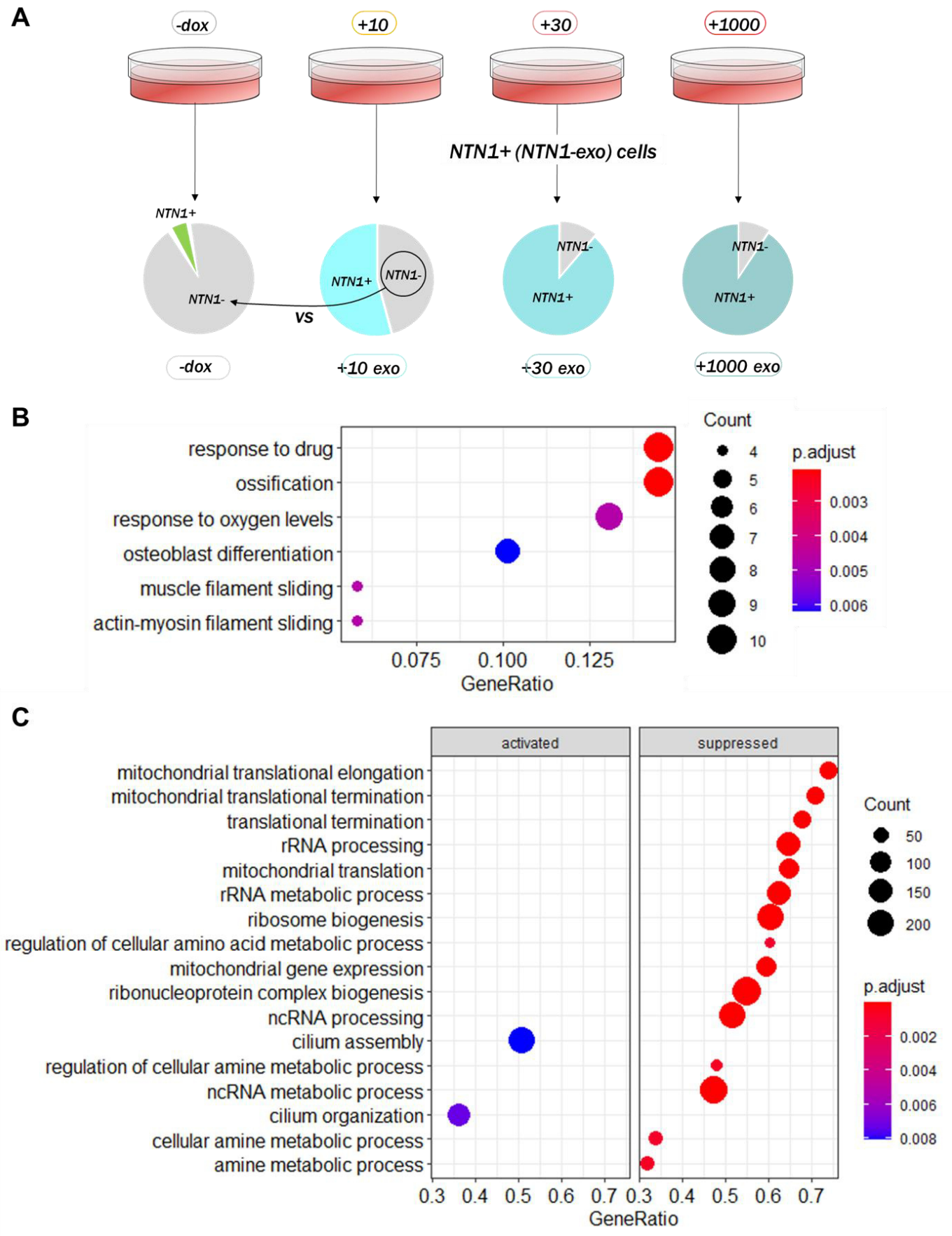

Figure 31. NTN1 exogenous expression has a paracrine effect on neighboring cells.
(**A**) Scheme representing the genes expression comparison performed for the subsequent analyses. (**B**) Gene Ontology analysis performed on upregulated genes (average Log2(FC)>0,25) of the pooled +dox NTN1-null populations (+10, +30 and +1000 conditions) vs –dox NTN1-null cells. (**C**) Gene Set Enrichment Analysis performed on all DEGs of the pooled +dox NTN1-null populations (+10, +30 and +1000 conditions) vs –dox NTN1-null cells.

IV.2. *DRAXIN*-positive TL2i-hSTAN1 do not undergo autocrine or paracrine effects from NTN1.

IV.2.a. DRAXIN-positive TL2i-hSTAN1 cells remain pluripotent upon induction

As previously investigated in the embryo and other primates PSCs, we nest asked if secreted Netrins other than *NTN1* are expressed in TL2i-hSTAN1, and if their expression is affected by induction. By dotplot and heatmap representations, we found that *NTN3*, *-4* and *-5* are expressed by infinitesimal fractions of cells regardless of dox treatment; however, we noticed strong expression of *DRAXIN* by a majority of cells in the -dox condition (**Figure 32A**). Upon *NTN1* induction, we observed a strong downregulation of DRAXIN in both the fraction of positive cells and average level of expression. On UMAP representations, it appears that *DRAXIN*- and *NTN1*-positive cells are mutually exclusive and cluster separately (**Figure 32B**). We confirmed this observation by calculating the correlation coefficient between *DRAXIN* and *NTN1* in each condition. While in -dox, no correlation could be established, we found a significant anti-correlation between the genes in all +dox conditions, consistently with our previous findings (**Figure 32C**).

Because *DRAXIN*-positive cells form a distinct cluster from their NTN1-exo counterparts upon induction, and because DRAXIN has been previously demonstrated to prevent NTN1 action in different contexts, we then asked if its expression could counteract *NTN1* pro-differentiation effect in TL2i-hSTAN1. We isolated and pooled together the *DRAXIN*+ populations of the +dox conditions, and generated a volcano plot representation with all DEGs from *DRAXIN*+ vs *DRAXIN*- cells. Interestingly, we found several pluripotency-associated genes, including *SOX2*, *OCT4*, *ESRG* and *NANOG* to be strongly enriched in *DRAXIN*+ cells (**Figure 33A**). Consistently, we found *NANOG* and *DRAXIN* to positively correlate in the whole dataset (**Figure 33B**), as previously suggested by their similar patterns of expression in UMAP representations. Using the most differentially expressed genes of the *DRAXIN* groups (Average $Log_2FC>0.25$ or <-0,25), we then interrogated the KEGG database, and found *DRAXIN*+ cells to be enriched for pathways regulating pluripotency and TGF-β/NODAL signaling (**Figure 33C**). We also noticed enrichment for cell cycle, DNA replication and base excision repair. *DRAXIN*-, on the other hand, are enriched for focal adhesion and actin cytoskeleton regulation, but also apoptosis. Additionally, while terms indicative of DNA replication, proliferation and stem cell self-renewal were confirmed, we found by GO analysis that *DRAXIN*+ cells undergo chromatin remodeling and DNA reconfiguration compared to their negative counterparts (**Figure 33D**). Collectively, these observations strongly suggest that

DRAXIN+ cells retain pluripotency upon induction and are shielded from *NTN1* pro-differentiation effects.

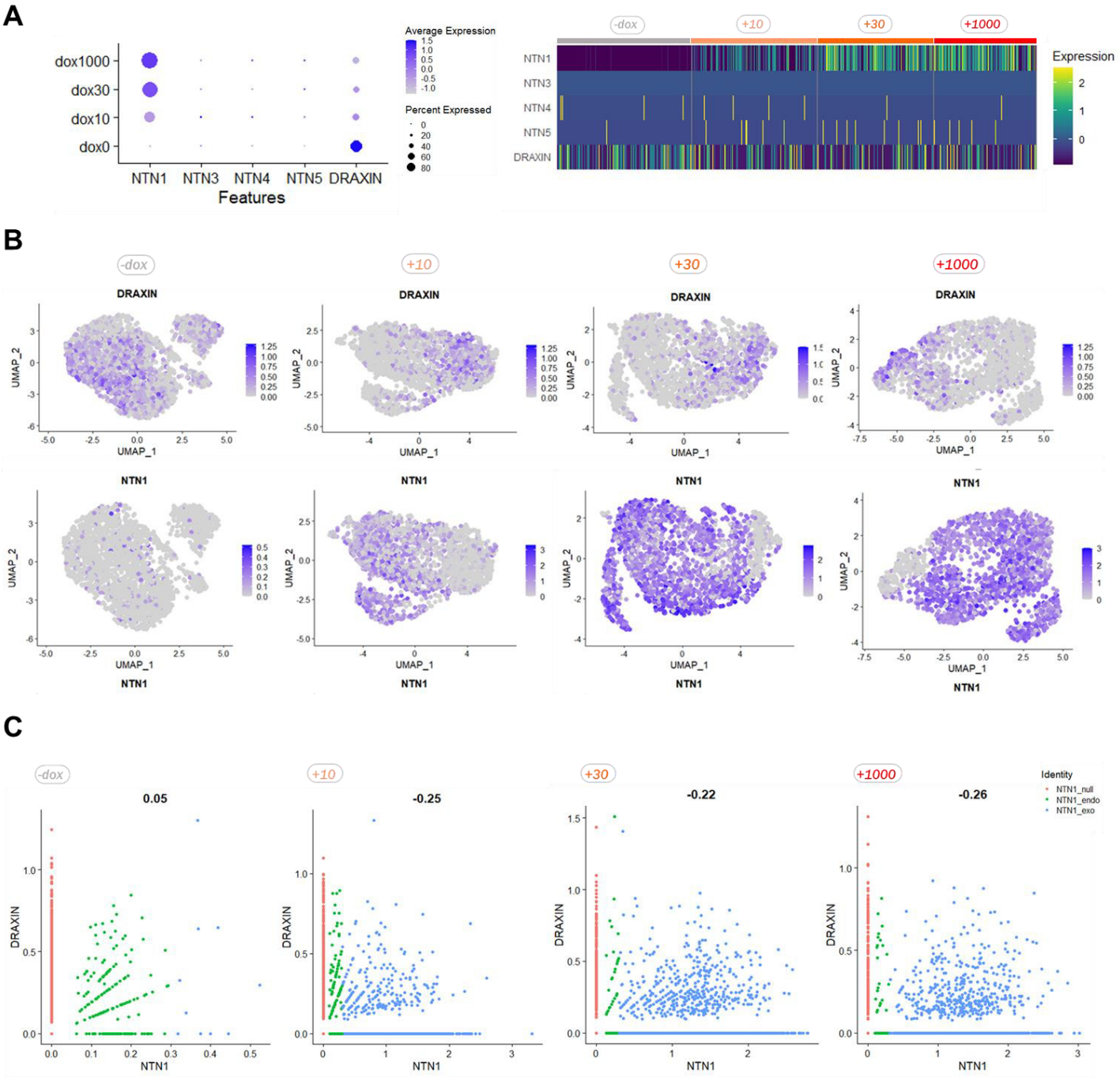

Figure 32. hSTAN1 cells express *DRAXIN* in anti-correlation with *NTN1* upon induction.
(**A**) Dotplot (left) and heatmap (right) showing the expression levels of secreted Netrins and Draxin in hSTAN1 cells of all four dox conditions. (**B**) Feature plots of *NTN1* and *DRAXIN* expression in hSTAN1 cells of all four dox conditions. (**C**) Correlation plots and correlation coefficients (-1<p<1 ; p=-1, complete anti-correlation, p=1, complete correlation, p=0, no correlation) of *NTN1* and *DRAXIN* in hSTAN1 cells of all four dox conditions.

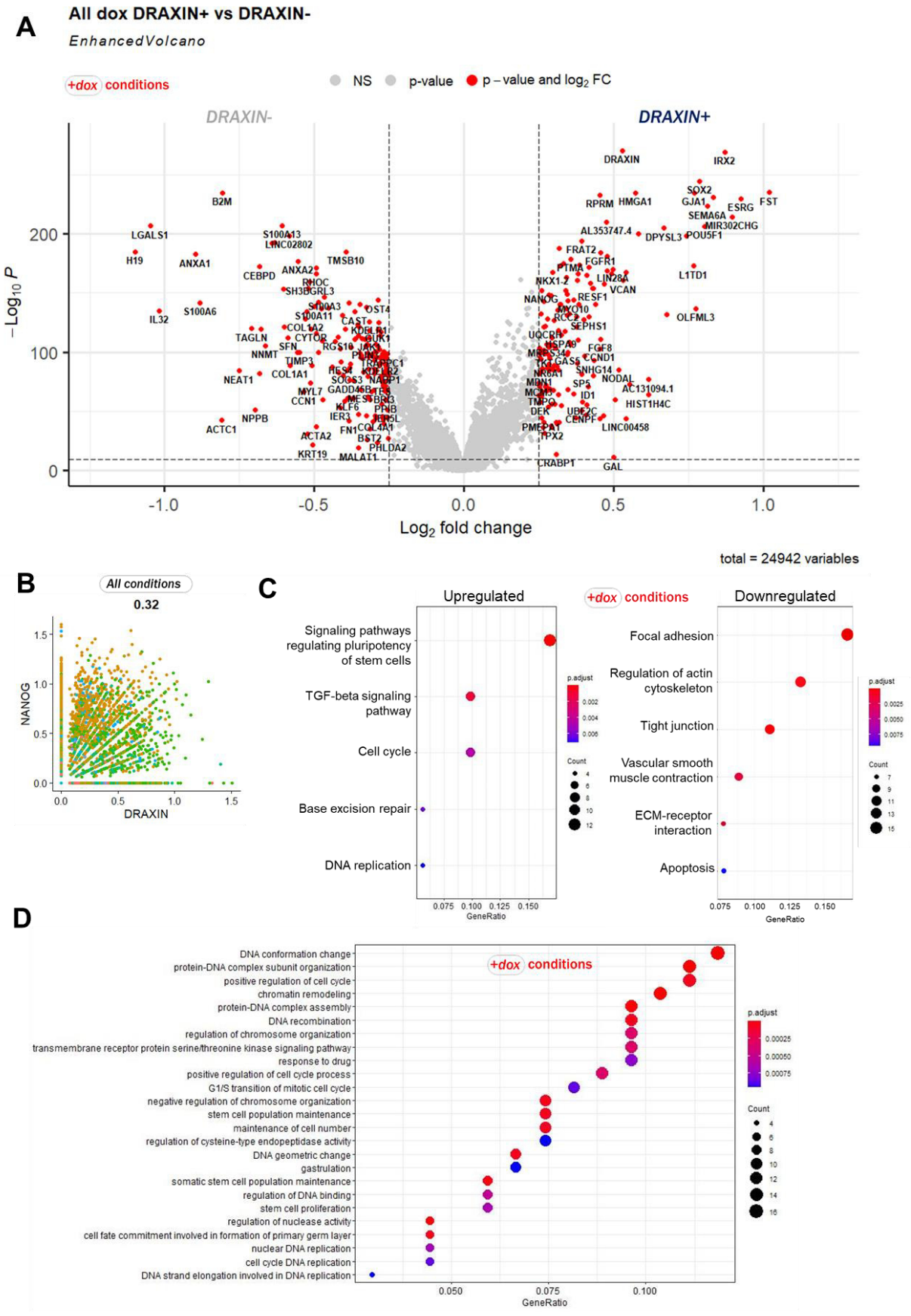

Figure 33. *DRAXIN*-positive hSTAN1 cells retain pluripotency upon induction.
(**A**) Volcano plot showing most differentially expressed genes of *DRAXIN*+ and *DRAXIN*- hSTAN1 cells. (**B**) Correlation plot and correlation coefficient (-1<p<1 ; p=-1, complete anti-correlation, p=1, complete correlation, p=0, no correlation) of *NANOG* and *DRAXIN* in hSTAN1 cells. (**C**) KEGG pathway analysis performed on all DEGs (average Log2(FC)>0,25 and <-0,25) of DRAXIN+ cells of the +dox contidions (**D**) Gene Ontology analysis performed on upregulated genes (average Log2(FC)>0,25) of DRAXIN+ cells of the +dox contidions.

IV.2.b. DRAXIN-positive cells constitute the most pluripotent compartment of the TL2i-hSTAN1 population

As previously showed, *NTN1* and *NANOG* anti-correlate upon induction, and NTN1-zero cells, despite undergoing paracrine effects from the NTN1-exo population, retain high *NANOG* and hallmarks from pluripotency. Because we demonstrated that *DRAXIN*+ cells remain pluripotent in treated conditions, we wondered if they epitomize entirely the pluripotent compartment of induced TL2i-hSTAN1, overlapping with NTN1-zero cells. For this, we identified and compared six subpopulations based on the co-expression of *DRAXIN* and *NTN1* (endogenous or exogenous). In absence of induction, we noticed that in the majority NTN1-zero fraction, more than half of the cells express *DRAXIN*, representing 56.8% of the whole population (**Figure 34A**). In induced conditions, despite an overall reduction compared to -dox, the *NTN1-DRAXIN+* group systematically represents more than half of NTN1-zero cells. By generating violin plots of *OCT4, SOX2, NANOG*, *DPPA4* and *SALL4* expression, we found that *NTN1-DRAXIN*+ cells exhibit higher levels of all considered pluripotency markers than their *DRAXIN*- counterparts (**Figure 34B**). Interestingly, we also found higher *OSN*, *DPPA4* and *SALL4* in NTN1-exo *DRAXIN*+ compared to NTN1-exo *DRAXIN*- cells. By performing a similar analysis in the -dox population, we observed overall higher levels of said markers, albeit to a lesser extent, in *DRAXIN*+ versus *DRAXIN*- cells (**Figure 34C**). Altogether, these findings reveal that *DRAXIN*-positive cells represent the most pluripotent compartment of TL2i-hSTAN1 cells, regardless of *NTN1* induction, and further suggest that *DRAXIN* has a shielding effect towards *NTN1*, alleviating both paracrine and autocrine effects.

IV.3. *NTN1* effect is partially due to *NEO1* activation.

IV.3.a. Netrin receptors expression in TL2i-hSTAN1

To characterize *NTN1* mode of action, we then asked what known netrin receptors are expressed by TL2i-hSTAN1 cells. We found that, among the UNC5 and DCC/NEO1 families, only *UNC5B* and *NEO1* are detected at significant levels (**Figure 35A**). We noticed that without induction, *UNC5B* is expressed by a majority of cells (56.1%), while *NEO1*+ only represent 40.2% of the population (**Figure 35B and C**). Upon induction, this pattern is inverted, *NEO1* taking over at the expense of *UNC5B* to reach 66.6% versus 29.6% of positive cells at the highest dox concentration, respectively. Moreover, while no correlation of expression could be established between *UNC5B* and *NEO1* in the whole dataset, we found a negative and positive

one with *NTN1*, respectively (**Figure 35D**). This shows that, upon induction, TL2i-hSTAN1 switch expression from *UNC5B* to *NEO1.*

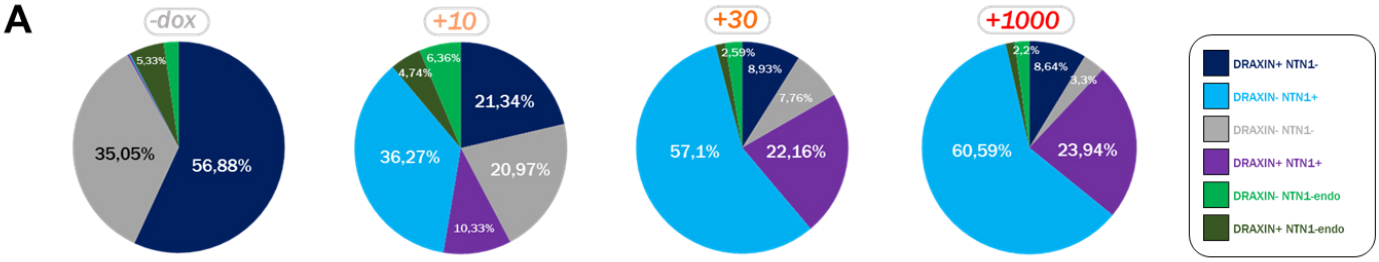

	-dox	+10	+30	+1000
DRAX+ NTN1-	56,88%	21,34%	8,93%	8,64%
DRAX- NTN1-	35,05%	20,97%	7,76%	3,30%
DRAX+ NTN1+	0,25%	10,33%	22,16%	23,94%
DRAX- NTN1+	0,17%	36,27%	57,10%	60,59%
DRAX+ NTN1endo	5,33%	4,74%	1,46%	1,32%
DRAX- NTN1endo	2,31%	6,36%	2,59%	2,20%

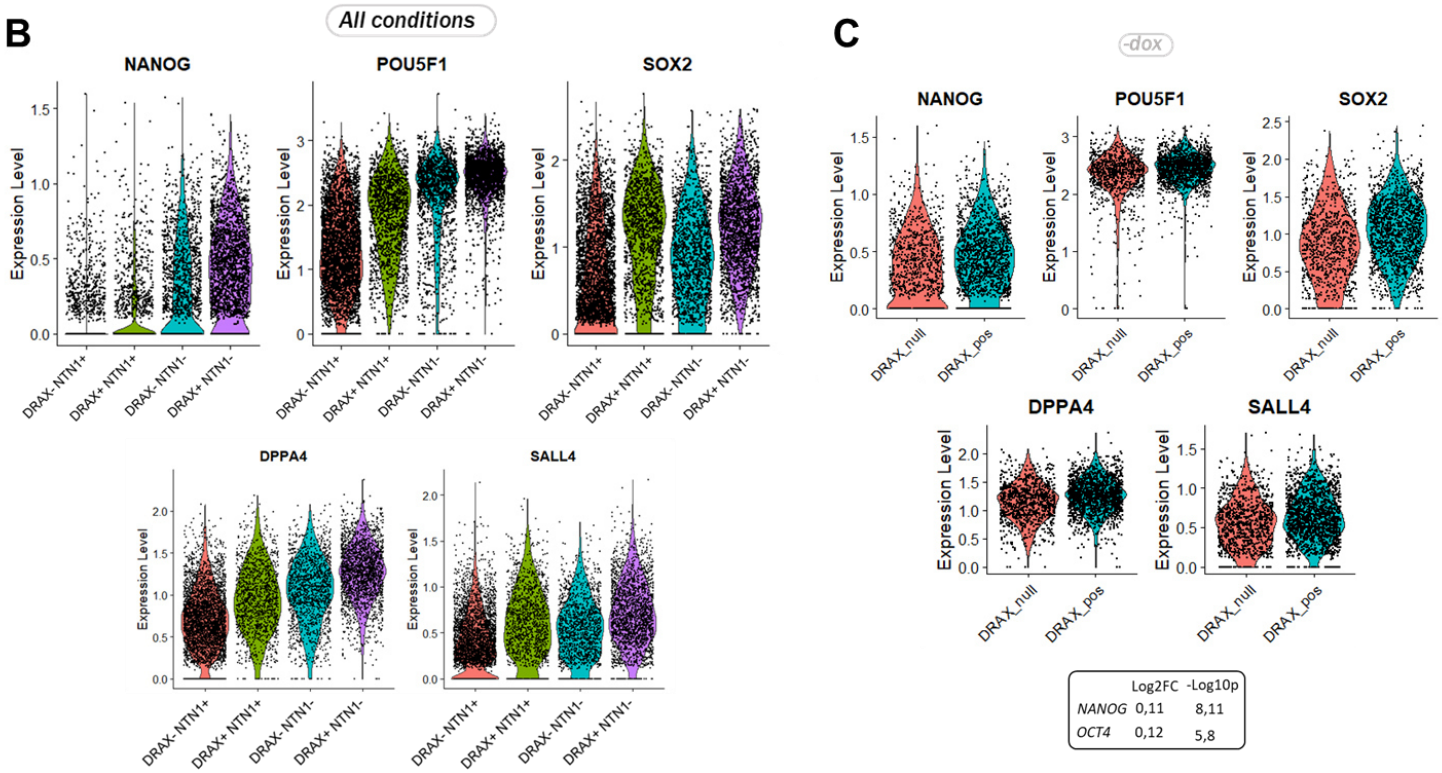

Figure 34. *DRAXIN*-positive hSTAN1 cells constitute the most pluripotent compartment of the hSTAN1 cell populations.

(**A**) Color pies and table showing *NTN1*/*DRAXIN* subpopulations distribution within hSTAN1 cells of all conditions. (**B**) Violin plots of pluripotency markers expression in *NTN1*/*DRAXIN* subpopulations of all dox conditions pooled. (**C**) Violin plots of pluripotency markers expression in *NTN1*/*DRAXIN* subpopulations in the –dox condition.

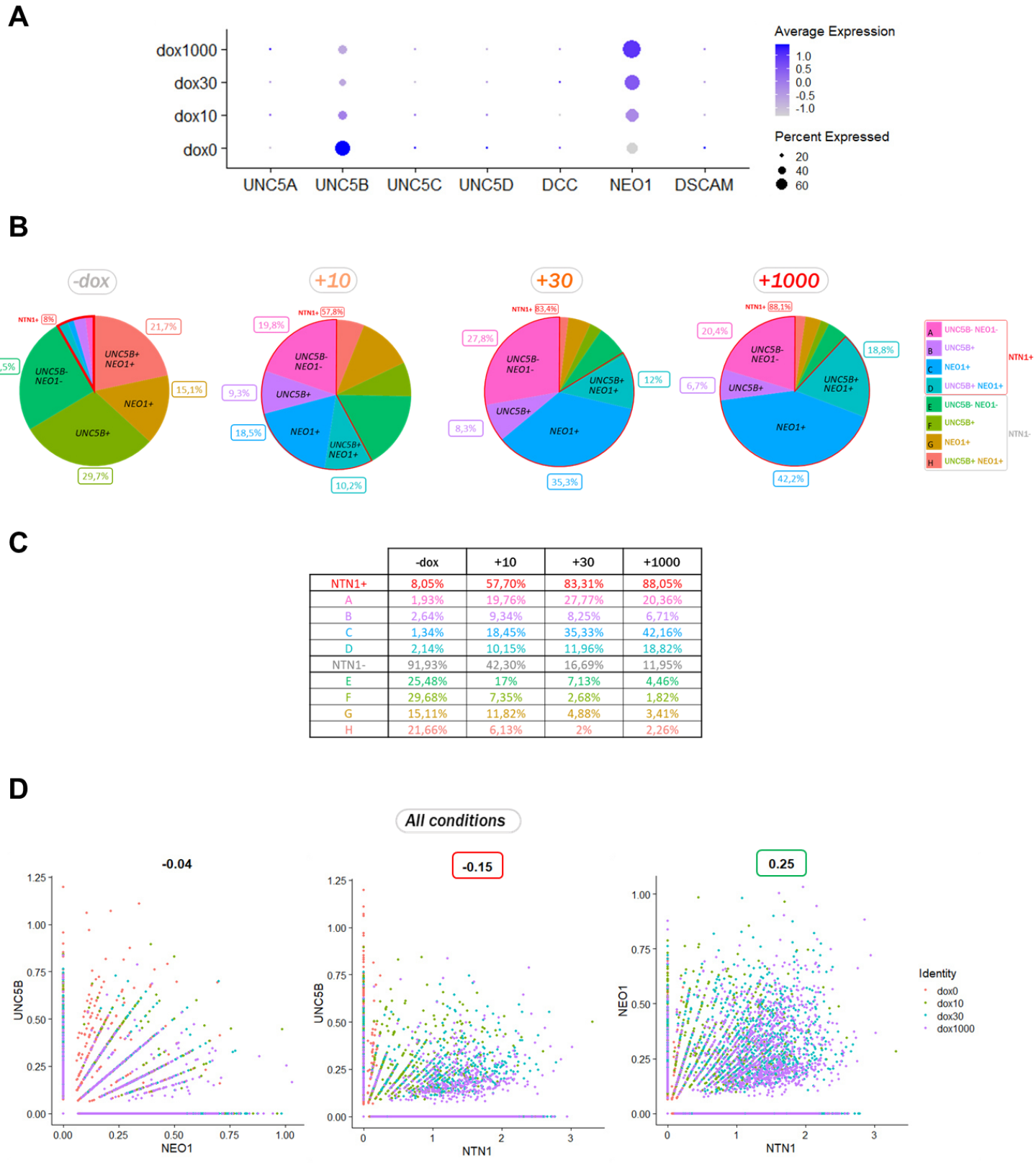

	-dox	+10	+30	+1000
NTN1+	8,05%	57,70%	83,31%	88,05%
A	1,93%	19,76%	27,77%	20,36%
B	2,64%	9,34%	8,25%	6,71%
C	1,34%	18,45%	35,33%	42,16%
D	2,14%	10,15%	11,96%	18,82%
NTN1-	91,93%	42,30%	16,69%	11,95%
E	25,48%	17%	7,13%	4,46%
F	29,68%	7,35%	2,68%	1,82%
G	15,11%	11,82%	4,88%	3,41%
H	21,66%	6,13%	2%	2,26%

Figure 35. hSTAN1 cells switch from *UNC5B* to *NEO1* expression upon *NTN1* induction.
(**A**) Dotplot of Netrin receptors expression in hSTAN1 cells of all dox conditions. (**B**) Color pies and (**C**) summary table of *UNC5B/NEO1* receptors subpopulations distribution in hSTAN1 cells. (**D**) Correlation plots and coefficients for *NEO1*, *UNC5B* and *NTN1* expression in all dox conditions.

We next sorted out 8 subpopulations (lettered A to H) based on the expression of *UNC5B*, *NEO1* and *NTN1*, and compared different configurations in the -dox condition (**Figure 36A**). We first collected DEGs of NTN1-zero UNC5B+ versus NEO1+ cells and generated volcano plots. As a result, we found that selected pluripotency markers are not significantly enriched in one or the other population, indicating that pluripotency does not rely on *UNC5B* or *NEO1* expression in absence of induction (**Figure 36B**). We noticed, however, that *NTN1*-endo expression leads to a change in enriched genes from both NEO1+ and UNC5B+ populations, suggesting that both receptors are responsive to a low-dose autocrine signal (**Figure 36C**). By comparing *UNC5B* and *NEO1*-positive cells to their negative counterparts, we observed that, in a non-induced context, *UNC5B* expression is associated with modest, but greater transcriptional changes that *NEO1* expression (**Figure 36D**). Collectively, these results indicate TL2i-hSTAN1 pluripotency is not affected by *UNC5B* or *NEO1* expression in a non-induced context, and that both receptors have an overall discrete effect on the cells transcriptome.

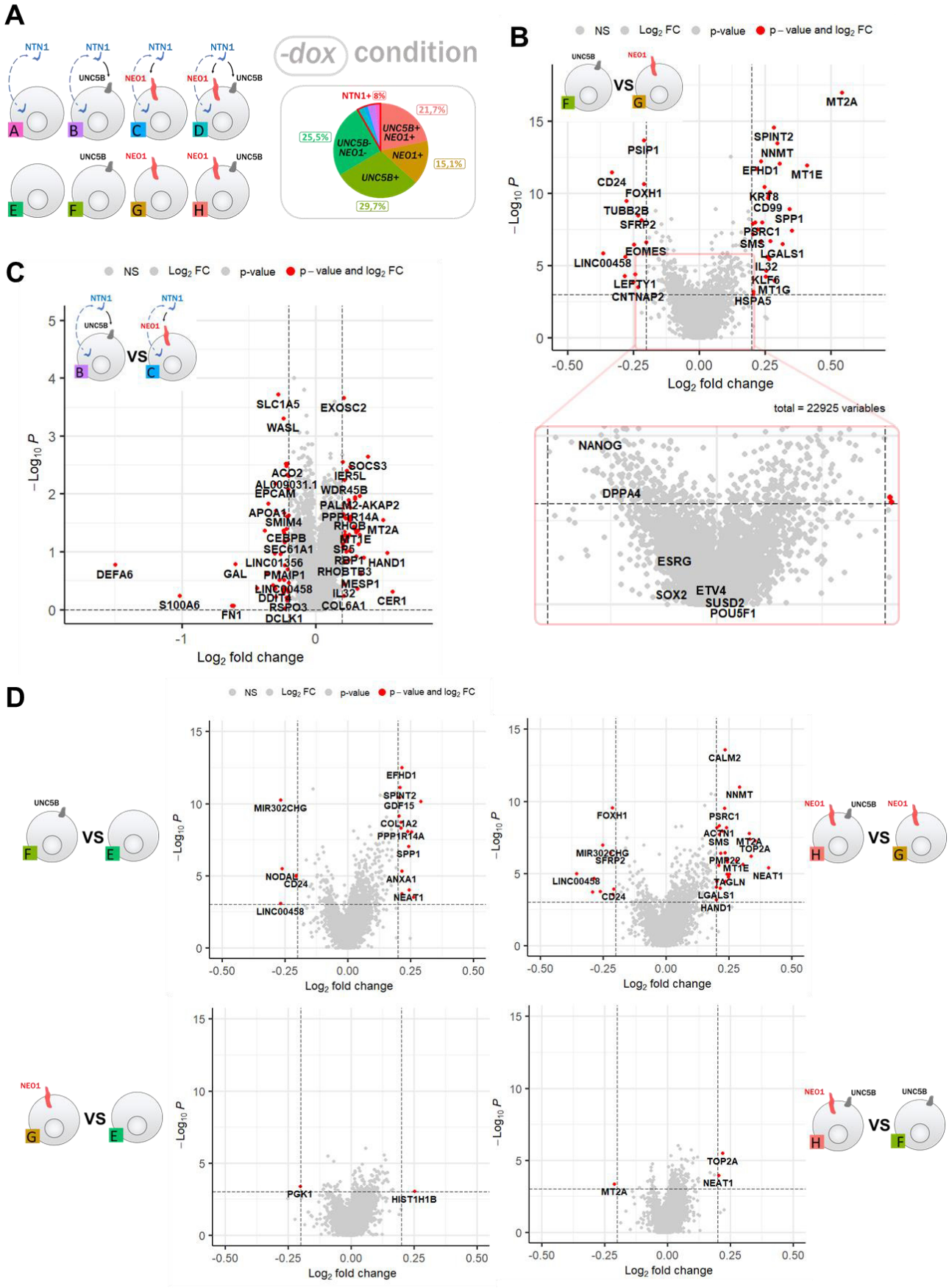

Figure 36. In absence of induction, pluripotency does not rely on *NEO1* or *UNC5B* expression.
(**A**) Schematic showing all the NTN1/UNC5B/NEO1 combinations (lettered A to G) present in hSTAN1 cells of the –dox condition (**B**) Volcano plot of DEGs in –dox-F (*UNC5B+*) vs –dox-G (*NEO1+*) cells. Bottom panel: enlargement highlighting pluripotency-associated genes. (**C**) Volcano plot of DEGs in –dox-B (*UNC5B+NTN1+*) vs –dox-C (*NEO1+NTN1+*) cells. (**D**) Equal-scaled Volcano plots of DEGs in four receptor configurations comparisons.

IV.3.b. NEO1-positive and NTN1-exo TL2i-hSTAN1 cells phenotype overlap

We then investigated *NEO1* and *UNC5B* expression impact on cell identity in treated conditions. For this, we first compared *NEO1*+ cells with or without *NTN1*-exo expression (collectively referred to as *NEO1*-specific) to all *NEO1*-negative cells in all +dox conditions (**Figure 37A**). With the differentially expressed genes from these populations, we generated a volcano plot and observed important downregulation of *NEO1*-specific cells for several pluripotency genes, including *OCT4*, *SOX2* and *NANOG*, along with *NODAL* and *LEFTY2* (**Figure 37B**). We performed gene set enrichment analysis interrogating GO databases and found that, while *NEO1*-negative cells are enriched for ribosomal biogenesis, rRNA metabolism and mitochondrial genes expression, all consensus terms of naïve-like cells, *NEO1*-specific return terms associated with endocytosis, Golgi-vesicle transport, cilia assembly and mitosis (**Figure 37C**). Interrogation of KEGG databases retrieved terms confirming the naïve-pluripotent identity of *NEO1*-negative cells, and enrichment of endocytosis for NEO1-specific cells (**Figure 37D**). Interestingly, the *NEO1*-specific population additionally display with this method enrichment for terms associated with osteoclast differentiation and focal adhesion. These results collectively suggest that cells expressing *NEO1* without *UNC5B* are engaged in differentiation processes, form cilia and undergo active proliferation, while *NEO1*-negative cells, regardless of *UNC5B* expression, retain a pluripotent identity.

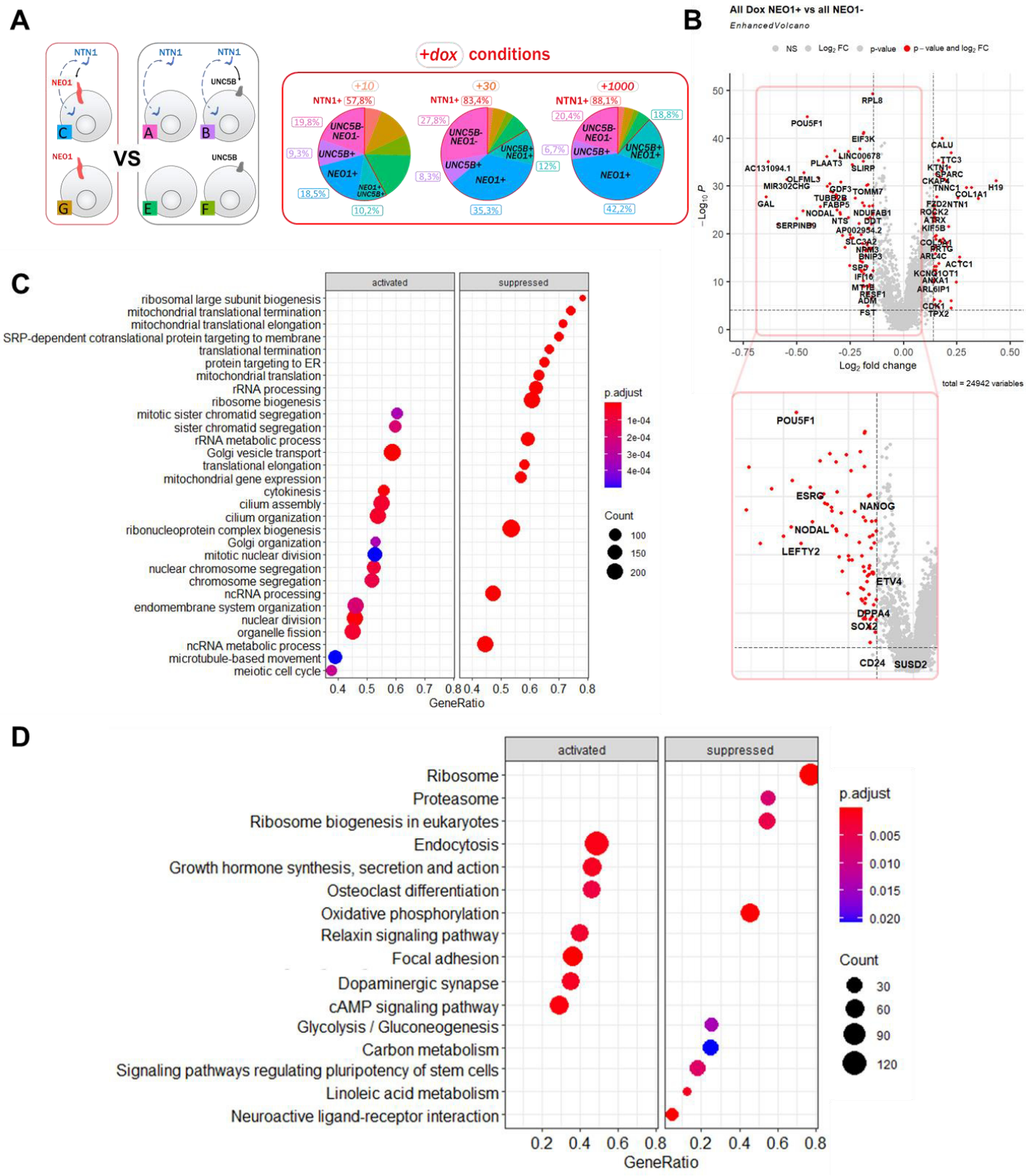

Figure 37. Upon induction, NEO1-positive hSTAN1 cells form focal adhesions and cilia, proliferate and undergo differentiation.

(**A**) Scheme depicting the groups compared in all +dox conditions for analyses performed in (**B**-**D**). Subpopulations expressing *NEO1* were pooled and compared to all cells without *NEO1* expression.(**B**) Volcano plots showing DEGs of *NEO1-specific* vs *NEO1*- cells in +dox conditions. Bottom panel: enlargement highlighting pluripotency and NODAL signaling-associated genes. (**C**) Gene Ontology GSEA analysis performed on all DEGs of *NEO1-specific* vs *NEO1*- cells in +dox conditions.(**D**) KEGG pathway GSEA analysis performed on all DEGs of *NEO1-specific* vs *NEO1*- cells in +dox conditions.

We next analyzed *UNC5B*-specific cells with a similar approach (**Figure 38A**). By using DEGs of *UNC5B*+*NTN1*- and *UNC5B+NTN1*+ versus all *UNC5B*-negative subpopulations, we generated a volcano plot and found that, to the opposite of *NEO1*-specific cells, *UNC5B*-specific are strongly enriched for *OCT4*, *ESRG*, *NODAL* and *LEFTY2* (**Figure 38B**). We noticed, however, that unlike the *NEO1*-negative population, other pluripotency markers, including *NANOG* and *SOX2,* are not significantly enriched in *UNC5B*-specific cells. We also observed a distinctive upregulation of the NODAL signaling gene *TDGF1* in the latter. Despite these differences, *NEO1-negative* and *UNC5B*-specific groups return partially similar GO-terms upon gene set enrichment analysis (namely ribosomal biogenesis and rRNA metabolism), while *UNC5B*-negative cells share common terms with their *NEO1*-specific counterparts (Golgi-vesicle transport and cilia assembly) (**Figure 38C**). By KEGG-pathway analysis, we confirmed that *UNC5B*-specific cells are enriched for terms associated with pluripotency (**Figure 38D**). Altogether, these results suggest distinct effects from *NEO1* and *UNC5B* expression in induced TL2i-hSTAN1. While the former is associated with actin-based morphological changes, cilia formation and differentiation, the latter is correlated to pluripotent characteristics.

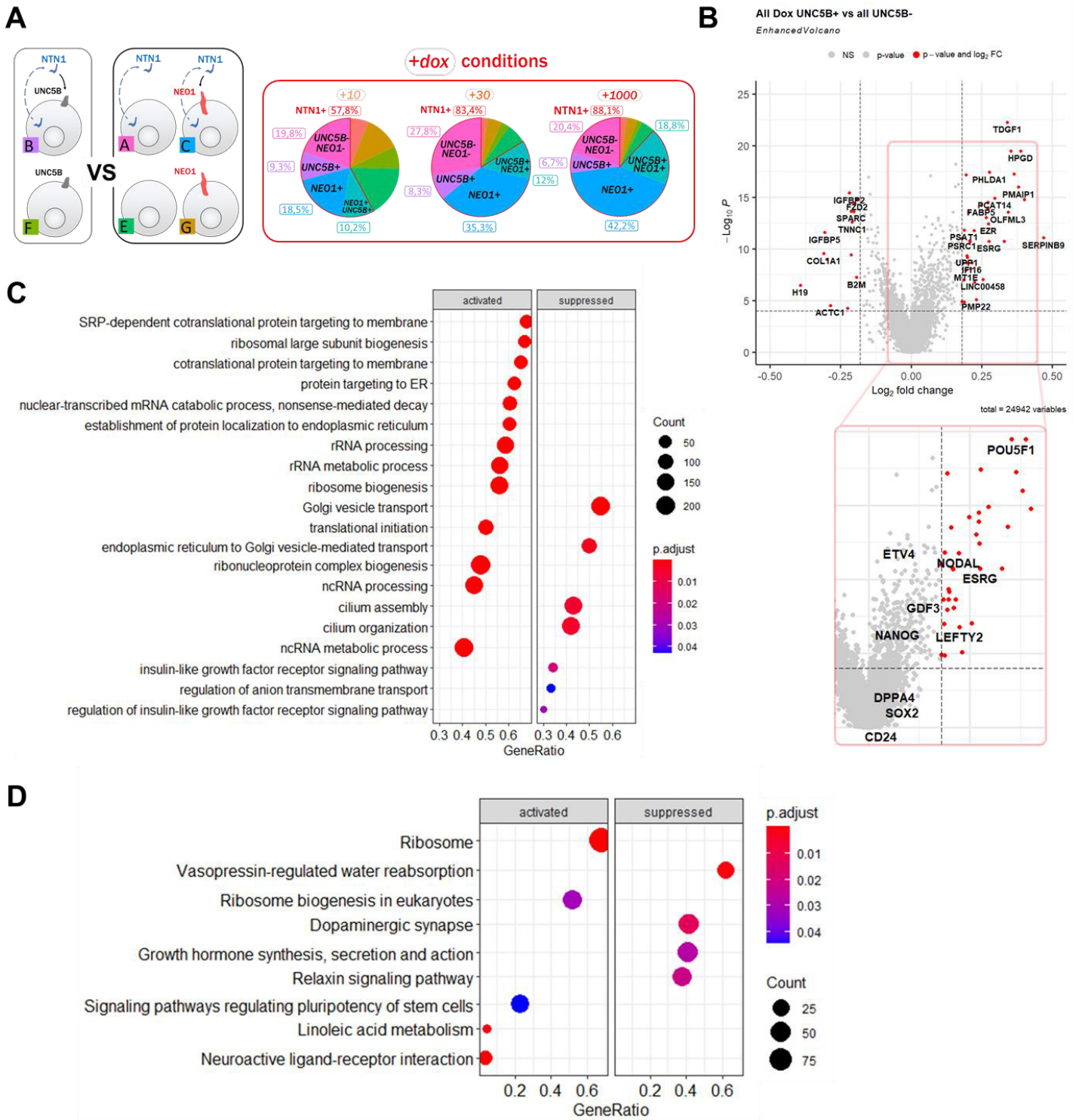

Figure 38. Upon induction, *UNC5B*-positive cells remain pluripotent and exhibit active transcription and translation.

(**A**) Scheme depicting the groups compared in all +dox conditions for analyses performed in (**B**-**D**). Subpopulations expressing *UNC5B* were pooled and compared to all cells without *UNC5B* expression.(**B**) Volcano plots showing DEGs of *UNC5B-specific* vs *UNC5B-* cells in +dox conditions. Bottom panel: enlargement highlighting pluripotency and NODAL signaling-associated genes. (**C**) Gene Ontology GSEA analysis performed on all DEGs of *UNC5B-specific* vs *UNC5B-* cells in +dox conditions.(**D**) KEGG pathway GSEA analysis performed on all DEGs of *UNC5B-specific* vs *UNC5B-* cells in +dox conditions.

IV.3.c. NEO1 and/or UNC5B activation in induced TL2i-hSTAN1is not the main cause of NTN1 effect.

To further understand these phenotypic differences, we then undertook to identify the genes expressed in response to one or the other receptor's activation. For this, we speculated that *NEO1* or *UNC5B* co-expressed with autocrine *NTN1* are strongly activated compared to a *NTN1-negative* context, where ligand is spatially distant and in limiting quantities. We thus compared *NEO1+NTN1+* and *UNC5B+NTN1+* (hereafter activated-NEO1 and -UNC5B,) to *NEO1+NTN1-* and *UNC5B+NTN1-* cells (hereafter silent-NEO1 and -UNC5B), respectively (**Figure 39A**). We generated volcano plots of these comparisons, in which the varying parameter is exogenous *NTN1* expression, and found for both *UNC5B*+ and *NEO1*+ cells important transcriptomic changes depending on ligand expression (**Figure 39B** and **Supplementary Figure S1**). In *NEO1*+ cells, we noticed that *NTN1* absence is associated with higher *NANOG, SOX2, OCT4, ESRG, DPPA4,* and NODAL signaling markers *NODAL, TDGF1, LEFTY2, FST. NEO1+NTN1+* on the contrary, express high levels of NTN1-exo top markers such as (*B2M, H19, COL1A1, LGALS1, ANXA1, ACTC1)* (**Supplementary Figure S2** and **Table S2**). For *UNC5B*+ cells, we observed similar impact of *NTN1* expression to a reduced extent (overall lower p-values). We then compared NTN1-exo cells expressing or not *NEO1* or *UNC5B*, to assess activated-receptors impact in a *NTN1*+ background. We found strikingly limited transcriptional effect of both *NEO1* and *UNC5B* in this context, with 8 (*NEO1, MALAT1, H19, COL1A1, TOP2A, TPX2, MKI67, UBE2C*) and 6 (*UNC5B, TDGF1, GAL, HIST1H1B, HIST1H4C*, UBE2C) upregulated genes, respectively (average $Log_2FC>0,2$ and p-value$<10^{-5}$) (**Figure 39C**). Moreover, *OCT4* is the only pluripotency gene downregulated upon one receptor (*NEO1*) expression. This intriguingly suggests that most transcriptomic effects observed in NTN1-exo cells are caused by the sole effect of *NTN1* rather by activation of its receptors, although activated NEO1 is associated with transcription of some top NTN1-exo markers.

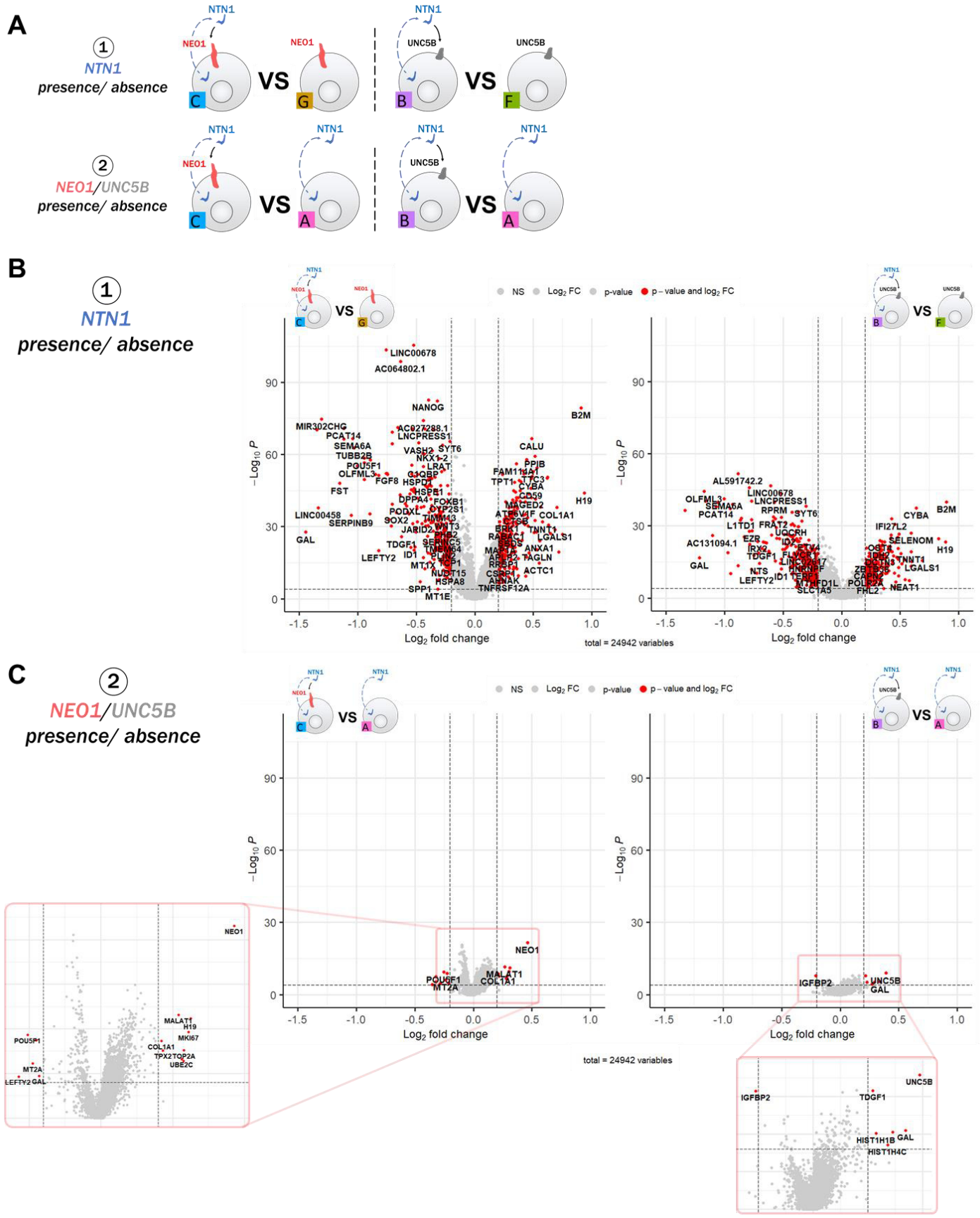

Figure 39. *NTN1* expression alone is responsible for greater transcriptional changes than *NEO1* or *UNC5B* expression and activation.

(**A**) Scheme depicting the groups compared in all +dox conditions for analyses performed in (**B**) and (**C**). (**B**) Volcano plots showing DEGs of *NTN1+NEO1+* and *UNC5B+* cells in +dox conditions vs *NTN1-NEO1+* and *UNC5B+* cells. (**C**) Volcano plots showing DEGs of *NTN1+NEO1+* or *UNC5B+* cells in +dox conditions vs *NTN1+NEO1-* and *UNC5B-* cells.

IV.3.d. UNC5B expression effect on TL2i-hSTAN1 cells is weaker than that of DRAXIN.

As precedingly observed, *NEO1*+ cells are associated in an induced context to differentiation of TL2i-hSTAN1, while *UNC5B* is correlated to maintenance of pluripotent characteristics. Because we previously suggested that *DRAXIN* acts as a shield against *NTN1* pro-differentiation cues and is thus also associated with pluripotency, we asked which of *UNC5B* or *DRAXIN* has the strongest pro-pluripotency effect. For this, we identified 4 subpopulations based on combined *UNC5B* and *DRAXIN* expression, and first compared *DRAXIN+UNC5B+* cells to *DRAXIN-UNC5B+*. By volcano plot representations, we found that *DRAXIN* expression yields important transcriptomic changes in a *UNC5B*+ context, with enrichment for both pluripotency and NODAL-signaling genes and concomitant downregulation of NTN1-exo markers (*B2M, H19, COL1A1, LGALS1, ANXA1, ACTC1)* (**Figure 40A**). Conversely, we observed sharply more discrete effects of *UNC5B* expression in a *DRAXIN*+ context, with a slight downregulation of NODAL-signaling members, and slight upregulation of *ETV4* and *OCT4* (average $Log_2Fc<0,2$) (**Figure 40B**). We consistently found with violin plot representations that *DRAXIN*+ cells systematically exhibit higher levels of some selected pluripotency and NODAL-associated genes than their *UNC5B*+ counterparts (**Figure 40C**). Among said genes, we found that only *ETV4* and, to a lesser extent, *NANOG* and *GDF3*, benefit from combined *DRAXIN* and *UNC5B* expression. Collectively, these data demonstrate that *DRAXIN* has a significantly stronger effect on TL2i-hSTAN1 pluripotency, and more generally transcriptome, than *UNC5B* expression.

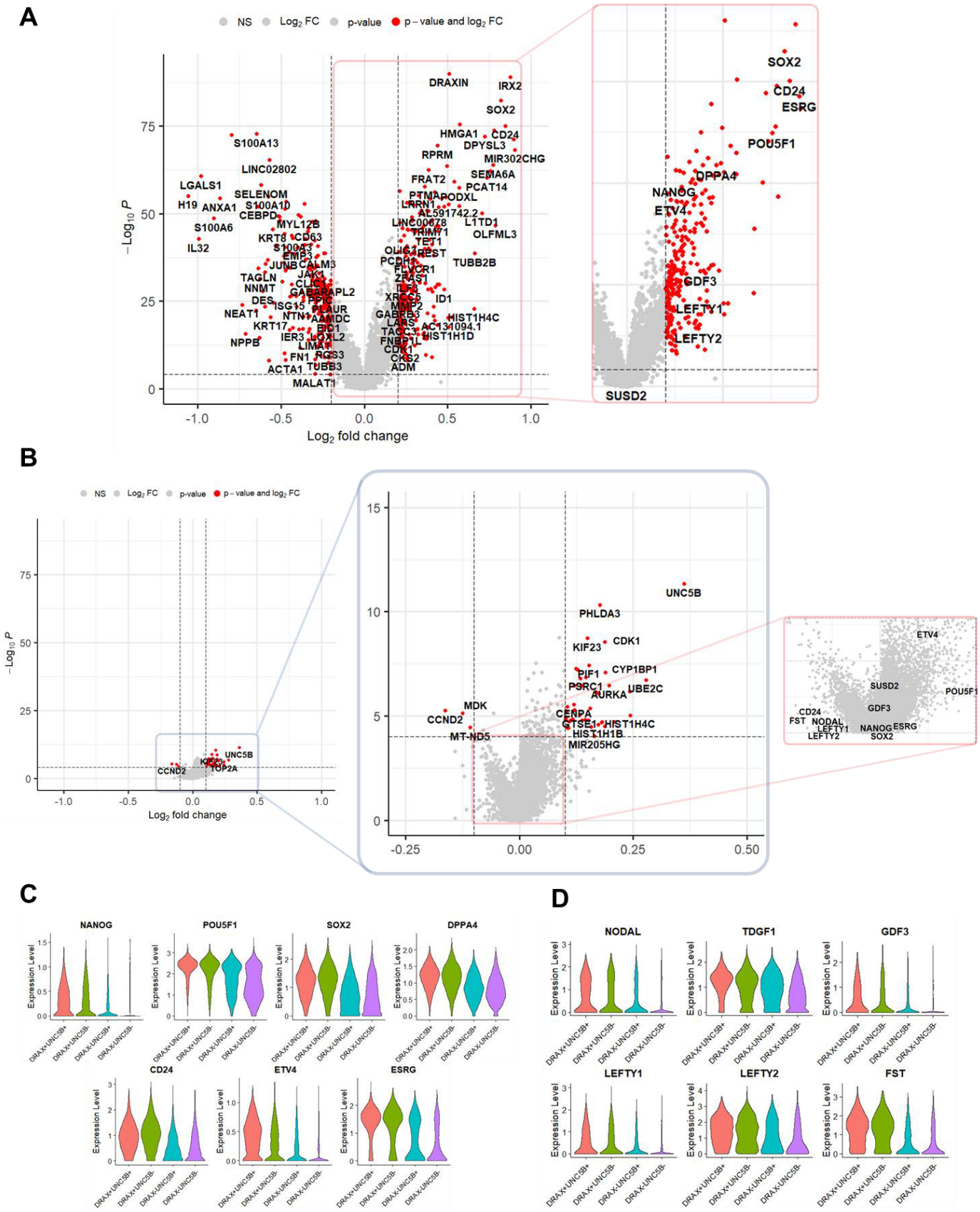

Figure 40. Pluripotency of hSTAN1 cells is more dependent on *DRAXIN* than *UNC5B* expression.
(**A**) Volcano plot showing DEGs of *DRAXIN+UNC5B+* vs *DRAXIN-UNC5B+* cells in all +dox conditions. (**B**) Volcano plot showing DEGs of *DRAXIN+UNC5B+* vs *DRAXIN+UNC5B-* cells in all +dox conditions. Left: volcano plot scaled to size of (**A**) volcano. Blue frame: enlargement of plot; Red frame: enalrgement with highlight of pluripotency and NODAL-signaling associated genes. (**C-D**) Violin plots of pluripotency (**C**) and NODAL-signaling associated (**D**) genes in *DRAXIN/UNC5B* subpopulations of hSTAN1 cells in all dox conditions.

Discussion

In this work, we asked if Netrin family genes, and more specifically *NTN1*, are involved in pluripotency regulation in primates as demonstrated in mouse, and could represent a new lever for the capture of *bona fide* primates' naïve pluripotency. Our main conclusion is that *NTN1* expression, unlike in macaques and mouse, is not associated to pluripotency in human but instead triggers differentiation to late mesodermal lineages. NETRIN-1 antagonist DRAXIN, on the contrary, is found enriched in the human naïve epiblast and is a potential new candidate for human pluripotency regulation, shielding PSCs against *NTN1* differentiating effect *in vitro*.

A. Netrin signaling in non-human primates' pluripotency

A.1 The *NTN1/UNC5B/NEO1* axis is a hallmark of naïve macaque cells

The first question we asked is how Netrin family genes are expressed in non-human primates' PSCs *in vivo* and *in vitro*. We found in analyzing publicly available single-cell RNA-seq data that, as for the mouse, the cynomolgus macaque's pre-implantation epiblast is enriched for *NTN1*, *UNC5B* and *NEO1*, and that *NTN1*-positive cells are associated with higher levels of pluripotency genes *OCT4*, *SOX2* and *NANOG*. *NTN1* antagonist *DRAXIN*, however, despite being expressed, is not associated with any difference in such markers' expression. Through bulk-RNA seq and qPCR analysis, we revealed that upon reprogramming to naïve-like pluripotency, primed rhesus macaque PSCs show an increase of *NTN1* and a converse decrease of *DRAXIN* while maintaining *UNC5B* and *NEO1* expression. This is consistent with our findings and previous reports that, while primed EpiSCs express no *Ntn1*, *bona fide* mouse naïve cells express the *Ntn1-Unc5b-Neo1* axis. By qPCR, we intriguingly observed in rhesus reprogrammed cell lines, along with *NTN1*, a co-upregulation of *NTN3.* Since *NTN3* expression was not detected in both rhesus PSCs bulk RNA-seq and embryos single-cell RNA-seq, and that *NTN1* and *-3* genes share the strongest sequences homology of the family (Van Raay et al., 1997), we hypothesize that this increase is due to a lack of specificity of the *NTN3* primers used for our qPCR experiment rather than an actual upregulation of the gene.

A.2 *NTN1* overexpression leads to pluripotency reinforcement of rhesus PSCs

Using a dox-inducible system, we showed that *NTN1* overexpression in rhesus macaque primed PSCs leads to discrete morphological changes, with a flattening and thinning of colonies not associated with visible increases in cell death or proliferation rate. Along with this transformation, we observed by qPCR analysis an increase of several pluripotency-associated genes in comparison to non-induced cells. These changes, despite being collectively in favor of pluripotency, are faint. Several factors could explain this observation: first, we used for these experiments the human *NTN1* gene, exhibiting a 99.34% sequence homology with its macaque counterpart. Although NTN1 binding sites to its receptors are here preserved, this could lead, for unknown reasons, to a weakening of the phenotype compared to rhesus NTN1. Second, we found that *NTN1*, as in the mouse, is associated in the macaque with the naïve epiblast, and to naïve-like reprogrammed PSCs rather than primed ones. It is a possibility that NTN1, in a context different from naïve pluripotency, does not trigger a pro-self-renewal effect or does so to a lesser extent. Such behavior would not be surprising, as several signals and pathways act in contrasting if not opposed fashion depending on the context; FGF/MEK/ERK, for example, is a potent differentiation axis in a naïve context, but is critical to the maintenance of pluripotency and self-renewal in the primed state of both primates and mouse (Hackett and Azim Surani, 2014; Weinberger et al., 2016).

A.3 *NTN4* expression is associated to primed pluripotency and gastrulation in macaque and mouse.

In the cynomolgus macaque embryo, we noticed at the peri-gastrulation stages a switch of expression from *NTN1* to another secreted netrin, NTN4, and an upregulation, in addition to *UNC5B* and *NEO1*, of another UNC5-family receptor, UNC5D. We also noticed that *DRAXIN*, despite being already expressed at the pre-implantation stages, is gradually increased upon implantation. Interestingly, we made consistent observations in rhesus PSCs. While *NTN4* and *UNC5D* are expressed at similar levels in primed cells, they are both downregulated upon reprogramming (**Figure 41**). *DRAXIN*, strongly expressed in the primed state, also shows a sharp downregulation depending on the reprogramming method. In mouse, although we did not observe *Unc5d* expression in the EpiSCs dataset at our disposal, we found *Ntn4* to be expressed, in contrast to the naïve 2i/LIF or epiblast cells. We thus speculate that, in the mouse and macaque, NTN1 and -4 represent antagonizing signals, the former regulating naïve, and the latter primed pluripotency or gastrulation. In the macaque, while NTN1 is likely to act through UNC5B and NEO1, NTN4 could act through UNC5D, co-expressed in the same context and embryonic stage. *DRAXIN*, strongly upregulated in primed cells *in vivo* and *in vitro*,

might here solely act to extinguish NTN1 signal in favor of NTN4. An element supporting this hypothesis is the important structural differences between NTN4, belonging to β- subfamily of netrins, compared to the other secreted netrins (NTN1, -3 and -5) belonging to the γ- group (Rajasekharan and Kennedy, 2009). It is worth noting that, although interaction between the latter and receptors UNC5 and NEO1/DCC has been demonstrated, a map or hierarchy of affinity remains to be established. This knowledge will be critical in future characterization of netrins and receptors' role in early mouse and primates' embryogenesis.

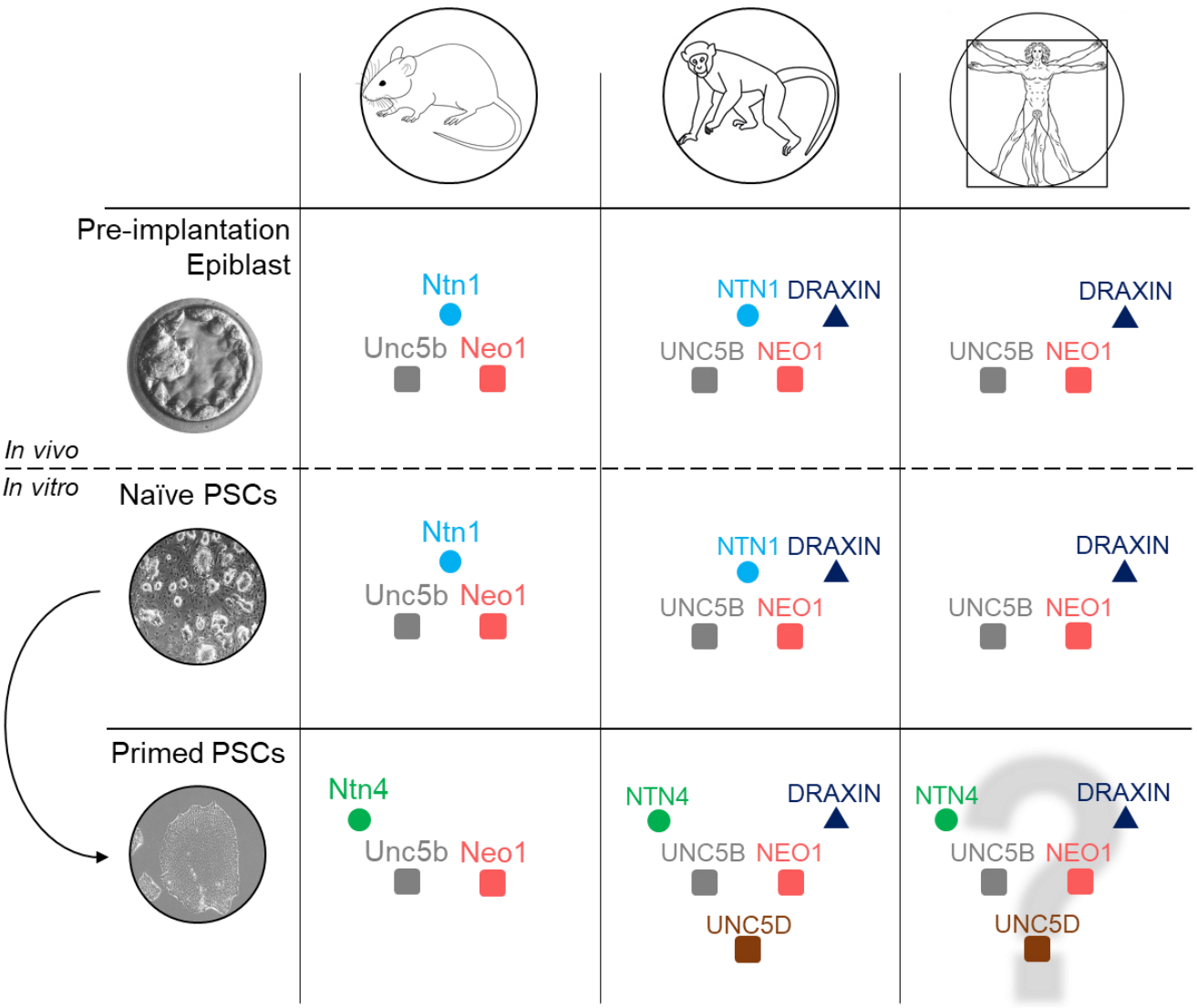

Figure 41: Netrin family genes expression in mouse and primates PSCs.

B. Netrin signaling in human pluripotency

B.1 *NTN1* expression is not a hallmark of human naïve pluripotency

By analyzing publicly available single-cell RNA-seq data, we investigated netrin family genes expression in the human pre-implantation embryo, and found that the naïve epiblast is enriched for *DRAXIN*, *NEO1* and *UNC5B*, but devoid of *NTN1* expression. *NTN1*-positive cells, contrary to the macaque, are not enriched but impoverished for pluripotency-associated genes. Interestingly, we showed that *DRAXIN*-positive cells on the other hand, show an upregulation of *OCT4* and *NANOG*. By exploring microarray data from the 5i/L/A and t2iLGöY protocols' original publications, we found that human PSCs reprogrammed with both methods display contrasting patterns of netrin family genes expression. We conclude that, contrary to the macaque or mouse, *NTN1* upregulation is not a hallmark of human naïve pluripotency. On the contrary, *DRAXIN* enrichment in the naïve epiblast and its correlation with high *OSN* expression, along with the complete absence of *NTN1* transcript in the same tissue, strongly suggest that NTN1 action is actively silenced in the human pre-implantation embryo. To verify this hypothesis, *in situ* observations of *NTN1* and *DRAXIN* transcripts and protein allocation will be instrumental.

B.2 *NTN1* overexpression leads to pluripotency exit of primed and naïve-like human PSCs.

Using the same tools as for rhesus macaque cells, we generated a human cell line, hSTAN1, expressing *NTN1* in response to doxycycline. In primed hSTAN1 PSCs, we demonstrated that NTN1 triggers an unambiguous pluripotency collapse. At the transcript level, we observed downregulation of numerous pluripotency-associated genes, including *OCT4*, *NANOG*, and the primed surface marker *CD24*, which we confirmed at the protein level through immunostaining. Interestingly, we observed that *OCT4*, *NANOG* and *CD24* decrease does not occur in a salt-and-pepper fashion, or by a homogenous reduction of signal in all cells, but is rather zone-specific, with clumps retaining expression of pluripotency genes in the central area of colonies. We noticed that this pattern anti-correlates with that of the NTN1-HA protein, aggregated in a net-like structure at the periphery of the colonies and impoverished in the middle. After reprogramming to the naïve-like state, we found that TL2i-hSTAN1 cells undergo similar changes, indicating that NTN1 affects self-renewal in the pluripotent state, whether primed or naïve. These observations were confirmed by our single-cell RNA-seq analysis of TL2i-hSTAN1 cells, through which we showed widespread downregulation of numerous pluripotency markers upon dox induction, and a clear-cut anti-correlation of *NTN1* and *NANOG* expression. We have moreover noticed that uninduced TL2i cells express primed

and formative pluripotency markers, and exhibit heterogeneous expression of naïve markers such as *KLF4*. *Bona fide* naïve cells, to the opposite of this pattern, are expected to express none of the former, and the latter in a homogeneous fashion. In preceding reports, it was already shown that human PSCs reprogrammed with different protocols exhibit transcriptional heterogeneity and expression of early lineage/ primed markers (Han et al., 2018; McCracken et al., 2020; Nguyen et al., 2018). This is consistent with the current knowledge that naïve-like human PSCs exhibit incomplete naïve characteristics (Aksoy et al., 2021), however, our findings reveal that the statement might be true to a greater extent than previously thought. Incidentally, a surprisingly low number of single-cell RNA-sequencing studies have been published on naïve-like human or non-human primates' cells to further confirm or infirm these observations, account being taken of the amount of efforts deployed by several groups to publish numerous reprogramming methods in the recent years.

B.3 NTN1 triggers commitment of naïve-like human PSCs to late mesodermal lineages.

B.3.1. Autocrine NTN1 induces striated muscle cell differentiation of TL2i-hSTAN1 cells.

Despite our finding that both primed hSTAN1 and naïve-like TL2i-hSTAN1 cells undergo pluripotency exit upon *NTN1* induction, we could not demonstrate any commitment to early lineages through qPCR analyses. This is a compelling observation, given that pluripotency and differentiation are two sides of a same coin, exit from the former triggering engagement in the latter. Surprisingly, we found that TL2i-hSTAN1 expressing autocrine NTN1, instead of committing to early lineages, express genes enriched for striated muscle cell differentiation, a late mesodermal lineage, and striated muscle structures such as myofibrils, sarcomeres and muscle filament. Muscle systems development, as any type of adult tissue differentiation, is a stepwise process during which cells of restricted potential gradually advance toward complete specification. In the case of striated muscle, three types of cells, myogenic progenitors (Expressing the PAX3 and PAX7 factors), myoblasts (Expressing MYF5 and MYOD1) and myocytes (Expressing MYOG1) precede the formation of more complex structures, the myotubes, myofibrils and myofibers, expressing the Major Histocompatibility Complex I (MHC-I) (Jiwlawat et al., 2018) (**Figure 42A**). When myocytes differentiation is directed from human iPSCs, the process takes up to 6 weeks in transgene-free conditions, reclaiming use of several pharmacological inhibitors and growth factors, and reclaims up to the double in duration to obtain myofibers (Jiwlawat et al., 2017; Shelton et al., 2016). In our

system, dox induction is applied for 72h, a strikingly shorter period of time, with a single protein being overexpressed. Furthermore, cells of origin are in a naïve-like state, *i.e.,* further away from differentiation in the development timeline than the primed human iPSCs used for said studies. When exploring expression of striated muscle precursors markers in TL2i-hSTAN1 cells, we found ~25% of the population to express the myogenic progenitor *PAX3* upon induction, versus ~90% expressing strong levels of *B2M,* coding for the Beta-2-Microglobulin protein, a member of the MHC-I complex (**Figure 42B**). We also noted that the 'net-like' aggregates observed in both primed and naïve-like hSTAN1 cells expressing NTN1 share structural similarities with myotubes formed by myocytes differentiated from human iPSCs (**Figure 42C**).

In mouse, it was demonstrated that Wnt activation (or GS3β inhibition) is necessary but not sufficient for myogenic differentiation (Suzuki et al., 2015). FGF2 (MEK/ERK activation), Hedgehog (Hh) activation and TGFβ inhibition are thus additionally used in numerous protocols to trigger efficient commitment (Brennan et al., 1991; Scata et al., 1999). Interestingly, TL2i-hSTAN1 cells are cultured in both GSK3β and MEK/ERK inhibition conditions, and we showed that upon induction, *NTN1*-negative cells, contrary to their NTN1-positive counterparts, are enriched for TGF-β/NODAL signaling genes. This suggests that *NTN1* overexpression allows to override MEK/ERK blockade and triggers TGF-β signaling inhibition, allowing progression through striated muscle commitment. These findings need to be further demonstrated at the protein and transcript level, but offer promising perspectives for muscle cells differentiation from human PSCs. An interesting approach in future studies will be to use recombinant NTN1 in a transgene-free PSCs culture system.

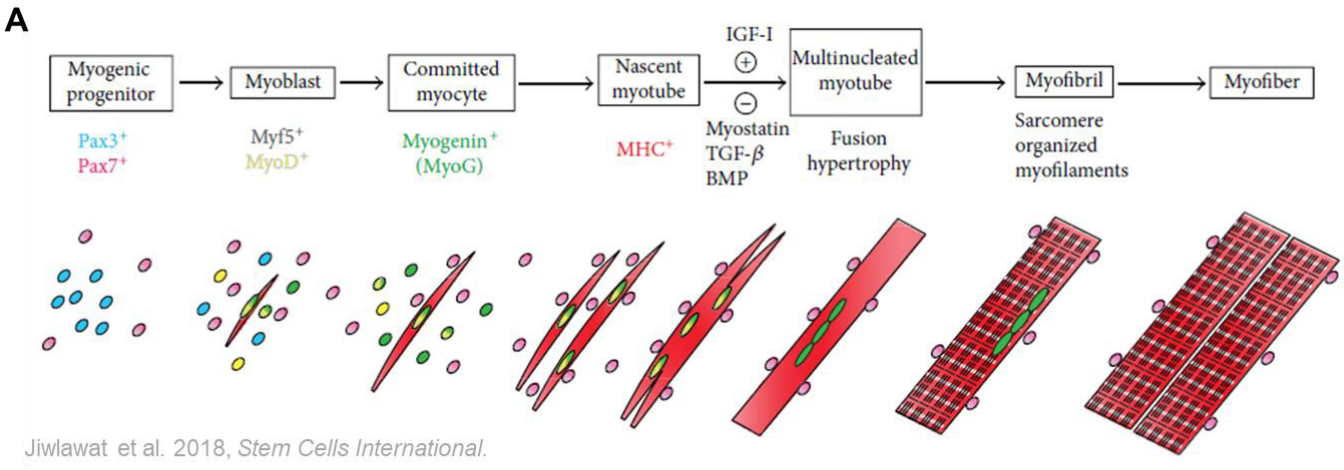

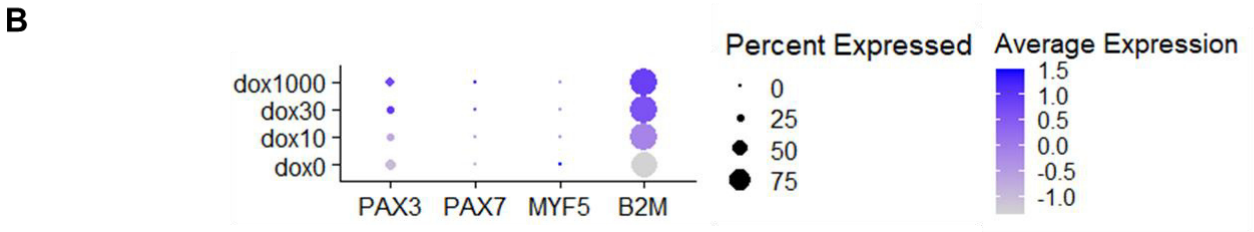

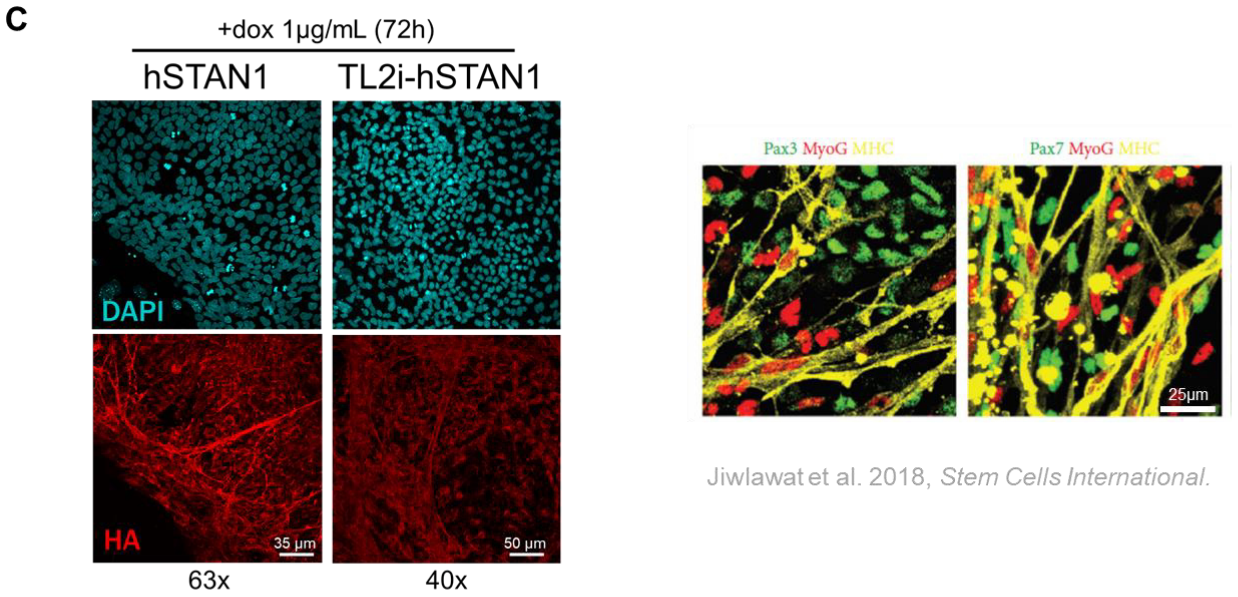

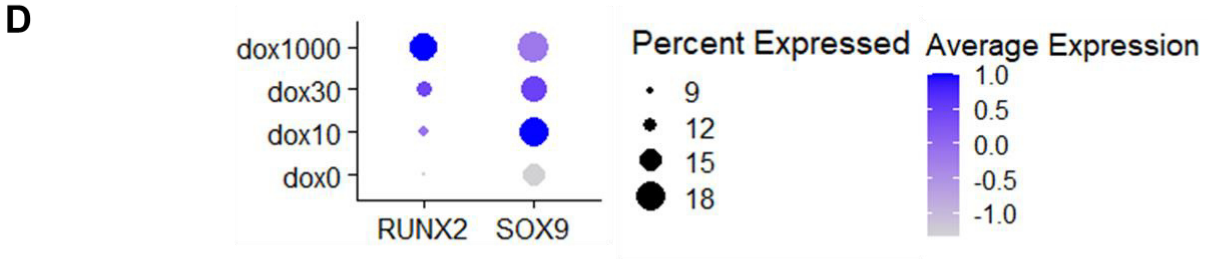

Figure 42: Skeletal muscle and osteoblastic differentiation of TL2i-hSTAN1 cells.

(**A**) Scheme depicting striated muscle differentiation (Jiwlawat et al 2018). (**B**) Dotplot of myogenic progenitors, myoblasts and myocytes markers expression in TL2i-hSTAN1 cells (**C**) Left: Immunostaining of primed and naive-like hSTAN1 cells submitted to 1µg/mL dox for 72h. Right: immunostaining of human iPSCs –derived myotubes (original picture from Jiwlawat et al. 2018). (**D**) Dotplot of osteoblasts progenitors *RUNX2* and *SOX9* expression in TL2i-hSTAN1 cells.

B.3.2. Paracrine NTN1 induces ossification and osteoblast differentiation

By comparing NTN1-zero TL2i-hSTAN1 in induced conditions to non-induced cells, we found a downregulation of pluripotency genes and upregulation of genes enriched for processes similar to NTN1-exo cells (*i.e.*, muscle filament and actin-myosin filament sliding), however, we also found the "ossification" and "osteoblast differentiation" terms to be enriched. We confirmed this finding by inspecting the expression of *RUNX2* and *SOX9*, both markers of osteoblast commitment, in TL2i-hSTAN1 (Rutkovskiy et al., 2016). We found the former to be strongly upregulated in a dox dose-dependent manner upon induction, and the latter to be upregulated, with a peak at 10ng/mL (**Figure 42D**). Collectively, these findings show that paracrine NTN1 has an effect only partially overlapping with autocrine NTN1 and triggers a distinct phenotype. Two hypotheses could explain this observation: 1) Paracrine NTN1 reaches to neighboring cells in residual quantities compared to autocrine NTN1, resulting in a low-dose effect triggering a different commitment. Incidentally, such an effect could not be tested with our inducible system, because of its surprisingly greater than expected efficiency, triggering strong *NTN1* overexpression with the low dox dose of 10 ng/mL. 2) NTN1 signal acts differently when captured from neighboring cells versus when secreted. Whether one, the other, or both of the hypotheses are true, autocrine and paracrine signals do not trigger opposed phenotypes, but differentiation into lineages belonging to the late mesodermal lineage. It is also worth noting that osteoblast, as striated muscle differentiation, reclaims Wnt activation or GSRβ inhibition; a major difference however, is the necessity of TGF-β signaling activation instead of inhibition. This suggests that, in our system, only autocrine NTN1 is able to trigger this pathway's inhibition, explaining at least partially the different outcomes observed in lineage engagement.

B.3.3. NTN1 signal triggers morphological changes in hSTAN1 cells.

In addition to differentiation, we found that hSTAN1 exposed to NTN1, whether primed or naïve, undergo morphological transformations. We noticed at the highest dox doses a thinning of colonies accompanied by an apparent fusion of cells, making

colonies appear as syncytia. During skeletal muscle differentiation, cell fusion is a mandatory step leading to the formation of myotubes, our finding is thus consistent in that context. We moreover found enrichment in NTN1-exo cells for terms confirming a morphological transformation, such as regulation of actin cytoskeleton, cellular component assembly involved in morphogenesis, and regulation of cell-substrate adhesion. A compelling finding, however, is the observation of a similar morphological change, although to a lesser extent, in rhesus STAN1 cells for which we demonstrated a reinforcement of pluripotency rather than differentiation. A possible explanation is that NTN1 itself, being an extracellular matrix and laminin-related protein, aggregates in macrostructures when overexpressed and induces mechanical pressure on the surrounding cells.

B.3.4. Cells exposed to NTN1 form cilia.

In both NTN1-exo and NTN1-zero cells from the induced conditions (undergoing paracrine NTN1), we found enrichment for terms associated for cilium assembly and organization. Primary cilia are microtubule-based structures functioning as sensory organelles in most adult cell types of vertebrates (Alaiwi et al., 2009). In addition to the detection of mechanical stresses, they have been shown to be paramount to the capture and processing of molecular signals including Hedgehog, Wnt and TGF-β (Bodle and Loboa, 2016) So is done by the gathering along the cilium of receptors and downstream effectors of a given pathway (Clement et al., 2013). Disruption of ciliogenesis has been shown to severely impair numerous processes, including proliferation and differentiation of adult stem cells and progenitors (Yuan et al., 2016). Interestingly, ciliogenesis has also been linked to the cell cycle, anti-correlating with mitosis (Plotnikova et al., 2009). It was indeed shown that cilia are assembled during the G_1 (or G_0) phase, last through the S phase, and are disassembled during G2 before entering the M phase. In our system, ciliogenesis in *NTN1*-positive cells could thus be explained by several scenarios: 1) NTN1 itself triggers cilia assembly, allowing enhanced capture of TGF-β ligands and growth factors, 2) NTN1 triggers differentiation toward lineages reclaiming pathways controlled by cilia, resulting in a cilium assembling as a feedback loop, or 3) Ciliogenesis is the reflect of *NTN1*-positive cells being differentiated, thus going through a longer G_1 phase than the rapidly proliferating

naïve-like *NTN1*-negative population. Regardless of the correct hypothesis, ciliogenesis and primary cilia in stem cell research have been so far overlooked considering the pathways to which they are tightly linked. Further investigations in this area will be instrumental in better understanding self-renewal and differentiation processes.

B.4 *DRAXIN* is a marker of human naïve pluripotency

B.4.1 DRAXIN shields TL2i-hSTAN1 cells against NTN1 pro-differentiation effect and preserves naive pluripotency

Upon induction, we noticed that TL2i-hSTAN1 cells exhibit anti-correlative *NTN1* and *DRAXIN* expression and a converse correlation between *NANOG* and *DRAXIN*. We further demonstrated that *DRAXIN*-positive cells in +dox conditions do not only retain pluripotency, but exhibit the highest expression levels of pluripotency and NODAL-signaling markers among the *NTN1*-negative fraction, thus qualifying as the most pluripotent compartment of the whole population. Most interestingly, this is also true for control TL2i-hSTAN1, where *DRAXIN*-positive cells exhibit the highest levels of *NANOG, OCT4, SOX2, DPPA4* and *SALL4*, though to a lesser extent than in the induced conditions. The antagonizing capacity of Draxin toward Ntn1 has been clearly demonstrated in the mouse, zebrafish and more recently human, and remains to this day this only characterized function of the molecule (Gao et al., 2015; Islam et al., 2009). Although correlation between *DRAXIN* expression and naïve pluripotency maintenance in TL2i-hSTAN1 cells does not represent a causal link *per se*, we therefore conclude that DRAXIN expression here actively protects against NTN1 mesodermal differentiation effects (**Figure 43**).

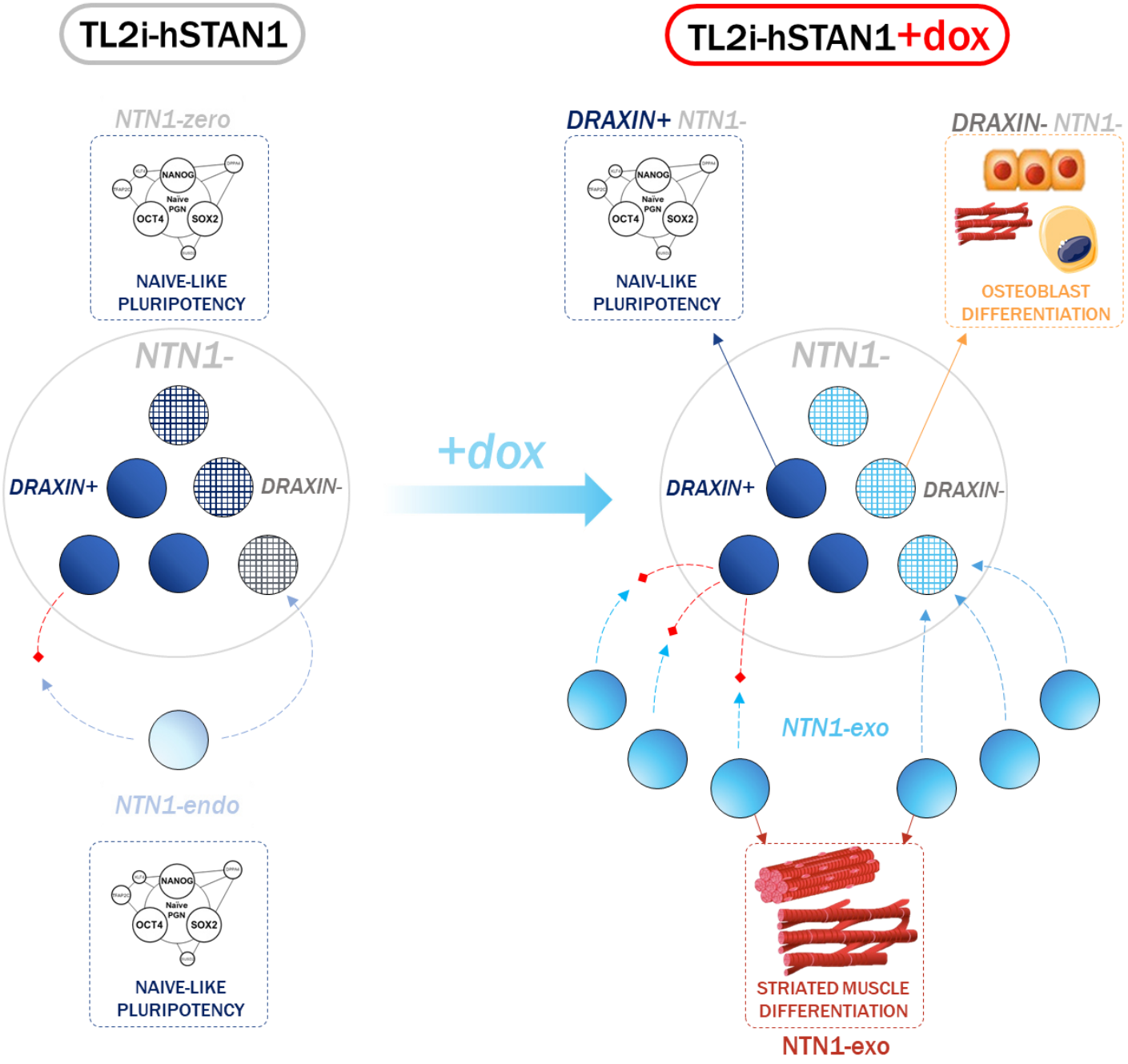

Figure 43. TL2i-hSTAN1 response to *NTN1* overexpression.

Scheme of *NTN1* overexpression on TL2i-hSTAN1 cells. Dashed grey/light blue arrows and dashed red lines represent NTN1 and DRAXIN action, respectively.

B.4.2 DRAXIN is associated with naïve pluripotency in the human pre-implantation embryo

As mentioned in part **B.1**, *DRAXIN*, but not *NTN1*, is enriched in the human naïve-epiblast. We also demonstrated that, contrary to the macaque, *DRAXIN*-positive cells display higher expression levels of *OCT4*, *NANOG,* and the naïve pluripotency markers *SUSD2* and *DPPA4*. We also found *NODAL* and the *GDF3*, *LEFTY1* and *-2* related genes to be enriched. KEGG pathway and GO analyses further demonstrated enrichment for signaling pathways regulating pluripotency along with oxidative phosphorylation, the preferential metabolic mode of naïve pluripotent stem cells. We moreover showed that *DRAXIN* is specifically enriched in the epiblast but absent from all other tissues, to the exception of a discrete expression in the primitive endoderm. We found, however, that the PE marker *GATA6* is the most downregulated gene of the *DRAXIN* population, indicating that DRAXIN is indeed a naïve-epiblast marker in human. DRAXIN enrichment in the human epiblast has no relevance in the current state of knowledge, where its only function is to antagonize NTN1 signal. If this is the case, the only explanation for this finding would be that NTN1 is exclusively devoted to differentiation in human, and is thus actively (and disproportionately) countered *in vivo* to avoid potential deleterious effects of a stochastic expression of NTN1 by a few cells. A second hypothesis, however, is that DRAXIN has a more potent role than previously characterized, and is either a driver of naïve pluripotency, maybe acting itself as a ligand, or prevents the action of one or several unreported molecules. One observation supporting this scenario is the fact that uninduced TL2i-hSTAN1 cells widely and strongly express *DRAXIN*, despite 8% of the population expressing, at low levels, its NTN1 interactant.

B.5 *NTN1* partially acts through NEO1*,* but not UNC5B to trigger pluripotency exit

In TL2i-hSTAN1 cells, we demonstrated upon induction a switch from a majority *UNC5B* to *NEO1* netrin receptors expression. More specifically, we found the *NEO1+UNC5B-* configuration to be predominant at the highest dox doses. By isolating the *NEO1*-positive population in all induced conditions, we showed that these cells are

downregulated for pluripotency and NODAL-signaling and undergo ciliogenesis, thus exhibiting an overlapping phenotype with the NTN1-exo cells. In analyzing *UNC5B*-positive cells in a similar way, we instead found enrichment for some, but not all pluripotency and NODAL-associated markers (*e.g.*, *OCT4, ESRG, TDGF1 NODAL* and *LEFTY2*; but not *NANOG*, *SOX2* and *GDF3*). We further found enrichment for signaling pathways regulating pluripotency and ribosome biogenesis, a term reported to be consensual in naïve-like human cells. This suggests that, in our system, *NEO1* and *UNC5B*-positive cells are respectively associated to differentiation and naïve-pluripotency maintenance. NTN1 might thus be a bipotent signal inducing two distinct outcomes depending the receptor bound. This hypothesis was suggested in the mouse by Huyghe and colleagues, in a mirror scenario where a majority activation of NEO1 promotes self-renewal versus a MAPK activation/ differentiation by UNC5B (Huyghe et al., 2020). Another hypothesis is that human NTN1 has a stronger affinity for NEO1 than for UNC5B, thus triggering differentiation in cells expressing the former, but barely affecting the background pluripotent phenotype in those expressing the latter. We attempted to answer this question by assessing NEO1 and UNC5B activation effect in our induced populations. Surprisingly, we found that NTN1 autocrine signal alone is responsible for significantly greater transcriptional changes than the simultaneous presence of NTN1/NEO1 or NTN1/UNC5B. In what we termed NEO1-activated cells, however, we found a downregulation of *OCT4*, and an upregulation of *H19*, *COL1A1* and *MALAT1*, NTN1-exo 2nd, 8th and 38th top markers, respectively. This represents a 6% of genes upregulated with an average Log2Fc above 0,25 in cells expressing *NTN1* alone. Conversely, UNC5B activation leads to no upregulation of NTN1-exo markers, but does lead to the upregulation of the NODAL receptor coding gene *TDGF1.* We conclude that *NTN1* overexpression effect in TL2i-hSTAN1 cells is in a minor way due to NEO1 binding, leading to *OCT4* downregulation and to *H19*, *COL1A1* and *MALAT1* upregulation (**Figure 44A**), but remains largely unexplained. The most likely hypothesis is that NTN1 is able to bind in our system one or several receptors different from the UNC, DCC/NEO1 and DSCAM families, and does so with greater affinity.

B.6 UNC5B and NEO1 are respectively associated to naive pluripotency and differentiation in the human pre-implantation embryo.

Consistently with our findings in TL2i-hSTAN1 cells, we found in the human pre-implantation embryo that *NEO1*-positive cells, despite being ubiquitously expressed at all stages and in all tissues including the naïve epiblast, are impoverished for pluripotency and NODAL-signaling markers. Interestingly, we also found in this population upregulation of genes enriched for ciliogenesis. In the mouse, primary cilia first appear at E6 in epiblast cells, and further propagate in early lineages, but are absent from extra-embryonic tissues (Lyu and Zhou, 2017). Upon implantation, the overall number of ciliated cells increases, correlating with progression in embryogenesis and thus differentiation/specification. If this paradigm is similar in human, *NEO1*-positive cells are hence not trophoblastic, and likely epitomize a fraction of cells undergoing specification.

Contrary to *NEO1*, we found that *UNC5B* is strongly enriched in the early epiblast and PE, but absent at all other stages. Further analysis demonstrated that *UNC5B*-positive cells are, contrary to their NEO1-positive counterparts, enriched for signaling pathways regulating pluripotency and oxidative phosphorylation, and exhibit expression of naïve pluripotency and NODAL-signaling markers. Despite its presence in the PE, we found that *UNC5B* anti-correlates with *GATA6* expression, demonstrating its human naïve epiblast marker status. We consider this finding of the utmost significance, because UNC5B enrichment cannot be explained by the presence of NTN1, which expression fades out at the 8-cell stage. Missing its putative ligand, we therefore hypothesize that UNC5B binds in the human embryo another “X” ligand (**Figure 44B**). This is supported by the fact that UNC5B, being a dependence receptor, should trigger apoptosis in absence of ligand binding, and thus epiblast collapse in the embryo in absence of ligand binding. A potential candidate for this unknown molecule is NTN4, expressed in the early ICM, EPI and PE, although no enrichment for pluripotency can be observed for *NTN4*-positive compared to *NTN4*-negative cells. Another possibility is that UNC5B binds other molecules from families distinct of Netrins, and for which interaction has not been thus far reported.

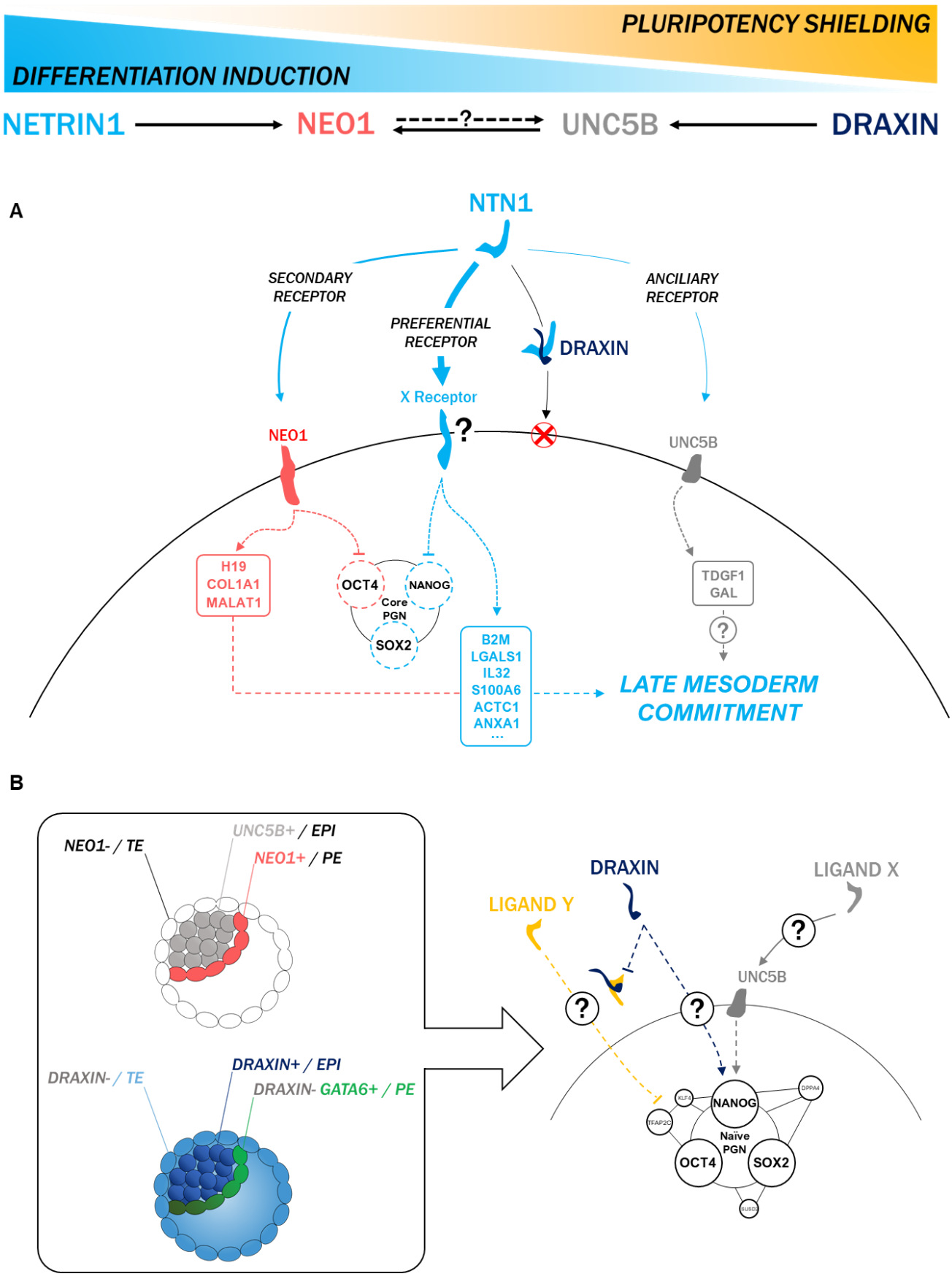

Figure 44. Graphical abstract: Netrin family members in human naive pluripotency regulation. (**A**) NTN1 effect on TL2i-hSTAN1 cells. Boxes represent genes expressed in response to NTN1 signal. (**B**) Left: *DRAXIN*, *NEO1* and *UNC5B* expression in the human pre-implantation embryo; Right: Hypothetical model of DRAXIN and UNC5B action on human epiblast cells pluripotency.

C. To sleep or not to sleep, discrepancies of Netrin-1 effect in the mouse, macaque and human.

In this work, we showed important discrepancies between Netrin family members involvement in pluripotency regulation of the mouse and primates. In the mouse, promotion of self-renewal and naïve pluripotency through the *Ntn1-Unc5b-Neo1* axis has been clearly demonstrated *in vitro*, and all three genes are found concomitantly expressed in the naïve epiblast, suggesting a similar role. In the macaque, we showed a conservation of the *NTN1-UNC5B-NEO1* axis *in vivo*, and a correlation between *NTN1* expression and pluripotency. Accordingly, we demonstrated that *NTN1* overexpression in primed macaque PSCs leads to an increase of pluripotency genes expression. Interestingly, we made drastically different findings in humans. First, we showed a complete absence of *NTN1* transcript after the 8-cell stage *in vivo*, and an impoverishment of pluripotency genes expression in *NTN1*-positive cells. Second, we demonstrated that *NTN1* overexpression rapidly triggers late mesodermal differentiation of naïve-like human PSCs. We thus showed that, while NTN1 promotes pluripotency in the mouse and macaque, it does precisely the opposite in human, where naïve pluripotency is quite contrarily associated with the NTN1 antagonist DRAXIN. Interestingly, *DRAXIN* expression in the early embryo is a major difference between the mouse and primates. Despite a strong homology between genes of the two groups and a similar putative function, *Draxin* is completely absent from the mouse early embryo, but is enriched in both the human and macaque's.

As mentioned in introduction of this work, one major difference between the mouse and primates that has been proposed to account for pluripotency regulation discrepancies is embryonic diapause. In eutherian mammals, this phenomenon, also known as discontinuous development, is the process by which a blastocyst enters a reversible dormant state upon unfavorable environmental conditions (Lopes et al., 2004). In mouse, this mechanism has been linked to the LIF/gp130/STAT3 and mTOR pathways, c-Myc activity, and has been shown to be a generally facilitating factor to mESCs derivation from blastocysts (Brook and Gardner, 1997; Bulut-Karslioglu et al., 2016; Evans and Kaufman, 1981; Scognamiglio et al., 2016). In primates, embryonic diapause has not yet been reported (Ptak et al., 2012), however, we speculate that genes coding for an ancestral molecular tooling might remain in regions silenced during early embryogenesis. If so is the case for macaques, it is possible that NTN1 belongs to this vestigial apparatus and thus has a pro-pluripotency effect, although dampened compared to the mouse. This would imply that the human genome, contrary to its non-human

primates' counterparts, has completely lost this heritage, only retaining the later functions of NTN1 in development, *i.e.,* neurogenesis and late mesodermal lineages differentiation. It seems, however, that Netrin family genes in general are not entirely disconnected from pluripotency regulation, as both *DRAXIN* and *UNC5B* associate with it in human. It is possible that what is observed with the *Ntn1-Unc5b-Neo1* axis in the mouse occurs in humans through a *X-UNC5B-DRAXIN* axis, X being an UNC5B ligand remaining to be identified. It is worth noting that, in attempts to identify potential candidates for X, we noticed several guiding molecules from families distinct of Netrins (Semaphorins, Slits and Repulsive Guidance Molecules) to be enriched in the naïve human epiblast or uninduced TL2i-hSTAN1 cells (**Supplementary Figure S3**). This strongly suggests that, as Netrins, these other guiding molecules have functions broader than their involvement and neurogenesis, and may constitute a new research avenue in early embryogenesis and pluripotency understanding.

D. Further studies

D.1 NETRIN1 effect.

In order to further understand Netrins and receptors function in primates' pluripotency regulation, several experiments will be instrumental. It will be first necessary to confirm that NTN1 exerts the effects observed in this work in other human and macaque cell lines; notably, *NTN1* overexpression effect in naïve-like rhesus PSCs has not been tested here. Assessing NTN1 effect through other means that the XLone system, *i.e.*, using other inducible systems or a transgene-free system with recombinant NTN1, would be of great interest. Incidentally, Netrin family genes expression in primed human PSCs remains to be overviewed and will reveal if, as for the macaque, NTN4 and UNC5D are the primed components of the family.

D.2 DRAXIN

In humans, we showed the central position of DRAXIN in the naïve pluripotency context. To establish if *DRAXIN* expression has a causal link with pluripotency maintenance, a *DRAXIN* knockout and converse overexpression in human PSCs will be critical, and will allow

to characterize potential underlying mechanisms. Another paramount information will be to establish if DRAXIN is expressed at the protein level in the human epiblast.

D.3 UNC5B and NEO1

In this work, we demonstrated a distinct effect of *NEO1* and *UNC5B* expression in human both *in vivo* and *in vitro*, however, both receptors function remains elusive. Whether other ligands are involved, and if so, what is the nature of these has to be elucidated. This could be addressed using mutant forms of NTN1, able to bind one but not the other, or none of the receptors. Complete knockouts of *NEO1* and *UNC5B* would also be instructive. We also suggested that, *in vivo*, UNC5B binds an unidentified ligand termed “X” therefore promoting naïve pluripotency. If this hypothesis is correct, the identification of X will be critical, and a complete KO of *UNC5B* in human PSCs should lead to pluripotency disruption.

Methods

Cell culture

All macaque and human cells were cultured at 37°C in 5% CO2, 5% O2 on 0.1% gelatin-coated dishes with murine embryonic fibroblasts (MEFs) growth-inactivated with mytomycine (Sigma) for 2 to 3 hours. All media used for culture were refreshed daily, and ROCK inhibitor Y27632 (Calbiochem) was used at 10µM for 24h following passages. Brightfield pictures were taken using Nikon's Eclipse Ti-S microscope.

Primed cells

Primed human (F-OS3-10) and macaque (LyonES) cells were cultured on 35mm dishes with 180 000 and 200 000 growth-inactivated MEFs per 35mm, respectively, using KnockOut Dulbecco's Modified Eagle's Medium (KO-DMEM) supplemented with 20% Knock Out Serum Replacement (KOSR, Gibco), 1% non-essential amino acids (NEAA, Gibco) 1mM glutamine (Gibco), 0.1mM β-Mercaptoethanol (Sigma), and 5ng/mL of FGF2 (Interchim) were used for routine culture, with daily medium refreshing. LyonES colonies were manually split and passaged every 4 to 5 days; F-OS3-10 every week.

TL2i

Primed to naïve conversion of F-OS3-10 cells was performed using the TL2i protocol from Chen et al. 2015. Basal culture medium for primed cells (described above) was supplemented with 10,000 U/mL hLIF, 250nM 4'-OHT, 3 mM CHIR99021 and 1 mM PD325901(Stemgent). TL2i medium was applied on primed cells with ROCKi during 24h; ROCKi was subsequently removed and cells were grown for a week, then routinely passaged by single-cell dissociation with trypsin-EDTA (Gibco) every 3 to 4 days. Stabilized TL2i-OS3 cells were cultured on 280 000 MEFs or 640 000 MEFS on 35 or 60mm dishes, respectively.

hSTAN1 cell line creation

F-OS3-10 cells were transfected with 2.5 µg for ~100 000 cells of the XLone-NTN1-HA transgene (obtained after modification of the XLone-GFP plasmid; Addgene #96930) using the Neon electroporation system (Invitrogen; 1050v, 20ms, 2 pulses). The hSTAN1 cells thus

obtained were subsequently plated on fresh MEFs (similar seeding to TL2i-OS3) and grown 2 weeks in medium supplemented with 250ng/mL of neomycin (G418). After two weeks of selection, cells were routinely cultured as TL2i-OS3, with permanent addition of Neomycin. Inductions were performed using doxycycline (Sigma) at 10, 30, 100, 300, 500, 1000 or 2000 ng/mL.

Western Blots

Cells used for western blots were pelleted through centrifugation and subsequently lysed in RIPA buffer, complemented with protease and phosphatase inhibitors. Lysates were then cleared by centrifugation (14 000 rpm for 30 min at 4°C) and protein concentration was assessed with the Bradford method. 15µg of proteins were used for subsequent steps. After SDS–PAGE and electroblotting on polyvinylidene difluoride, membranes were incubated with a HA specific primary antibody (Sigma), diluted at 1 :1 000. Blots were incubated with horseradish peroxidase-coupled anti-rabbit immunoglobulin G (Jackson ImmunoResearch, diluted at 1 : 10 000) and developed with Clarity Western ECL Substrate (BIO-RAD).

Immunofluorescence

Cells were fixed on coverslips with 4% Paraformaldehyde for 30min at room temperature (RT), and permeabilized with 0.4% Triton X-100 (Sigma) for 10min. Non-specific binding sites were blocked with PBS containing 5% of donkey serum (Biowest) and 0.1% Triton X-100 for 30min at RT. Cells were incubated overnight at 4°C with primary antibodies raised against HA (Sigma), NANOG (R&D Systems), OCT4 (CliniSciences), SOX2 (Bio-Techne), CD24 (Beckton & Dickintson Biosciences), diluted at a concentration of 1:200 in the blocking solution. After four rinses with PBS, cells were subsequently stained with secondary antibodies conjugated to Alexa Fluor-647, -594 and -488 (ThermoFischer), and diluted at 1/1000th in the blocking solution for 1 hour at RT in the dark. Nuclear staining was performed by applying DAPI (Invitrogen ; diluted at 1:8000 in the blocking solution) on the cells for 8min at RT. After 3 rinses in PBS, coverslips were mounted on microscope slides and analyzed using confocal laser scanning microscopy system (Leica Microsystems, SP5). All incubations were performed under continuous gentle agitation.

Quantitative PCR

RNA was extracted using RNAeasy kits with on-column DNAse digestion and reverse transcription carried out with the High Capacity cDNA Reverse Transcription Kit (Applied Biosystems) according to the manufacturer's recommendations. qRT-PCR was performed using specific primers (listed in Supplemental Table S3) and Fast SYBR® Green Master Mix on the StepOnePlus™ system (Applied Biosystems).

Bioinformatics

Single-cell RNA sequencing

Cell suspension (1200 cells per µl) was added to 10x Genomics Chromium Single Cell Controller (10x Genomics) to achieve 2500 encapsulated cells per condition (4 samples). The next steps for cDNA synthesis and library preparation were done following the manufacturer's instructions (chemistry V3). All Libraries have been sequenced simultaneously using the Novaseq 6000 platform (Illumina) in order to target 150k reads per cell. Cell Ranger version 5.0.1 was used to align reads on the mouse reference genome GRCm38 mm10 to exclude MEFs and the human reference genome GRCh38, and to produce the count matrix.

Analysis of single-cell RNA-sequencing data

Quality control and filtering. We filtered 2414, 2333, 2065 and 1835 cells for dox0, dox10, dox30 and dox1000, respectively, based on two-quality control criteria: the number of genes per cell and the fraction of counts from mitochondrial genes per cell. Cells with <4500 genes or >10000 and with >10% mitochondrial genes fraction were removed.

Clustering analysis. Filtering and Data analysis were performed using the R package Seurat (version 4). First, genes expressed in less than 3 cells were removed in each dataset. Gene expression was normalized using sctransform workflow in which the 3000 most variable genes were identified. Then, the 4 independent datasets were aggregated, scaled with cell cycle and mitochondria expression regression and used for PCA at 50 dimensions. We then performed clustering (30 PCs; resolution = 0.5) yielding 10 final clusters. The clusters were visualized in

two dimensions using the RunUMAP() function (minimum distance = 0.3; n_neighbors = 30 L; umap.method = ‘umap-learn’; metric = ‘correlation’). We finally performed differential expression analysis using the *Findmarkers()* function of Seurat.

Volcano plots from differentially expressed genes were generated using the Enhanced Volcano package (v3.13) for R. Gene Ontology, KEGG pathway and Gene Set Enrichment analyses were carried out using the ClusterProfiler (v3.18.1) and DOSE (v3.16) packages.

Supplementary Data

Supplementary Table S1: Primates PSCs' naive reprogramming protocols

Protocol	LIF	NODAL/TGFB signaling	"2i"		MAPK inhibition				AMPKi	Chromatin remodeler	other
			GSK3i	MEKi	BRAFi	SRCi	PKCi	JNKi	p38i			
NHSM (Gafni et al. 2013)	yes	MEFs + TGFB1	yes	yes	no	no	yes	yes	yes	no	no	-
3i/L (Chan et al. 2013)	yes	MEFs	yes	yes	no	no	no	no	no	yes	no	-
4i (Fang et al. 2014)	yes	MEFs	yes	yes	no	no	no	yes	yes	no	no	-
2iL/Toggle (Ware et al. 2014)	yes	MEFs	yes	yes	no	no	no	no	no	no	HDACi	sequential use of HDACi and 2i/LIF
t2iLGö (Takashima et al. 2014)	yes	MEFs	yes	yes	no	no	yes	no	no	no	no	transitory NANOG and KLF2 overexpression
5i/L/A (Theunissen et al. 2014)	yes	MEFs + Activin A	yes	yes	yes	yes	yes	optional	no	no	no	-
TL2i (Chen et al. 2015)	yes	MEFs	yes	yes	no	no	no	no	no	no	no	transitory STAT3 overactivation
nPSCs (Duggal et al. 2015)	yes	MEFs	yes (x2)	yes	no	no	no	no	no	no	VPA (HDACi)	-
YAP-PSCs (Qin et al. 2016)	yes	MEFs	yes (x2)	yes	no	no	no	no	no	no	no	Hippo inhibition through LPA or YAP overexpression
LCDM/EPSCs (Yang et al. 2017)	yes	MEFs	yes	yes	no	no	no	no	no	no	no	Use of MiH and DiM
PXGL (Guo et al. 2017)	yes	MEFs	yes (2x)	yes	no	no	yes	no	no	no	VPA + Ascorbic Acid	transitory use of VPA + Ascorbic Acid
LCDM2/EPSCs (Gao et al. 2019)	yes	MEFs + Activin A	yes (x3)	yes	optional	yes	no	optional	no	no	Ascorbic Acid	-
CDK8i-PSCs (Lynch et al. 2020)	yes	MEFs	yes	yes	no	no	no	no	no	no	CDK8/19i	-

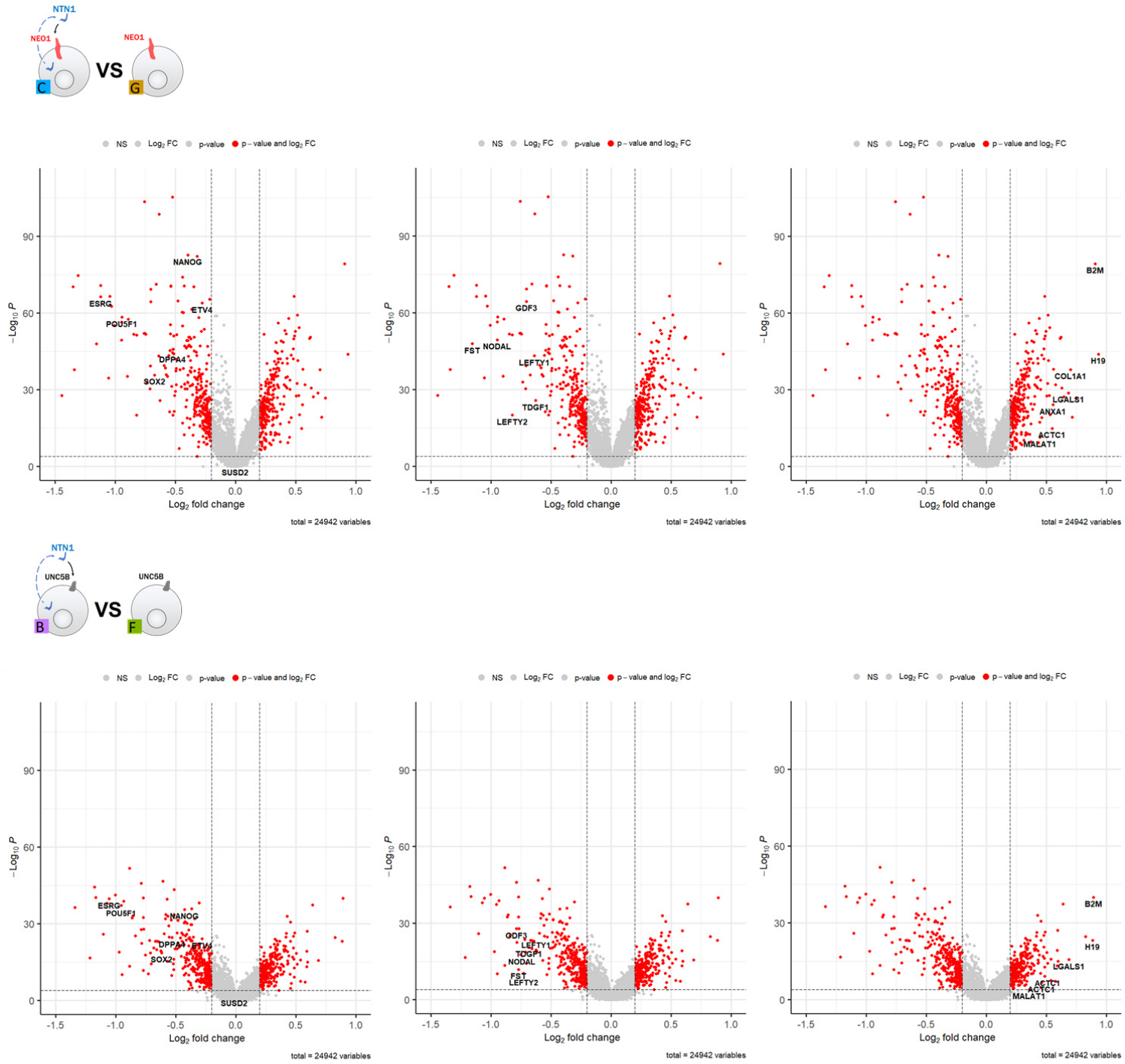

Supplementary Figure S1: Pluripotency, TGF-B signaling and NTN1-exo markers in *UNC5B+* or *NEO1+* *NTN1-/+* cells.

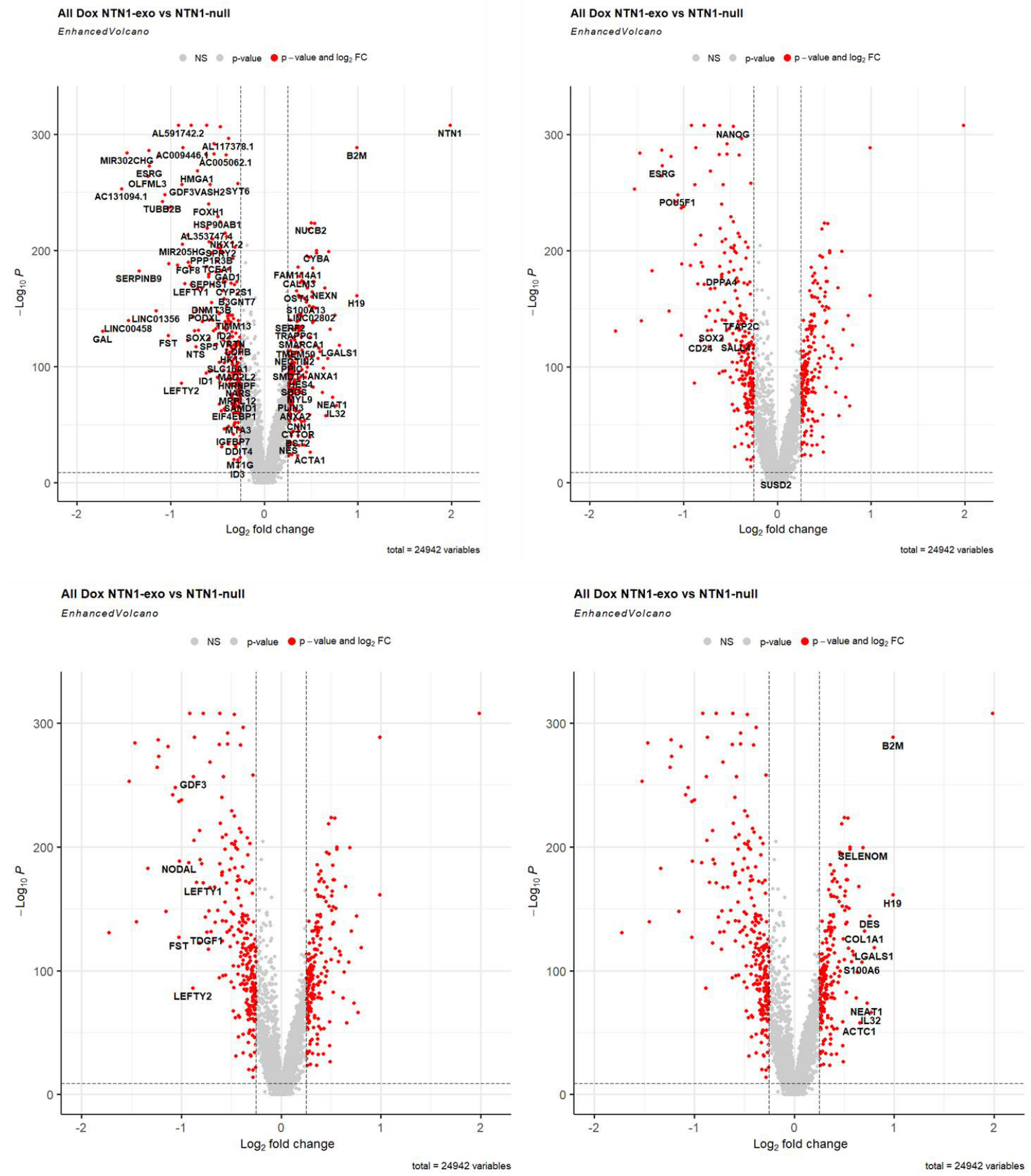

Supplementary Figure S2: Volcano plots of NTN1-exo and NTN1-null differentially expressed genes.

Supplementary Table S2: NTN1-zero and NTN1-exo top 50 markers.

	NTN1-zero upregulated		NTN1-exo upregulated	
Rank	gene name	avg_log$_2$FC	gene name	avg_log$_2$FC
1	GAL	-1,72476121	NTN1	1,98600433
2	AC131094.1	-1,52254608	H19	0,99098325
3	MIR302CHG	-1,46507926	B2M	0,9882133
4	LINC00458	-1,45108542	LGALS1	0,80378261
5	SERPINB9	-1,336434	IL32	0,76853265
6	OLFML3	-1,24350225	DES	0,75342256
7	PCAT14	-1,23528146	NEAT1	0,72978366
8	ESRG	-1,2291596	COL1A1	0,70304391
9	LINC01356	-1,15623906	SELENOM	0,68596752
10	SEMA6A	-1,13529881	S100A6	0,67787535
11	TUBB2B	-1,09004883	ACTC1	0,65502756
12	POU5F1	-1,06161718	NEXN	0,64515242
13	L1TD1	-1,02602912	ANXA1	0,63212611
14	FST	-1,02519645	TAGLN	0,62002416
15	NODAL	-1,02192737	CEBPD	0,59345996
16	GJA1	-1,00146724	TNNT1	0,58526649
17	PLAAT3	-0,92540184	ISG15	0,57262176
18	AL591742.2	-0,91862396	CYBA	0,55901862
19	LEFTY2	-0,88322564	TTC3	0,55559836
20	GDF3	-0,88258679	HLA-B	0,54688762
21	MIR205HG	-0,87444299	COL1A2	0,54171445
22	AC009446.1	-0,87223151	CALU	0,53637561
23	IRX2	-0,84773793	SPARC	0,53288398
24	DPYSL3	-0,81814722	CD99	0,52555659
25	CD24	-0,81681552	SH3BGRL3	0,52403188
26	FGF8	-0,81309796	CALR	0,5228721
27	TUBB2A	-0,79836584	SFN	0,52132563
28	AC064802.1	-0,78353692	PPIB	0,51627344
29	LEFTY1	-0,78237782	TIMP1	0,51624205
30	FABP5	-0,75875566	CD59	0,51110511
31	TDGF1	-0,74393155	LINC02802	0,5082251
32	NTS	-0,73026956	TNNC1	0,50458177
33	PMAIP1	-0,72376865	TIMP3	0,50267126
34	HMGA1	-0,71461648	NUCB2	0,50022673
35	PHLDA1	-0,71146922	TPM2	0,48961353
36	SOX2	-0,70227057	ACTA1	0,48789582
37	EZR	-0,66638232	ACTA2	0,48759947
38	HPGD	-0,66410612	MALAT1	0,48483104
39	PODXL	-0,6386069	MAGED1	0,48189041
40	RPRM	-0,62205199	MAGED2	0,47996704
41	ID1	-0,61993457	KDELR1	0,47681746
42	RESF1	-0,61741973	CDH3	0,46142735
43	LINC00678	-0,61728739	TUBA1A	0,45772278
44	AL353747.4	-0,61046739	IFI27L2	0,45564526
45	FOXH1	-0,59634356	JUNB	0,44907441
46	SEPHS1	-0,59494808	FTL	0,44773895
47	DPPA4	-0,59290411	S100A13	0,44655348
48	FRAT2	-0,59119994	PALLD	0,43624465
49	UGP2	-0,58960183	S100A4	0,43269298
50	PSAT1	-0,58863132	CAST	0,42689401

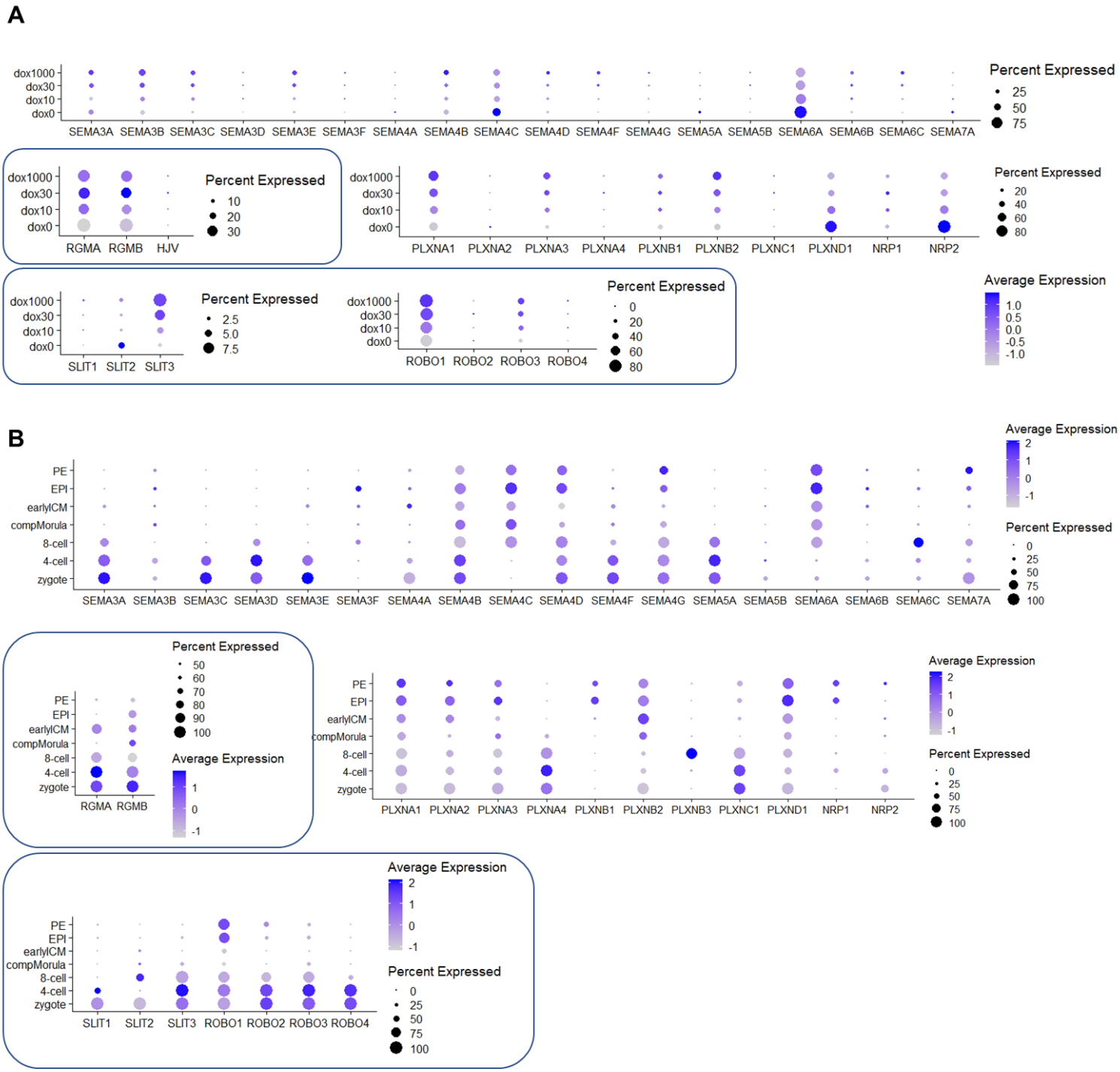

Supplementary Figure S3: Guiding molecules expression in naive human cells.
Dotplots displaying expression of Semaphorins, Repulsive Guidance Molecules (RGMs), Slits, and receptors in TL2i-hSTAN1 cells (**A**) or the human pre-implantion embryo (**B**).

Supplementary Table S3: Primer sequences used for qPCR analyses

	Human	
	Forward	Reverse
ALPPL2	TCTCCGACTGCTTCCAGACA	GTTCTCCTCCTCAACTGGGAT
CD24	GCGGGGGCGAAGAAGATTTA	GAGACCACGAAGAGACTGGC
C-MYC	TTCGGGTAGTGGAAAACCAG	CAGCAGCTCGAATTTCTTCC
DRAXIN	AGGCTGCACCAAGATCATCC	CTACCGGATGCGTCAGAGTC
EOMES	GGATCTTGCGGAGGACTGG	AAAGGAAACATGCGCCTGCC
ESRRB	CTCAGACCATTCCACGGAGG	ATCCTGTTCAGCAGCCCTCT
FST	CCTGAGAAAGGCTACCTGCC	TCTTCACAGGACTTTGCTTTGAT
GATA6	AGAAGCGCGTGCCTTCATC	ATAGCAAGTGGTCTGGGCAC
KLF2	AGAGGGTCTCCCTCGATGAC	CTCGTCAAGGAGGATCGTGG
KLF4	CAAGCCAAAGAGGGGAAGAC	CGGTAGTGCCTGGTCAGTTC
KLF5	AGATGTTCGCTCGTGCAGTA	TCTGCCCTTTGGTTAACAGC
NANOG	CAATGGTGTGACGCAGGGAT	GGACTGGATGTTCTGGGTCTG
NEO1	GGGCATGAGTCAGAGGACAG	TTTCGAACGGATTGCTGGGG
NES	CTGGCGCACCTCAAGATGTC	CTCCAGCTTGGGGTCCTGAAA
NTN1-HA	GTGTCCCAAAATCAAGCCCC	TGGAACATCGTATGGGTAGGC
NTN3	CGCCCTGTGTTAAGACCCC	TTAGGCTGATGCGGTAGCTG
NTN4	TGTTCCGGGAGAAGGACTGA	TAGCATTCTGACCGCAGGTG
NTNG1	GCACTGCAAATACCTGTATCCC	GCTAGCCTAGACTTGGTTTGGT
OCT4	ATGTGGTCCGAGTGTGGTTC	AGCGGCCTCAAAATCCTCTC
PAX6	CCATCACCAATCAGCATAGGAAT	GTGCTGCTGTTGTTGCTTGA
PECAM1	CCAGTGTCCCCAGAAGCAAA	TCCGATGACAACCACTGCAA
PITX2	CACCATCCCCAGCCGTTAG	GCTTTTATCTTTCTCTGCGGC
SOX17	TTCGTGTGCAAGCCTGAGAT	TAATATACCGCGGAGCTGGC
SOX2	TCTTGGTTCCATGGGTTCGG	CTGGAGTGGGAGGAAGAGGT
UNC5A	CCAGAACTACTTCCGCTCCC	AAGTAGGCTGCTTGGCTGTA
UNC5B	TGCTGGGTGAGCCTTAGTTG	GCCAGAATCAGTGCCTCGTT
UNC5C	GGTACCACAAAGAGCCGGAA	TCAACCATTCCACCTCAGCC
UNC5D	TTCGACTCGGGACCCTCAT	CATTGTCAGTTCCTCGGGCA
UPP1	GAGTGGGCTTGGTGAGGTG	TGACGGGGCAATCATTGTGA

	Macaque	
	Forward	Reverse
BMP4	TCGCCCAGGTTCACTACAAC	CATAGGTCCCTGCAGTAGCG
CDH2	CATCCAGACCGACCCAAACA	TCCCTTGGCTAATGGCACTT
CDX2	CTTGAGTCCGGTGTCTTCCC	GGTGACAGTGGGGTTTAGCA
C-MYC	GCCCCTCAACGTTAGCTTCA	TCCTCCTCGTCGCAGTAGAA
DCC	TGGCAAGTTTGGAAGGACTCA	CGGGAATCTGCCATTTCTCATC
DNMT3L	TCTCGCTTCCTGGAGATGGA	CTGCTCCTTATGGCCGGAAT
DPA3	CGCCAGTAACGAATCCCCTT	ATTTCCCTGAGGACTGGTGC
DPPA4	GCTGCTGACAGGTGAACTCT	CCACTCACAAAGCAACAGGC
DPPA5	GGTCGTGGTTTACGGTTCCT	AGTTTGAGCATCCCTCGCTC
DRAXIN	CATGGCCTTGTTCGACTGGA	TACCCCGGTGTTTCTCTTTCT
EOMES	TGCCTACCAAAACACCGACA	TCTGATGGGATGAATCGTAGTTGT
FGF5	GAGGCTCTAGCAGCAGACAG	CTGCTCCAAGCCACTTCCTT
FGFR1	CTTAGGCAAACCCCTGGGAG	ACGGTTGGGTTTGTCCTTGT
GATA4	GCACCCCAATCTCGTAGATATGTT	ACAGATAGTGACCCGTCCCA
GATA6	ACACAACCTACAGCCTCAGG	GAGCCCATCTTGACCCGAAT
HAND1	AAAAGGGATCTGCAGCACGAA	CCTCGGCTCACTGGTTTAACT
ICAM1	ATCTACAGCTTTCCGGCACC	TGGGCCTCACACTCCACTAT
KLF4	CCCTACCTCGGAGAGAGACC	GGATGGGTCAGCGAATTGGA
KLF5	CAGCCACCAGAGTGAAACGA	CGGTCTGGTGTGAGCTGAAT
MIXL1	GAGTCAAGGATCCAGGTATGGT	GGCCTAGCCAAAGGTTGGAA
NANOG	AGTCCTGCTTGCAGTTCCAG	TCAGGTTGCATGTTCGTGGA
NEO1	CTTGAACATGCACCAGCCAC	GGATCTGATGCAGGTGTCCG
NTN4	AGCAGCAGCAACACAGACAT	TAGAAGCGCAGAAAACCCCT
OCT4	ATGTGGTCCGAGTGTGGTTC	AGCGGCCTCAAAATCCTCTC
PITX2	TCTGCAGGCCTGAAAGAAGG	AGGAAGCGACAGGGAAAGTG
SOX1	CTGACGCATATCTAGCGCCT	TCTGTACAAAAGCCAGGCCG
TFAP2C	ACGTCCTTAGTAGAAGGTGAAGC	TTCGTCCTCCGAGATGAGGT
UNC5A	TGCTTGTCCTCATCCTCGTTTA	GATGGGGGTTGTCTGCTTTGC
UNC5B	AACAGCCACCTGCTGGA	TGTCTGTGTCGAAGTCACGG
UNC5C	CATGCAGACTGCTCCTGATTC	TACAGAGATCGCCAGGCAAA

Bibliography

Aksoy, I., Rognard, C., Moulin, A., Marcy, G., Masfaraud, E., Wianny, F., Cortay, V., Bellemin-Ménard, A., Doerflinger, N., Dirheimer, M., et al. (2021). Apoptosis, G1 Phase Stall, and Premature Differentiation Account for Low Chimeric Competence of Human and Rhesus Monkey Naive Pluripotent Stem Cells. Stem Cell Reports *16*, 56–74.

Alaiwi, W.A.A., Lo, S.T., and Nauli, S.M. (2009). Primary cilia: Highly sophisticated biological sensors. Sensors *9*, 7003–7020.

Allen, B.L., and Taatjes, D.J. (2015). The Mediator complex: A central integrator of transcription. Nat. Rev. Mol. Cell Biol.

Andrews, G.L., Tanglao, S., Farmer, W.T., Morin, S., Brotman, S., Berberoglu, M.A., Price, H., Fernandez, G.C., Mastick, G.S., Charron, F., et al. (2008). Dscam guides embryonic axons by Netrin-dependent and -independent functions. Development *135*, 3839–3848.

Aouadi, M., Bost, F., Caron, L., Laurent, K., Le Marchand Brustel, Y., and Binétruy, B. (2006). p38 Mitogen-Activated Protein Kinase Activity Commits Embryonic Stem Cells to Either Neurogenesis or Cardiomyogenesis. Stem Cells *24*, 1399–1406.

Arakawa, H. (2004). Netrin-1 and its receptors in tumorigenesis. Nat. Rev. Cancer *4*, 978–987.

Au, K.F., Sebastiano, V., Afshar, P.T., Durruthy, J.D., Lee, L., Williams, B.A., Van Bakel, H., Schadt, E.E., Reijo-Pera, R.A., Underwood, J.G., et al. (2013). Characterization of the human ESC transcriptome by hybrid sequencing. Proc. Natl. Acad. Sci. U. S. A. *110*.

Avilion, A.A., Nicolis, S.K., Pevny, L.H., Perez, L., Vivian, N., and Lovell-Badge, R. (2003). Multipotent cell lineages in early mouse development depend on SOX2 function. Genes Dev. *17*, 126–140.

Barallobre, M.J., Pascual, M., Del Río, J.A., and Soriano, E. (2005). The Netrin family of guidance factors: Emphasis on Netrin-1 signalling. Brain Res. Rev. *49*, 22–47.

Beddington, R.S.P., and Robertson, E.J. (1999). Axis development and early asymmetry in mammals. Cell *96*, 195–209.

Bernet, A., and Fitamant, J. (2008). Netrin-1 and its receptors in tumour growth promotion. Expert Opin. Ther. Targets *12*, 995–1007.

Betschinger, J., Nichols, J., Dietmann, S., Corrin, P.D., Paddison, P.J., and Smith, A. (2013). Exit from pluripotency is gated by intracellular redistribution of the bHLH transcription factor Tfe3. Cell *153*, 335–347.

Blakeley, P., Fogarty, N.M.E., Valle, I., Wamaitha, S.E., Hu, T.X., Elder, K., Snell, P., Christie, L., Robson, P., Niakan, K.K., et al. (2015). Erratum to Defining the three cell lineages of the human blastocyst by single-cell RNA-seq (Development, (2015) 142, 3151-3165). Dev. *142*, 3613.

Bodle, J.C., and Loboa, E.G. (2016). Concise Review : Primary Cilia : Control Centers for Stem Cell Lineage Specification and Potential Targets for Cell-Based Therapies. Stem Cells 1445–1454.

Boroviak, T., and Nichols, J. (2017). Primate embryogenesis predicts the hallmarks of human naïve pluripotency. Dev. *144*, 175–186.

Boroviak, T., Loos, R., Lombard, P., Okahara, J., Behr, R., Sasaki, E., Nichols, J., Smith, A., and Bertone, P. (2015). Lineage-Specific Profiling Delineates the Emergence and Progression of Naive Pluripotency in Mammalian Embryogenesis. Dev. Cell *35*, 366–382.

Bourillot, P.Y., Santamaria, C., David, L., and Savatier, P. (2020). GP130 signaling and the control of naïve pluripotency in humans, monkeys, and pigs. Exp. Cell Res. *386*, 111712.

Bourque, G., Burns, K.H., Gehring, M., Gorbunova, V., Seluanov, A., Hammell, M., Imbeault, M., Izsvák, Z., Levin, H.L., Macfarlan, T.S., et al. (2018). Ten things you should know about transposable elements 06 Biological Sciences 0604 Genetics. Genome Biol. *19*, 1–12.

Boussouar, A., Tortereau, A., Manceau, A., Paradisi, A., Gadot, N., Vial, J., Neves, D., Larue, L., Battistella, M., Leboeuf, C., et al. (2020). Netrin-1 and its receptor DCC are causally implicated in melanoma progression. Cancer Res. *80*, 747–756.

Bradford, D.K., Cole, S.J., and Cooper, H.M. (2009). Netrin-1: Diversity in development. Int. J. Biochem. Cell Biol. *41*, 487–493.

Bradley, A., Evans, M., Kaufman, M.H., and Robertson, E. (1984). Formation of germ-line chimaeras from embryo-derived teratocarcinoma cell lines. Nature *309*, 255–256.

Bredenkamp, N., Stirparo, G.G., Nichols, J., Smith, A., and Guo, G. (2019). The Cell-Surface Marker Sushi Containing Domain 2 Facilitates Establishment of Human Naive Pluripotent Stem Cells. Stem Cell Reports *12*, 1212–1222.

Bredesen, D.E., Ye, X., Tasinato, A., Sperandio, S., Wang, J.J.L., Assa-munt, N., and Rabizadeh, S. (1998). p75NTR and the concept of cellular dependence: seeing how the Other Half Die. Cell Death Differ. *5*, 365–371.

Bredesen, D.E., Mehlen, P., and Rabizadeh, S. (2004). Apoptosis and Dependence Receptors: A Molecular Basis for Cellular Addiction. Physiol. Rev. *84*, 411–430.

Brennan, T.J., Edmondson, D.G., Li, L., and Olson, E.N. (1991). Transforming growth factor β represses the actions of myogenin through a mechanism independent of DNA binding. Proc. Natl. Acad. Sci. U. S. A. *88*, 3822–3826.

Brons, I.G.M., Smithers, L.E., Trotter, M.W.B., Rugg-Gunn, P., Sun, B., Chuva De Sousa Lopes, S.M., Howlett, S.K., Clarkson, A., Ahrlund-Richter, L., Pedersen, R.A., et al. (2007). Derivation of pluripotent epiblast stem cells from mammalian embryos. Nature *448*, 191–195.

Brook, F.A., and Gardner, R.L. (1997). The origin and efficient derivation of embryonic stem cells in the mouse. Devlopmental Biol. *94*, 5709–5712.

Buecker, C., Chen, H.H., Polo, J.M., Daheron, L., Bu, L., Barakat, T.S., Okwieka, P., Porter, A., Gribnau, J., Hochedlinger, K., et al. (2010). A murine ESC-like state facilitates transgenesis and homologous recombination in human pluripotent stem cells. Cell Stem Cell *6*, 535–546.

Buecker, C., Srinivasan, R., Wu, Z., Calo, E., Acampora, D., Faial, T., Simeone, A., Tan, M., Swigut, T., and Wysocka, J. (2014). Reorganization of enhancer patterns in transition from naive to primed pluripotency. Cell Stem Cell *14*, 838–853.

Buehr, M., Meek, S., Blair, K., Yang, J., Ure, J., Silva, J., McLay, R., Hall, J., Ying, Q.L., and Smith, A. (2008). Capture of Authentic Embryonic Stem Cells from Rat Blastocysts. Cell *135*, 1287–1298.

Bulut-Karslioglu, A., Biechele, S., Jin, H., MacRae, T.A., Hejna, M., Gertsenstein, M., Song, J.S., and Ramalho-Santos, M. (2016). Inhibition of mTOR induces a paused pluripotent state. Nature *540*, 119–123.

Burdon, T., Stracey, C., Chambers, I., Nichols, J., and Smith, A. (1999). Suppression of SHP-2 and ERK signalling promotes self-renewal of mouse embryonic stem cells. Dev. Biol. *210*, 30–43.

Burdon, T., Smith, A., and Savatier, P. (2002). Signalling, cell cycle and pluripotency in embryonic stem cells. Trends Cell Biol. *12*, 432–438.

Carter, M.G., Smagghe, B.J., Stewart, A.K., Rapley, J.A., Lynch, E., Bernier, K.J., Keating, K.W., Hatziioannou, V.M., Hartman, E.J., and Bamdad, C.C. (2016). A Primitive Growth Factor, NME7AB, Is Sufficient to Induce Stable Na€ıve State Human Pluripotency; Reprogramming in This Novel Growth Factor Confers Superior Differentiation. Stem Cells 847–859.

Chambers, I., Silva, J., Colby, D., Nichols, J., Nijmeijer, B., Robertson, M., Vrana, J., Jones, K., Grotewold, L., and Smith, A. (2007). Nanog safeguards pluripotency and mediates germline development. Nature *450*, 1230–1234.

Chan, Y.S., Göke, J., Ng, J.H., Lu, X., Gonzales, K.A.U., Tan, C.P., Tng, W.Q., Hong, Z.Z., Lim, Y.S., and Ng, H.H. (2013). Induction of a human pluripotent state with distinct regulatory circuitry that resembles preimplantation epiblast. Cell Stem Cell *13*, 663–675.

Chen, H., Aksoy, I., Gonnot, F., Osteil, P., Aubry, M., Hamela, C., Rognard, C., Hochard, A., Voisin, S., Fontaine, E., et al. (2015). Reinforcement of STAT3 activity reprogrammes human embryonic stem cells to naive-like pluripotency. Nat. Commun. *6*.

Cheng, S., Pei, Y., He, L., Peng, G., Reinius, B., Tam, P.P.L., Jing, N., and Deng, Q. (2019). Single-Cell RNA-Seq Reveals Cellular Heterogeneity of Pluripotency Transition and X Chromosome Dynamics during Early Mouse Development. Cell Rep. *26*, 2593-2607.e3.

Chew, J., Tam, W., Yeap, L., Li, P., Ang, Y., Lim, B., Robson, P., and Ng, H. (2005). Reciprocal Transcriptional Regulation of. Society *25*, 6031–6046.

Chia, N.Y., Chan, Y.S., Feng, B., Lu, X., Orlov, Y.L., Moreau, D., Kumar, P., Yang, L., Jiang, J., Lau, M.S., et al. (2010). A genome-wide RNAi screen reveals determinants of human embryonic stem cell identity. Nature.

Cirulli, V., and Yebra, M. (2007). Netrins: Beyond the brain. Nat. Rev. Mol. Cell Biol. *8*, 296–306.

Clement, C.A., Ajbro, K.D., Koefoed, K., Vestergaard, M.L., Veland, I.R., HenriquesdeJesus, M.P.R., Pedersen, L.B., Benmerah, A., Andersen, C.Y., Larsen, L.A., et al. (2013). TGF-β Signaling Is Associated with Endocytosis at the Pocket Region of the Primary Cilium. Cell Rep. *3*, 1806–1814.

Collier, A.J., and Rugg-Gunn, P.J. (2018). Identifying Human Naïve Pluripotent Stem Cells − Evaluating State-Specific Reporter Lines and Cell-Surface Markers. BioEssays *40*.

Collier, A.J., Panula, S.P., Schell, J.P., Chovanec, P., Plaza Reyes, A., Petropoulos, S., Corcoran, A.E., Walker, R., Douagi, I., Lanner, F., et al. (2017). Comprehensive Cell Surface Protein Profiling Identifies Specific Markers of Human Naive and Primed Pluripotent States. Cell Stem Cell *20*, 874-890.e7.

Coronado, D., Godet, M., Bourillot, P.Y., Tapponnier, Y., Bernat, A., Petit, M., Afanassieff, M., Markossian, S., Malashicheva, A., Iacone, R., et al. (2013). A short G1 phase is an intrinsic determinant of naïve embryonic stem cell pluripotency. Stem Cell Res. *10*, 118–131.

Dahéron, L., Opitz, S.L., Zaehres, H., Lensch, W.M., Andrews, P.W., Itskovitz-Eldor, J., and Daley, G.Q. (2004). LIF/STAT3 Signaling Fails to Maintain Self-Renewal of Human Embryonic Stem Cells. Stem Cells.

Du, X.Y., Huang, J., Xu, L.Q., Tang, D.F., Wu, L., Zhang, L.X., Pan, X.L., Chen, W.Y., Zheng, L.P., and Zheng, Y.H. (2012). The proto-oncogene c-src is involved in primordial follicle activation through the PI3K, PKC and MAPK signaling pathways. Reprod. Biol. Endocrinol.

Duboule, D. (1994). Temporal colinearity and the phylotypic progression: A basis for the stability of a vertebrate Bauplan and the evolution of morphologies through heterochrony. Development *120*, 135–142.

Duggal, G., Warrier, S., Ghimire, S., Broekaert, D., Van der jeught, M., Lierman, S., Deroo, T., Peelman, L., Van Soom, A., Cornelissen, R., et al. (2015). Alternative Routes to Induce Na€ıve Pluripotency in Human Embryonic Stem Cells. Stem Cells 1517–1527.

Dunglison, G.F., Barlow, D.H., and Sargent, I.L. (1996). Leukaemia inhibitory factor significantly enhances the blastocyst formation rates of human embryos cultured in serum-free medium. Hum. Reprod. *11*, 191–196.

Dupont, C., and Gribnau, J. (2013). Different flavors of X-chromosome inactivation in mammals. Curr. Opin. Cell Biol.

Dutta, D., Ray, S., Home, P., Larson, M., Wolfe, M.W., and Paul, S. (2011). Self-renewal versus lineage commitment of embryonic stem cells: Protein kinase C signaling shifts the balance. Stem Cells *29*, 618–628.

Enver, T., Soneji, S., Joshi, C., Brown, J., Iborra, F., Orntoft, T., Thykjaer, T., Maltby, E., Smith, K., Dawud, R.A., et al. (2005). Cellular differentiation hierarchies in normal and culture-adapted human embryonic stem cells. Hum. Mol. Genet. *14*, 3129–3140.

Escamilla-Del-Arenal, M., Da Rocha, S.T., and Heard, E. (2011). Evolutionary diversity and developmental regulation of X-chromosome inactivation. Hum. Genet.

Esteban, M.A., Wang, T., Qin, B., Yang, J., Qin, D., Cai, J., Li, W., Weng, Z., Chen, J., Ni, S., et al. (2010). Vitamin C Enhances the Generation of Mouse and Human Induced Pluripotent Stem Cells. Cell Stem Cell.

Evans, M.J., and Kaufman, M.H. (1981). Establishment in culture of pluripotential cells from mouse embryos. Nature *292*, 154–156.

Fang, R., Liu, K., Zhao, Y., Li, H., Zhu, D., Du, Y., Xiang, C., Li, X., Liu, H., Miao, Z., et al. (2014). Generation of naive induced pluripotent stem cells from rhesus monkey fibroblasts. Cell Stem Cell *15*, 488–497.

Fearon, E.R., Cho, K.R., Nigro, J.M., Kern, S.E., Simons, J.W., Ruppert, J.M., Hamilton, S.R., Preisinger, A.C., Thomas, G., Kinzler, K.W., et al. (1990). Identification of a chromosome 18q gene that is altered in colorectal cancers. Science (80-.). *247*, 49–56.

Fei, T., Zhu, S., Xia, K., Zhang, J., Li, Z., Han, J.D.J., and Chen, Y.G. (2010). Smad2 mediates Activin/Nodal signaling in mesendoderm differentiation of mouse embryonic stem cells. Cell Res. *20*, 1306–1318.

Festuccia, N., Osorno, R., Halbritter, F., Karwacki-Neisius, V., Navarro, P., Colby, D., Wong, F., Yates, A., Tomlinson, S.R., and Chambers, I. (2012). Esrrb is a direct Nanog target gene that can substitute for Nanog function in pluripotent cells. Cell Stem Cell *11*, 477–490.

Forcet, C., Stein, E., Pays, L., Corset, V., Llambi, F., Tessier-Lavigne, M., and Mehlen, P. (2002). Netrin-1-mediated axon outgrowth requires deleted in colorectal cancer-dependent MAPK activation. Nature *417*, 443–

447.

Francescone, R., Vendramini-Costa, D.B., Franco-Barraza, J., Wagner, J., Muir, A., Lau, A.N., Gabitova, L., Pazina, T., Gupta, S., Luong, T., et al. (2021). Netrin G1 promotes pancreatic tumorigenesis through cancer-associated fibroblast–driven nutritional support and immunosuppression. Cancer Discov. *11*, 446–479.

Fu, X., Cui, K., Yi, Q., Yu, L., and Xu, Y. (2017). DNA repair mechanisms in embryonic stem cells. Cell. Mol. Life Sci. *74*, 487–493.

Gafni, O., Weinberger, L., Mansour, A.A., Manor, Y.S., Chomsky, E., Ben-Yosef, D., Kalma, Y., Viukov, S., Maza, I., Zviran, A., et al. (2013). Derivation of novel human ground state naive pluripotent stem cells. Nature *504*, 282–286.

Gan, W.B., Wong, V.Y., Phillips, A., Ma, C., Gershon, T.R., and Macagno, E.R. (1999). Cellular expression of a leech netrin suggests roles in the formation of longitudinal nerve tracts and in regional innervation of peripheral targets. J. Neurobiol. *40*, 103–115.

Gao, X., Metzger, U., Panza, P., Mahalwar, P., Alsheimer, S., Geiger, H., Maischein, H.M., Levesque, M.P., Templin, M., and Söllner, C. (2015). A floor-plate extracellular protein-protein interaction screen identifies Draxin as a secreted Netrin-1 antagonist. Cell Rep. *12*, 694–708.

Gao, X., Nowak-Imialek, M., Chen, X., Chen, D., Herrmann, D., Ruan, D., Chen, A.C.H., Eckersley-Maslin, M.A., Ahmad, S., Lee, Y.L., et al. (2019). Establishment of porcine and human expanded potential stem cells. Nat. Cell Biol. *21*, 687–699.

Göke, J., Lu, X., Chan, Y.S., Ng, H.H., Ly, L.H., Sachs, F., and Szczerbinska, I. (2015). Dynamic transcription of distinct classes of endogenous retroviral elements marks specific populations of early human embryonic cells. Cell Stem Cell *16*, 135–141.

Goldschneider, D., and Mehlen, P. (2010). Dependence receptors: A new paradigm in cell signaling and cancer therapy. Oncogene *29*, 1865–1882.

Goto, T., Hara, H., Sanbo, M., Masaki, H., Sato, H., Yamaguchi, T., Hochi, S., Kobayashi, T., Nakauchi, H., and Hirabayashi, M. (2019). Generation of pluripotent stem cell-derived mouse kidneys in Sall1-targeted anephric rats. Nat. Commun. *10*.

Grabole, N., Tischler, J., Hackett, J.A., Kim, S., Tang, F., Leitch, H.G., Magnúsdóttir, E., and Surani, M.A. (2013). Prdm14 promotes germline fate and naive pluripotency by repressing FGF signalling and DNA methylation. EMBO Rep. *14*, 629–637.

Grandin, M., Meier, M., Delcros, J.G., Nikodemus, D., Reuten, R., Patel, T.R., Goldschneider, D., Orriss, G., Krahn, N., Boussouar, A., et al. (2016). Structural Decoding of the Netrin-1/UNC5 Interaction and its Therapeutical Implications in Cancers. Cancer Cell *29*, 173–185.

Guenebeaud, C., Goldschneider, D., Castets, M., Guix, C., Chazot, G., Delloye-Bourgeois, C., Eisenberg-Lerner, A., Shohat, G., Zhang, M., Laudet, V., et al. (2010). The Dependence Receptor UNC5H2/B Triggers Apoptosis via PP2A-Mediated Dephosphorylation of DAP Kinase. Mol. Cell *40*, 863–876.

Guo, G., Yang, J., Nichols, J., Hall, J.S., Eyres, I., Mansfield, W., and Smith, A. (2009). Klf4 reverts developmentally programmed restriction of ground state pluripotency. Development *136*, 1063–1069.

Guo, G., Huss, M., Tong, G.Q., Wang, C., Li Sun, L., Clarke, N.D., and Robson, P. (2010). Resolution of Cell Fate

Decisions Revealed by Single-Cell Gene Expression Analysis from Zygote to Blastocyst. Dev. Cell *18*, 675–685.

Guo, G., Von Meyenn, F., Santos, F., Chen, Y., Reik, W., Bertone, P., Smith, A., and Nichols, J. (2016). Naive Pluripotent Stem Cells Derived Directly from Isolated Cells of the Human Inner Cell Mass. Stem Cell Reports *6*, 437–446.

Guo, G., von Meyenn, F., Rostovskaya, M., Clarke, J., Dietmann, S., Baker, D., Sahakyan, A., Myers, S., Bertone, P., Reik, W., et al. (2018). Erratum: Correction: Epigenetic resetting of human pluripotency (doi:10.1242/dev.146811) (Development (Cambridge, England) (2017) 144 15 (2748-2763) PII: dev166397).

Hackett, J.A., and Azim Surani, M. (2014). Regulatory principles of pluripotency: From the ground state up. Cell Stem Cell *15*, 416–430.

Hackett, J.A., Dietmann, S., Murakami, K., Down, T.A., Leitch, H.G., and Surani, M.A. (2013). Synergistic mechanisms of DNA demethylation during transition to ground-state pluripotency. Stem Cell Reports *1*, 518–531.

Hall, J., Guo, G., Wray, J., Eyres, I., Nichols, J., Grotewold, L., Morfopoulou, S., Humphreys, P., Mansfield, W., Walker, R., et al. (2009). Oct4 and LIF/Stat3 Additively Induce Krüppel Factors to Sustain Embryonic Stem Cell Self-Renewal. Cell Stem Cell *5*, 597–609.

Han, X., Chen, H., Huang, D., Chen, H., Fei, L., and Cheng, C. (2018). Mapping human pluripotent stem cell differentiation pathways using high throughput single-cell RNA-sequencing. 1–19.

Hanken, J., and Carl, T.F. (1996). The shape of life: Genes, development, and the evolution of animal form. Trends Ecol. Evol.

Hanna, J., Cheng, A.W., Saha, K., Kim, J., Lengner, C.J., Soldner, F., Cassady, J.P., Muffat, J., Carey, B.W., and Jaenisch, R. (2010). Human embryonic stem cells with biological and epigenetic characteristics similar to those of mouse ESCs. Proc. Natl. Acad. Sci. U. S. A. *107*, 9222–9227.

Harbour, J.W., and Dean, D.C. (2000). The Rb/E2F pathway: Expanding roles and emerging paradigms. Genes Dev. *14*, 2393–2409.

Harbour, J.W., Luo, R.X., Dei Santi, A., Postigo, A.A., and Dean, D.C. (1999). Cdk phosphorylation triggers sequential intramolecular interactions that progressively block Rb functions as cells move through G1. Cell *98*, 859–869.

Harris, R., Sabatelli, L.M., and Seeger, M.A. (1996). Guidance cues at the Drosophila CNS midline: Identification and characterization of two Drosophila Netrin/UNC-6 homologs. Neuron *17*, 217–228.

Hayashi, K., Lopes, S.M.C. de S., Tang, F., and Surani, M.A. (2008). Dynamic Equilibrium and Heterogeneity of Mouse Pluripotent Stem Cells with Distinct Functional and Epigenetic States. Cell Stem Cell *3*, 391–401.

Hayashi, K., Ohta, H., Kurimoto, K., Aramaki, S., and Saitou, M. (2011). Reconstitution of the mouse germ cell specification pathway in culture by pluripotent stem cells. Cell *146*, 519–532.

Hedgecock, E.M., Culotti, J.G., and Hall, D.H. (1990). The unc-5, unc-6, and unc-40 genes guide circumferential migrations of pioneer axons and mesodermal cells on the epidermis in C. elegans. Neuron *4*, 61–85.

Hikita, S.T., Kosik, K.S., Clegg, D.O., and Bamdad, C. (2008). MUC1* mediates the growth of human pluripotent stem cells. PLoS One *3*.

Hill, C.S. (2016). Transcriptional control by the SMADs. Cold Spring Harb. Perspect. Biol. *8*.

Hough, S.R., Laslett, A.L., Grimmond, S.B., Kolle, G., and Pera, M.F. (2009). A continuum of cell states spans pluripotency and lineage commitment in human embryonic stem cells. PLoS One *4*.

Huang, K., Maruyama, T., and Fan, G. (2014). The naive state of human pluripotent stem cells: A synthesis of stem cell and preimplantation embryo transcriptome analyses. Cell Stem Cell *15*, 410–415.

Huang, L., Chen, D., Liu, D., Yin, L., Kharbanda, S., and Kufe, D. (2005). MUC1 oncoprotein blocks glycogen synthase kinase 3β-mediated phosphorylation and degradation of β-catenin. Cancer Res.

Huang, S.M.A., Mishina, Y.M., Liu, S., Cheung, A., Stegmeier, F., Michaud, G.A., Charlat, O., Wiellette, E., Zhang, Y., Wiessner, S., et al. (2009). Tankyrase inhibition stabilizes axin and antagonizes Wnt signalling. Nature.

Huelsken, J., Vogel, R., Brinkmann, V., Erdmann, B., Birchmeier, C., and Birchmeier, W. (2000). Requirement for β-catenin in anterior-posterior axis formation in mice. J. Cell Biol. *148*, 567–578.

Humiêcka, M., Szpila, M., Køś, P., Maleszewski, M., and Szczepańska, K. (2017). Mouse blastomeres acquire ability to divide asymmetrically before compaction. PLoS One *12*, 1–15.

Huyghe, A., Furlan, G., Ozmadenci, D., Galonska, C., Charlton, J., Gaume, X., Combémorel, N., Riemenschneider, C., Allègre, N., Zhang, J., et al. (2020). Netrin-1 promotes naive pluripotency through Neo1 and Unc5b co-regulation of Wnt and MAPK signalling. Nat. Cell Biol. *22*, 389–400.

Irie, N., and Kuratani, S. (2014). The developmental hourglass model: A predictor of the basic body plan? Dev. *141*, 4649–4655.

Ishii, N., Wadsworth, W.G., Stern, B.D., Culotti, J.G., and Hedgecock, E.M. (1992). UNC-6, a laminin-related protein, guides cell and pioneer axon migrations in C. elegans. Neuron *9*, 873–881.

Islam, S.M., Shinmyo, Y., Okafuji, T., Su, Y., Naser, I. Bin, Ahmed, G., Zhang, S., Chen, S., Ohta, K., Kiyonari, H., et al. (2009). Draxin, a repulsive guidance protein for spinal cord and forebrain commissures. Science (80-.). *323*, 388–393.

Jeronimo, C., and Robert, F. (2017). The Mediator Complex: At the Nexus of RNA Polymerase II Transcription. Trends Cell Biol.

Van Der Jeught, M., Heindryckx, B., O'Leary, T., Duggal, G., Ghimire, S., Lierman, S., Van Roy, N., Chuva De Sousa Lopes, S.M., Deroo, T., Deforce, D., et al. (2014). Treatment of human embryos with the TGFβ inhibitor SB431542 increases epiblast proliferation and permits successful human embryonic stem cell derivation. Hum. Reprod. *29*, 41–48.

Jiang, S., Richaud, M., Vieugué, P., Rama, N., Delcros, J., Siouda, M., Sanada, M., Redavid, A., Ducarouge, B., Hervieu, M., et al. (2021). Targeting netrin-3 in small cell lung cancer and neuroblastoma. EMBO Mol. Med. *13*, 1–14.

Jiwlawat, N., Lynch, E., Jeffrey, J., Van Dyke, J.M., and Suzuki, M. (2018). Current progress and challenges for skeletal muscle differentiation from human pluripotent stem cells using transgene-free approaches. Stem Cells Int. *2018*.

Jiwlawat, S., Lynch, E., Glaser, J., Smit-Oistad, I., Jeffrey, J., Van Dyke, J.M., and Suzuki, M. (2017). Differentiation and sarcomere formation in skeletal myocytes directly prepared from human induced pluripotent stem cells using a sphere-based culture. Differentiation *96*, 70–81.

Kalantry, S. (2011). Recent advances in X-chromosome inactivation. J. Cell. Physiol. *226*, 1714–1718.

Kashyap, V., Rezende, N.C., Scotland, K.B., Shaffer, S.M., Persson, J.L., Gudas, L.J., and Mongan, N.P. (2009). Regulation of Stem cell pluripotency and differentiation involves a mutual regulatory circuit of the Nanog, OCT4, and SOX2 pluripotency transcription factors with polycomb Repressive Complexes and Stem Cell microRNAs. Stem Cells Dev. *18*, 1093–1108.

Kaufman, M.H. (1992). The Atlas of Mouse Development. J. Med. Genet. *30*, 350–351.

Keino-Masu, K., Masu, M., Hinck, L., Leonardo, E.D., Chan, S.S.Y., Culotti, J.G., and Tessier-Lavigne, M. (1996). Deleted in Colorectal Cancer (DCC) encodes a netrin receptor. Cell *87*, 175–185.

Kennedy, T.E., Serafini, T., de la Torre, J.R., and Tessier-Lavigne, M. (1994). Netrins are diffusible chemotropic factors for commissural axons in the embryonic spinal cord. Cell *78*, 425–435.

Kim, H., Wu, J., Ye, S., Tai, C.I., Zhou, X., Yan, H., Li, P., Pera, M., and Ying, Q.L. (2013). Modulation of β-catenin function maintains mouse epiblast stem cell and human embryonic stem cell self-renewal. Nat. Commun. *4*.

Kim, K., Zhao, R., Doi, A., Ng, K., Unternaehrer, J., Cahan, P., Hongguang, H., Loh, Y.H., Aryee, M.J., Lensch, M.W., et al. (2011). Donor cell type can influence the epigenome and differentiation potential of human induced pluripotent stem cells. Nat. Biotechnol. *29*, 1117–1119.

Kinoshita, M., and Smith, A. (2018). Pluripotency Deconstructed. Dev. Growth Differ. *60*, 44–52.

Kinoshita, M., Barber, M., Mansfield, W., Cui, Y., Spindlow, D., Stirparo, G.G., Dietmann, S., Nichols, J., and Smith, A. (2021). Capture of Mouse and Human Stem Cells with Features of Formative Pluripotency. Cell Stem Cell *28*, 453-471.e8.

Kobayashi, T., Yamaguchi, T., Hamanaka, S., Kato-Itoh, M., Yamazaki, Y., Ibata, M., Sato, H., Lee, Y.S., Usui, J. ichi, Knisely, A.S., et al. (2010). Generation of Rat Pancreas in Mouse by Interspecific Blastocyst Injection of Pluripotent Stem Cells. Cell *142*, 787–799.

Kolodziejczyk, A.A., Kim, J.K., Tsang, J.C.H., Ilicic, T., Henriksson, J., Natarajan, K.N., Tuck, A.C., Gao, X., Bühler, M., Liu, P., et al. (2015). Single Cell RNA-Sequencing of Pluripotent States Unlocks Modular Transcriptional Variation. Cell Stem Cell *17*, 471–485.

Krueger, F., Madeja, Z., Hemberger, M., McMahon, M., Cook, S.J., and Gaunt, S.J. (2009). Down-regulation of Cdx2 in colorectal carcinoma cells by the Raf-MEK-ERK 1/2 pathway. Cell. Signal.

Kurek, D., Neagu, A., Tastemel, M., Tüysüz, N., Lehmann, J., Van De Werken, H.J.G., Philipsen, S., Van Der Linden, R., Maas, A., Van Ijcken, W.F.J., et al. (2015). Endogenous WNT signals mediate BMP-induced and spontaneous differentiation of epiblast stem cells and human embryonic stem cells. Stem Cell Reports *4*, 114–128.

Lee, N.G., Jeung, I.C., Heo, S.C., Song, J., Kim, W., Hwang, B., Kwon, M.G., Kim, Y.G., Lee, J., Park, J.G., et al. (2020). Ischemia-induced Netrin-4 promotes neovascularization through endothelial progenitor cell activation via Unc-5 Netrin receptor B. FASEB J. *34*, 1231–1246.

Leonardi, G.C., Candido, S., Carbone, M., Raiti, F., Colaianni, V., Garozzo, S., Cinà, D., McCubrey, J.A., and Libra, M. (2012). BRAF mutations in papillary thyroid carcinoma and emerging targeted therapies (Review). Mol. Med. Rep.

Leung-Hagesteijn, C., Spence, A.M., Stern, B.D., Zhou, Y., Su, M.W., Hedgecock, E.M., and Culotti, J.G. (1992). UNC-5, a transmembrane protein with immunoglobulin and thrombospondin type 1 domains, guides cell and pioneer axon migrations in C. elegans. Cell *71*, 289–299.

Li, Q. V., Dixon, G., Verma, N., Rosen, B.P., Gordillo, M., Luo, R., Xu, C., Wang, Q., Soh, C.L., Yang, D., et al. (2019). Genome-scale screens identify JNK–JUN signaling as a barrier for pluripotency exit and endoderm differentiation. Nat. Genet. *51*, 999–1010.

Liang, J., Wan, M., Zhang, Y., Gu, P., Xin, H., Jung, S.Y., Qin, J., Wong, J., Cooney, A.J., Liu, D., et al. (2008). Nanog and Oct4 associate with unique transcriptional repression complexes in embryonic stem cells. Nat. Cell Biol. *10*, 731–739.

Liu, D., Wang, X., He, D., Sun, C., He, X., Yan, L., Li, Y., Han, J.D.J., and Zheng, P. (2018). Single-cell RNA-sequencing reveals the existence of naive and primed pluripotency in pre-implantation rhesus monkey embryos. Genome Res. *28*, 1481–1493.

Liu, G., Beggs, H., Jürgensen, C., Park, H.T., Tang, H., Gorski, J., Jones, K.R., Reichardt, L.F., Wu, J., and Rao, Y. (2004). Netrin requires focal adhesion kinase and Src family kinases for axon outgrowth and attraction. Nat. Neurosci. *7*, 1222–1232.

Liu, G., Li, W., Wang, L., Kar, A., Guan, K.L., Rao, Y., and Wu, J.Y. (2009). DSCAM functions as a netrin receptor in commissural axon pathfinding. Proc. Natl. Acad. Sci. U. S. A. *106*, 2951–2956.

Liu, P., Wakamiya, M., Shea, M.J., Albrecht, U., Behringer, R.R., and Bradley, A. (1999). Requirement for Wnt3 in vertebrate axis formation. Nat. Genet. *22*, 361–365.

Llambi, F., Causeret, F., Bloch-Gallego, E., and Mehlen, P. (2001). Netrin-1 acts as a survival factor via its receptors UNC5H and DCC. EMBO J. *20*, 2715–2722.

Lopes, F.L., Desmarais, J.A., and Murphy, B.D. (2004). Embryonic diapause and its regulation. Reproduction *128*, 669–678.

Lv, B., Song, C., Wu, L., Zhang, Q., Hou, D., Chen, P., Yu, S., Wang, Z., Chu, Y., Zhang, J., et al. (2015a). Netrin-4 as a biomarker promotes cell proliferation and invasion in gastric cancer. Oncotarget *6*, 9794–9806.

Lv, J., Sun, X., Ma, J., Ma, X., Zhang, Y., Li, F., Li, Y., and Zhao, Z. (2015b). Netrin-1 induces the migration of Schwann cells via p38 MAPK and PI3K-Akt signaling pathway mediated by the UNC5B receptor. Biochem. Biophys. Res. Commun. *464*, 263–268.

Lynch, C.J., Bernad, R., Martínez-Val, A., Shahbazi, M.N., Nóbrega-Pereira, S., Calvo, I., Blanco-Aparicio, C., Tarantino, C., Garreta, E., Richart-Ginés, L., et al. (2020). Global hyperactivation of enhancers stabilizes human and mouse naive pluripotency through inhibition of CDK8/19 Mediator kinases. Nat. Cell Biol. *22*, 1223–1238.

Lyu, R., and Zhou, J. (2017). The Multifaceted Roles of Primary Cilia in the Regulation of Stem Cell Properties and Functions. J. Cell. Physiol. *232*, 935–938.

Mahanta, S., Fessles, S.P., Park, J., and Bamdad, C. (2008). A minimal fragments of MUC1 mediates growth of cancer cells. PLoS One.

Martello, G., Sugimoto, T., Diamanti, E., Joshi, A., Hannah, R., Ohtsuka, S., Göttgens, B., Niwa, H., and Smith, A. (2012). Esrrb is a pivotal target of the Gsk3/Tcf3 axis regulating embryonic stem cell self-renewal. Cell Stem Cell *11*, 491–504.

Martello, G., Bertone, P., and Smith, A. (2013). Identification of the missing pluripotency mediator downstream of leukaemia inhibitory factor. EMBO J. *32*, 2561–2574.

Martin, G.R. (1981). Isolation of a pluripotent cell line from early mouse embryos cultured in medium conditioned by teratocarcinoma stem cells. Proc. Natl. Acad. Sci. U. S. A. *78*, 7634–7638.

Masaki, H., Kato-Itoh, M., Umino, A., Sato, H., Hamanaka, S., Kobayashi, T., Yamaguchi, T., Nishimura, K., Ohtaka, M., Nakanishi, M., et al. (2015). Interspecific in vitro assay for the chimera-forming ability of human pluripotent stem cells. Dev. *142*, 3222–3230.

Masui, S., Nakatake, Y., Toyooka, Y., Shimosato, D., Yagi, R., Takahashi, K., Okochi, H., Okuda, A., Matoba, R., Sharov, A.A., et al. (2007). Pluripotency governed by Sox2 via regulation of Oct3/4 expression in mouse embryonic stem cells. Nat. Cell Biol. *9*, 625–635.

Matus, D.Q., Pang, K., Marlow, H., Dunn, C.W., Thomsen, G.H., and Martindale, M.Q. (2006). Molecular evidence for deep evolutionary roots of bilaterality in animal development. Proc. Natl. Acad. Sci. U. S. A. *103*, 11195–11200.

McCracken, I.R., Taylor, R.S., Kok, F.O., De La Cuesta, F., Dobie, R., Henderson, B.E.P., Mountford, J.C., Caudrillier, A., Henderson, N.C., Ponting, C.P., et al. (2020). Transcriptional dynamics of pluripotent stemcell-derived endothelial cell differentiation revealed by single-cell RNA sequencing. Eur. Heart J. *41*, 1024–1036.

McDermott, M.S.J., Chumanevich, A.A., Lim, C.U., Liang, J., Chen, M., Altilia, S., Oliver, D., Rae, J.M., Shtutman, M., Kiaris, H., et al. (2017). Inhibition of CDK8 mediator kinase suppresses estrogen dependent transcription and the growth of estrogen receptor positive breast cancer. Oncotarget.

Mehlen, P., and Bredesen, D.E. (2004). The dependence receptor hypothesis. Apoptosis *9*, 37–49.

Mehlen, P., Rabizadeh, S., Snipas, S.J., Assa-Munt, N., Salvesen, G.S., and Bredesen, D.E. (1998). The DCC gene product induces apoptosis by a mechanism requiring receptor proteolysis. Nature *395*, 801–804.

Meisse, D., Van de Casteele, M., Beauloye, C., Hainault, I., Kefas, B.A., Rider, M.H., Foufelle, F., and Hue, L. (2002). Sustained activation of AMP-activated protein kinase induces c-Jun N-terminal kinase activation and apoptosis in liver cells. FEBS Lett. *526*, 38–42.

Merrill, B.J. (2012). Wnt pathway regulation of embryonic stem cell self-renewal. Cold Spring Harb. Perspect. Biol. *4*, 1–17.

Messmer, T., von Meyenn, F., Savino, A., Santos, F., Mohammed, H., Lun, A.T.L., Marioni, J.C., and Reik, W. (2019). Transcriptional Heterogeneity in Naive and Primed Human Pluripotent Stem Cells at Single-Cell Resolution. Cell Rep. *26*, 815-824.e4.

Mitsui, K., Tokuzawa, Y., Itoh, H., Segawa, K., Murakami, M., Takahashi, K., Maruyama, M., Maeda, M., and Yamanaka, S. (2003). The homeoprotein nanog is required for maintenance of pluripotency in mouse epiblast and ES cells. Cell *113*, 631–642.

Miyazono, K., Kamiya, Y., and Morikawa, M. (2010). Bone morphogenetic protein receptors and signal transduction. J. Biochem.

Mo, J., Park, H.W., and Guan, K. (2014). The Hippo signaling pathway in stem cell biology and cancer. EMBO Rep.

Morgani, S., Nichols, J., and Hadjantonakis, A.K. (2017). The many faces of Pluripotency: In vitro adaptations of a continuum of in vivo states. BMC Dev. Biol. *17*, 10–12.

Nagaria, P., Robert, C., and Rassool, F. V. (2013). DNA double-strand break response in stem cells: Mechanisms to maintain genomic integrity. Biochim. Biophys. Acta - Gen. Subj. *1830*, 2345–2353.

Nakamura, T., Okamoto, I., Sasaki, K., Yabuta, Y., Iwatani, C., Tsuchiya, H., Seita, Y., Nakamura, S., Yamamoto, T., and Saitou, M. (2016). A developmental coordinate of pluripotency among mice, monkeys and humans. Nature *537*, 57–62.

Neganova, I., Chichagova, V., Armstrong, L., and Lako, M. (2017). A critical role for p38MAPK signalling pathway during reprogramming of human fibroblasts to iPSCs. Sci. Rep. *7*, 1–13.

Nemashkalo, A., Ruzo, A., Heemskerk, I., and Warmflash, A. (2017). Morphogen and community effects determine cell fates in response to BMP4 signaling in human embryonic stem cells. Dev. *144*, 3042–3053.

Nguyen, Q.H., Lukowski, S.W., Chiu, H.S., Senabouth, A., Bruxner, T.J.C., Christ, A.N., Palpant, N.J., and Powell, J.E. (2018). Single-cell RNA-seq of human induced pluripotent stem cells reveals cellular heterogeneity and cell state transitions between subpopulations. Genome Res. *28*, 1053–1066.

Niakan, K.K., and Eggan, K. (2013). Analysis of human embryos from zygote to blastocyst reveals distinct gene expression patterns relative to the mouse. Dev. Biol. *375*, 54–64.

Nichols, J., and Smith, A. (2009). Naive and Primed Pluripotent States. Cell Stem Cell *4*, 487–492.

Nichols, J., Zevnik, B., Anastassiadis, K., Niwa, H., Klewe-Nebenius, D., Chambers, I., Schöler, H., and Smith, A. (1998). Formation of pluripotent stem cells in the mammalian embryo depends on the POU transcription factor Oct4. Cell *95*, 379–391.

Nichols, J., Chambers, I., Taga, T., and Smith, A. (2001). Physiological rationale for responsiveness of mouse embryonic stem cells to gp130 cytokines. Development *128*, 2333–2339.

Niwa, H., Burdon, T., Chambers, I., and Smith, A. (1998). Self-renewal of pluripotent embryonic stem cells is mediated via activation of STAT3. Genes Dev. *12*, 2048–2060.

Nowotschin, S., Setty, M., Kuo, Y.Y., Liu, V., Garg, V., Sharma, R., Simon, C.S., Saiz, N., Gardner, R., Boutet, S.C., et al. (2019). The emergent landscape of the mouse gut endoderm at single-cell resolution. Nature *569*, 361–367.

Ohinata, Y., Ohta, H., Shigeta, M., Yamanaka, K., Wakayama, T., and Saitou, M. (2009). A Signaling Principle for the Specification of the Germ Cell Lineage in Mice. Cell *137*, 571–584.

Okita, K., Ichisaka, T., and Yamanaka, S. (2007). Generation of germline-competent induced pluripotent stem cells. Nature *448*, 313–317.

Okumura-Nakanishi, S., Saito, M., Niwa, H., and Ishikawa, F. (2005). Oct-3/4 and Sox2 regulate Oct-3/4 gene in embryonic stem cells. J. Biol. Chem. *280*, 5307–5317.

Ozmadenci, D., Féraud, O., Markossian, S., Kress, E., Ducarouge, B., Gibert, B., Ge, J., Durand, I., Gadot, N., Plateroti, M., et al. (2015). Netrin-1 regulates somatic cell reprogramming and pluripotency maintenance. Nat. Commun. *6*, 1–11.

Pastor, W.A., Chen, D., Liu, W., Kim, R., Sahakyan, A., Lukianchikov, A., Plath, K., Jacobsen, S.E., and Clark,

A.T. (2016). Naive Human Pluripotent Cells Feature a Methylation Landscape Devoid of Blastocyst or Germline Memory. Cell Stem Cell *18*, 323–329.

Pastor, W.A., Liu, W., Chen, D., Ho, J., Kim, R., Hunt, T.J., Lukianchikov, A., Liu, X., Polo, J.M., Jacobsen, S.E., et al. (2018). TFAP2C regulates transcription in human naive pluripotency by opening enhancers. Nat. Cell Biol. *20*, 553–564.

Pelish, H.E., Liau, B.B., Nitulescu, I.I., Tangpeerachaikul, A., Poss, Z.C., Da Silva, D.H., Caruso, B.T., Arefolov, A., Fadeyi, O., Christie, A.L., et al. (2015). Mediator kinase inhibition further activates super-enhancer-associated genes in AML. Nature.

Petropoulos, S., Edsgärd, D., Reinius, B., Deng, Q., Panula, S.P., Codeluppi, S., Plaza Reyes, A., Linnarsson, S., Sandberg, R., and Lanner, F. (2016). Single-Cell RNA-Seq Reveals Lineage and X Chromosome Dynamics in Human Preimplantation Embryos. Cell *165*, 1012–1026.

Plotnikova, O. V., Pugacheva, E.N., and Golemis, E.A. (2009). Primary cilia and the cell cycle. (Elsevier).

Plusa, B., Piliszek, A., Frankenberg, S., Artus, J., and Hadjantonakis, A.K. (2008). Distinct sequential cell behaviours direct primitive endoderm formation in the mouse blastocyst. Development *135*, 3081–3091.

Ptak, G.E., Tacconi, E., Czernik, M., Toschi, P., Modlinski, J.A., and Loi, P. (2012). Embryonic diapause is conserved across mammals. PLoS One *7*.

Qin, H., Blaschke, K., Wei, G., Ohi, Y., Blouin, L., Qi, Z., Yu, J., Yeh, R.F., Hebrok, M., and Ramalho-santos, M. (2012). Transcriptional analysis of pluripotency reveals the hippo pathway as a barrier to reprogramming. Hum. Mol. Genet.

Qin, H., Diaz, A., Blouin, L., Lebbink, R.J., Patena, W., Tanbun, P., Leproust, E.M., McManus, M.T., Song, J.S., and Ramalho-Santos, M. (2014). Systematic identification of barriers to human Ipsc generation. Cell.

Qin, H., Hejna, M., Liu, Y., Percharde, M., Wossidlo, M., Blouin, L., Durruthy-Durruthy, J., Wong, P., Qi, Z., Yu, J., et al. (2016). YAP Induces Human Naive Pluripotency. Cell Rep. *14*, 2301–2312.

Van Raay, T.J., Foskett, S.M., Connors, T.D., Klinger, K.W., Landes, G.M., and Burn, T.C. (1997). The NTN2L gene encoding a novel human netrin maps to the autosomal dominant polycystic kidney disease region on chromosome 16p13.3. Genomics *41*, 279–282.

Rabizadeh, S., Oh, J., Zhong, L., Yang, J., Bitler, C.M., Butcher, L.L., Bredesen, D.E., Pechersky, D.M., Tikhonov, V., Pertsev, N.N., et al. (1993). Induction of Apoptosis by the Low-Affinity NGF Receptor. Science (80-.). *261*, 345–348.

Rajasekharan, S., and Kennedy, T.E. (2009). Protein family review The netrin protein family. Genome Biol. *10*, 239.

Ramalho-Santos, M., Yoon, S., Matsuzaki, Y., Mulligan, R.C., and Melton, D.A. (2002). “Stemness”: Transcriptional profiling of embryonic and adult stem cells. Science (80-.).

Randolph, L.N., Bao, X., Zhou, C., and Lian, X. (2017). PiggyBac system for human pluripotent stem cells and derivatives. Sci. Rep. 1–8.

Ren, X.R., Ming, G.L., Xie, Y., Hong, Y., Sun, D.M., Zhao, Z.Q., Feng, Z., Wang, Q., Shim, S., Chen, Z.F., et al. (2004). Focal adhesion kinase in netrin-1 signaling. Nat. Neurosci. *7*, 1204–1212.

Rodda, D.J., Chew, J.L., Lim, L.H., Loh, Y.H., Wang, B., Ng, H.H., and Robson, P. (2005). Transcriptional regulation of Nanog by OCT4 and SOX2. J. Biol. Chem. *280*, 24731–24737.

Roode, M., Blair, K., Snell, P., Elder, K., Marchant, S., Smith, A., and Nichols, J. (2012). Human hypoblast formation is not dependent on FGF signalling. Dev. Biol. *361*, 358–363.

Rutkovskiy, A., Stensløkken, K.-O., and Vaage, I.J. (2016). Osteoblast Differentiation at a Glance. Med. Sci. Monit. Basic Res. *22*, 95–106.

S.J. Dunn, and G. Martello, B. Yordanov, S. Emott, A.. S. (2014). Defining an essential transcription factor program for naïve pluripotency. Science (80-.). *344*, 1156–1161.

Sasai, Y., Lu, B., Steinbeisser, H., and Robertist, E.M. De (1995). Regulation of neural induction by the Chd and Bmp-4 antagonistic patterning signals in Xenopus. Nat. Lett. *376*, 333–336.

Sato, N., Meijer, L., Skaltsounis, L., Greengard, P., and Brivanlou, A.H. (2004). Maintenance of pluripotency in human and mouse embryonic stem cells through activation of Wnt signaling by a pharmacological GSK-3-specific inhibitor. Nat. Med. *10*, 55–63.

Savatier, P., Lapillonne, H., Van Grunsven, L.A., Rudkin, B.B., and Samarut, J. (1996). Withdrawal of differentiation inhibitory activity/leukemia inhibitory factor up-regulates D-type cyclins and cyclin-dependent kinase inhibitors in mouse embryonic stem cells. Oncogene *12*, 309–322.

Savatier, P., Lapillonne, H., Jirmanova, L., Vitelli, L., and Samarut, J. (2002). Analysis of the cell cycle in mouse embryonic stem cells. Methods Mol. Biol. *185*, 27–33.

Scata, K.A., Bernard, D.W., Fox, J., and Swain, J.L. (1999). FGF receptor availability regulates skeletal myogenesis. Exp. Cell Res. *250*, 10–21.

Schrode, N., Xenopoulos, P., Piliszek, A., Frankenberg, S., Plusa, B., and Hadjantonakis, A.K. (2013). Anatomy of a blastocyst: Cell behaviors driving cell fate choice and morphogenesis in the early mouse embryo. Genesis *51*, 219–233.

Schwarz, B.A., Bar-Nur, O., Silva, J.C.R., and Hochedlinger, K. (2014). Nanog is dispensable for the generation of induced pluripotent stem cells. Curr. Biol. *24*, 347–350.

Scognamiglio, R., Cabezas-Wallscheid, N., Thier, M.C., Altamura, S., Reyes, A., Prendergast, Á.M., Baumgärtner, D., Carnevalli, L.S., Atzberger, A., Haas, S., et al. (2016). Myc Depletion Induces a Pluripotent Dormant State Mimicking Diapause. Cell *164*, 668–680.

Serafini, T., Kennedy, T.E., Gaiko, M.J., Mirzayan, C., Jessell, T.M., and Tessier-Lavigne, M. (1994). The netrins define a family of axon outgrowth-promoting proteins homologous to C. elegans UNC-6. Cell *78*, 409–424.

Serafini, T., Colamario, S.A., Leonardo, E.D., Wang, H., Beddington, R., Skarnes, W.C., and Tessier-Lavigne, M. (1996). Netrin-1 Is Required for Commissural Axon Guidance in the Developing Vertebrate Nervous System. Cell *87*, 1001–1014.

Shahbazi, M.N., and Zernicka-Goetz, M. (2018). Deconstructing and reconstructing the mouse and human early embryo. Nat. Cell Biol. *20*, 878–887.

Shakiba, N., White, C.A., Lipsitz, Y.Y., Yachie-Kinoshita, A., Tonge, P.D., Hussein, S.M.I., Puri, M.C., Elbaz, J., Morrissey-Scoot, J., Li, M., et al. (2015). CD24 tracks divergent pluripotent states in mouse and human cells. Nat.

Commun. *6*.

Shelton, M., Kocharyan, A., Liu, J., Skerjanc, I.S., and Stanford, W.L. (2016). Robust generation and expansion of skeletal muscle progenitors and myocytes from human pluripotent stem cells. Methods *101*, 73–84.

Shipony, Z., Mukamel, Z., Cohen, N.M., Landan, G., Chomsky, E., Zeliger, S.R., Fried, Y.C., Ainbinder, E., Friedman, N., and Tanay, A. (2014). Dynamic and static maintenance of epigenetic memory in pluripotent and somatic cells. Nature *513*, 115–119.

Silva, J., Nichols, J., Theunissen, T.W., Guo, G., van Oosten, A.L., Barrandon, O., Wray, J., Yamanaka, S., Chambers, I., and Smith, A. (2009). Nanog Is the Gateway to the Pluripotent Ground State. Cell *138*, 722–737.

Silva, S.S., Rowntree, R.K., Mekhoubad, S., and Lee, J.T. (2008). X-chromosome inactivation and epigenetic fluidity in human embryonic stem cells. Proc. Natl. Acad. Sci. U. S. A. *105*, 4820–4825.

Smagghe, B.J., Stewart, A.K., Carter, M.G., Shelton, L.M., Bernier, K.J., Hartman, E.J., Calhoun, A.K., Hatziioannou, V.M., Lillacci, G., Kirk, B.A., et al. (2013). MUC1* Ligand, NM23-H1, Is a Novel Growth Factor That Maintains Human Stem Cells in a More Naïve State. PLoS One *8*, 1–15.

Smith, A. (2017). Formative pluripotency: The executive phase in a developmental continuum. Dev. *144*, 365–373.

Smith, A.G. (2013). Embyronic-Derived Stem Cells: Of Mice and Men. Annu. Rev. Cell 2364–2373.

Smith, Z.D., and Meissner, A. (2013). DNA methylation: Roles in mammalian development. Nat. Rev. Genet.

Smith, A.G., Heath, J.K., Donaldson, D.D., Wong, G.G., Moreau, J., Stahl, M., and Rogers, D. (1988). Inhibition of pluripotential embryonic stem cell differentiation by purified polypeptides. Nature *336*, 688–690.

Staab, J., Herrmann-Lingen, C., and Meyer, T. (2013). CDK8 as the STAT1 serine 727 kinase? JAK-STAT.

Stirparo, G.G., Boroviak, T., Guo, G., Nichols, J., Smith, A., and Bertone, P. (2018). Erratum: Correction: Integrated analysis of single-cell embryo data yields a unified transcriptome signature for the human pre-implantation epiblast (doi: 10.1242/dev.158501) (Development (Cambridge, England) (2018) 145 3 PII: dev169672). Development *145*.

Sumi, T., Oki, S., Kitajima, K., and Meno, C. (2013). Epiblast Ground State Is Controlled by Canonical Wnt/β-Catenin Signaling in the Postimplantation Mouse Embryo and Epiblast Stem Cells. PLoS One *8*.

Sun, K.L.W., Correia, J.P., and Kennedy, T.E. (2011). Netrins: Versatile extracellular cues with diverse functions. Development *138*, 2153–2169.

Sung, P.J., Rama, N., Imbach, J., Fiore, S., Ducarouge, B., Neves, D., Chen, H.W., Bernard, D., Yang, P.C., Bernet, A., et al. (2019). Cancer-associated fibroblasts produce netrin-1 to control cancer cell plasticity. Cancer Res. *79*, 3651–3661.

Suzuki, A., Pelikan, R.C., and Iwata, J. (2015). WNT/β-catenin signaling regulates multiple steps of myogenesis by regulating step-specific targets. Mol. Cell. Biol. *35*, 1763–1776.

Taft, R.A. (2008). Virtues and limitations of the preimplantation mouse embryo as a model system. Theriogenology *69*, 10–16.

Takahashi, K., and Yamanaka, S. (2006). Induction of Pluripotent Stem Cells from Mouse Embryonic and Adult

Fibroblast Cultures by Defined Factors. Cell *126*, 663–676.

Takahashi, K., and Yamanaka, S. (2015). A developmental framework for induced pluripotency. Dev. *142*, 3274–3285.

Takahashi, K., Tanabe, K., Ohnuki, M., Narita, M., Ichisaka, T., Tomoda, K., and Yamanaka, S. (2007). Induction of Pluripotent Stem Cells from Adult Human Fibroblasts by Defined Factors. Cell *131*, 861–872.

Takahashi, S., Kobayashi, S., and Hiratani, I. (2018). Epigenetic differences between naïve and primed pluripotent stem cells. Cell. Mol. Life Sci. *75*, 1191–1203.

Takashima, Y., Guo, G., Loos, R., Nichols, J., Ficz, G., Krueger, F., Oxley, D., Santos, F., Clarke, J., Mansfield, W., et al. (2014). Resetting transcription factor control circuitry toward ground-state pluripotency in human. Cell *158*, 1254–1269.

Tan, T., Wu, J., Si, C., Ji, W., Niu, Y., Carlos, J., Belmonte, I., Tan, T., Wu, J., Si, C., et al. (2021). Article Chimeric contribution of human extended pluripotent stem cells to monkey embryos ex vivo ll ll Article Chimeric contribution of human extended pluripotent stem cells to monkey embryos ex vivo. 2020–2032.

Tanikawa, C., Matsuda, K., Fukuda, S., Nakamura, Y., and Arakawa, H. (2003). p53RDL1 regulates p53-dependent apoptosis. Nat. Cell Biol. *5*, 216–223.

Tesar, P.J., Chenoweth, J.G., Brook, F.A., Davies, T.J., Evans, E.P., Mack, D.L., Gardner, R.L., and McKay, R.D.G. (2007). New cell lines from mouse epiblast share defining features with human embryonic stem cells. Nature *448*, 196–199.

Theunissen, T.W., Powell, B.E., Wang, H., Mitalipova, M., Faddah, D.A., Reddy, J., Fan, Z.P., Maetzel, D., Ganz, K., Shi, L., et al. (2014). Erratum: Systematic identification of culture conditions for induction and maintenance of naive human pluripotency (Cell Stem Cell (2014) 15 (471-487)). Cell Stem Cell *15*, 523.

Theunissen, T.W., Friedli, M., He, Y., Planet, E., O'Neil, R.C., Markoulaki, S., Pontis, J., Wang, H., Iouranova, A., Imbeault, M., et al. (2016). Molecular Criteria for Defining the Naive Human Pluripotent State. Cell Stem Cell *19*, 502–515.

Thiagarajan, R.D., Morey, R., and Laurent, L.C. (2014). The epigenome in pluripotency and differentiation. Epigenomics *6*, 121–137.

Thomson, J.A. (1998). Embryonic stem cell lines derived from human blastocysts. Science (80-.). *282*, 1145–1147.

Toyooka, Y., Shimosato, D., Murakami, K., Takahashi, K., and Niwa, H. (2008). Identification and characterization of subpopulations in undifferentiated ES cell culture. Development *135*, 909–918.

Tsakiridis, A., Huang, Y., Blin, G., Skylaki, S., Wymeersch, F., Osorno, R., Economou, C., Karagianni, E., Zhao, S., Lowell, S., et al. (2014). Distinct Wnt-driven primitive streak-like populations reflect in vivo lineage precursors. Dev. *141*, 1209–1221.

Tsukiyama, T., and Ohinata, Y. (2014). A modified EpiSC culture condition containing a GSK3 inhibitor can support germline-competent pluripotency in mice. PLoS One *9*, e95329.

Vallier, L., Reynolds, D., and Pedersen, R.A. (2004). Nodal inhibits differentiation of human embryonic stem cells along the neuroectodermal default pathway. Dev. Biol. *275*, 403–421.

Vallier, L., Alexander, M., and Pedersen, R.A. (2005). Activin/Nodal and FGF pathways cooperate to maintain pluripotency of human embryonic stem cells. J. Cell Sci. *118*, 4495–4509.

Villa-Diaz, L.G., Pacut, C., Slawny, N.A., Ding, J., O'Shea, K.S., and Smith, G.D. (2009). Analysis of the factors that limit the ability of feeder cells to maintain the undifferentiated state of human embryonic stem cells. Stem Cells Dev. *18*, 641–651.

Ware, C.B., Wang, L., Mecham, B.H., Shen, L., Nelson, A.M., Bar, M., Lamba, D.A., Dauphin, D.S., Buckingham, B., Askari, B., et al. (2009). Histone Deacetylase Inhibition Elicits an Evolutionarily Conserved Self-Renewal Program in Embryonic Stem Cells. Cell Stem Cell *4*, 359–369.

Weinberger, L., Ayyash, M., Novershtern, N., and Hanna, J.H. (2016). Dynamic stem cell states: Naive to primed pluripotency in rodents and humans. Nat. Rev. Mol. Cell Biol. *17*, 155–169.

Wernig, M., Meissner, A., Foreman, R., Brambrink, T., Ku, M., Hochedlinger, K., Bernstein, B.E., and Jaenisch, R. (2007). In vitro reprogramming of fibroblasts into a pluripotent ES-cell-like state. Nature *448*, 318–324.

Wianny, F., Bernat, A., Huissoud, C., Marcy, G., Markossian, S., Cortay, V., Giroud, P., Leviel, V., Kennedy, H., Savatier, P., et al. (2008). Derivation and Cloning of a Novel Rhesus Embryonic Stem Cell Line Stably Expressing Tau-Green Fluorescent Protein. Stem Cells *26*, 1444–1453.

Williams, R.L., Hilton, D.J., Pease, S., Willson, T.A., Stewart, C.L., and Gearing, D.P. (1988). Myeloid leukaemia inhibitory factor maintains the developmental potential of embryonic stem cells. Nature *336*, 684–687.

Wray, J., Kalkan, T., Gomez-Lopez, S., Eckardt, D., Cook, A., Kemler, R., and Smith, A. (2011). Inhibition of glycogen synthase kinase-3 alleviates Tcf3 repression of the pluripotency network and increases embryonic stem cell resistance to differentiation. Nat. Cell Biol. *13*, 838–845.

Wu, J., and Belmonte, J.C.I. (2015a). Metabolic exit from naive pluripotency. Nat. Cell Biol. *17*, 1519–1521.

Wu, J., and Belmonte, J.C.I. (2015b). Metabolic exit from naive pluripotency. Nat. Cell Biol. *17*, 1519–1521.

Wu, J., Kubota, J., Hirayama, J., Nagai, Y., Nishina, S., Yokoi, T., Asaoka, Y., Seo, J., Shimizu, N., Kajiho, H., et al. (2010). P38 Mitogen-activated protein kinase controls a switch between cardiomyocyte and neuronal commitment of murine embryonic stem cells by activating myocyte enhancer factor 2C-dependent bone morphogenetic protein 2 transcription. Stem Cells Dev. *19*, 1723–1734.

Wu, J., Okamura, D., Li, M., Suzuki, K., Luo, C., Ma, L., He, Y., Li, Z., Benner, C., Tamura, I., et al. (2015). An alternative pluripotent state confers interspecies chimaeric competency. Nature *521*, 316–321.

Wu, J., Platero Luengo, A., Gil, M.A., Suzuki, K., Cuello, C., Morales Valencia, M., Parrilla, I., Martinez, C.A., Nohalez, A., Roca, J., et al. (2016). Generation of human organs in pigs via interspecies blastocyst complementation. Reprod. Domest. Anim. *51*, 18–24.

Wu, J., Platero-Luengo, A., Sakurai, M., Sugawara, A., Gil, M.A., Yamauchi, T., Suzuki, K., Bogliotti, Y.S., Cuello, C., Morales Valencia, M., et al. (2017). Interspecies Chimerism with Mammalian Pluripotent Stem Cells. Cell *168*, 473-486.e15.

Xu, X., Yan, Q., Wang, Y., and Dong, X. (2017). NTN4 is associated with breast cancer metastasis via regulation of EMT-related biomarkers. Oncol. Rep. *37*, 449–457.

Xue, L., Cai, J.Y., Ma, J., Huang, Z., Guo, M.X., Fu, L.Z., Shi, Y.B., and Li, W.X. (2013). Global expression

profiling reveals genetic programs underlying the developmental divergence between mouse and human embryogenesis. BMC Genomics *14*, 1.

Yamaji, M., Ueda, J., Hayashi, K., Ohta, H., Yabuta, Y., Kurimoto, K., Nakato, R., Yamada, Y., Shirahige, K., and Saitou, M. (2013). PRDM14 ensures naive pluripotency through dual regulation of signaling and epigenetic pathways in mouse embryonic stem cells. Cell Stem Cell *12*, 368–382.

Yan, L., Yang, M., Guo, H., Yang, L., Wu, J., Li, R., Liu, P., Lian, Y., Zheng, X., Yan, J., et al. (2013). Single-cell RNA-Seq profiling of human preimplantation embryos and embryonic stem cells. Nat. Struct. Mol. Biol. *20*, 1131–1139.

Yang, Y., Liu, B., Xu, J., Wang, J., Wu, J., Shi, C., Xu, Y., Dong, J., Wang, C., Lai, W., et al. (2017). Derivation of Pluripotent Stem Cells with In Vivo Embryonic and Extraembryonic Potency. Cell *169*, 243-257.e25.

Yao, K., Ki, M.O., Chen, H., Cho, Y.Y., Kim, S.H., Yu, D.H., Lee, S.Y., Lee, K.Y., Bae, K., Peng, C., et al. (2014). JNK1 and 2 play a negative role in reprogramming to pluripotent stem cells by suppressing Klf4 activity. Stem Cell Res. *12*, 139–152.

Yin, K., Wang, L., Zhang, X., He, Z., Xia, Y., Xu, J., Wei, S., Li, B., Li, Z., Sun, G., et al. (2017). Netrin-1 promotes gastric cancer cell proliferation and invasion via the receptor neogenin through PI3K/AKT signaling pathway. Oncotarget *8*, 51177–51189.

Yin, K., Dang, S., Cui, L., Fan, X., Xie, R., Qu, J., Shang, M., and Chen, J. (2018). Netrin-1 promotes metastasis of gastric cancer by regulating YAP activity. Biochem. Biophys. Res. Commun. *496*, 76–82.

Ying, Q.-L., Nichols, J., Chambers, I., and Smith, A. (2003a). BMP Induction of Id Proteins Suppresses Differentiation and Sustains Embryonic Stem Cell Self-Renewal in Collaboration with STAT3. Cell *115*, 281–292.

Ying, Q.L., Stavridis, M., Griffiths, D., Li, M., and Smith, A. (2003b). Conversion of embryonic stem cells into neuroectodermal precursors in adherent monoculture. Nat. Biotechnol. *21*, 183–186.

Ying, Q.L., Wray, J., Nichols, J., Batlle-Morera, L., Doble, B., Woodgett, J., Cohen, P., and Smith, A. (2008). The ground state of embryonic stem cell self-renewal. Nature *453*, 519–523.

Yoshida, K., Chambers, I., Nichols, J., Smith, A., Saito, M., Yasukawa, K., Shoyab, M., Taga, T., and Kishimoto, T. (1994). Maintenance of the pluripotential phenotype of embryonic stem cells through direct activation of gp130 signalling pathways. Mech. Dev. *45*, 163–171.

Young, R.A. (2011). Control of the embryonic stem cell state. Cell *144*, 940–954.

Yuan, X., Cao, J., He, X., Serra, R., Qu, J., Cao, X., and Yang, S. (2016). Ciliary IFT80 balances canonical versus non-canonical hedgehog signalling for osteoblast differentiation. Nat. Commun. *7*.

Zhang, J., Nuebel, E., Daley, G.Q., Koehler, C.M., and Teitell, M.A. (2012). Metabolic regulation in pluripotent stem cells during reprogramming and self-renewal. Cell Stem Cell *11*, 589–595.

Zhou, W., Choi, M., Margineantu, D., Margaretha, L., Hesson, J., Cavanaugh, C., Blau, C.A., Horwitz, M.S., Hockenbery, D., Ware, C., et al. (2012). HIF1α induced switch from bivalent to exclusively glycolytic metabolism during ESC-to-EpiSC/hESC transition. EMBO J. *31*, 2103–2116.

Zimmerlin, L., Park, T.S., Huo, J.S., Verma, K., Pather, S.R., Talbot, C.C., Agarwal, J., Steppan, D., Zhang, Y.W., Considine, M., et al. (2016). Tankyrase inhibition promotes a stable human naïve pluripotent state with improved

functionality.

Zwaka, T.P., and Thomson, J.A. (2003). Homologous recombination in human embryonic stem cells. Nat. Biotechnol. *21*, 319–321.